INDUCED VOLTAGE ELECTROMAGNETIC FLOWMETERS

by

M.K. BEVIR

A Thesis submitted to the University of Warwick for the degree of Doctor of Philosophy

April 1969

ABSTRACT

This thesis analyses the behaviour of electromagnetic flowmeters in which the flowrate of a suitably conducting liquid is measured by means of the e.m.f. induced between two electrodes by the motion in a magnetic field. The distortion of the field by the induced currents is assumed negligible, thus excluding the more highly conducting liquid metals, but the method is well-known to be suitable for certain liquid metals, water-based liquids and blood. Attention is concentrated entirely on the flowmetering device itself and not on any associated electronics.

The idea of the contribution of each element of fluid moving with velocity $\underline{v}$ in a magnetic field $\underline{B}$ to the total electrode e.m.f. is first put on a sound mathematical basis by the introduction of a weight vector

$$\underline{W} = \underline{B} \wedge \nabla q$$

where ∇q is a vector entirely determined by the flowmeter and electrode geometry. The contribution is $\underline{W}.\underline{v}$ per unit volume.

The ultimate aim of the flowmeter designer is to make the meter sensitivity (the electrode e.m.f. divided by the flowrate) entirely independent of the flow pattern, i.e. of $\underline{v}$. The behaviour of a flowmeter is specified entirely by $\underline{W}$ and the necessary condition on $\underline{W}$ to achieve this sensitivity independence (an ideal meter) is found to be curl $\underline{W} = 0$.

It is shown that there is no magnetic field that will achieve this if point electrodes are used. The condition on $\underline{W}$ weakens progressively as more assumptions are made about the flow pattern and weight functions suitable for different types of velocity profile are defined. The effects of different types of electrode are also discussed.

This basic theory is then applied, first to a class of ideal uniform field flowmeters with transverse line electrodes. These meters can, moreover, be used as valves and flowmeters simultaneously. Their performance has been experimentally checked.

Secondly the theory of long flowmeters (in which all quantities are assumed invariant in the flow direction) is exhaustively discussed.

Thirdly the practically important case of circular meters with non-conducting walls, point electrodes and short magnetic fields is examined. In view of the difficulty of manufacturing a magnetic field that may be mathematically desirable, this problem is by-passed by first choosing a technologically simple method of producing magnetic fields for these meters using coils specified by certain parameters and then analysing the relevant weight function in terms of these parameters. Design tables for the case of rectilinear axisymmetric flow are presented (one specimen), and experimental tests described which check the performance of designs produced from these tables.

A different method of producing the magnetic field is suggested which saves power consumption and enables the field to be more accurately designed, but to which the tables mentioned above still apply.

Finally some outstanding problems are discussed.

PREFACE

Since October 1965 I have been working as a research student under Professor J.A. Shercliff at the University of Warwick. During that time I have been on leave from the English Electric Company's Mechanical Engineering Laboratories at Whetstone, near Leicester and been given a grant by them. I wish to record my gratitude to the Company for supporting me over the last few years, and for giving the University a grant which enabled me to attend the 6th Symposium on Magnetohydrodynamics at Riga in September 1968.

My main field has been the theory of the electromagnetic flow measurement of liquids. The flowrate is measured by the voltage induced between two electrodes by motion in a magnetic field (Faraday's Law) under conditions where the magnetic field is not significantly distorted by the currents induced by the motion, and the voltage is effectively measured on open circuit. Though much of the theory may be applied to any flow measurement situation I have concentrated on flow in pipes and the improvement of modern flowmeter design. At one time there were hopes of not only measuring the flowrate, but also analysing the velocity profiles. However, precisely those characteristics which make an electromagnetic flowmeter good at measuring the mean velocity (in some sense) make it bad at picking up local velocities, and this part of the project was dropped.

Six or nine months were spent on a different project, which is not reported in this thesis. This was the flow of electrolyte in a long circular pipe under a pressure gradient and streamwise body force varying quadratically with radius. The force is produced electromagnetically by imposing quadrupole current and magnetic fields (lying in planes perpendicular to the pipe) the conditions being such that there is no interaction between the fluid motion

and imposed fields. The aim is to produce artificial velocity profiles in normal fluid mechanic pipe flow by the use of carefully controlled non-uniform body forces, so that the turbulence in abnormal shear flow profiles and the stability of the laminar profiles may be examined. A small amount of elementary analysis of the laminar profiles has been done, and the experimental apparatus half-constructed. The problem of getting the necessary non-uniform current distribution inside a circular pipe has been solved by using porous walls (impervious to the flow) and electrodes lying outside them.

The flowmetering work is fully reported in this thesis. The material has been arranged as a general survey of the theory followed by the experimental results, with three reports containing details of the theory in the appendix. This enables the flowmeter designer to get a good idea of the scope of the mathematical work without having to read it unless he particularly wishes to.

Most of the theoretical results in this thesis are in analytical form, from which numerical results have been obtained using a digital computer when necessary. Though there are situations when numerical analysis may be preferable, the geometry of many flowmetering problems is sufficiently simple to be amenable to algebraic analysis.

During the first year the analysis was restricted to long flowmeters and it was only then that, spurred on by the work of Ketelsen (6), we started tackling the problem of short meters.

The first and third reports in the appendix result from this work on short meters and formed the basis of papers given in the autumn of 1968, by Prof. J.A. Shercliff to the 12th International Congress of Applied Mechanics at Stanford and myself to the 6th Symposium on Magnetohydrodynamics at the Latvian Academy of Sciences at Riga. The second report, though it contains the work on long flowmeters done before the other two, was written up after them in a shorter and neater form after the advantages of couching the theory in terms of the virtual current (defined on page 4 of the first report) were realised.

The reader will notice that to some extent the work of other people is discussed after the basic theory has been introduced. The reason is that some of their work has been simplified to ease analysis and some is inaccurate. Different notations have been used and it is easier to discuss the work in a common notation and with an awareness of what is being ignored.

I should like to take this opportunity of thanking my supervisor, Professor J.A. Shercliff, for his advice and criticism throughout my work, Dr. G. Rowlands for convincing me that in practical situations separable solutions are often the only way of solving Laplace's equation, Dr. C.J.N. Alty for reading this thesis in draft, Dr. R.C. Baker, Dr. C.J. Mills, Dr. D.G. Wyatt and George Kent Ltd for discussions on flowmetering and the requirements of practical designs. Finally I should like to thank Mr. A.E. Webb and Mr. A.C. Ross for their work in the construction of the apparatus and Miss J.A. Green who had to read my writing when typing this thesis.

CONTENTS

NOMENCLATURE

a	radius of flowmeter
A	coefficient in Fourier Series
b	radius of iron sheath
B	coefficient in Fourier Series, magnetic field component
$\underline{B}$	magnetic field vector
Bo	Uniform or reference magnetic field
D	Flowmeter internal diameter
d	Canvas pipe diameter
E(k)	Complete Elliptic Integral of the second kind, modulus k.
F	Magnetic field potential $\underline{B} = \nabla F$
f(z)	Magnetic field potential: $B_x - iB_y = f'(z) \equiv \frac{df}{dz}$; $i = \sqrt{-1}$
G	Virtual current potential, current $= \nabla G$
g(z)	Virtual current potential: $\frac{\partial G}{\partial x} - \iota \frac{\partial G}{\partial y} = g'(z) \equiv \frac{dg}{dz}$; $\iota = \sqrt{-1}$
H	Manometer reading
I_m, J_m	Bessel Functions
$j_{m,s}^{[\prime]}$	s^{th} zero of $J_m(p) = 0$ $\left[\text{of } \frac{dJ_m}{dp} = 0\right]$
K	Bessel Function, Complete Elliptic Integral of the first kind
L	length of coil
m,n	integers
p	pitch of conducting wall made of alternate conducting and insulating strips
Q	Flowrate
r	co-ordinate radius
R	distance from origin $\sqrt{x^2 + y^2 + z^2}$
S	sensitivity
t	canvas pipe thickness, potential (if it exists) such that $\nabla t = \underline{B} \wedge \nabla G$
T	Ratio of iron sheath diameter to flowmeter diameter
U	Electric potential

ΔV Electric potential difference

$\underline{V}$ Velocity vector (V_x , V_y , V_z)

v Velocity component, normally in stream-wise direction

w Conducting wall thickness

$\underline{W}$ Weight vector $\underline{B} \wedge \nabla G \equiv (W_x , W_y , W_z)$

W $\equiv W_z$ (the only surviving component in long flowmeter theory)

$\overline{W} = \int_{z=-\infty}^{+\infty} W_z \, dz$, asymmetric rectilinear profile weight function

$\overline{W}' = \frac{1}{2\pi} \int_0^{2\pi} \overline{W} d\theta$, axisymmetric rectilinear profile weight function

$[x,y,z]$ Cartesian co-ordinates

$z, \overline{z}$ $x + iy$, $x - iy$ in long flowmeter theory

α electrode (or pole piece) half angle, Fourier integral exponent

β Fourier integral exponent

γ Angle between virtual current stream line and electrode axis in a long flowmeter

θ Polar co-ordinate

$\pi/2 - \theta_0$ Coil half angle

κ Wall conductivity

λ Canvas wall conductivity factor, variably conducting wall parameter

σ Fluid conductivity

$\tau, d\tau$ Volume, volume element

ϕ Co-ordinate in spherical polars (R, θ , ϕ), potential in plane geometries.

ψ Stream function in plane geometries

1. INTRODUCTION

The basic equation for the induced electric potential U of a fluid in motion in a magnetic field, given for example by Shercliff (8a, p12), is

$$\nabla^2 U = \text{div}\,(\underline{v} \wedge \underline{B}) \qquad (2.1)$$

together with suitable boundary conditions on any walls present. Subsidiary conditions available, if needed, are div $\underline{v} = 0$ (incompressible flow), div $\underline{B} = 0$ (always) and curl $\underline{B} = 0$ (if the distortion of the magnetic field due to the induced currents is negligible). Throughout this thesis the applied field $\underline{B}$ will be assumed steady or varying sinusoidally with time, and only the potential U due to the motion will be considered. The out of phase potentials due to electromagnetic induction must be otherwise taken care of.

Various methods of obtaining solutions of (2.1) have been tried. In (8a) Shercliff has used separation of variables (e.g. for laminar flow in an insulating rectangular pipe and uniform magnetic field) image systems (in the case of the weight function for a circular flowmeter with point electrodes and a uniform field), and plain juggling making simple assumptions about the velocity profile and using the fact that the field is Laplacian (in the solutions for wall velometers with the fluid half-space bounded by an insulating plane).

Baker has obtained a very elegant set of solutions for such wall velometers with insulating walls (2a) and also for circular flowmeters (both internal and external) (2b), initially by separation of variables. At first he assumed the velocity was in one direction only and dependent only on distance from the wall (radius in the circular case),

and that the magnetic field lay in the plane perpendicular to the flow. (He also considered an axisymmetric magnetic field for the wall velometer). The notation is in figure 1. He gives the solution everywhere in the fluid, but on the wall it takes the form ($U(\infty) = B(\infty) = 0$)

$$\text{half space } x > 0: \quad U = 2 \int_0^\infty V_z(x)\ B_y(2x,y,z)\, dx \qquad (2.2)$$

$$\begin{matrix}\text{circular pipe} \\ \text{(radius a)}\end{matrix} : U = \frac{2}{a} \int_0^a v_z(r)\ B_\theta\left(\frac{r^2}{a},\theta\right) r\, dr \qquad (2.3)$$

with slight changes in notation. Disregard the dependence of B_y on z in (2.2) for the moment. Although these formulae take account of ohmic losses, the total signal is found by simply multiplying the velocity at one station by twice the transverse component of magnetic field at a different but related station regardless of the magnetic field anywhere else.

Because $\underline{B}$ is a plane solution of Laplace's equation, the magnetic field (under certain assumptions about symmetry and singularities) is specified everywhere by its value along a line, so it is not possible to vary the field anywhere without varying it along the relevant lines. This follows from a theorem in the theory of complex variables which may also be used to prove (2.2) and (2.3) (for the latter see page 9, report 2).

The factors 2 in (2.2) and (2.3) appear embarrassing, especially in the case when the moving fluid is confined to a thin layer close to the wall and the magnetic field is fairly uniform there, so that $B_y(2x,y,z) \simeq B_y(x,y,z)$. How, one may ask, do we get twice the expected potential? The answer is that (2.2) applies in its present form only when $\underline{B} \to 0$ at ∞; half the signal comes from the motion of the shear layer in B_y as expected and the other half from the motion in B_x for large y, i.e. from the distant motion in the other transverse field component, which is implied if the field goes to zero at infinity. It can be shown that the signal in the (non-Laplacian) field created by reversing the sign of B_y is zero.

Similar statements apply to (2.3). The potential using the (non-Laplacian) field (B_r, $-B_\theta$) found by reversing the sign of B_θ for a Laplacian field is also zero.

(2.2) also holds even when the magnetic field $\underline{B}$ is three dimensional. This means that for a wall velometer with two point electrodes it is necessary only to arrange the difference in B_y along the two perpendiculars to the wall through the electrodes to get a specified response, the field everywhere else can be left to look after itself. (2.2) also holds if the wall can be removed, though the potential is then halved and any motion and field in the half space $x < 0$ must be taken account of. It is more likely that the motion and field will be symmetrical, in which case (2.2) holds without alteration.

The generalisation of (2.2) immediately leads one to ask if (2.3) can be similarly generalised because, if this were the case, the problem of designing short flowmeters with rectilinear flow with an axisymmetric profile would have been solved. The answer is no, and the reason must be connected with the two facts that, firstly, circles in two dimensions and half planes, in two and three dimensions, have simple image systems and, secondly, the magnetic field is Laplacian. Circular pipes in three dimensions do not have simple image systems. It is still possible to attempt the solution of the flowmeter equation (2.1) by separating the variables (see page 7 of report 3) though the terms no longer add up neatly to give the transverse component of the magnetic field at an easily recognisable position.

There are, however, two difficulties using separable solutions. The first is the need to take account of variation of velocity in two dimensions (in the case of a pipe arbitrary variation over the pipe cross-section) and the second is the mixed boundary value conditions relevant when the electrodes are not small.

In this thesis another approach is adopted, which is an extension of the idea of the weight function originally given by Shercliff (e.g. 8a, p.29) (which has, incidentally, been abused by being applied outside the context of long flowmeters). The idea indicates the use of Green's functions. (The term Green's function will henceforth be used generically implying that the function is suited to the boundary conditions).

2. OUTLINE THEORY

2.1. The Basic Theorem

Analysis, given on pages 3 and 4 of the first report, shows that the signal of a flowmeter is

$$\int \underline{v} \cdot \underline{W} \, d\tau \qquad (2.4)$$

where the volume integral is taken over the whole of the fluid space of the flowmeter and $\underline{W}$ is a weight vector, given by

$$\underline{W} = \underline{B} \wedge \nabla \zeta \qquad (2.5)$$

$\nabla\zeta$ is a vector that does not depend on $\underline{B}$ but only on the shape of the electrodes and the flowmeter (and the electrical boundary conditions on the walls). Here it has been given the name "virtual current" since if unit current is passed between the electrodes by placing a suitable voltage across them, the resulting current distribution is $\nabla\zeta$. ζ is the potential associated with the virtual current. This theorem holds even if the conductivity of the liquid is non-uniform, though the distribution of $\nabla\zeta$ is of course altered. The result may also be derived by modelling the fluid by a resistance network and using the reciprocity theorem in the form used by electrical engineers. The current is called 'virtual' because although there will in general be currents circulating (which must of course depend on $\underline{v}$) the virtual current is fictitious and only a means of thinking about the problem.

In this thesis we deal only with cases in which the magnetic field is unperturbed by currents induced by the motion thus excluding high conductivity liquid metals. With this assumption $\underline{B} = \nabla F$ where F, as well as ζ, in the case of fluid with uniform conductivity, is a solution of Laplace's equation.

It can now immediately be seen why certain well-known types of flowmeter have desirable characteristics. Consider, for example, a rectangular flowmeter with large electrodes of high conductivity covering opposite walls and long in the flow direction. The virtual current is obviously uniform, even if the other walls, or the fluid, have conductivities varying with the distance between the electrodes, though not if they vary in the other direction. In a uniform magnetic field the weight vector would have only one component, which would be constant and in the flow direction.

Axial current flowmeters (Shercliff 8b) are another example. Suppose the liquid passes through a highly conducting circular pipe which forms one of the electrodes, the other being a wire placed on the centre-line of the pipe.

If the flowmeter is long, it is clear that the virtual current is radial, $\propto \frac{1}{r}$ in strength, and does not depend on the conductivity of the fluid or on contact resistance provided they are axisymmetric. It is clear that an azimuthal magnetic field $\propto r$ will make $\underline{W}$ uniform and in the flow direction. Such a field is provided by a uniform current flow along the fluid.

2.2. The Design Problem

We now turn to the basic problem which is to make a flowmeter whose signal depends only on the flowrate and is independant of the shape of the flow pattern. From here on such flowmeters are called "ideal", though the term is sometimes used in connection with a flow pattern about which some restrictive assumption has been made.

The first stage of the problem is to work out a suitable condition on $\underline{W}$ to ensure that a flowmeter is ideal, or range of conditions depending on assumed forms of flow-patterns, since only $\underline{W}$ itself appears explicitly in equation (2.1).

The second stage is to choose the magnetic field and virtual current so that the condition selected is satisfied, if this is possible.

The third stage is to produce the required magnetic field and virtual current. This is where difficulties can arise. Suppose we have written down mathematical expressions for the field and virtual current potentials (for F and G) satisfying Laplace's equation and each containing a set of unknown coefficients which we are at liberty to choose.

The use of a suitable (as yet undiscussed) condition on $\underline{W}$ would result in relations between the sets of coefficients, that might either specify the sets completely, or else allow some element of choice. Put another way, the condition on $\underline{W}$ would either result in the specification of the magnetic field and virtual current, or in the specification of a range of matching fields and currents.

The problem would then arise of producing them practically. Though any magnetic field can be produced by putting suitable coils around the flowmeter (and surrounding them with high permeability iron if so desired) there is no guarantee that the coils would be easy to make. In general, it would also be too difficult to manufacture the electrical boundary conditions required on the wall of the flowmeter to realise the stipulated virtual current.

For these reasons we have reversed the procedure. The virtual current has been analysed first for electrode arrangements that are easy to realise in practice (and which normally have undesirable effects on the weight vector $\underline{W}$), and secondly for arrangements that are possible in practice and which have less undesirable effects.

In the second report, on long flowmeters, where attention has been concentrated on what is possible rather than what is practicable, the magnetic field has been chosen after considering what field is best suited to a particular virtual current. The method requires the choice of a mathematical function and the resulting field is not always easy to reproduce.

On the other hand in the third report, which is an analysis of the case of a circular flowmeter with diametrically opposed electrodes, assuming rectilinear flow, with special emphasis on flow with axi-symmetric velocity profiles, a range of magnetic fields which are easy to produce are analysed in terms of certain parameters describing the

range. The behaviour of the relevant weight function resulting from these fields is set out in tables. The design is then found by selecting a suitable number of these basic fields so that the weight function has the correct behaviour. Normally two, sometimes three, of these fields are necessary.

The main advantage of this method is that while we do not know (and do not care) what the magnetic field is, we know how to make it. The corresponding disadvantage is that it must be made in the prescribed manner, or by using some other technique that satisfies the same magnetic boundary conditions. If these conditions are different the analysis does not apply at all.

2.3. Conditions on the Weight Vector $\underline{W}$

The minimum assumption we may make about the flow is that it is incompressible (div $\underline{v} = 0$) for, if it is not, the volumetric flow rate is different at various cross-sections and is therefore not uniquely defined. On page 5 of the first report the necessary and sufficient condition on $\underline{W}$ for an ideal meter (assuming $\underline{W} \to 0$ far from the electrodes) is shown to be curl $\underline{W} = 0$. On page 12 of the same report it is also shown that whenever point electrodes are used this condition cannot be achieved. Since this is so, and since most practical flowmeters use point electrodes, further conditions must be imposed on the velocity so that the flowmeter becomes ideal. The most useful necessary and sufficient conditions are summarised in the following table.

Assumption on $\underline{v}$	Condition on $\underline{W}$
div $\underline{v} = 0$	curl $\underline{W} = 0$ (1)
$\underline{v} = [0,0,V(x,y,z)]$	W_z = function of z (2)
$\underline{v} = [0,0,V(x,y)]$	$\overline{W}(x,y) = \int_{-\infty}^{\infty} W\, dz$ = constant (3)
$\underline{v} = [0,0,V(r)]$	$\overline{W}'(r) = \frac{1}{2\pi} \int_{0}^{2\pi} \overline{W}\, d\theta$ = constant (4)

A condition intermediate between (1) and (2) is possible if, for example, $\underline{v}$ is confined to a plane.

Condition 1 is the most desirable; as mentioned above it cannot be achieved using point electrodes but it can be satisfied using a uniform magnetic field and line electrodes in specially shaped flowmeter channels (p.7, first report). Whether it can be achieved in other circumstances is still an open question, though it is unlikely.

Condition 4 (p.9, report 1), normally only required for circular flowmeters, makes the maximum assumption about the flow (apart from slug flow): that it is rectilinear and axisymmetric. This assumption has been made or implied in most flowmeter designs until recently. Condition 4 may be achieved in many ways: for example with a uniform field and any electrode system (p.6, report 1) or with any matching* electrode arrangement and magnetic field. Even for one particular arrangement, such as point electrodes, there are many suitable magnetic fields. The justification for this remark is not merely some existence theorem, (see the remarks on p.8 of report 3), but also that report 3 describes a set of design tables which do demonstrate many ways of achieving designs of constant $\overline{W}'$.

The possibility of achieving condition 3, for an asymmetric rectilinear velocity profile is not so well established. Pages 13 and 14 of report 1 suggest that this is possible in principle with point electrodes but that in practice difficulties will be experienced in a region whose distance from the electrode is small compared with the flowmeter wall thickness. The analysis there is not entirely satisfactory and the question is discussed further on page 13 of this thesis.

---

*The term matching is used in the sense given in the middle of p.8 of report 3, which only suggests the existence of matching solutions but does not show how to find them. This would involve mathematical inversion of equation 16 (p.7 same report) which may be very difficult (as in the classical problem of moments) and would still leave the designer with a mathematical specification of the magnetic field once he had selected the electrode arrangement.

It is possible to produce a set of tables for this case similar to (but much bulkier than) the design tables for the axisymmetric case. When report 1 was written it was thought such tables would be too large for practical use, but with drastic pruning their size can be reduced and tables for this case are being prepared.

Conditions (3) and (4) also apply in the theory of long flowmeters, when they take simplified forms. In such flowmeters the magnetic field and virtual current are assumed to be perpendicular to and invariant along the main stream direction, and the weight vector $\underline{W}$ has only one component W which is also in that direction. Under certain conditions (p.3 report 2) other flowmeters may be analysed as if they were long. Report 2 deals almost entirely with long flowmeters and the mathematical situation is clear. To achieve condition (4) either the magnetic field or the virtual current must be uniform and the other may then be arbitrary: to achieve (3) both must be uniform. The rest of the report is concerned with analysing situations that either approximate to these conditions, or can be easily realised in practice.

The velocity distribution assumed in condition (2) will never occur in practice, since the assumption of rectilinear flow and the continuity condition requires $\frac{\partial v_z}{\partial z} = 0$. Condition (2) has, however, been used as the basis of some designs. Its shortcoming is that it is either too weak or unnecessarily strong. If the flow is rectilinear then condition (3) is all that is necessary: if the flow is not rectilinear then condition (2) is not sufficient since in general there will also be velocity components transverse to the streamwise direction which will contribute to the output voltage; we must have condition (1) or some variant of it.

2.4. The Effect of Large Electrodes.

For the purposes of discussion, the possible electrode systems can be listed, in order of increasing manufacturing difficulty, as follows:

a) Point electrodes (in practice small circular discs)

b) Line electrodes, transverse to the flow (p.10 report 1) (p.12 report 2)

c) Long electrodes (report 2), in particular long quadrant electrodes.

d) Anything more complicated, such as multiple electrode systems, or some of the schemes suggested in report 2, using walls of variable conductivity.

To get some idea of the strength of the singularity at the edge of the electrodes, consider the virtual current potential function when the first three electrode systems are set in an otherwise non-conducting plane (or in free space, since the solutions are symmetric), assuming that the far end of a line electrode and far edge of a long electrode are sufficiently distant to be considered at infinity (see figure 2 for sketch and notation).

In order to simplify the comparison assume that each of these electrodes is situated in a uniform transverse magnetic field with the flow rectilinear and invariant in the flow direction. Then the integrated form of the virtual current is relevant, i.e. $\frac{\partial \bar{\varphi}}{\partial y} = \int_{\infty} \frac{\partial \varphi}{\partial y} dz$, since these are essentially long flowmeter situations.

For a point electrode $\varphi \propto \frac{1}{R}$ and for a semi-infinite line electrode $\varphi \propto \int^{x} \frac{dx}{R}$ or $\log(R + x)$, a much weaker singularity. The integrated virtual current, represented using the complex variable $z' = x + iy$ as $\frac{\partial \bar{\varphi}}{\partial x} - \iota \frac{\partial \bar{\varphi}}{\partial y} \equiv \frac{d\bar{\varphi}}{dz}$, has the form $\frac{1}{z'}$, for a point electrode, $\log z'$ for a transverse line electrode and $\frac{1}{\sqrt{z'}}$ for a large electrode (which, being already invariant in the flow direction, needs no integration).

The weakest of these singularities is $\log z'$. $\frac{\partial \bar{\varphi}}{\partial y} = \theta'$ and in a uniform field the weight function is uniform over the electrodes and always finite.

The other component $\frac{\partial \bar{\varphi}}{\partial x} = \log r'$, which must be taken into account if the field is inclined to the electrode; though it tends to infinity at the electrode edge it does so very weakly. The weakness of this logarithmic singularity is the reason why the long flowmeter performance of the curved line electrodes studied on page 12

of report 2 is so good. In figure 3 the lines of constant $\frac{\partial \bar{\varphi}}{\partial y}$ for the integrated virtual current for a transverse line electrode with two ends at $x = \pm a$ are shown. $\frac{\partial \bar{\varphi}}{\partial x} - i\frac{\partial \bar{\varphi}}{\partial y}$ is $\frac{1}{2\pi a} \log \frac{z'-a}{z'+a}$ and the lines are a set of coaxial circles through the electrode ends, the value of $\frac{\partial \bar{\varphi}}{\partial y}$ on a circle being the angle subtended there by the electrode. $\frac{\partial \bar{\varphi}}{\partial y}$ is always finite and is uniform over the electrode. The effect of the slight curvature if the electrode is small and set in a curved wall is remarkably small.

The point electrode has the strongest singularity, for which $\frac{\partial \bar{\varphi}}{\partial y} = \frac{-y}{r^2}$ which is $\propto \frac{1}{y}$ on the perpendicular to the plane through the electrode and zero on the plane itself. The lines of constant $\frac{\partial \bar{\varphi}}{\partial y}$ are the limit of figure 3 as the electrode length tends to zero and are to be seen in Shercliff's original weight function (see report 2 figure 2a).

For the large electrode $\frac{\partial \bar{\varphi}}{\partial y} = \frac{1}{\sqrt{|x|}}$ on the electrode and is zero on the wall. The singularity for this case is worse than for the transverse line electrodes. In practice the use of long electrodes not only lengthens the flowmeter, but also results in reduction of output signal unless the electrodes are sufficiently short for the long flowmeter assumption to be invalid. For these reasons long large electrodes should not be regarded as practical competitors to point and transverse line electrodes.

Point electrodes, although they have a potentially bad performance, are very simple to make. In practice of course they are not points but circular discs in a virtually flat plane, a well-known problem in potential theory. The virtual current $\frac{\partial \varphi}{\partial y}$ on the disc $\propto \frac{1}{\sqrt{1-r^2}}$ (r being the radius from the centre of the disc, whose edge is at r = 1) with the typical $\frac{1}{\sqrt{}}$ singularity at the edge. On a hemisphere of radius one disc diameter, the virtual current is within $\pm 20\%$ of the value for an infinitesimal point electrode (it must average out to the same value since the flux is the same). The integrated virtual current is within $\pm 10\%$ on a similar circle: in fact the integrated current distribution is the same as for a line electrode one diameter long. This remarkable fact is true for any elliptically shaped electrode, the equivalent line electrode having the same length as the axis of the electrode perpendicular to the flow. This can easily be

seen in the case of the circle since $\left(\frac{\partial \bar{\varphi}}{\partial y}\right)_{y=0} = \int \left(\frac{\partial \varphi}{\partial y}\right)_{y=0} dz$ [where $\left(\frac{\partial \varphi}{\partial y}\right)_{y=0} \propto \frac{1}{\sqrt{1-r^2}}$ for $r < 1$, $= 0$ for $r > 1$] is independent of x, and similar formulae apply for an elliptical electrode. Marked curvature of the disc would affect the virtual current distribution both before and after integration, but not affect the essential logarithmic nature of the integrated virtual current. Slight curvature can be presumed to have little effect.

In general we may be confident that the point electrode approximation will be good far from the electrode compared with its size. Only within, say, one electrode diameter will the departure from this approximation be marked, and this will probably ease the problem of finding a suitable magnetic field.

2.5. The Effect of Various Flow Patterns

In this section we discuss, in rather general terms, whether it is possible to design the magnetic field distribution so that using either point or transverse line electrodes the flowmeter sensitivity is independent of specified classes of flow pattern, namely

a) axisymmetric rectilinear flow
b) asymmetric rectilinear flow
c) flow pattern unspecified.

The conditions on the weight vector $\underline{W}$ have already been discussed on page 7. On the simplest view the problem is to make the magnetic field ($\underline{B} = \nabla F$) small where the virtual current $\nabla \varphi$ is large, so that their product is constant. It is not in fact as easy as this since the magnetic field and virtual current are vectors with, in general, three components; the product $\underline{W}$ is a vector product and the relevant weight functions are integrals so that in some cases locally infinite values of a component of $\underline{W}$ can be tolerated provided the integral is not infinite.

Axisymmetric Rectilinear Flow

We consider here the case (a) of circular flowmeters with axisymmetric profiles and point electrodes, or equivalent schemes in other geometries when the profile depends only on one variable (e.g. flows past a wall where the velocity depends only on distance from the wall). With a uniform transverse magnetic field, which is obviously non-zero at the electrode, the axisymmetric weight function $\overline{W}'$ is well-known to be uniform, so one would not expect infinite values of $\overline{W}'$ because of the singularity at the electrodes using a non-uniform magnetic field. This is clearly shown in report 3 where the effect of shortening the magnetic field is merely to add correction terms to the value of $\overline{W}'$ for the uniform field case.

Asymmetric Rectilinear Flow

Making the asymmetric weight function $\overline{W}$ uniform is not nearly so easy, using point electrodes. Report 2 shows it is impossible using a long non-uniform magnetic field. The question is then whether the extra freedom gained by allowing the magnetic field to vary three dimensionally will make it possible. In fact the magnetic field cannot be adjusted arbitrarily at every position: it is a Laplacian field and once it, or its potential F, is specified on the surface of the flowmeter, it is specified everywhere inside. This fact is the basis of report 3 and also the reason why attempts to satisfy condition (2) on page 7 exactly are likely to be unsuccessful as there is not enough freedom in $\underline{B}$ to be able to specify it over a volume. In long flowmeter theory, specifying the magnetic field along a radius (i.e. one dimensionally) (see Baker (2b) or report 2, p.9) completely specifies it and the axisymmetric weight function $\overline{W}'$; we may plausibly expect the situation to extend to short flowmeters and to be able to arrange the distribution of the field, or its potential F, over the surface to produce a specified distribution of the asymmetric weight function $\overline{W}$. For point electrodes it now becomes necessary to make the magnetic field zero at the electrodes. The appendix of report 1 models the conditions close to a point electrode by assuming it lies on an infinite flat plane so that, in the notation of report 1, figure 5

$$G \propto \frac{1}{R}$$

the potential due to a point source, so that

$$\overline{W} = \int_{-\infty}^{\infty} \frac{1}{R^3} \frac{\partial F}{\partial \phi} \, dz \qquad (2.6)$$

There is only one non-singular magnetic field with the right order of smallness at the electrode to make $\overline{W}$ finite and the necessary symmetry, (p.13 report 1), and it happens to be two dimensional, causing the same behaviour at the electrodes as shown in report 2 figure 2a.

If we allow fields with singularities at the electrodes, the possibilities are not so obvious. It is clear from (2.6) however that if $\overline{W}$ is to be independent of ϕ , $\frac{\partial F}{\partial \phi}$ must be as well ($\frac{\partial F}{\partial \phi}$ is itself a solution of Laplace's equation). This case was also analysed on p.13 of report 1 by considering the case $F = \phi R^2 P_2^0 (\cos\theta)$ which would be the first term in the expansion of such a magnetic field that was zero at the electrode. It was found that $\overline{W}$ was an integral diverging logarithmically as $\frac{z}{r} \to \infty$. This difficulty has been glossed over in the appendix since the expansion is not valid for large z: it suggests however that $\overline{W} \sim \log r$ for small r (and not constant as stated in the appendix).

In order to clarify the situation suppose $\frac{\partial F}{\partial \phi}$ is the same as the potential due to a ring of radius c and charge Q , whose axis is the z-axis, and whose centre is the origin in figure 4. This is an axisymmetric solution of Laplace's equation that goes to zero at ∞ ; on the z-axis it is $\frac{Qc}{4\pi\sqrt{z^2+c^2}}$ and may be expanded around the origin (for $R < c$) as

$$\frac{Qc}{4\pi c}\left[1 - \frac{R^2}{2c^2} P_2^0(\cos\theta) + \frac{3}{8}\cdot\frac{R^4}{c^4} P_4^0(\cos\theta) + \ldots\ldots\right] \qquad (2.7)$$

which may be written as

$$\frac{Q}{4\pi c}\left[1 + \frac{r^2 - 2z^2}{4c^2} + \frac{3}{8c^4}\left(z^4 - 3z^2r^2 + \frac{3}{8}r^4\right) + \ldots\ldots\right] \qquad (2.8)$$

The resulting $\overline{W}$ (found from (2.6) and (2.8) by expanding the elliptic integral) is:

$$\frac{Qc}{2\pi r^2 c}\left[1 + \frac{r^2}{2c^2}\left(1 - \log\frac{4c}{r}\right) + O(r^4)\right] \qquad (2.9)$$

We may superimpose these fields for different values of Q and c. We find

$$\overline{W} \propto \left[\frac{1}{r^2} \sum_c \frac{Q_c}{c} + \left(1 + \log \frac{r}{A}\right) \sum_c \frac{Q_c}{c^3} + \sum_c \frac{Q_c \log c}{c^3} + O(r^2) \right] \tag{2.10}$$

We see clearly now that it is not sufficient to suppress the first term in (2.10) by choosing $\sum_c \frac{Q_c}{c} = 0$, we must also choose $\sum_c \frac{Q_c}{c^3} = 0$ to suppress the logarithmic singularity: in general $\sum_c \frac{Q_c \log c}{c^3} \neq 0$ so that $\overline{W}$ would have the desired uniformity near the electrode. This behaviour is due to the field far away from the electrode since the order of smallness of the magnetic field near the electrode now more than cancels out the singularity of $\nabla \varphi$.

Put another way, the magnetic field component $\frac{\partial F}{\partial \Phi}$ on the axis is

$$\frac{Q_c}{4\pi} \frac{1}{\sqrt{z^2 + c^2}}$$

Taking $\frac{1}{R^3} \equiv \frac{1}{z^3}$, if we ignore the misrepresentation at the origin, the resulting weight function $\overline{W}$ is

$$\frac{Q_c}{4\pi} \int_{-\infty}^{\infty} \frac{1}{\sqrt{z^2 + c^2}} \frac{dz}{z^3}$$

and it is seen by expanding $\frac{1}{\sqrt{z^2 + c^2}}$ as a power series for small z/c that $\sum \frac{Q_c}{c}$ and $\sum \frac{Q_c}{c^3}$ must be zero to make the integral finite.

Unfortunately it is not possible to suppress the magnetic field at the electrode and make the distant field responsible for $\overline{W}$ using non-singular magnetic fields since $\frac{\partial F}{\partial \phi} = 0$ on the z-axis for these.

The implications of this piece of analysis (which is a rather inferior existence theorem) are that the magnetic field coils shown in report 1 figure 6a will produce an asymmetric weight function $\overline{W} \propto \log r$ at a point electrode. The coils necessary to make $\overline{W}$ uniform would, from (2.7), be the lines of constant $R^{2n} P_{2n}(\cos\theta)$, for $n \geq 2$, not $R^2 P_2(\cos\theta)$, and would have at least five, not three, branches either side of the z-axis. The conclusions about the possibility of achieving uniform $\overline{W}$ with point electrodes are unaltered; it is

not possible near the electrodes unless the coils are so close that they approximately produce a magnetic field with a singularity along the z-axis through the electrode. While the suggestion, made on page 13/14 of the first report, that $\overline{W}$ be made 1 on the wall and -1 on the radius is possible, I am inclined now to think it a bad one since if we have to assume that the velocity profile depends only on distance from the wall in the electrode region there are many other possibilities.

In practice the departure of $\mathcal{G}$ from the formula $\frac{1}{R}$ assumed in order to examine the singularities of $\overline{W}$ will have an effect but only far from the electrode. So will small circular electrodes, at which the magnetic field should be small but finite, since under these conditions the integrated version of the virtual current is relevant and for a circular electrode we have already seen this is large, but finite.

There is always the possibility, too, that even with coils and iron sheath very close to the electrodes, unwanted magnetic fields could occur, since we cannot control the normal component locally: it is controlled by conditions elsewhere. The only harmful field (using the relevant symmetry) is the non-singular one we have mentioned before on page 14.

It would be better to regard the above analysis in the same light as on page 14 of report 1: suggesting what coil shapes to try, but relying on the precise analysis of report 3 for calculating the coil performance.

Flow Pattern Unspecified

Page 12 report 1 shows that an ideal flowmeter (insensitive to any flow pattern) cannot be achieved with point electrodes. On page 6 a class of ideal flowmeters is described, a simple rectangular one with transverse line electrodes being shown in figure 1 of that report. If this rectangle is distorted into a circular pipe the electrodes become quadrants as in figure 4b of that report and we may hope that its ideal performance in a uniform field is not too

impaired. Report 2 computes $\overline{W}$ for such a meter using a uniform field and a non-uniform long field for different electrode angles (figures 2c, 2d and 2e). The non-uniform field gives very good results, especially for electrodes rather larger than quadrants and there is every hope that there will be some practicable short magnetic fields that will make this meter a very good approximation to an ideal meter in a circular pipe. Fortunately the virtual current can be calculated by the same sort of formulae as for point electrodes on page 6 of report 3 since the boundary condition on the virtual current potential φ on the line electrode is $\frac{\partial \varphi}{\partial n} =$ δ-function (suitably normalised) and $\frac{\partial \varphi}{\partial n} = 0$ everywhere else; that is, there are no mixed boundary value problems.

3. THE WORK OF OTHERS

The work of Shercliff and Baker has already been referred to in the introduction. Shercliff's book (8a) summarises the state of the art in electromagnetic flowmeasurement (including liquid metals) in 1962 while Baker's work was the immediate background to my own. Other people in this country, such as Mills and Wyatt, are well-known in the field of blood flowmetering and experts on the electronics and the practical side of head design.

In this section the theoretical work of some people abroad is discussed.

3.1. H.KANAI

H. Kanai has been working on electromagnetic blood flowmeters in Japan since about 1960, particularly on the problem of asymmetric and pulsatile flows. He is at present (1969) on leave at the Bockus Research Institute in Pennsylvania.

His work has been published in a number of Japanese journals and he is about to publish an account in English, probably in "Medical and Biological Engineering". We have copies of his papers, including an advance copy of the English one (4) which appears to contain a synopsis of his Japanese work. The remarks below are based on correspondence with him and his English paper, since we have not been able to translate his Japanese work.

The English paper starts with a two dimensional solution of the flowmeter equation (2.1) for a flowmeter with point electrodes and a conducting wall, using Green's functions which he finds by matching solutions via the usual boundary conditions. (He does not use complex

variable methods). The result is expressed as a weight function ($W_y B_x + W_x B_y$) on V(x,y) the streamwise velocity, where he now assumes the wall conductivity zero to avoid intractable expressions. (W_x, $-W_y$) agree with the components of the virtual current $g'(z) = \frac{i}{z^2+1}$ (page 8 report 2). He defines a function equivalent to the axisymmetric weight function W', normalised for a given non-uniform field so that the signal for a parabolic velocity profile is one.

He then defines a function $\mathcal{E} = \sqrt{2\int_0^1 (1-W'^2) r\,dr}$ (in our notation), essentially the root mean square departure of W' from 1, and discusses flowmeters with three types of air-cored coil: (a) infinitely long rectangular coils, (b) Helmholz-type coils of varying proportions, (c) short curved rectangular coils lying on the flowmeter wall. Although he admits the need for a proper three dimensional analysis with short coils, he uses the above (W_x, $-W_y$) with the actual magnetic field components (B_x, B_y) in the electrode plane, to make some allowance for the short coil lengths (which appear to be about one internal diameter).

Graphs of $\mathcal{E}$ against various coil parameters suggest which coils have an approximately uniform W'. He also calculates the sensitivities for different axisymmetric profiles. These agree with the experimental results obtained by observing the change in sensitivity when the flow changed from laminar to turbulent to within 1 to 3% for different coils, not bad considering the theory does not take account of end shorting. Normally the error in applying strict long flowmeter theory to short flowmeters becomes noticeable when the coils are shorter than twice the flowmeter internal diameter . The experimental results seem to agree with those of Clark and Wyatt (3) in predicting that a rectangular coil subtending a half-angle of approximately 55° at the centre of the flow-meter gives no change of sensitivity as the Reynold's number increases, when the coil length is approximately one diameter.

Kanai then considers the case of axisymmetric pulsating flow under a sinusoidally time dependent pressure gradient. He predicts the velocity profiles whose shape depends on the frequency and finds

the calculated sensitivities vary in size with frequency by 6% or more (as well as in phase), though this can be reduced to 1% by using the rectangular coil mentioned before.

He then measures another pulsatile flow with nett flow using different coils, first measuring the flow rate as a function of time with the different coils and then, Fourier-analysing the observed flow rate as measured by a uniform field (Helmholz) coil, he predicts what the performance of the other coils should be. He finds that the behaviour of a 45° rectangular coil is almost indistinguishable from a Helmholz coil, and says that the effect of high harmonics (in time) are important by which he means, I think, that he has ignored them and hence his predicted flow rate graph is less sharp edged than the measured one.

Finally he calculates a weight function W for asymmetric flow, as set up in a tube bent in a large radius of 10 to 30 pipe diameters, using the velocity distributions measured by Adler (whose paper I have not read) to predict the sensitivity for different coils orientated at different angles to the plane of the bend, called the setting angles. He also defines another $\varepsilon \propto \sqrt{\frac{1}{S}\int (1-W)^2 dS}$ as a measure of flowmeter behaviour, and finds that for no coil is it anything like zero, (see report 2, page 7: there is little hope of making W uniform for a long meter with point electrodes). He ignores the swirl (which I believe will produce no signal, see page 26) though he admits it ought to be discussed. His calculations show the change in sensitivity with setting angle for different coils, and his experiments the change with Reynolds number for a uniform field and 45° coil at different setting angles. The results agree with the calculations except, as he notes, the experimental variation of sensitivity of the Helmholz coil with Reynolds number is larger than predicted.

The general impression given is that the analysis, despite its two dimensional nature, by and large predicts the experimental results to within about $\pm$ 2%, though in some cases the weight function normalisation does not seem to be clear, since the laminar profile sensitivities are not always unity (which they should be on his definition).

Kanai seems to be unsatisfied with the experimental results since he says in a letter "the experimental results are not in good agreement with the theoretical results". All the calculations seem to use numerical integration at some stage. He appears also to have decided against using iron-cored circuits and does not think it is possible to design a desirable magnetic field from the weight function which could imply that, like me, he prefers to analyse the weight function for fields that can be easily manufactured. In private correspondence he also says that he does not think it is possible to design a coil to produce a desirable magnetic field which has been calculated from ∇G .

3.2. RUMMEL AND KETELSEN

In the last few years Ketelsen, of Fisher and Porter in Göttingen and Rummel, at the Technical University of Hanover, have developed a new range of electromagnetic flowmeters using diametrically opposed point electrodes and deliberately short non-uniform magnetic fields. They have described their work briefly in some papers and also taken out a number of patents. Their work has two main features.

First a description of how the flow at any position in a flowmeter contributes to the signal in terms of a weight function which they compare with Shercliff's and second the definition of a range of coil shapes and iron circuits which will produce the necessary non-uniform field. They claim that the change in sensitivity of their new flowmeters when exposed to different flow patterns is at least ten times less than with the old uniform field meter with the same flow.

While the idea of using a deliberately non-uniform field is undoubtedly a good one one must feel a certain reservation about the theoretical side of their work because none of the papers or patents that we have seen show any sign that the weight function is a vector, not a scalar. Their weight function is, in our notation, the virtual current component $\frac{\partial G}{\partial y}$ (figure 5) parallel to the electrode axis and they appear to take

$$W_z = B_x \frac{\partial q}{\partial y}$$

and ignore the other components of $\underline{W}$. In fact from (2.5)

$$W_z = B_x \frac{\partial q}{\partial y} - B_y \frac{\partial q}{\partial x}$$

showing that both transverse magnetic field components must be taken into account and there are other components of $\underline{W}$ as well, though these do not affect rectilinear flow in which only V_z is assumed to exist.

One further point is that in their earlier work they took $W_z = f(z)$ as the condition on $\underline{W}$ for asymmetric rectilinear flow, and only in their later work, e.g. (6c), do they point out the sufficiency of making $\overline{W} = \int_{-\infty}^{\infty} W_z \, dz$ a constant (see page 9). It is not clear on which principle their flowmeters are designed.

There are other more minor criticisms which stem however from the assumption that the weight function is a scalar.

Their method of finding $\frac{\partial q}{\partial y}$ is unspecified, except that it is an analog method. It might, for example, have been found by measuring the electric field set up by imposing a voltage across the electrodes or by placing an electric dipole suitable oriented (i.e. a probe with twin points maintained at different voltages) and measuring the voltage across the electrodes. Both methods are mathematically equivalent, though they do not say they have used either.

They found that the plots of constant $\frac{\partial q}{\partial y}$ (which is proportional to W_z in the case of a uniform field B_x = constant, $B_y = 0$) differ from Shercliff's original plot even in the electrode plane which one would expect since their's takes account of the three dimensional variation of the virtual current while Shercliff's is essentially two dimensional and is the virtual current produced by line electrodes of infinite length in the flow direction. For reasons given on page 5 of report 1 (or page 3, report 2) Shercliff's is valid for point electrodes provided the magnetic field and velocity profile do not vary in the flow direction, since the z-integration in the volume

integral (2.1) then only affects the three dimensional virtual current yielding Shercliff's two dimensional virtual current. Indeed Rummel and Ketelsen (6a) found that such integration, presumably numerical, of their virtual current gave Shercliff's weight function, which it ought.

Their plot of $\frac{\partial G}{\partial y}$ in the electrode plane (6a and 6b) demonstrates an essential difference between the three and two dimensional virtual currents: that, if d is the distance from an electrode, as we approach an electrode along the radius $\frac{\partial G}{\partial y} \sim \frac{1}{d}$ in the two dimensional case and $\sim \frac{1}{d^2}$ in the three dimensional case.

There is not sufficient information in the published work that we have seen to say more about the theoretical side of their work. They do not say, for instance, how they calculated the necessary magnetic field. In private correspondence they have indicated that they feel analytical solutions are of only limited use, so it may be that their methods were numerical or involved some sort of analog for the magnetic field as well as the virtual current.

3.3. V.I. MEZBURD

Mezburd is working at Tallinn, in Estonia, on the design of industrial flowmeters with short fields. I met him at Riga where we discussed the analytical formula of the virtual current ∇G (report 3, page 16), and the best condition on $\underline{W}$ for asymmetric rectilinear flow. At the moment he is measuring ∇G by injecting dipoles into a flowmeter at different orientations. His magnetic field is predicted (numerically I think) from the weight function and then suitable coils are found, mathematically and experimentally, that produce this field. His work is not yet finished.

He is also experimenting with the case where a flat piece of non-conducting material is placed perpendicular to the flow at different stations, partially blocking the flow. He finds considerable changes in sensitivity, using a uniform field and point electrodes, as one might

expect (private correspondence).

3.4. L.M. KORSUNSKII

In 1964 Korsunskii published a book called "Electromagnetic Liquid Measuring Devices", (5), drawing on work inside and outside the U.S.S.R. up to the early 1960's. (60% of the 200 references are non-Soviet). The book, of course, is in Russian but appears to have a fairly comprehensive coverage, including a certain amount of electronic circuitry, though the sections of liquid metal flowmeasurement will have been superseded by the booklet produced by the Latvian Academy of Sciences (10). We had difficulty getting hold of Korsunskii's book until Mezburd gave us a copy at Riga.

A section of particular interest has been translated; it concerned rectangular flowmeters with a uniform field and large well conducting electrodes parallel to the field. Korsunskii refers to the work of Arnold (1) which described a meter with long rectangular electrodes (Arnold's analysis did not consider the effect of the circulating currents) and also to Thürleman who, Korsunskii says, considered the case $\underline{v} = [0,0,v(y)]$. Korsunskii's analysis as given in his book assumes $\underline{v} = [0,0,v(x,y)]$ with large electrodes and $\underline{v} = 0$ on the walls. Apparently Holdaway solved this case as well. Korsunskii describes some experiments measuring the sensitivity variations of the meter for different Reynold's numbers and with plates perpendicular to the flow partially cut away in various patterns. He does not say if the plates are conducting or insulating nor does he give any dimensions, but the electrodes appear from the figures to be about one channel height long and the obstructing plates two channel heights up stream. The variation of sensitivity appears from his table of results to be well inside $\pm \frac{1}{2}\%$.

He shows no sign of realising that the meter can be generalised to include any velocity distribution and electrode system invariant in the magnetic field direction (as described in report 1, page 7),

though he does note that an essential feature of his flowmeter is that the electrodes are long in the field direction, pointing out that point electrodes will not do. One would suspect that with some of his flow disturbers his condition $\underline{v} = [0,0,V(x,y)]$ would be flagrantly violated. His experiments would then confirm that $\underline{v}$ may be arbitrary (subject only to div $\underline{v} = 0$).

4. SHORT SUMMARY OF THE THREE REPORTS

4.1. The first report sets the idea of a weight function on a sound mathematical basis, proving equation (2.1) for $\underline{W}$. The conditions on $\underline{W}$ for ideal flowmeters are proved (pages 5, section 2.1. and 8, section 4.1) and devices that can be used as simultaneous valves and flowmeters described (p.6, section 3). The end of section 4.1. (page 9) examines the conditions under which swirl is likely to affect a flowmeter signal.

More may be said regarding swirl than section 4.1. suggests. We consider flows not varying in the flow direction. Such swirl would occur, for example, in flow through a curved pipe, though there it would be called secondary flow. Whatever the motion in planes perpendicular to the flow it will contribute nothing to the signal in a meter with symmetry about the electrode plane (i.e. F and G even in z), because the components of $\underline{W}$ in these planes are odd in z, (see figure 5 for notation)

i.e.

$$\left[W_x , W_y\right] (x,y,z) = - \left[W_x , W_y\right] (x,y,-z)$$

whereas

$$W_z (x,y,z) = W_z (x,y,-z)$$

This swirl's contribution to the e.m.f. upstream is cancelled out by its contribution downstream. However if the swirl varies in the streamwise direction it may in general contribute to the signal.

Section 4.2. describes certain types of flowmeter which, although of limited practical interest, are ones which, instead of having a short electrode system and long magnetic field, have long electrodes and a short field. The last paragraph of this section is misleading. The approximation is similar, not the same, and in fact leads to a

different $\underline{W}$ and $\overline{W}$ because the two flowmeters are not dual in the sense of page 4 (last line but one). $\overline{W}$ for quadrant electrodes and a plane magnetic field is the same as in report 2 figure 2b first drawing, and for (quadrant) transverse line electrodes and a uniform field figure 2c, first drawing.

The appendix to this report is mainly concerned with the analysis of the behaviour of $\underline{W}$ and $\overline{W}$ near point electrodes (see page 13 in the thesis).

4.2. The second report deals with long flowmeters, the assumption being that neither the magnetic field nor the virtual current vary in the flow direction. The analysis is based entirely on the use of complex variables.

Some general remarks on the necessity for a uniform field or virtual current for axisymmetric profiles and both for asymmetric profiles are proved first. Next the not very fruitful cases of rectangular and square flowmeters using point electrodes are analysed. Then the case of circular flowmeters, using three types of electrode: point, long quadrant, and transverse line (using the integrated virtual current), all with suitable non-uniform (long) fields as well as uniform ones. The transverse line electrodes have the best performance.

Next some rather artificial methods of making the virtual current uniform are discussed and finally the performance of external flowmeters, which have the electrodes on the outer surface and the magnetic field windings inside, is analysed.

4.3. The third report is concerned with design of circular flowmeters with diametrically opposed point electrodes, in which the magnetic field is produced in a technologically simple way, described on pages 3, 4 and 5. The weight functions $\overline{W}$ and $\overline{W}'$ are analysed (pages 6, 7 and 8) and a set of design tables for $\overline{W}'$ explained in some detail, pages 9 - 15.

A specimen of these tables is shown in figure 4 of the report, but it should be noted that in later versions of these tables the last three tables are multiplied by a factor $\frac{4}{\pi}$ to enable a direct comparison with the first one to be made.

Since there had been some uncertainty about the values of the virtual current ∇G in such a flowmeter, on pages 16 - 19 analytical formulae are given for it and numerical values computed from these for the fall off of ∇G up and down the flowmeter axis. The formulae, at any rate in the form given there, are not immediately suitable for finding ∇G everywhere in the electrode plane.

5. EXPERIMENTAL WORK

Of the theoretical work summarised in the preceding sections the axisymmetric design tables and the combined valve and flowmeter are most likely to be of direct practical use. Some experiments to check the predictions were done.

Since there had also been some uncertainty about the value of the virtual current for point electrode meters some simple measurements of it were made which are described in section 5.5.

5.1. Apparatus

However, before describing these experiments we set out the reasons for our choice of flowmeasuring system. It was as simple as possible: a single flow loop with experimental flowmeter, master flowmeter, pump and reservoir tank in series. If accurate results are required, around 1% say, one of the main difficulties is to find a suitable master flowmeter. Positive displacement pumps may be used or time taken to fill a known volume can be measured, but even if accurate flow measurement can be achieved accurate measurement of the coil currents and flowmeter signal is also necessary and absolute electrical measurements in a laboratory with few standards are surprisingly difficult to make. We decided to tolerate poor absolute accuracy, but to design the system so that a comparison between two sensitivites could be made to an accuracy of better than 1%, using the master flowmeter to ensure only that the same flow rate had been achieved in both cases.

A schematic diagram of the flow circuit is shown in figure 6. Construction was generally in P.V.C. pipe 3" ID, $3\frac{1}{2}$" OD, and the experimental flowmeters were built into 2 foot lengths of pipe with flanges for easy interchangeability. A British Standard Venturi and U-tube manometer were used as the master flowmeter (the bubble clearing system is not shown in the diagram). In practice the flow rate was adjusted till the manometer reading H was only approximately the same, in the region $85 < H < 100$ cms.

Assuming that the square root law was accurate over this range, and allowing errors of $\pm$ 0.1% cm at each end for measuring would allow a repeatability of $\pm$ 0.1%, provided allowance was made for the variation of viscosity in the liquid as the temperature rose because of heat dissipated in the pumping. Using the British Standard Venturi corrections for viscosity variation, and assuming copper sulphate solution (used for reasons given later) and water have the same rate of change of viscosity with temperature (and after allowing for the change in density due to temperature) the correction required was to increase the manometer reading of 0.5% as the temperature changed from 20°C to 30°C. This covered normal working conditions and the correction was assumed linear between these temperatures. In practice it was rarely required.

The magnetic field coils were supplied with currents in the range of 2 to 8 amps from a Variac transformer run off the 50c/s mains and connected by a current transformer to a Kent Veriflux Mark II converter. This electronic device produces a current (in the range 0 to 20 mA) proportional to the flowmeter output voltage component in phase with the magnetic field current divided by this current, thus removing the effects of variations in the current supply and the out of phase voltages induced in the flowmeter $\left(\frac{\partial B}{\partial t}\right)$. The output signal of the valve/flowmeter was a few millivolts rms but of the circular flowmeters initially only about 50 μV rms, and later 100 μV when the pump capacity was increased raising the mean velocity to 5 ft/sec. Since this was well below the recommended signal voltage for the Veriflux, the voltage was boosted by inserting a 10:1 step up transformer (the same as the step-down transformer in the first stage

of the converter) and the impedance matched by replacing the stainless steel electrodes and tap water by copper electrodes and 4% copper sulphate solution. The impedance between the $\frac{1}{4}$" diameter electrodes ranged between 500 and 200 ohms, depending on how recently the electrode surface had been cleaned: this was done by passing a D.C. current between the electrodes and the (single) earth, a copper gauze suspended in the tank.

The input impedance of the Veriflux is 20. 10^6 MΩ and 1000 H. Ignoring any capacitive impedance of the electrodes, as long as their resistive impedance is maintained at 200 Ω a drop in signal of 0.1% will be introduced. We cleaned the electrodes before each test, checked their impedance, and ignored this drop. We later found that the system was also partially earthed by the pumps, but this extra earth seemed to make no difference.

The flowmeter output signal, after the 10:1 step up transformer, and the reference voltage from the current transformer were monitored continually on a large Tektronix dualtrace oscilloscope whose most sensitive range using the A.C. differential amplifier was 10 μV/cm peak to peak. In general we found there was a small inphase voltage at no flow of up to 1% of full flow signal compared to the value obtained by shorting the input to the step-up transformer. This could be lessened by electrolytic cleaning of the electrodes and the zero was checked after the end of each run.

Another effect removed by cleaning the electrodes was the mechanical modulation of the large D.C. voltages (a fraction of a volt with different materials) between the electrodes and ground when the pumps were running. The correlation between the wave-form of this effect on the scope and the main valve when chattering at different frequencies was excellent.

One other trouble was random jumps in the Veriflux of some 5% of full scale deflection which was cured by changing some of the circuit boards.

The D.C. current output from the Veriflux (0 - 20 mA) was passed through a 500 Ω resistance ($\pm$ 0.2% standard) and the voltage measured

on a digital voltmeter. Oscillations in this voltage reading due to flow pulsations were damped out by putting a 5 - 15,000 μF condensor across the resistance. At one time we used a stopwatch to time an electrical relay counter operated by the Veriflux which gave very repeatable results ($\pm$ 0.1%).

We found that in the range we were working a variation in the supply current of 10% made a change in zero reading on the digital voltmeter of 0.4%, but the supply current was kept constant to better than 1% using an Avometer so this effect was small. A variation in quadrature of 10% of the main flow signal caused a 0.3% change in the voltmeter zero reading. This may have been because the quadrature was not strictly out of phase: it was only checked on the oscilloscope. For test purposes we ensured that the quadrature was the same before and after a run.

Even keeping the coil current and quadrature constant, we found unexplained variations in zero reading and full flow reading on the digital voltmeter of up to $\pm$ 0.1%. For this reason the increase in voltage output ΔV caused by the flow can be relied on to $\pm$ 0.2% and combined with the manometer error gives the sensitivity

$$S = \frac{\Delta V}{\sqrt{\Delta H}} \qquad (5.1)$$

to $\pm$ 0.3%. The ratio between two sensitivities should therefore be accurate to $\pm$ 0.6%. Though we expect a sensitivity repeatability to be within $\pm$ 0.3% it was normally better than this, except for the canvas pipe, and the results quoted are averages with their limits of repeatability. This definition of sensitivity in (5.1) is inversely proportional to the nominal setting of the Veriflux (quoted in mA/ft/sec), which was adjusted to make the flow signal nearly full scale.

We also made some absolute measurements. The venturi was calibrated to $\pm$ 5% using a tank and stopwatch, the current transformer to $\pm$ 2% using an Avometer which we had made some attempt to calibrate, and the output signal of the flowmeter calculated from the digital voltmeter reading, for which allowance must be made for the accuracy of the input impedance of the Veriflux (81 $\pm \frac{1}{2} \Omega$) and the standard

resistance on the D.C. output (± .2%). In all this gives a total absolute accuracy in the region of ± 8%, apart from flowmeter manufacturing errors.

5.2. Artificial Velocity Profiles

Before we move on to describing the flowmeter construction and experiments in detail, there is one outstanding experimental problem.

With the chosen experimental system we must not only compare the sensitivities of two different flowmeters using normal turbulent flow in a pipe, but also check the variation of sensitivity with change in profile. We cannot vary the flow rate to achieve laminar flow since the measurement system does not allow it, nor can we artifically increase the viscosity, with treacle or cellulose for example, since this is messy and would upset the calibration of the venturi. Some other method of creating artificial profiles must be found.

A plastic plate was tried first, bolted in front of the flowmeter flange (4 diameters upstream) and drilled with axisymmetric rings of small holes and one large central one. The resulting profile was measured using a pitot tube and inclined manometer. The aim was to reproduce a parabolic profile at the flowmeter cross-section although the flow was turbulent, by drilling out the rings by trial and error. We did not achieve this as we could not remove the jet-like point of inflexion in the profile: the variation in the profile along the flowmeter was large, too, and rather non-linear.

Following others, we then tried placing an axially disposed canvas tube in the flowmeter and pumping liquid through it, to get a "top hat" profile whose rounding off could be estimated from standard pipe flow profiles. Liquid soaked canvas will upset the sensitivity by an amount depending on its conductivity compared to that of the liquid. This conductivity factor depends on the geometrical structure of the material, not the liquid. If a thin walled canvas tube of thickness t, diameter d and conductivity factor λ , is set concentrically in a

flowmeter of diameter D the sensitivity S is given by

$$\frac{1}{S} = 1 + \frac{2t}{d}\,\frac{(1-\lambda)\left[(1-\lambda) - (1+\lambda)\left(\frac{d}{D}\right)^2\right]}{2\lambda} \qquad (5.2)$$

for axisymmetric flow in the canvas pipe in a uniform magnetic field.

The thickness of canvas material t in our experiments was .025", d = 1.8", D = 3.0". The sensitivity in (52) is plotted in figure 7 for this case, from which it can be seen that there is a region $.47 < \lambda < 1.0$ in which the presence of the canvas pipe actually increases the signal slightly (which we might expect: for example a thin wall of high resistance at d = D simply makes the flowmeter smaller and thus increases the signal: having such a wall inside introduces another effect; a drop in output voltage due to the increase in resistance experienced by the currents passing across the wall. These two effects compete with each other). We had hoped that the canvas pipe conductivity would lie somewhere in this range: in fact it was smaller. Dr.Wyatt kindly measured the conductivity of a canvas sample prior to prolonged immersion in copper sulphate solution and found $\lambda = 0.10$. There are indications however that the immersion may alter λ: in practice the drop of sensitivity in our experiments (where end-shorting is important) due to the canvas was in the region of 4%, though the results were not repeatable to better than 1%. This would indicate a value of λ near 0.15, $\lambda = 0.10$ giving a drop of 6%, though the analysis in (5.2) of course does not allow for end-shorting.

Since the canvas tube caused errors well above the intended experimental accuracy ($\pm$ 0.2%) we decided to use the original idea of the plate as well, but abandoned the hope of achieving an artificial parabolic profile and simply drilled a hole in the centre of a piece of $\frac{1}{2}$" thick P.V.C. with quarter-round edges on the entrance side, sufficiently large to let the required flow through (1.3" diameter) and measured the profile, which is shown in figure 8 and table 1. The shaded area at the edges represents uncertainty about the velocity at the wall and numerical predictions of sensitivity using the

predicted weight function distribution are made for both cases, hence the two figures in table 3 for the predicted sensitivity using the plate. The formula for sensitivity for a circular flowmeter used was:

$$S = \frac{\int_0^1 \bar{W}'(r)\, v(r)\, r\, dr}{\int_0^1 v(r)\, r\, dr} \qquad (5.3)$$

This was calculated using Simpson's Rule and dividing the range into ten segments (i.e. using Simpson's Rule five times). The numerical error when $v(r) = 1 - r^7$, representing a fairly sharp fall away at the profile edge, was .05%. The predicted $\bar{W}'(r)$ was taken from an earlier version of the tables in which a factor $4/\pi$ had been left out. This factor has to be included in order to compare the performance of a flowmeter with coils carrying a certain current and the same meter with the uniform field produced by the same Amp-Turns spread over the diameter.

These three profiles:

(a) Normal turbulent flow: figures taken from Shlicting (7), $Re = 15 \times 10^4$

(b) Flow through 1.3" diameter hole in plate 12" upstream

(c) Normal turbulent flow in the canvas pipe 1.8" diameter,

were used for testing each experimental meter and are shown in figure 8 and table 1. The results using the uniform field produced by the magnet in figures 9 and 10, for which there should be no change of sensitivity, showed (table 2) a drop of 1.1% with the plate and a drop of 6.3/7.5% with the canvas tube compared to normal flow. We cannot really estimate the canvas conductivity from this since the field is obviously not uniform enough so that part of the drop is due to the change in profile: all we can say is that a figure in the region 2 - 5% due to the canvas alone does not conflict with the evidence.

Table 1 - Velocity Profiles

Radius (wall ≡ 1.0)	Normal Turbulent Profile $Re = 15 \times 10^4$ (Schlicting)	Flat Plate Profile	Canvas Pipe Profile Wall radius 0.6
0	1.00	1.00	1.00
0.1	0.99	0.99	assumed same
0.2	0.98	0.965	profile as
0.3	0.97	0.93	first column
0.4	0.96	0.88	
0.5	0.94	0.82	
0.6	0.90	0.76	0.43
0.7	0.86	0.695	
0.8	0.82	0.63	
0.9	0.74	0.56	
1.0	0.43	0.45/0.30	

Notes: Explicit calculation showed that the slight variation in profile due to changing Reynold's number affected the predicted sensitivity for the normal turbulent profile, since the weight function distribution was highly non-uniform but did not affect the canvas pipe sensitivity appreciably since the weight function in $0 < r < 0.6$ was much more uniform. The increase of Reynold's number for the same flow in the smaller canvas pipe was therefore ignored, hence the third column of this table.

Table 2 - Canvas Pipe Behaviour

1. Circular Flowmeter with Approximately Uniform Field

	Normal Profile	Plate Profile	Canvas Pipe
Sensitivity	$929\frac{1}{2} \pm \frac{1}{2}$	$919\frac{1}{2} \pm \frac{1}{2}$	860/871
% change	reference	-1.1%	-7.5/6.3%

2. Valve/Flowmeter with same field (in the fully open position)

	No Obstruction	Canvas Pipe
Sensitivity	$958\frac{1}{2} \begin{smallmatrix} + \frac{1}{2} \\ - 1 \end{smallmatrix}$	$931/947\frac{1}{2}$
% change	reference	-2.9%/-1.1%

5.3. Circular Flowmeter with Point Electrodes: Experiments

A diagram and photograph of one of these flowmeters is shown in figures 11 and 12. The electrodes were set diametrically opposite each other in the centre of a two foot length of perspex pipe 3" I.D., $3\frac{1}{2}$" O.D. (nominally) and connected to the Veriflux using electrostatically screened internally twisted cable set in grooves in the pipe surface. Quadrature was adjusted by tying a piece of string to the longer of the electrode leads and pulling it to and fro in a suitably placed groove.

At first the electrodes were recessed in order to reduce the in-phase signals due to eddy currents entering them across a layer of non-uniform contact capacitance (Wyatt 9b) but after disagreement between the measured and theoretical signals of a few percent, it was thought that this might be due to fluid eddies in the recesses and the non-uniformity of the magnetic field there. These recesses were therefore removed by using flush fitting copper electrodes, but the errors still persisted and were finally traced to the canvas tube which had been used for creating artificial velocity profiles (page 34).

The pipe was screened with aluminium foil over the central 6" section and the magnetic field coils were set in an outer plastic pipe, 1 foot long, split into two halves for assembly. Thin paper was used for insulation where necessary, and one or more layers of transformer iron .013" thick by 1 foot long were wrapped around the flowmeter and held in place by jubilee clips.

Three sets of magnetic field coils and suitable outer plastic pipes and positioning pieces were made, all 0.2" (nominally) deep in the radial direction. The first two sets were single pairs of rectangular coils, made to check the sensitivities predicted by the tables. Their mean dimensions were 3" (one diameter) long, subtending 30° at the flowmeter centre line, and $\frac{3}{4}$" (one quarter diameter), subtending 90°. Each was wound with shellac-insulated copper wire, of 0.020" diameter with 100 turns in a cross-section 0.2" square. For both these sets the output voltage was in the region of 100 μV rms and the coil current 2.00 amps.

The third set of coils was a double pair, designed to have a uniform axisymmetric weight function. The coils were considerably larger in area, the first having nominal dimensions 3" long (one diameter) subtending 168° with 50 turns, the second 2¼" (¾ diameter) subtending 84° with 295 turns. Both were wound in the same wire as before to the same depth of 0.2", ten layers deep. In practice the dimensions were different and were not easy to measure accurately. The predicted weight function was based on the actual coil size, not the design size, and is non-uniform for that reason. The coil current had to be reduced to 1.70 amps to avoid over-heating.

With the single coils only one layer of transformer iron was thought necessary. Tests showed that the leakage field was about 0.7 gauss (far from sinusoidal) over the coils and much less elsewhere, compared to a typical field of 56 gauss which the coil currents (200 turns with 2.0 amps i.e. 400 Amp-Turns) would maintain over the diameter (approximately 10 cms between the iron) if the field inside was uniform. In practice the iron layer covered the pipe surface nearly twice and the gap was kept away from the region of high flux density.

With the twin coil flowmeter the total current was 690 turns at 1.70 amps or 1170 Amp-Turns, that is some three times higher. The same iron sheath 12" long and nearly twice round was used, and a piece 6" long was added to increase the depth to 5 layers in the centre. The leakage flux was now approximately 0.8 gauss over the coils. The flowmeter signal, which had been around 100 μV rms for the single coil meters, was now around 1.1 mV rms, this improvement being due partly to the increase in Amp-Turns, and partly to the increase in coil size.

The leakage field due to the finite value of the iron permeability indicates a drop in the flowmeter absolute sensitivity in the order of 1%. This drop is unlikely to be important when comparing the sensitivities of two profiles and cannot be detected in our experiments because of the very poor absolute accuracy. Another factor affecting the value of the absolute sensitivity is the accuracy of the coil manufacture. For a single coil flowmeter the ratio between sensitivities is only slightly affected by small manufacturing errors, but the

performance of the twin coil flowmeter depends on the sum of the absolute performances of its two coils, which were difficult to measure accurately after manufacture. Absolute errors here will affect the shape as well as size of the final weight function distribution.

The results for all three flowmeters, predicted and experimental, are given in table 3. It can be seen that the predicted weight function for the coils in the twin coil meter are very different and any error in the proportions which they contribute to the final signal has a marked effect on the final weight function. In my opinion this entirely accounts for the discrepancy between predicted and observed performance, especially in view of the accuracy to which the theory predicts the observed performance of the single coil flowmeters. Assuming a sensitivity drop solely due to the presence of the canvas pipe of 3.7% in both the single coil cases, apart from any effect of profile variation, makes the predicted sensitivities equal to the experimental observations. This figure of 3.7% which is necessary must be compared with the figures in table 2 page 37 which have been discussed on pages 35&47. We do not necessarily expect them to be the same since the magnetic fields are different, but merely to be of the same order.

Though no-one would pretend that the tables have yet been exhaustively tested, the accuracy of the predicted rise of 30% in one of the single coil meters after making this allowance of 3.7% for the canvas pipe gives one provisional confidence in their predictions.

The reason for the two sets of experimental results for the twin coil meter is that during a repeat run of the first experiment the small permanent rise of sensitivity recorded was found. No definite reason has been found, but it is probably due to a small movement of one of the coils when hot. The relative change in sensitivities is very small. If we allow the figure of 3.7% for the canvas pipe we find that the experimental sensitivity drops were approximately twice the predicted ones. This indicates that the actual weight function distribution was more non-uniform than predicted and higher at r = 1.

It can easily be explained, either by not having enough $\bar{W}'_b$ in the total weight function, or by slight error in the angle of coil (b) since the performance of $\bar{W}'$ is very sensitive to this angle at r = 1. Additional sources of error are that T was rather larger than 1.30 (in fact 1.32), though this would alter only the absolute sensitivity appreciably (a drop of around 2%), and that the coils were slightly unsymmetrically placed on the flowmeter.

The assumptions of theory which may be invalidated in practice and other factors affecting the performance are

1) Infinitely long iron sheaths of infinite permeability
2) Infinitely long insulating pipe
3) Point electrodes
4) Uniform liquid conductivity
5) Lack of precise knowledge of the velocity profile.

In report three, page 20 it was shown that in practice the minimum length of linear and sheath to avoid noticeable effects on the performance is about $1\frac{1}{2}$ diameters: in this experiment we have at least 4. The finite permeability of the iron which we have already referred to should affect the absolute signal by $<1\%$ and relative signals less. The finite size of practical electrodes was discussed on page 11: since no effort has been made to tailor the field at the electrode, and the velocity profile is axisymmetric this will have a negligible effect. The liquid conductivity, even if not uniform cannot be very non-uniform and with a moving liquid the effect of any non-uniformity would be expected to be random. The effect of uncertainties in the profile have already been mentioned: the experimental figures in table 3 lie well between the limits of uncertainty assumed.

All in all there is no reason why the theory should not hold as well as it seems to: if any major discrepancies are found in the future they will probably be due to errors in numerical computation. The sizes of the effect of the canvas pipe in different situations are entirely compatible with the differences between theory, which assumes no canvas pipe, and the experiments.

The variation of the predicted output voltage (table 2) compared to the experimental results (0%, + 7%, - 7%) is the most unsatisfactory feature of these experiments. Since the sign of the discrepancy depends on the flowmeter the fault is likely to lie with the flowmeters rather than the lack of calibration of the venturi and electronics and calls for an investigation into more accurate methods of producing the necessary magnetic fields (see page 50). With errors of $\pm$ 7% it is just possible that inaccurate manufacture of the field coils, together with some uncertainty about the iron diameter, could be the explanation.

Table 3 – Weight function $\bar{W}'$ and predicted and experimental sensitivities †

Radius	Single Coil $T = 1.32$ $L/D = 1$ H.A. = 15°	Single Coil $T = 1.32$ $L/D = 1/4$ H.A. = 45°	Twin Coil T = 1.30 Inside Coil (a) $.55 \leq L/D \leq .75$ $39\frac{3}{4}° < H.A. \leq 58\frac{1}{4}°$	Twin Coil T = 1.30 Outside Coil (b) $L/D = 1.00$ H.A. = 81.8°	Twin Coil T = 1.30 Combined Weight Function $\bar{W}' = \frac{295\,\bar{W}'_a + 50\,\bar{W}'_b}{345}$
r = 0.1	$\bar{W}'$ = .1324	.1074	$\bar{W}'_a$ = .3181	$\bar{W}'_b$ = .5159	$\bar{W}'$ = .3468
0.2	.1334	.1092	.3222	.5221	.3512
0.3	.1341	.1121	.3287	.5342	.3585
0.4	.1331	.1156	.3365	.5375	.3656
0.5	.1282	.1191	.3443	.5883	.3797
0.6	.1178	.1213	.3491	.6408	.3914
0.7	.1009	.1201	.3452	.7231	.4000
0.8	.0786	.1117	.3229	.8533	.3998
0.9	.0539	.0923	.2687	1.0664	.3843
1.0	.0308	.0617	.1757	1.4160	.3555
Sensitivities					
Flat profile: predicted	.0937	.1071	.3102	.8062	.3821
Parabolic profile: "	.1131	.1141	.3309	.6652	.3793

† The predicted and experimental sensitivities are given on the next page as a % increase or decrease based on the sensitivity of the normal turbulent profile flow. The figures in square brackets are the actual experimental or numerical values.

Table 3 - continued predicted and experimental sensitivities.

Sensitivities	Single Coil	Single Coil	Twin Coil T = 1.30 Combined Weight Function	
			1st experiment	2nd experiment
Turbulent profile: predicted	.0988	.1095	.3821	.3821
" " : experimental	747 ± 1	923 ± 1	$914\frac{1}{2} \pm 1$	$932\frac{1}{2}\ ^{+1\frac{1}{2}}_{-1}$
Plate profile: predicted	[.1005/.1015]	[.1094/.1101]	[.3808/.3811]	[.3808/.3811]
Plate profile: % change	+1.7%/+2.7%	-0.1%/+0.6%	-0.35%/-0.25%	
Plate profile: experimental	$[764(+2\frac{1}{2}-1\frac{1}{2})]$	$[924(+2-1\frac{1}{2})]$	$[909(+\frac{1}{2}-1)]$	$[924\frac{1}{2}(+3\frac{1}{2}-3)]$
Plate profile: % change	+2.3%	+0.1%	-0.6%	-0.9%
Canvas pipe: predicted	[.1304]	[.1150]	[.3677]	[.3677]
Canvas pipe: % change	+32.0%	+5.0%	-3.8%	
Canvas pipe: experimental	$[955\frac{1}{2}/961]$	$[929/941\frac{1}{2}]$	$[813\frac{1}{2}/815\frac{1}{2}]$	$[827\frac{1}{2}/833]$
Canvas pipe: % change	+27.9%/+28.6%	+0.6%/+2.0%	-11.1%/-10.9%	-11.3%/-10.7%
Output voltage: predicted*	96 μV	106 μV	1.08 mV	1.08 mV
" " : experimental (for H=90cms)	96 μV	99 μV	1.13 mV	1.15 mV
Nominal Veriflux Range in ft/sec/10 mA	1.500	1.250	17.0	17.0

Notes:

1) * The predicted voltages contain the factor $4/\pi$: the predicted sensitivities do not.
2) All % changes in sensitivity are with respect to the normal turbulent flow profile.
3) H.A. denotes the half-angle subtended by the coil at the flowmeter centre.

5.4. Valve/Flowmeter Experiments

The aim of this experiment was to demonstrate the behaviour of a simple example of the class of ideal meters described on pages 6, 7 and 8 of report one. The flowmeter design is shown in figures 13 and 14 and in the first version the magnetic field windings were made unnecessarily long to ensure the field was uniform. For this reason no design effort was made to compress the virtual current lines into a region smaller than they naturally occupy.

The flowmeter was made out of a square perspex pipe, 1 foot long, whose external size was 4" x 4", with a central square hole 2" x 2". At the ends the cross-section changed abruptly to 3" I.D., $3\frac{1}{2}$" O.D. circular pipe with flanges.

In the centre of the square pipe a 3" diameter stopcock, with a 2" x 2" central hole was placed, with electrodes made out of $\frac{1}{4}$" diameter stainless steel set half-proud in the stopcock walls and copper-plated on the exposed half. The stopcock could just cut off the flow, though in practice there was some leakage which we had expected because overlap was so small. The flow was stopped completely by using the main valve in the circuit.

Originally the magnetic field was produced by approximately 760 turns of copper wire wound uniformly around the top and bottom of the flowmeter to a depth of $\frac{1}{2}$". Around this 6 layers of 12" wide transformer iron 0.013" thick were wrapped, in L sections covering alternate corners and held together by Sellotape. The electrode wires were taken through the centre of the stopcock handle. Unfortunately there was a short in the windings which we could not trace and, since a uniform magnetic field was required for testing the behaviour of the canvas pipe, the magnet shown in figures 9 and 10 was quickly assembled and used for this experiment after we had cut off the original windings.

With a coil current of 8.0 amps, the field strength predicted for this magnet was 174 gauss, assuming iron of infinite permeability and no small air gaps. Measurements with the search coil indicated a

field of 135 gauss and the valve/flowmeter signal indicated 155 gauss. The search coil absolute measurements may be wrong, since they were made with A.C. (50 c/s) and it was a D.C. search coil with a brass covering. The figure of 155 gauss seems reasonable, since there were air gaps, and in fact the magnet had to be run at 5.0 amps instead of 8.0 to prevent excessive chattering.

A plot of the transverse field component, made measuring the voltage with the search coil using an RMS voltmeter with a resolution of ½% or better, is also shown in figure 9. The field is not as uniform as might be desired but had to do.

The sensitivity of this flowmeter for different positions of the stopcock is shown in figure 15. The last figure is possibly suspect since the valve was so nearly shut that the pumps could only produce 50 cms head on the venturi instead of the normal 90. The small changes of sensitivity (well within ± 1%) are quite consistent with the non-uniformity of the magnetic field in view of the marked changes of vortex pattern behind the stopcock when partially closed. Normally one would expect a 1% variation in field uniformity over the region of appreciable virtual current to cause a much smaller variation in sensitivity as the profile changed, but with reverse flow the variation would be of the same order of size as the field non-uniformity. The reader is referred to the remarks on page 24 about Korsunskii's work with ideal meters.

The requirement of a uniform field and line electrodes might be modified. Once the decision has been taken to install a valve in a pipe line, obstruction to the flow is no longer a disadvantage of the flowmeter, in which case the valve and electrode geometry can be altered to compress the lines of appreciable virtual current into a smaller region. The magnetic field now need only be uniform over this volume: experimental tests would be required with different ways of producing an approximately uniform field to find out to what extent non-uniformity could be tolerated.

The normal industrial argument put forward against line electrodes is that they may become partially covered with insulating material

thereby introducing meter errors that may not be noticed. (Point electrodes so covered simply cease to work). Since the only induced currents in this meter are due to the variation of velocity in the magnetic field direction the ends of the electrodes would be the critical regions, carrying the relatively high current from the boundary layers. Tests would show the effect of covering these ends with insulating material, but there is also the possibility of doing away with line electrodes by removing the electrode region from the motion, so that departures from two dimensionality in the virtual current only occur where there is no or little motion. This would mean some form of liquid trap which might, of course, trap air. Whether this is feasible depends on the application.

As a final experiment, the canvas pipe was inserted in the meter with the stopcock fully open and the loss of sensitivity due to the presence of the canvas measured. The results (table 2, p. 37) indicate a drop of about 2% due to the canvas alone, since this meter rules out the profile effects. Some difficulty was experienced with air bubbles since the flowmeter started leaking at this stage. In addition the canvas tube had recently been washed in detergent to remove some grease and this may have affected its conductivity, so the result is not reliable.

5.5. Virtual Current Measurements

It was thought advisable to check the rate of fall of the virtual current along the centre line of a circular flowmeter with point electrodes in order to verify the theoretical calculation on page 16 of report 3. At the same time we took the opportunity to estimate the effect of material of differing conductivity placed at the ends of a flowmeter. The experiments were done quickly and not very accurately.

A 3" I.D. plastic pipe was cut in half axially and both ends were sealed off with plastic walls to form a trough (figure 16). It was then half filled with electrolyte ($CuSO_4$ solution) and two small electrodes were placed in holes at one end just below the liquid level.

It thus simulated a quarter of a flowmeter, the virtual current being generated by putting an A.C. voltage (about 10 volts, 50 c/s) across the electrodes and being measured along the z-axis using a two-pronged probe made of copper-plated platinum wire and an oscilloscope. The voltage measurements are only accurate to about 5%. The maximum probe voltage was about 65mV, peak to peak, noise $< 1\%$.

Provision was made for placing semi-circular pieces of plastic and copper at various distances from the electrodes. In practice it was found that only at the nearest position, $z/R = 2$, did they have an appreciable effect.

The virtual current is plotted in figure 16, as fractions of its value at $z = 0$, for the cases with copper and plastic walls at $z/R = 2$ and also for the case with no partition. At the lower end of the curve this latter case falls exactly between the other two and one would suspect it to do so everywhere. In fact without the partition the results were not very repeatable, two different tests yielding differences of about 5% (one lying below the two cases and the other above). More accurate experiments would resolve the differences.

The theoretical points lie where one might expect for $z = 2R$ and just above the other two curves for $z = \frac{R}{2}$ and $z = R$. Given the rather poor accuracy of the experiment we can say that the results agree with the theory. They also show that extreme variations in the boundary condition at $z = 2R$ affects the shape of the distribution of virtual current very little. The effect on the relative sensitivities for different profiles will be small, especially with a non-uniform field which is small at $z = 2R$ where most of the virtual current variation occurs. The effect on the absolute sensitivities cannot be found from these experiments: it could easily be in the region of 1% without being noticed.

6. CONCLUSION AND POSSIBLE DEVELOPMENTS

The work presented in this thesis raises a number of difficulties which need attention before the results can be confidently used by the flowmeter designer, and also suggests a number of areas in which further work could be done.

1. One of the difficulties shown by the experimental tests for the design tables for the axisymmetric weight function $\bar{W}'$ is the poor predictability of the absolute signal. It is true that most present day designs, with so-called uniform fields, suffer from this fault and calibration is always done after manufacture. I am told that even if the absolute sensitivity could be predicted to, say, 1% the customer would still demand calibration. It is expensive, however, and it would be worth many thousands of pounds a year in this country alone if calibration could be dispensed with.

   The trouble lies in the difficulty of manufacturing the coils accurately, and in the side effects that can take place in the iron circuit, e.g. induced fields due to eddy currents and the non-infinite magnetic permeability of the iron. No-one really knows how large these effects are.* It may be that different methods of producing the magnetic field would be preferable, as in (2) below.

   An elementary preliminary step would be to produce a uniform field meter with a really uniform field and to see whether its sensitivity was predictable. The theory is not in dispute here,

---

* At the time of writing tests on some industrial flowmeters have shown that eddy current effects are far from small. Elementary analysis shows that stainless steel liners have a large effect and using the iron pipe as the magnetic yoke a lesser but not negligible effect. In both cases the effect is proportional to the size.

and such an experiment might show up some of the side effects.

2. In certain applications the power dissipation of the coils is an embarrassment. Combined with the difficulty of manufacturing coils accurately, this leads to the idea of producing the magnetic field in a physically different way, while satisfying the same mathematical conditions, so that the design tables may be used. Figure 17 shows the idea schematically. The coils are replaced by slots in the iron, such that the iron would fall apart if not held together in some different way. The difference in magnetic potential between the various parts of the circuit is maintained by Amp-Turns wound on a yoke outside the meter. The advantages are:

(a) since the main field is low, the cross-section of the yoke can be reduced till the flux in it is approaching saturation, thus reducing the winding turn length.

In a typical case, where the main field was around 100 gauss, and saturation took place at 10,000 gauss the yoke area could be reduced by up to 100 times and the turn length by up to 10, thus saving up to 10 times the power (though the inductance is unaltered).

(b) the iron pole pieces can be made accurately, the equivalent coil size being measured from the centre of the gap. The larger the gap, the more the magnetic field departs from design (though only in the regions close to the gap), and the smaller the inductance of the system. A good rule of thumb is that the gap width should be no larger than the distance from the pole pieces to the inside of the flowmeter (which in most cases will be the wall thickness), though the errors due to the gap size would probably not be noticeable till it was much larger.

It may be a disadvantage that the iron can no longer be relied on for strength: this must now come from the inside wall of the flowmeter.

Magnetic materials other than iron could be used, to avoid eddy currents for example. This would require a careful assessment of the strength, cost and magnetic performance of the readily

available materials.

3. A set of tables for the asymmetric weight function $\bar{W}$ are at present under production. There is no doubt that the necessary magnetic field, if feasible in practice, will be much more complicated, and the winding of suitable coils will probably be so difficult that the technique described in (2) will have to be used, where the windings can be fixed on outside wherever convenient.

4. The assumption of asymmetric rectilinear flow in a circular pipe will only be valid in certain circumstances, such as flow in a curved pipe, where the swirl (being also invariant in the stream-wise direction) should have no effect (see page 26). Immediately after a valve, however, the flow may well be far from rectilinear and a meter capable of coping with this will probably have to have some form of transverse line electrode. This problem can be (p.17) analysed by an extension of the techniques described in report 3.

5. In some cases where a flowmeter is placed after a valve in a circular pipe, so that the meter requires a transverse line electrode, it may be feasible to design the meter and valve together, as described on page 7 of report 1. The principle of these meters has been established in this thesis both theoretically and experimentally, but practical tests would be required to see how far the ideal conditions (such as a uniform field) could be relaxed without seriously affecting the meter performance.

6. In some circumstances, for instance in blood flow measurement where the meter has to be placed around the vein or artery, the large angle subtended at the flowmeter centre by one of the coils of a uniform axisymmetric weight function flowmeter when high permeability material is placed all around the flowmeter is an embarrassment, since the gap between the coils or pole pieces is not large enough to slip the vein through. The material immediately over the electrodes is the cause of the trouble: if we could design a flowmeter without it we could make the subtended angle smaller.

Finding analytic formulae for a short magnetic field under these circumstances is not easy, because the boundary conditions are mixed. Figure 18 shows diagrammatically the flowmeter we have in mind. If it is long however, then the magnetic field has already been found on page 10 of report 2, though in that context it was the virtual current. The axisymmetric weight function for this long meter is:

$$\bar{W}' = \frac{1}{\sqrt{1 + r^2/4 + 2r/2 \cos 2\alpha}}$$

which, for T = 1.2 and $\alpha = 53^\circ$, is uniform to $\pm$ 5%. It is reasonable to suppose that if we shorten the magnetic poles to a convenient length, say one diameter, and suitably pare them away so that they have some sort of saddle-shape we shall achieve a short flowmeter with a uniform $\bar{W}'$. Since the analysis of this problem is difficult it might have to be done numerically.

There is of course a range of saddle shaped coils which would also produce a uniform $\bar{W}'$ when the rest of the flowmeter was covered with magnetic material. These could be found using the present tables (and will not be rectangular).

7. The virtual current for point electrode circular meters has been used in an analytic form in this thesis because it was possible to specify the magnetic field analytically. Anyone designing a flowmeter and producing the field by some other means may only be able to specify it numerically, in which case they would need numerical values of the virtual current. Though these can be measured, it would be very simple to compute them from the analytic formula. The fact that it does not converge in the electrode plane could be overcome by extrapolation, using the fact that the virtual current is symmetric in z (the co-ordinate in the flow direction).

It would probably be possible to produce a first order approximation to an analytical formula for the virtual current for short insulating liners in conducting pipes that were not too short (say one diameter) if it was thought useful.

Though interest in the theory of flowmeters has been renewed in the last few years, stimulated largely by the work of Rummel and Ketelsen (6), the concluding remarks above show that much remains to be done if meter sensitivities are to be analytically predictable to within the commonly accepted engineering tolerance of 1%. It is clear that in the production of accurately known magnetic fields closer attention must be paid to ill understood side effects and eddy current losses, either by eliminating them or analysing them accurately. The competing claims of different shapes of electrode, too, warrant consideration and a careful assessment of their practical merits is required.

The subject has reached a stage where new information is available to the flowmeter designer, but further tests on experimental designs are required before industry can be confident that the outstanding problems have been overcome. Such tests are unlikely to be done by a single manufacturer and there is a good case for some form of centrally sponsored development work that would result in new designs and information being readily available to industry in a directly useful form. This would prevent the fragmentation of effort that occurs at present and also the premature abandonment of development work before the practical problems have been properly sorted out.

7. REFERENCES

(not including those at the end of each report in the appendix)

1.	Arnold J.S.	Rev. Sci. Inst. 22. p.43 1951
2.	Baker R.C.	a) 1968 J.F.M. 33.1.p.73 b) 1968 Brit. J. Appl. Phys. (J. Phys. D) 2.1. p.815.
3.	Clark, Delia and Wyatt D.G.	Electromagnetic Flowmeter Symposium, Oslo, 1967.
4.	Kanai H.	Private correspondence and preview of English paper.
5.	Korsunskii L.M.	Electromagnetic Flow Measuring Devices (State Committee for Standards, etc., Moscow 1964).
6.	Rummel Th. and Ketelsen B.	a) Regelungs Technik 1966, 6. p.262 b) Die Elektrische Ausrüstung, 5.4. p.131, 1968. c) Patent application 6514384, 1966.
7.	Schlicting H.	Boundary Layer Theory. McGraw-Hill (4th edition).
8.	Shercliff J.A.	a) The Theory of Electromagnetic Flow Measurement. (C.U.P.) 1962. b) J. Nucl. Energy, part B 1959, 1. p.5.
9.	Wyatt D.G.	a) see Clark & Wyatt b) Med. & Biol. Eng. 4. p.17. 1966.
10.	Kalnin R.K. (Editors) Kisis A.Ya. Krumin Ya.K.	Electromagnetic Measurement of the Parameters of M.H.D. Processes. Latvian Academy of Sciences, 1968.

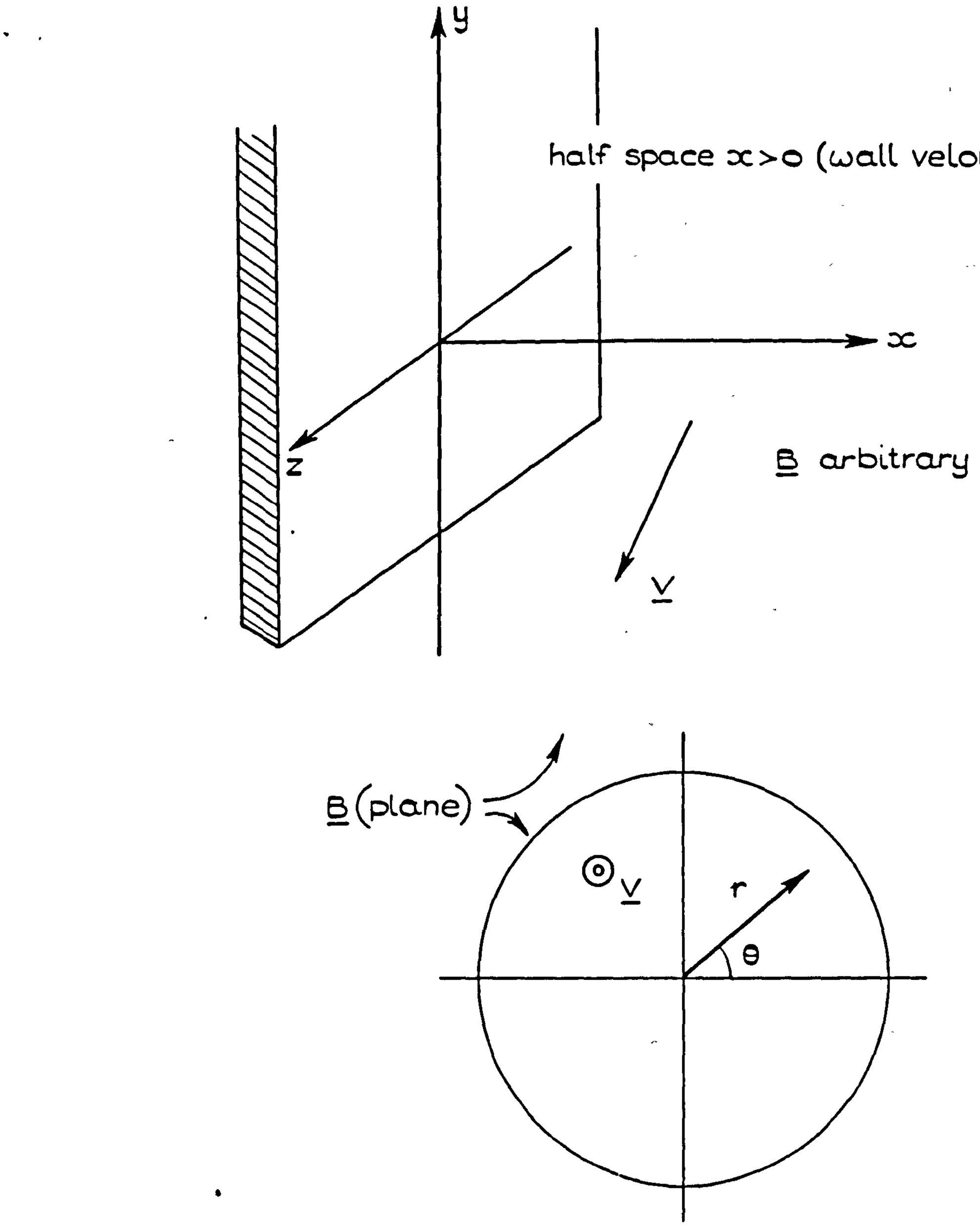

BAKER'S SOLUTION : NOTATION

FIGURE 1

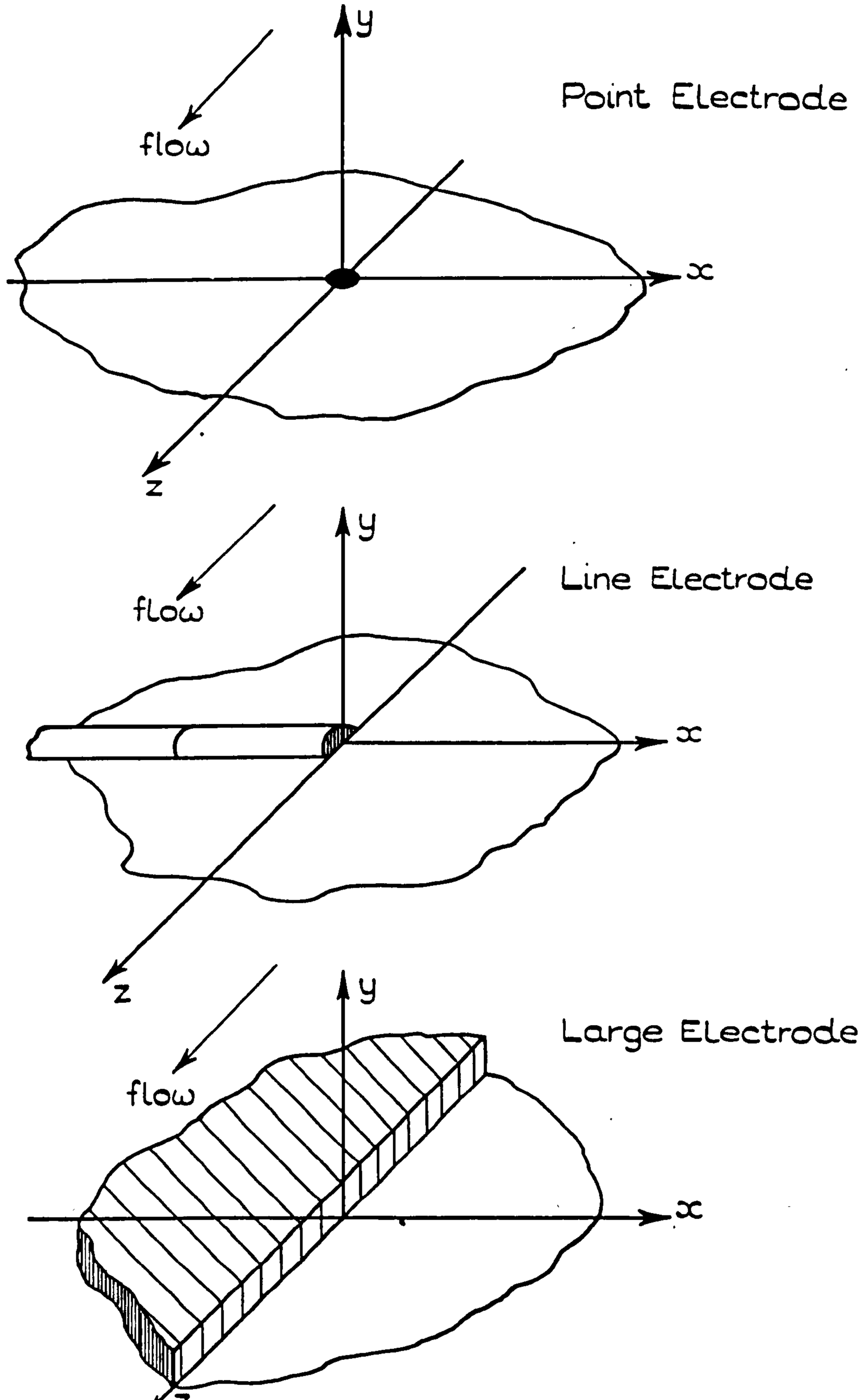

THE BASIC TYPES OF ELECTRODE.

FIGURE 2.

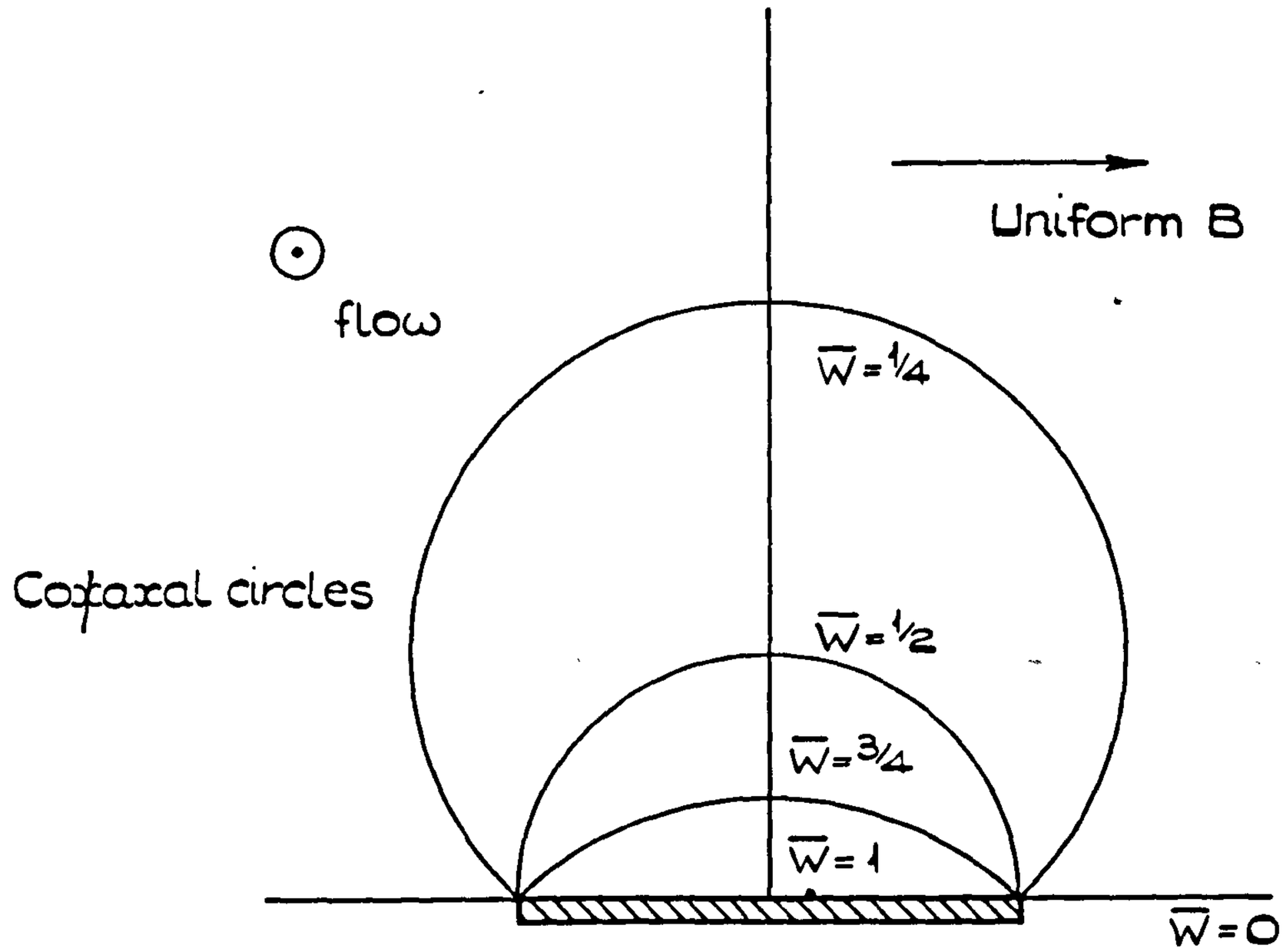

LINES OF Constant $\overline{W}$ FOR A TRANSVERSE LINE ELECTRODE.

FIGURE 3.

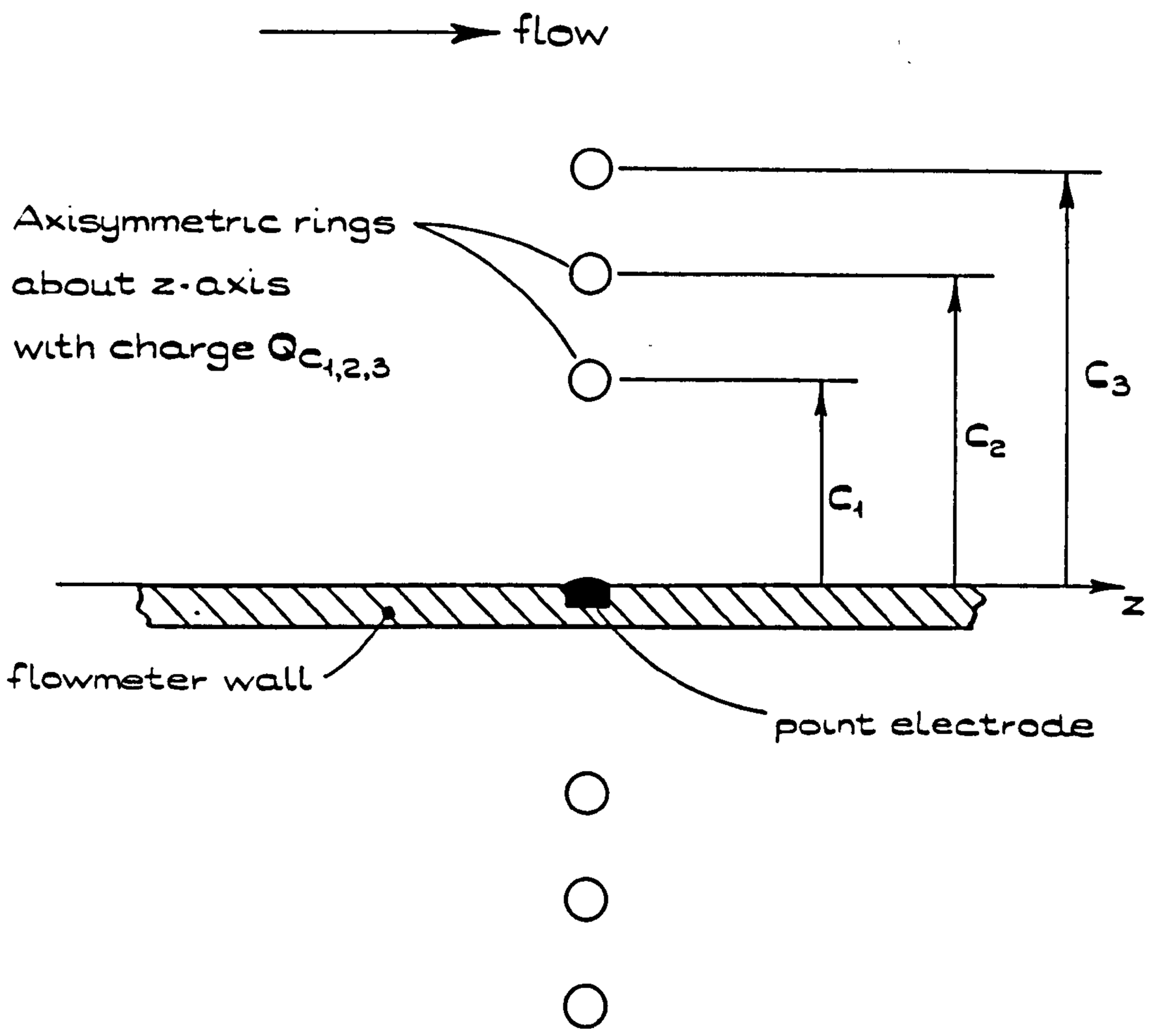

FICTITIOUS SYSTEM OF CHARGED RINGS RESULTING IN A $\frac{\partial F}{\partial \theta}$ THAT WOULD PRODUCE A UNIFORM $\bar{W}$ AT A POINT ELECTRODE.

FIGURE 4.

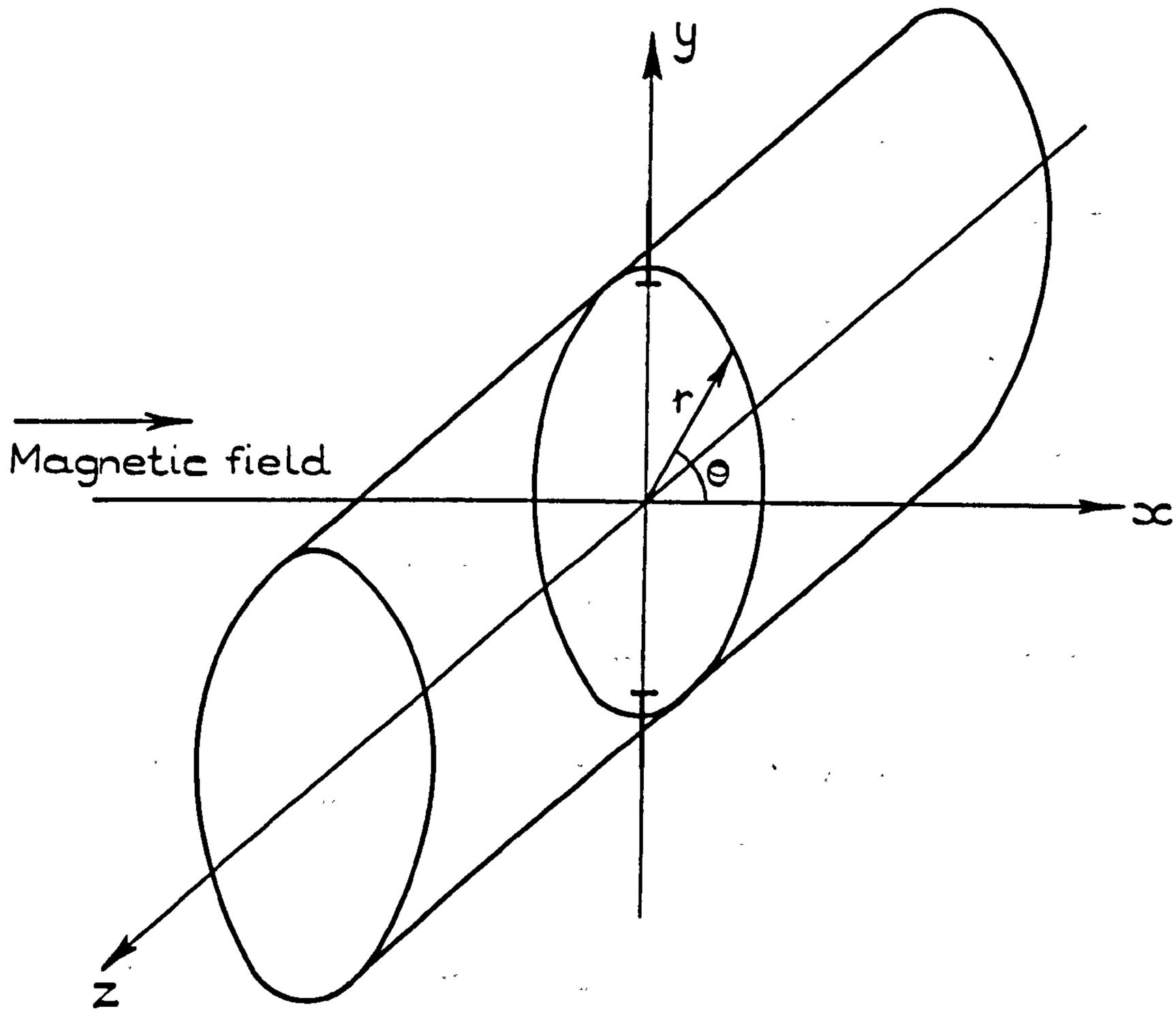

COORDINATE AXES FOR A CIRCULAR FLOWMETER

FIGURE 5.

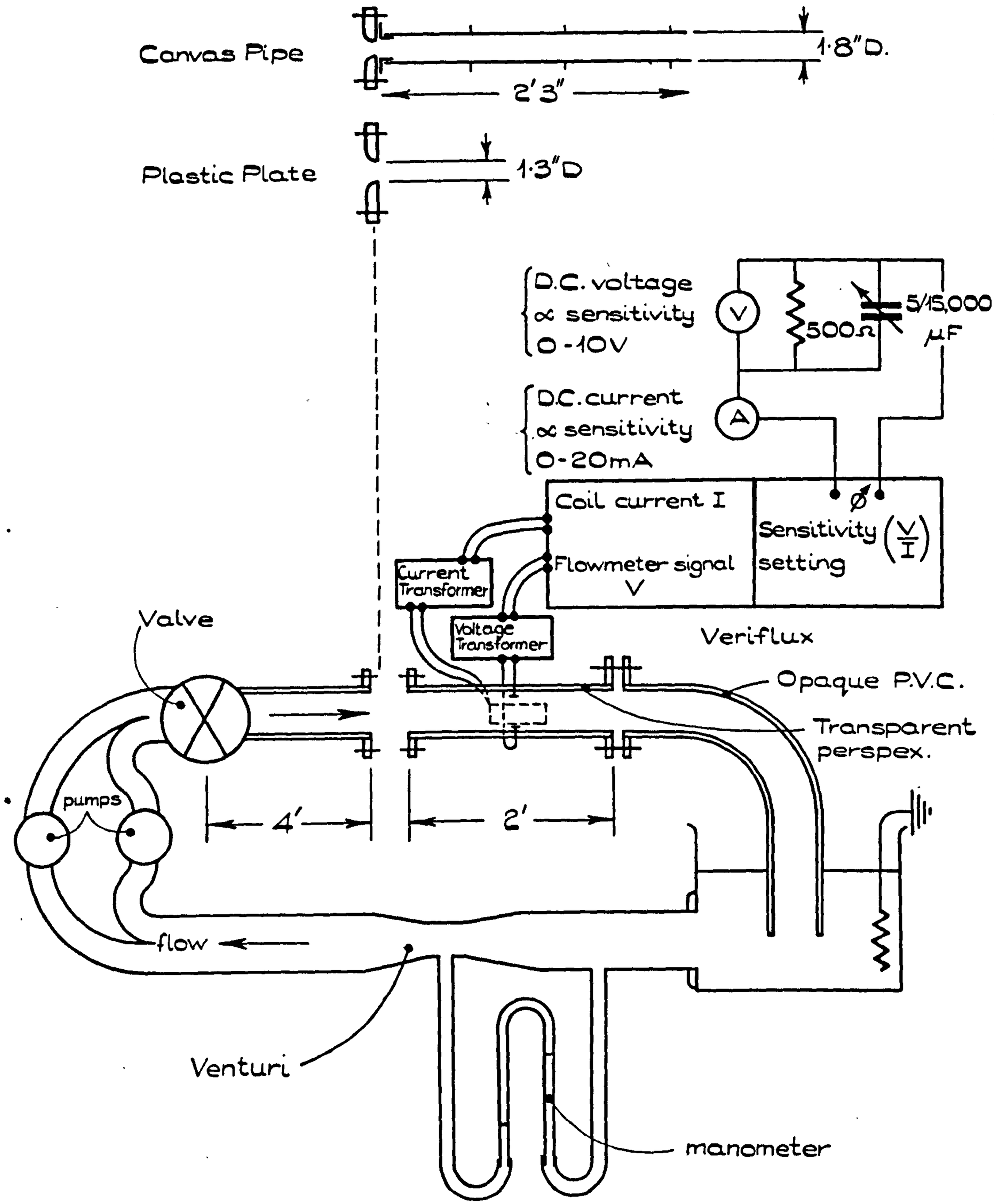

FLOW CIRCUIT AND ELECTRONICS.

FIGURE 6.

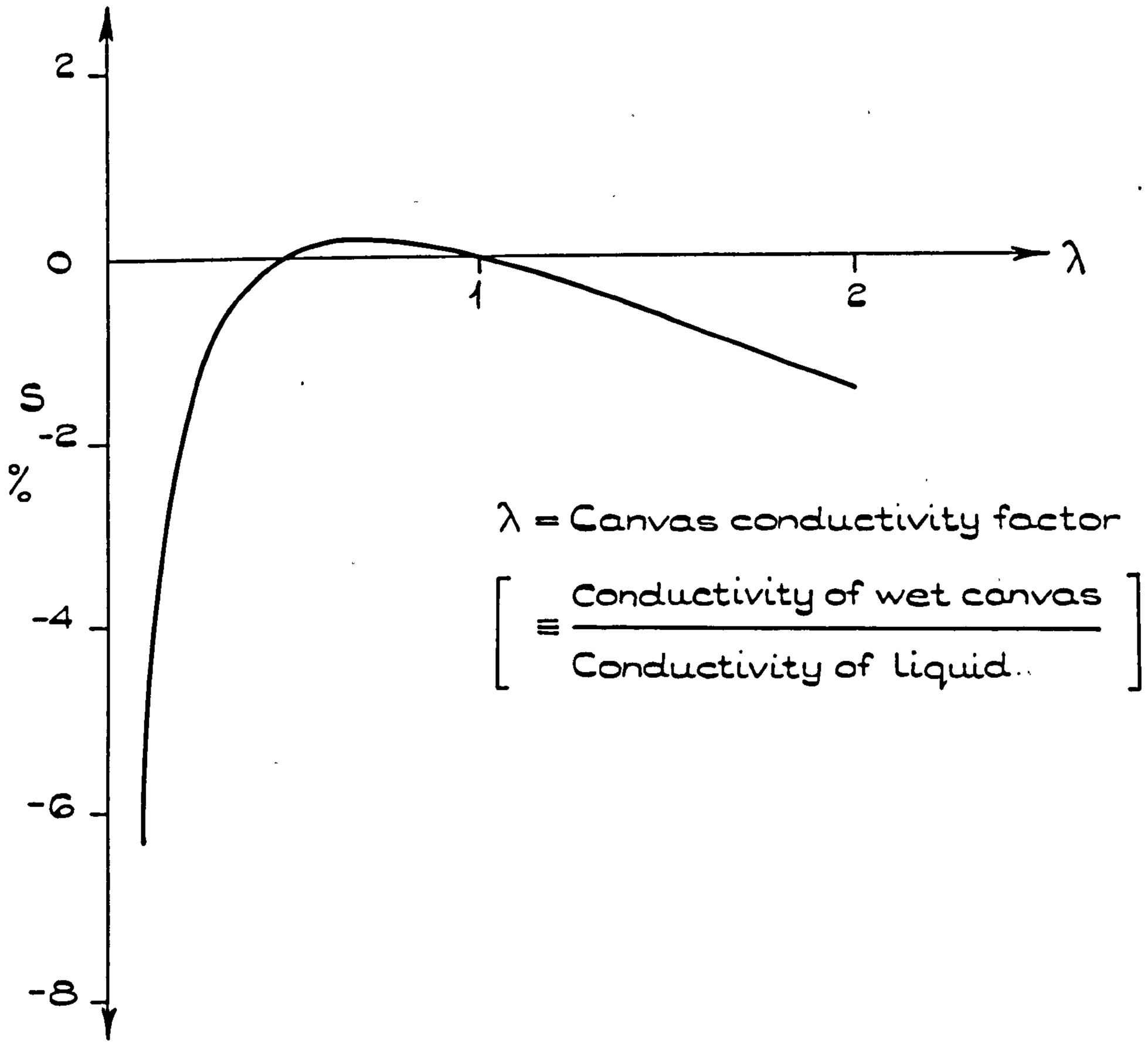

THEORETICAL SENSITIVITY S OF UNIFORM FIELD FLOWMETER WITH AXISYMMETRIC PROFILE AND CANVAS PIPE.

FIGURE 7.

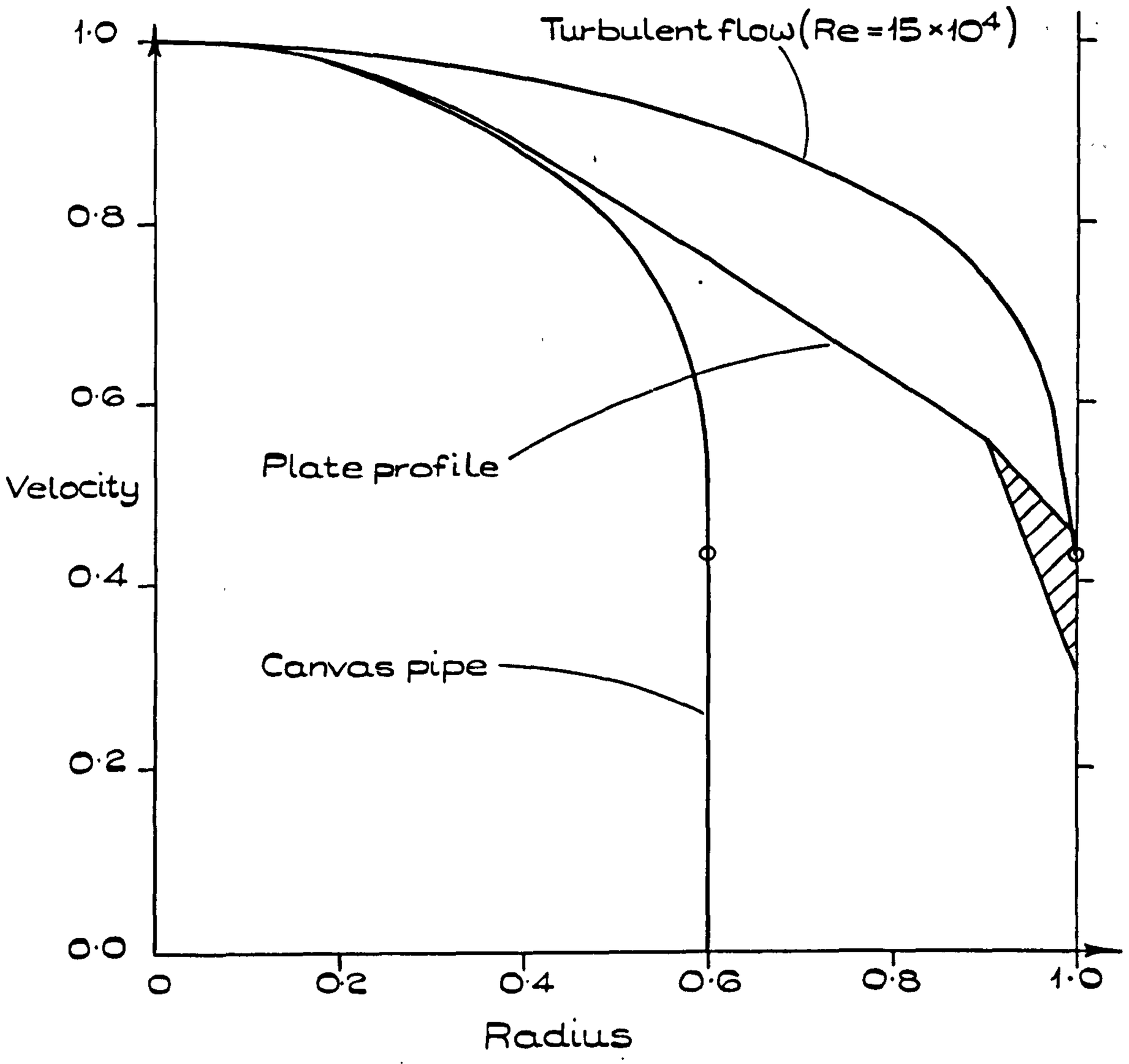

VELOCITY PROFILES USED FOR EXPERIMENTS

FIGURE 8.

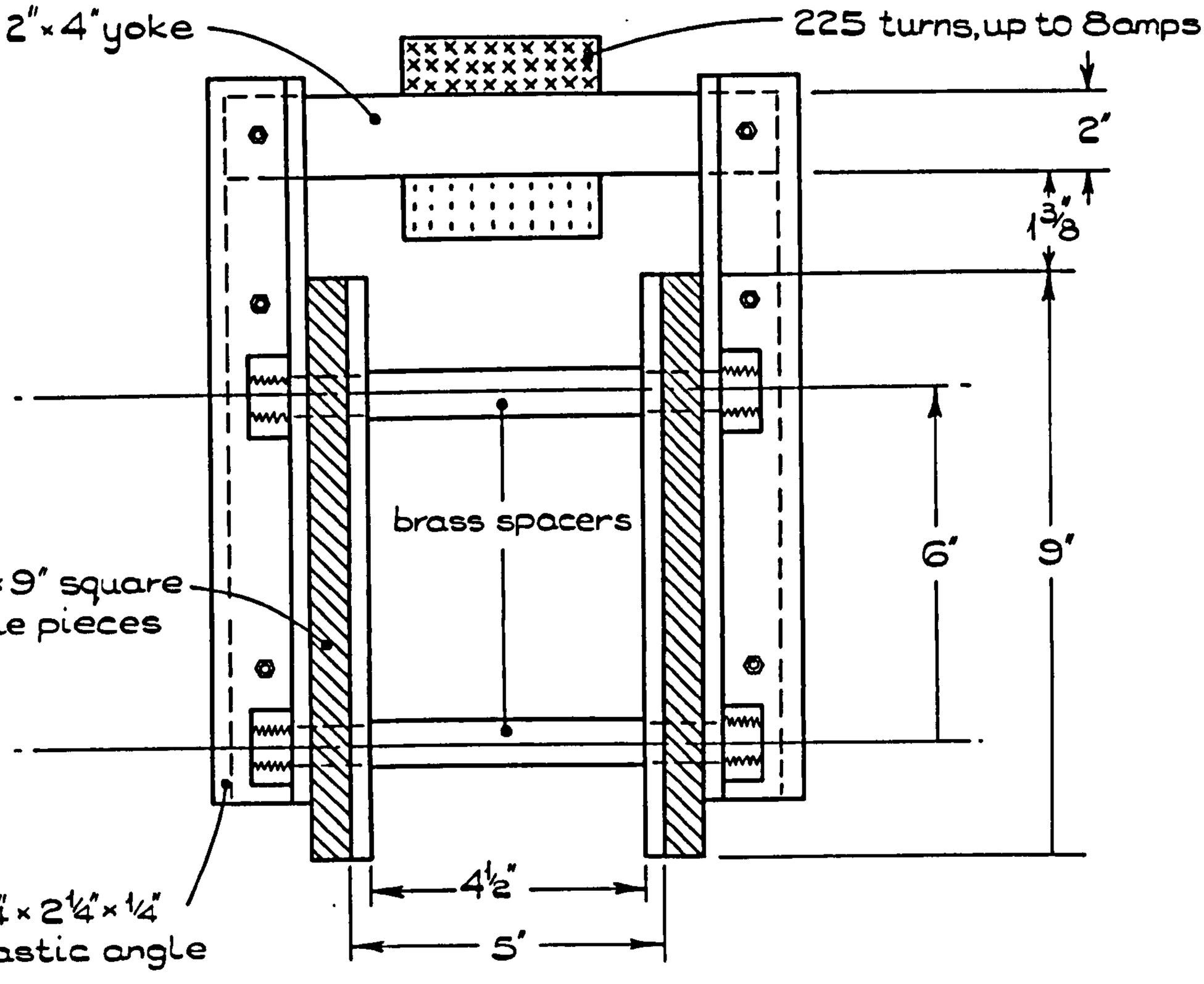

ELEVATION OF UNIFORM FIELD MAGNET.

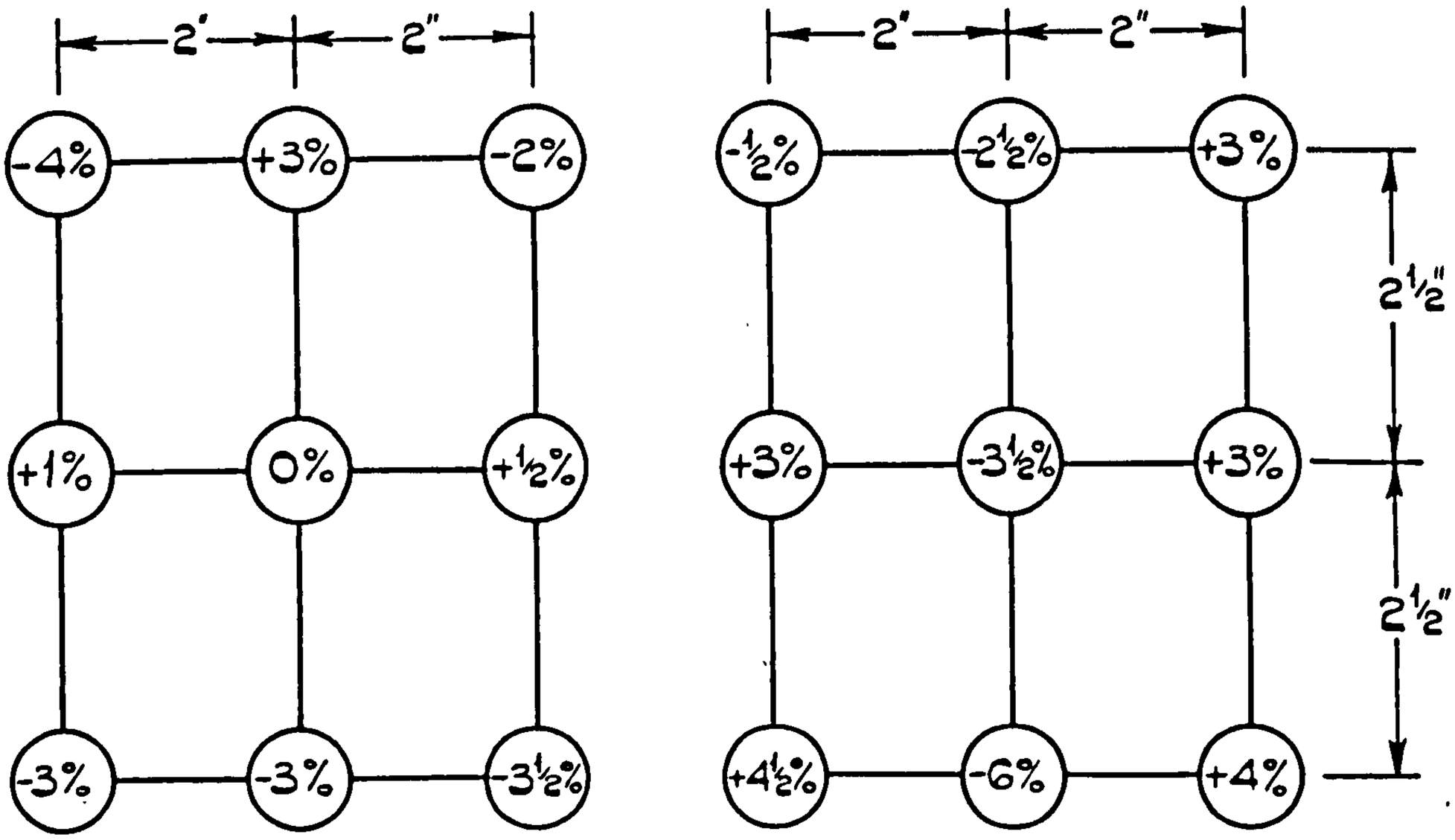

CENTRE CROSS SECTION

2½" FROM CENTRE SECTION.

TRANSVERSE FIELD NON-UNIFORMITY.

FIGURE 9.

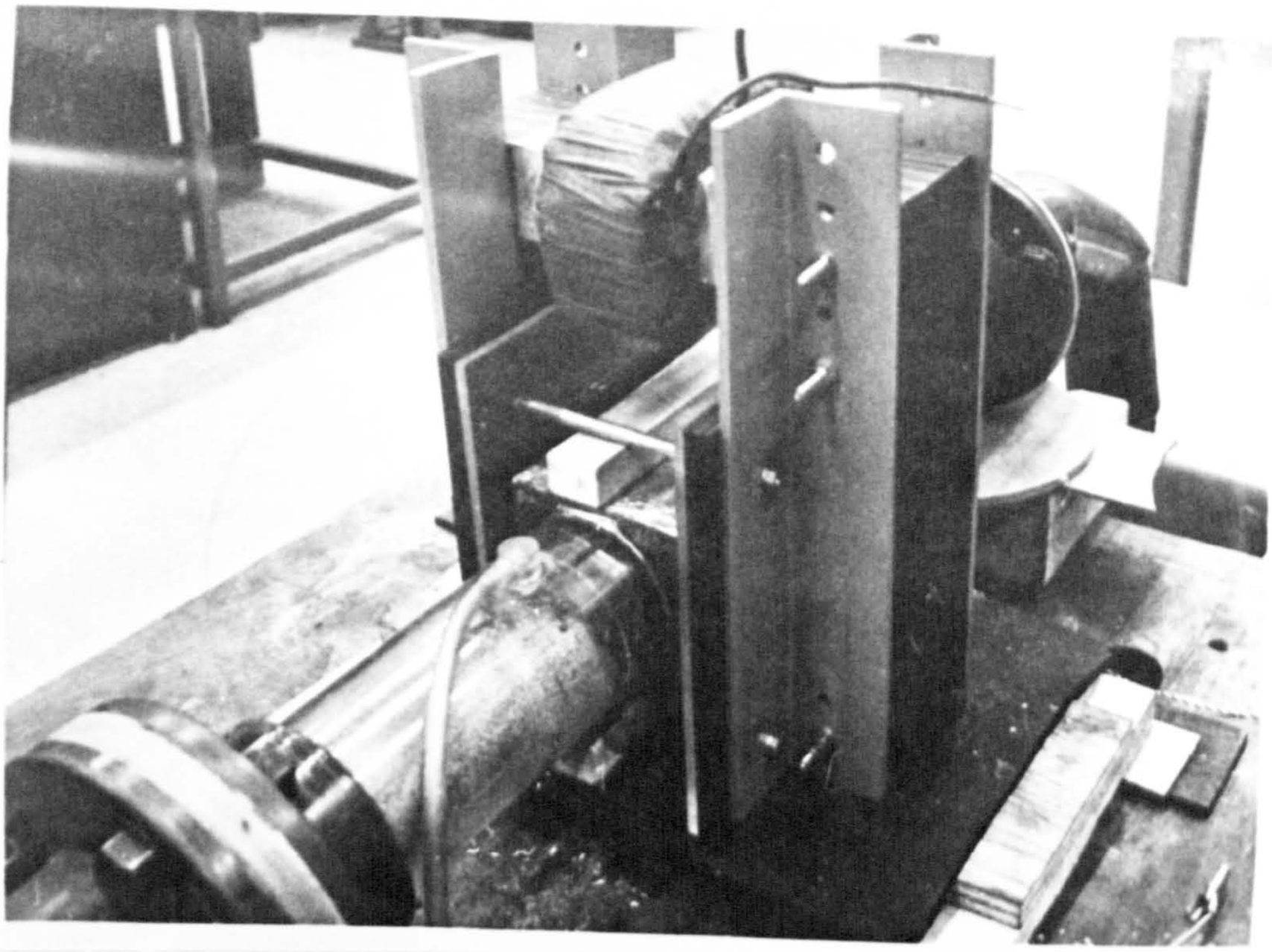

UNIFORM FIELD MAGNET

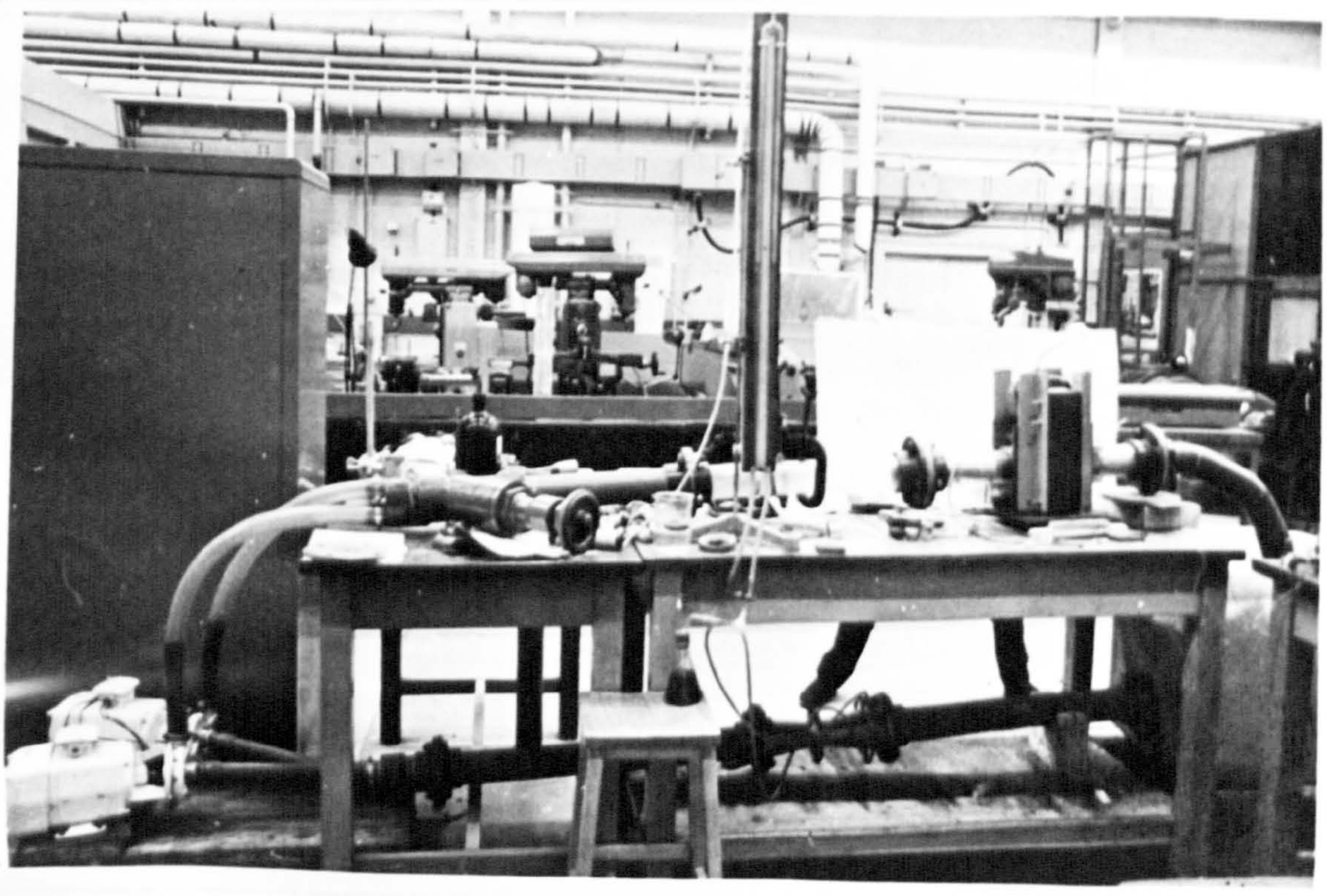

GENERAL ARRANGEMENT OF APPARATUS

FIGURE 10

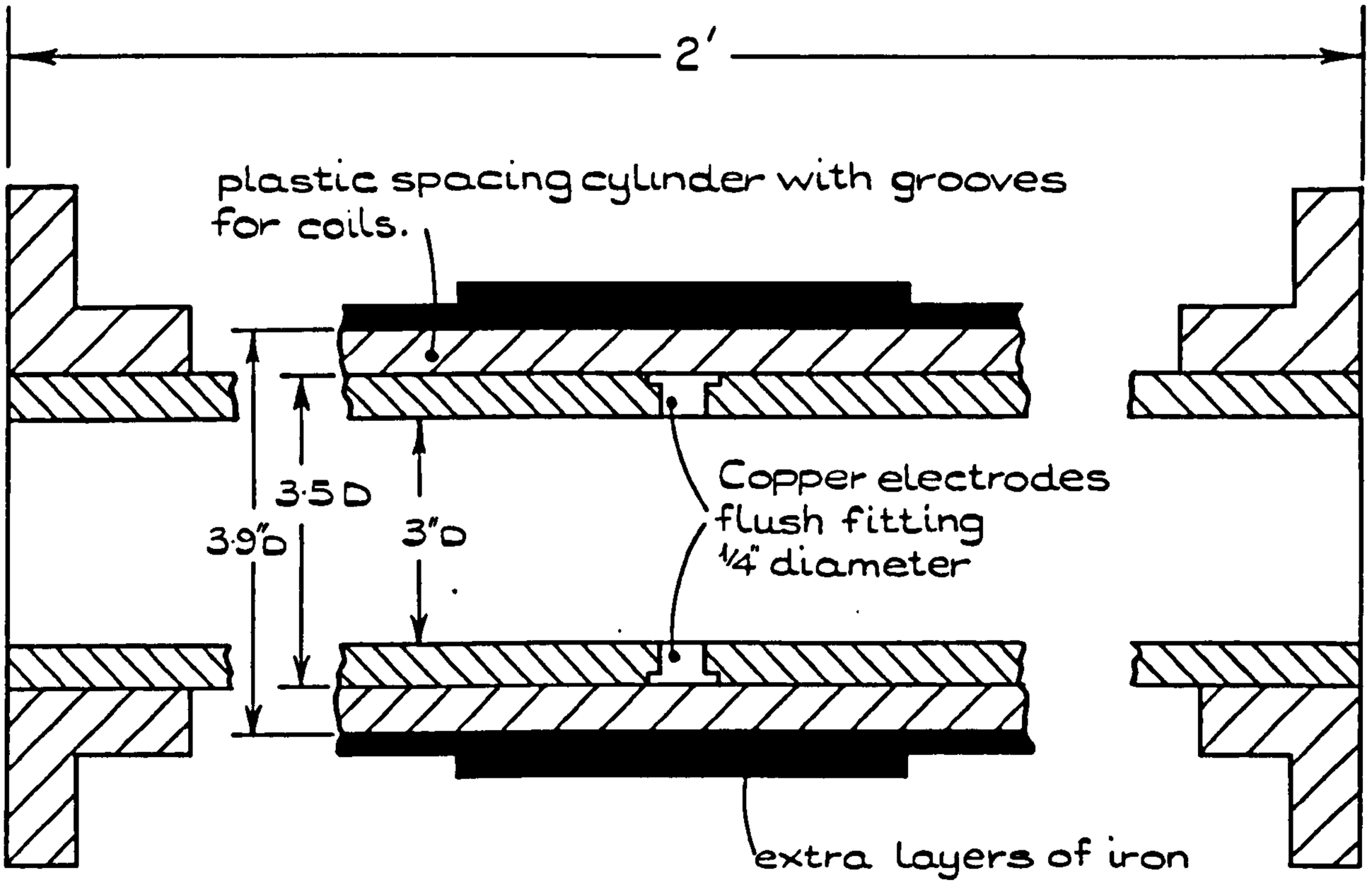

CROSS-SECTION OF CIRCULAR FLOWMETER (SCHEMATIC)

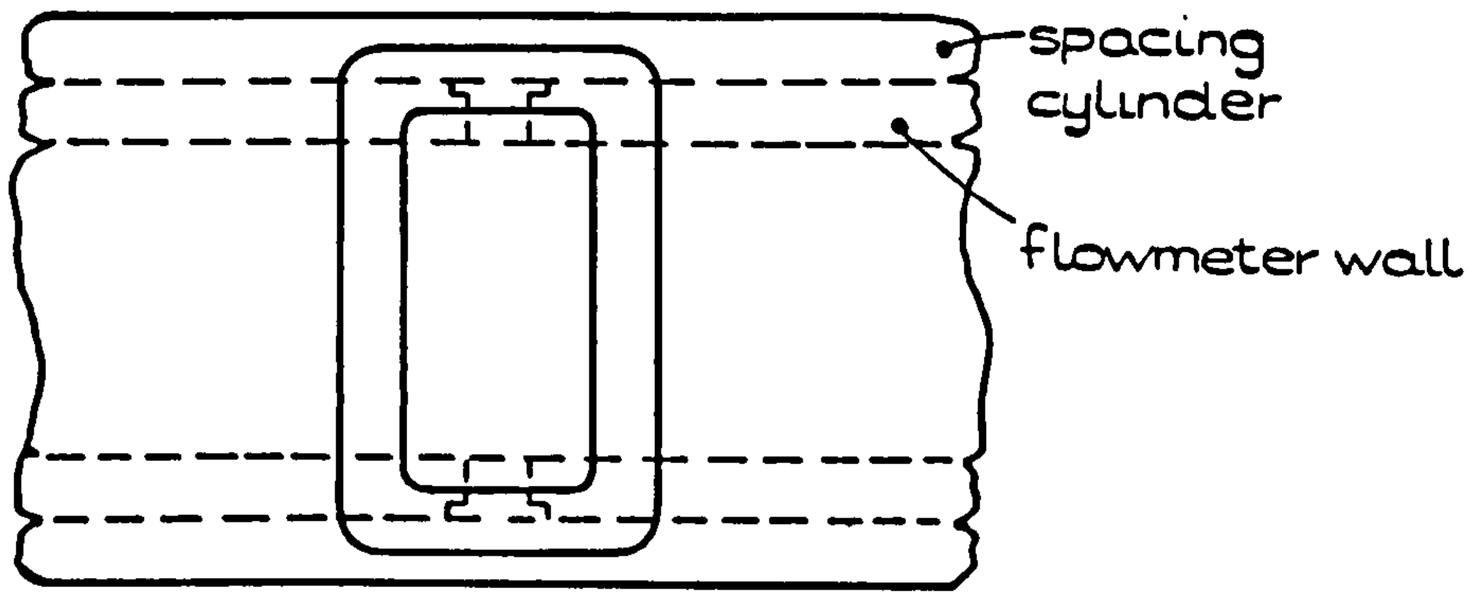

SIDE VIEW OF PLASTIC SPACING CYLINDER SHOWING TYPICAL COIL GROOVE.

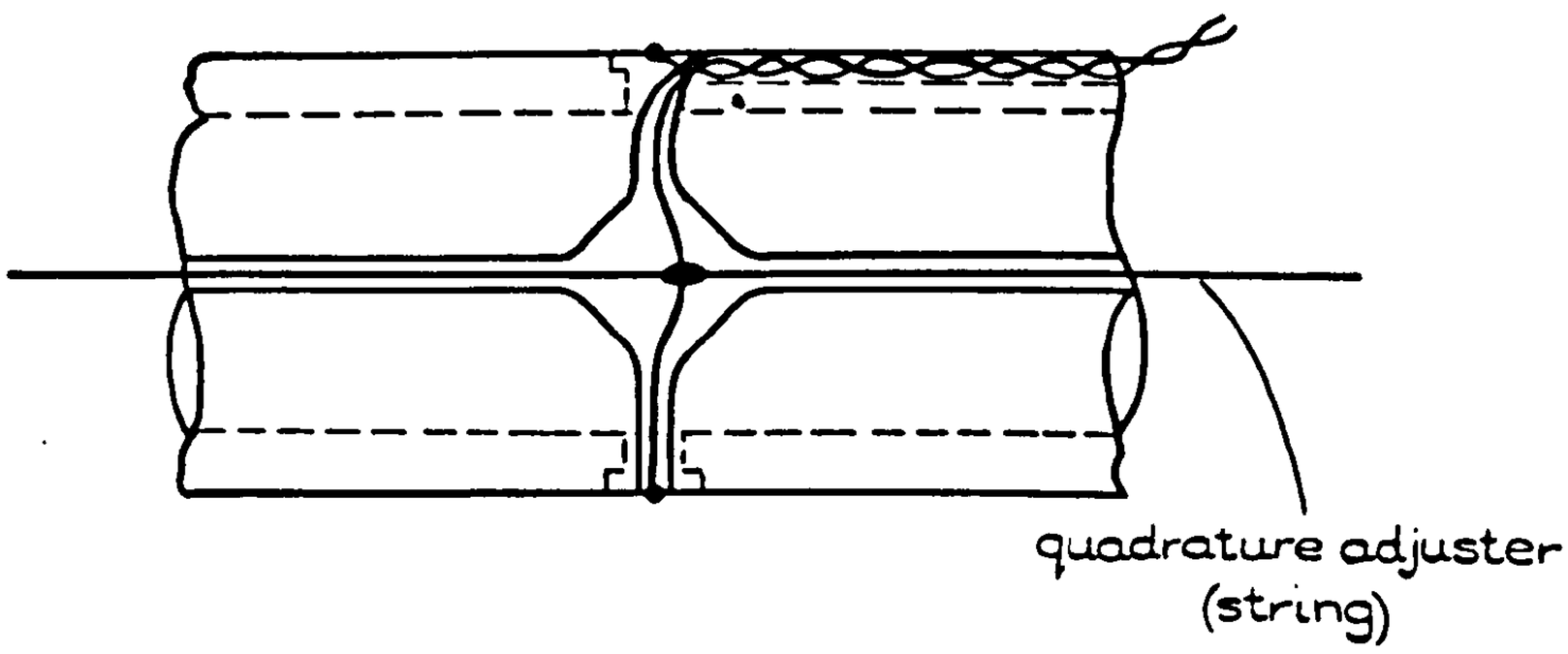

SIDE VIEW OF OUTSIDE OF INNER PLASTIC PIPE, SHOWING GROOVES CARRYING ELECTRODE WIRES

FIGURE 11.

FIGURE 12

FLOWMETER WITH SINGLE IRON SHEATH

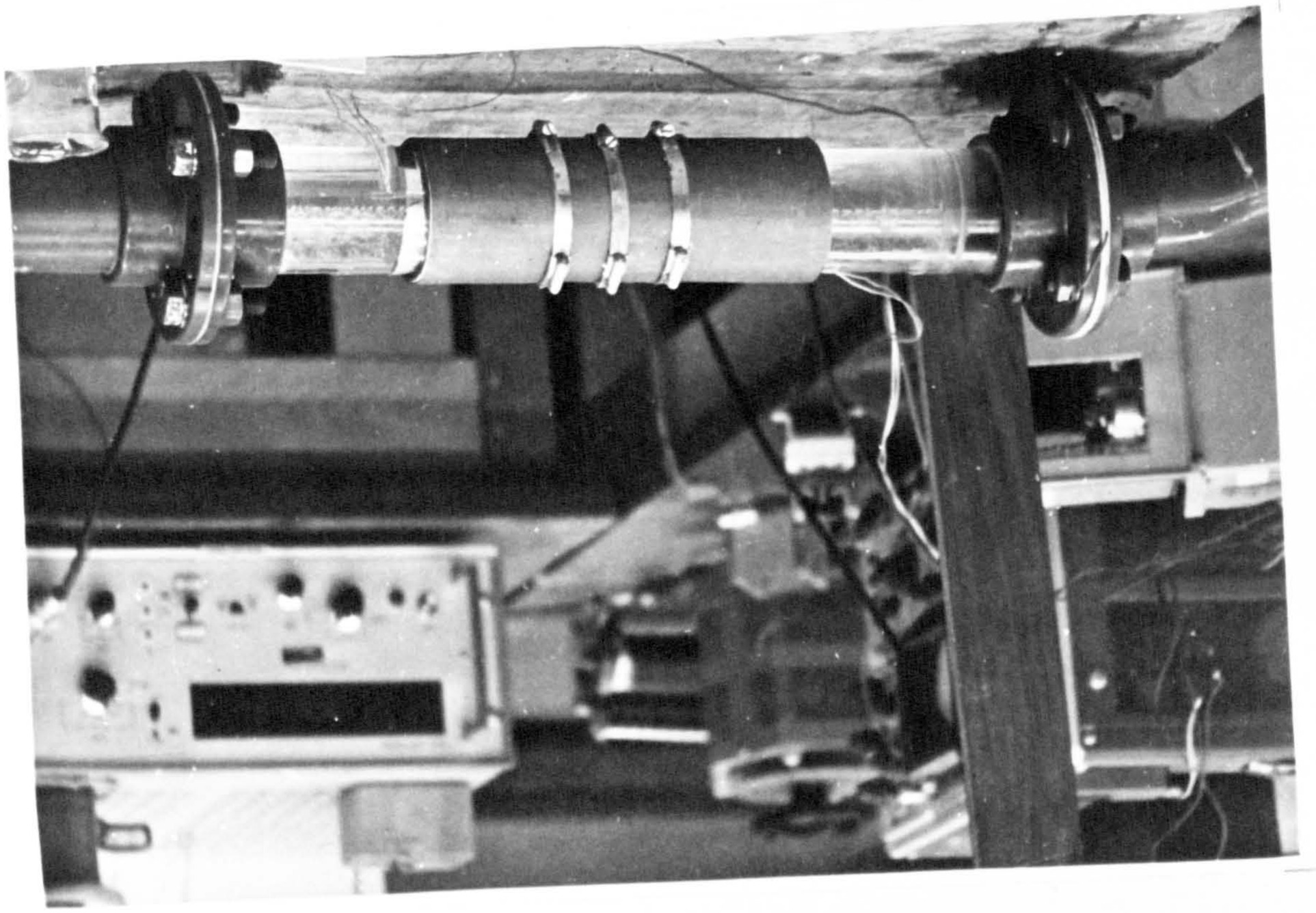

TWIN-COIL FLOWMETER WITHOUT IRON SHEATH

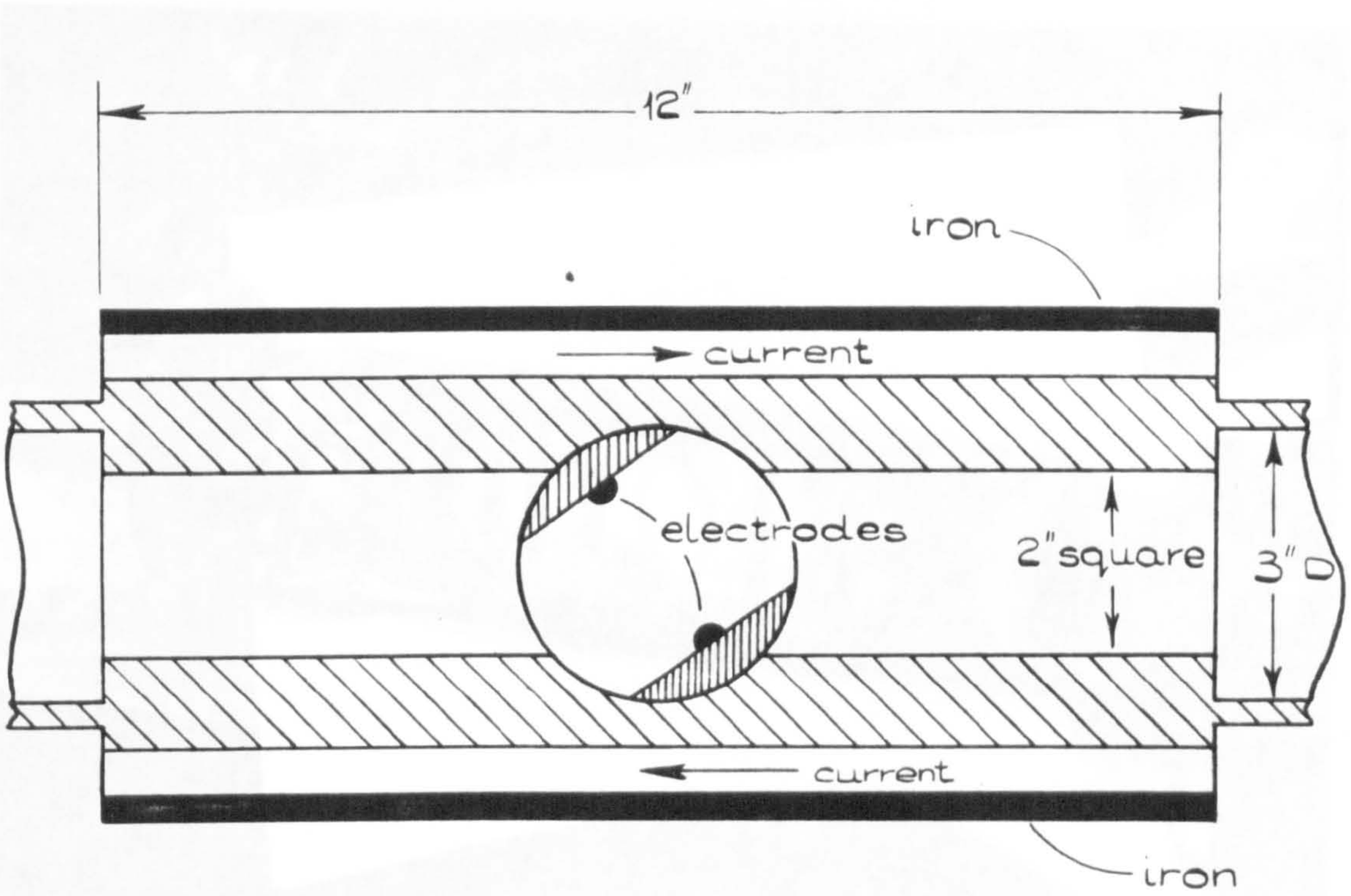

VALVE/FLOWMETER CROSS-SECTION (WITH ORIGINAL WINDINGS)

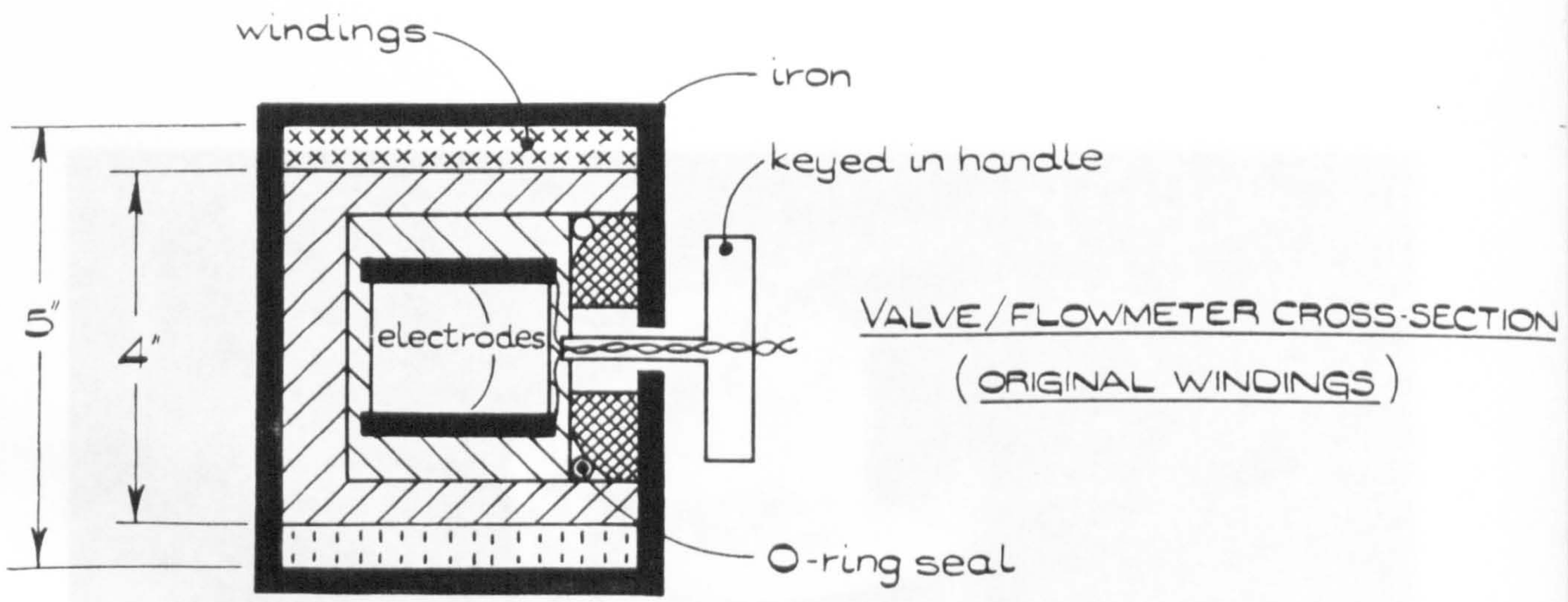

VALVE/FLOWMETER CROSS-SECTION
(ORIGINAL WINDINGS)

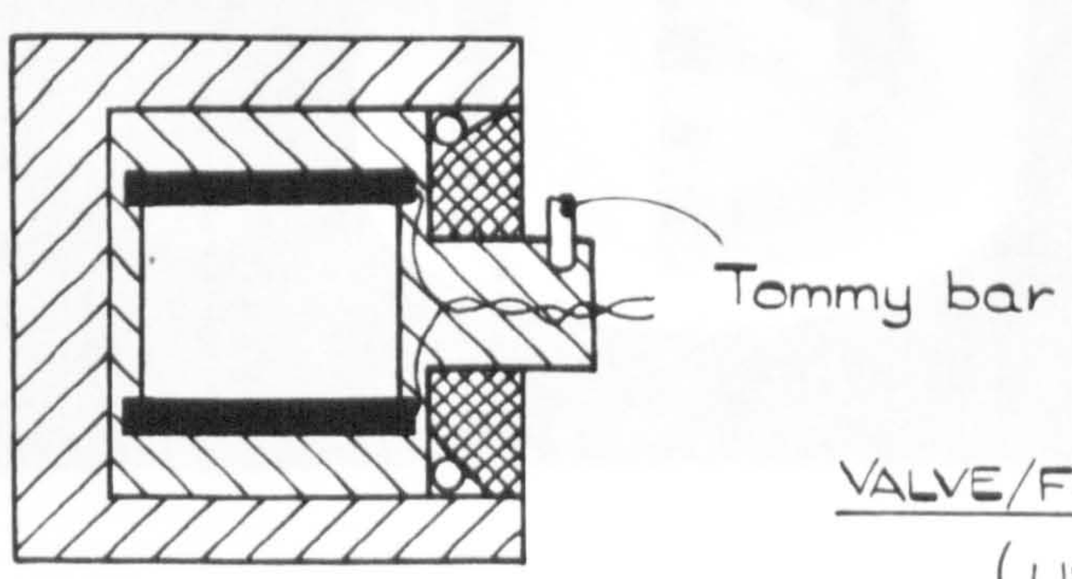

VALVE/FLOWMETER CROSS-SECTION
(USING MAGNET)

FIGURE 13.

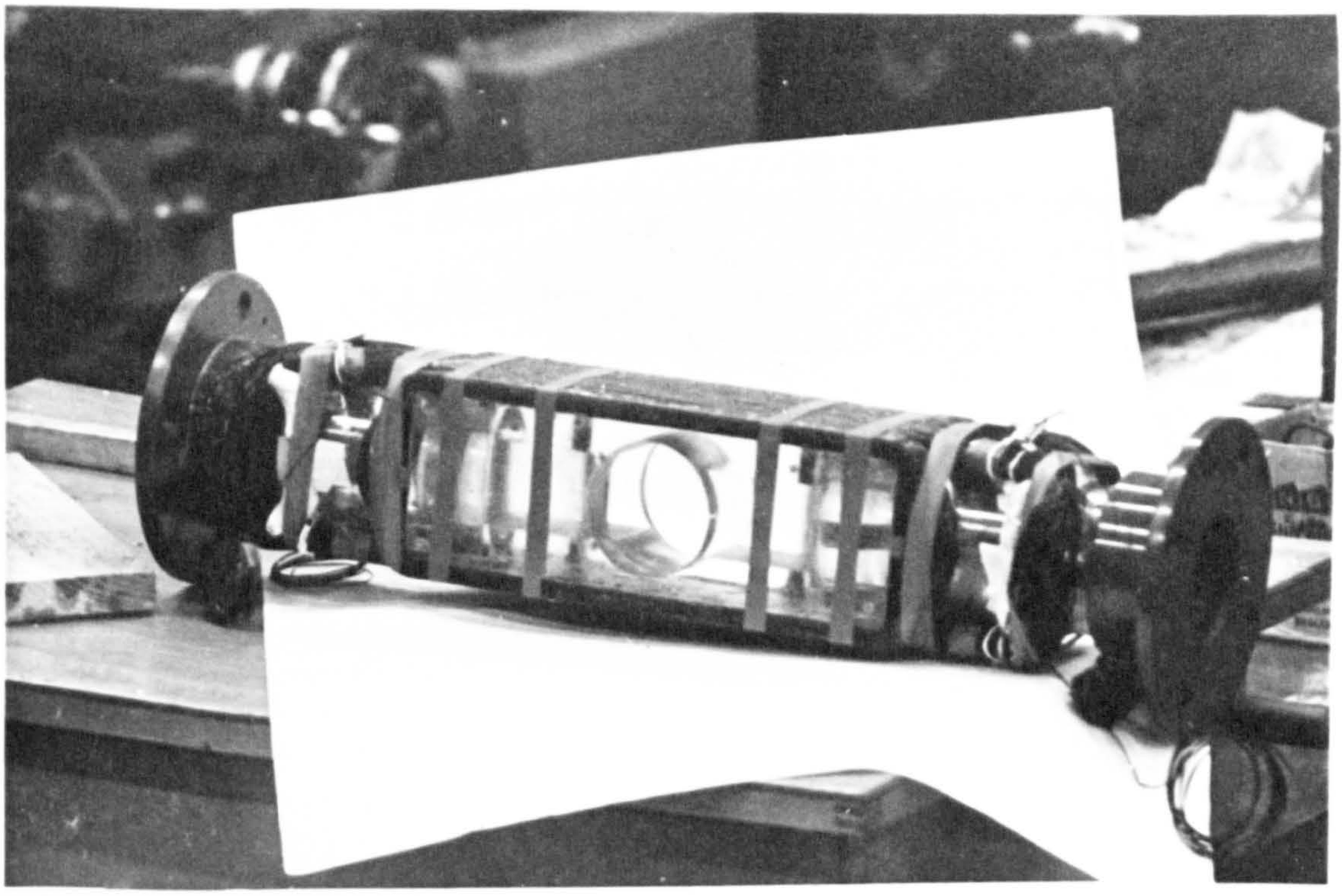

VALVE FLOWMETER WITHOUT STOP-COCK

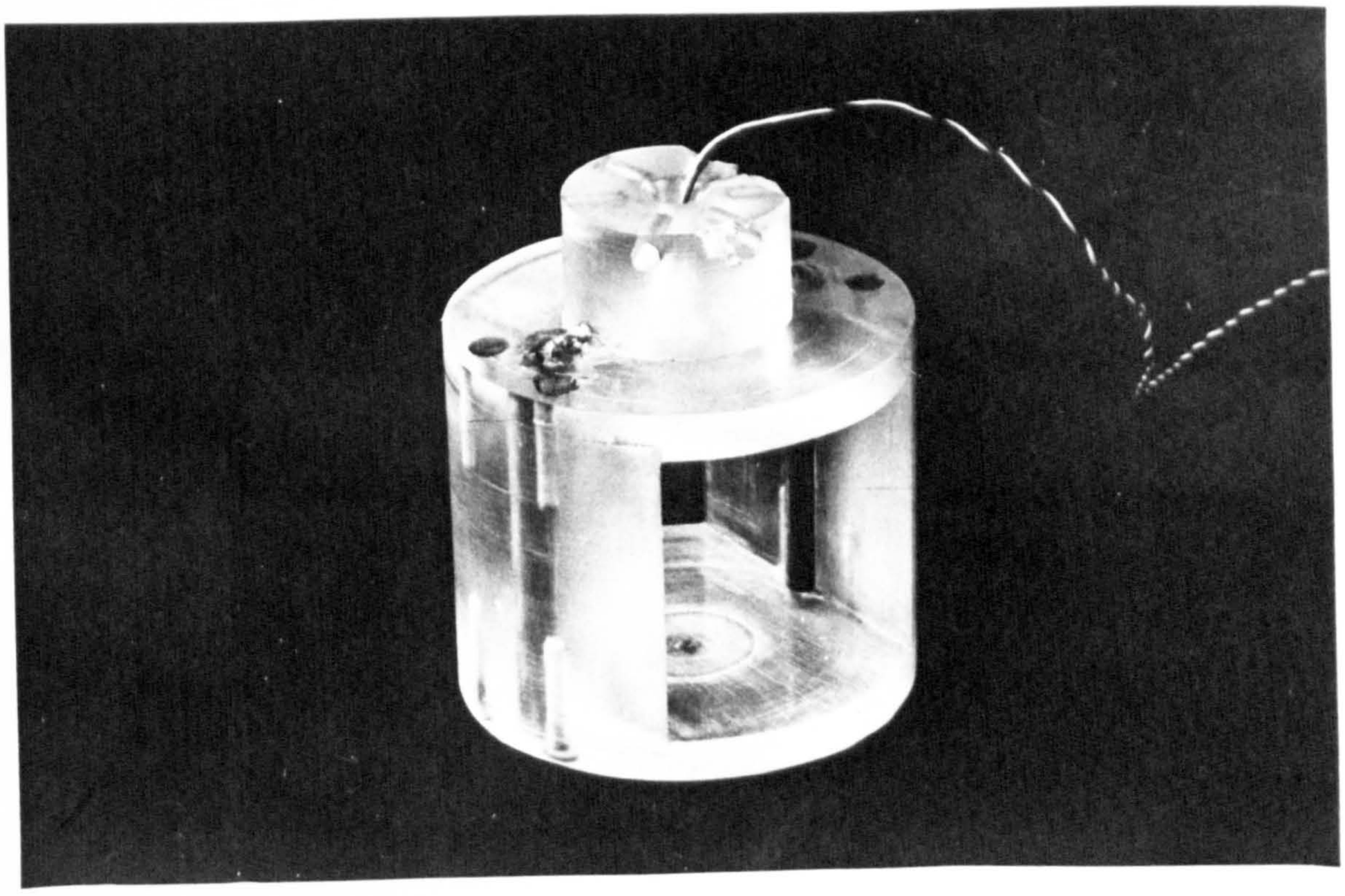

VALVE FLOWMETER STOP-COCK

FIGURE 14

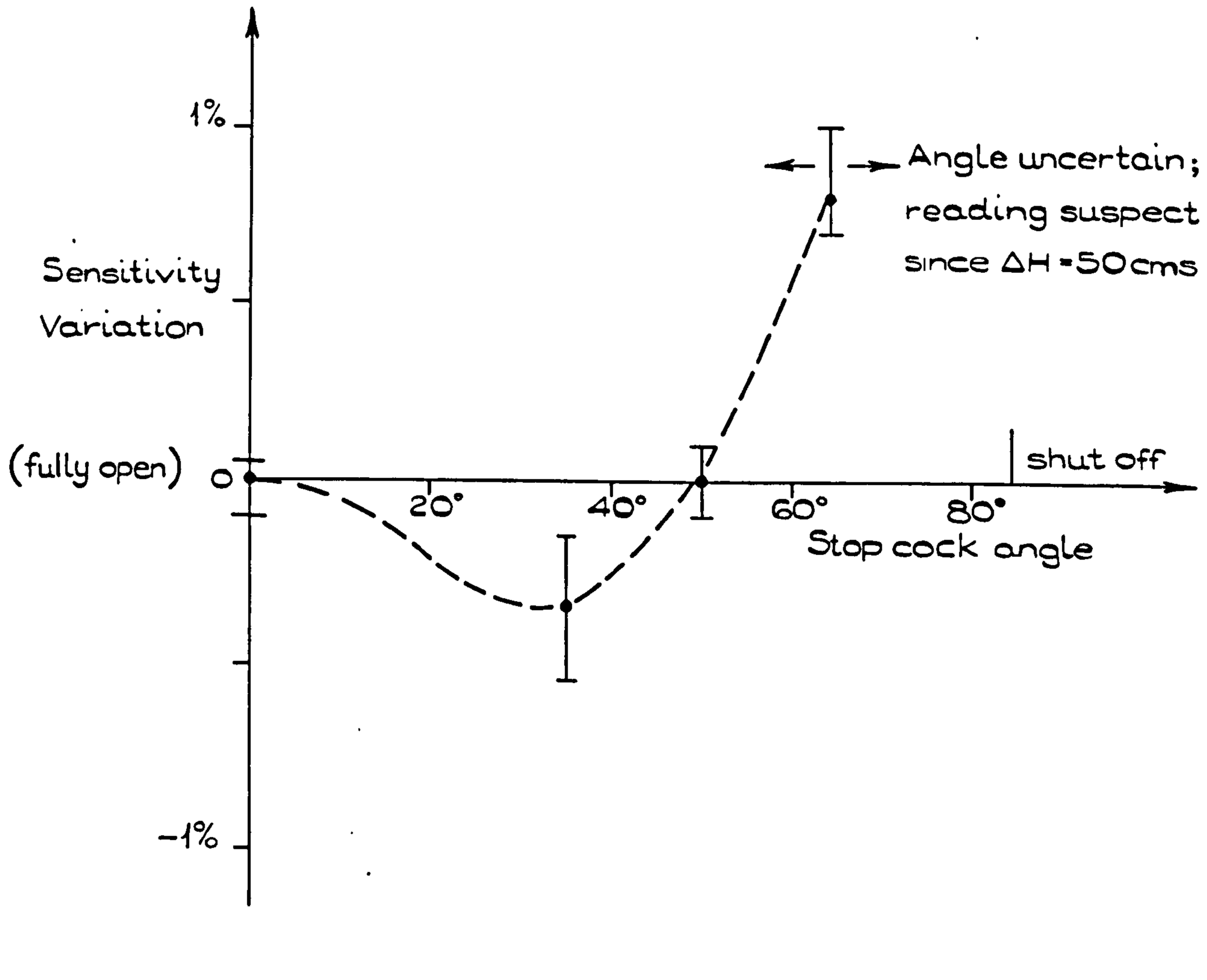

VALVE FLOWMETER SENSITIVITY DEPENDENCE ON STOP-COCK POSITION.

FIGURE 15.

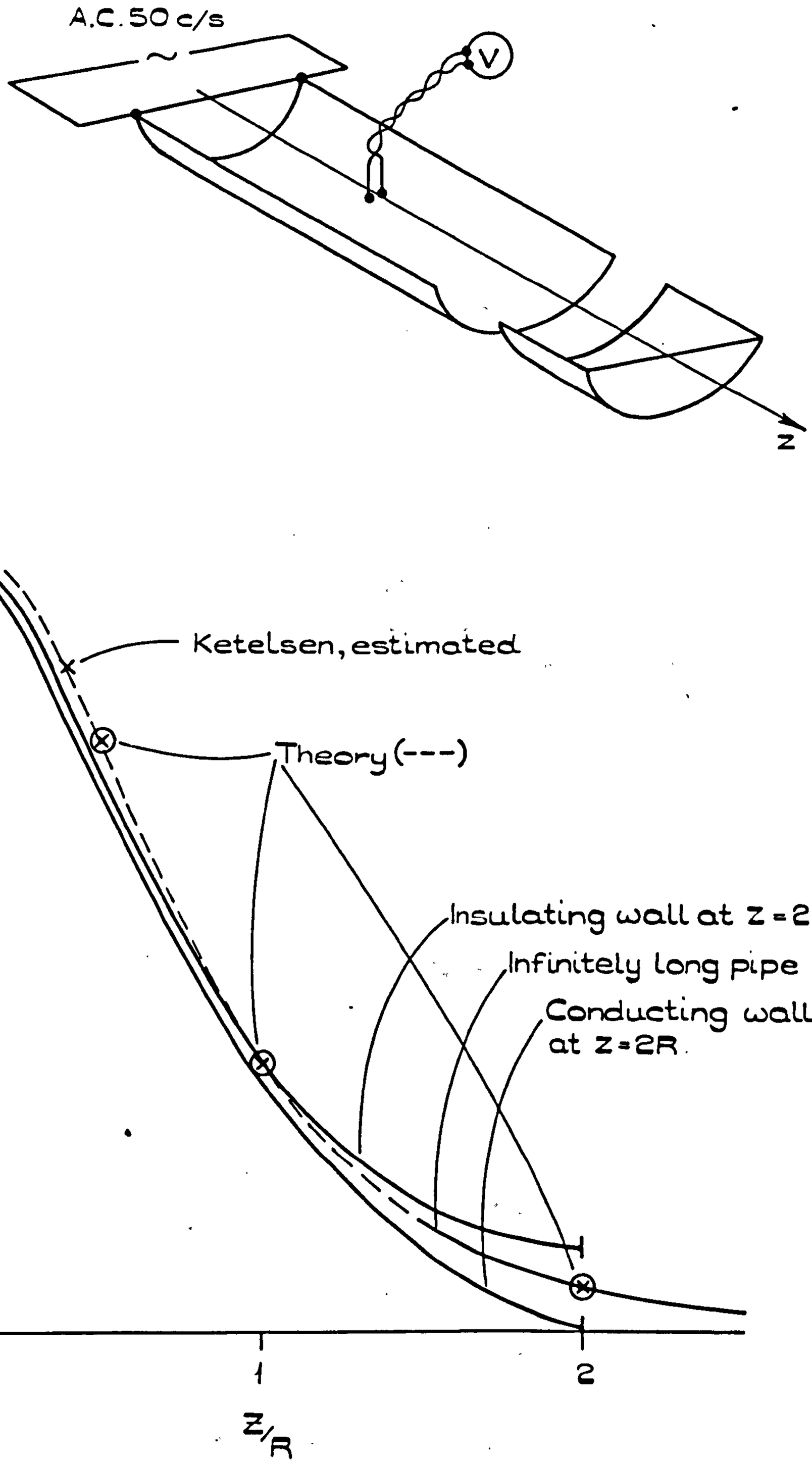

VIRTUAL CURRENT ON FLOWMETER AXIS

FIGURE 16.

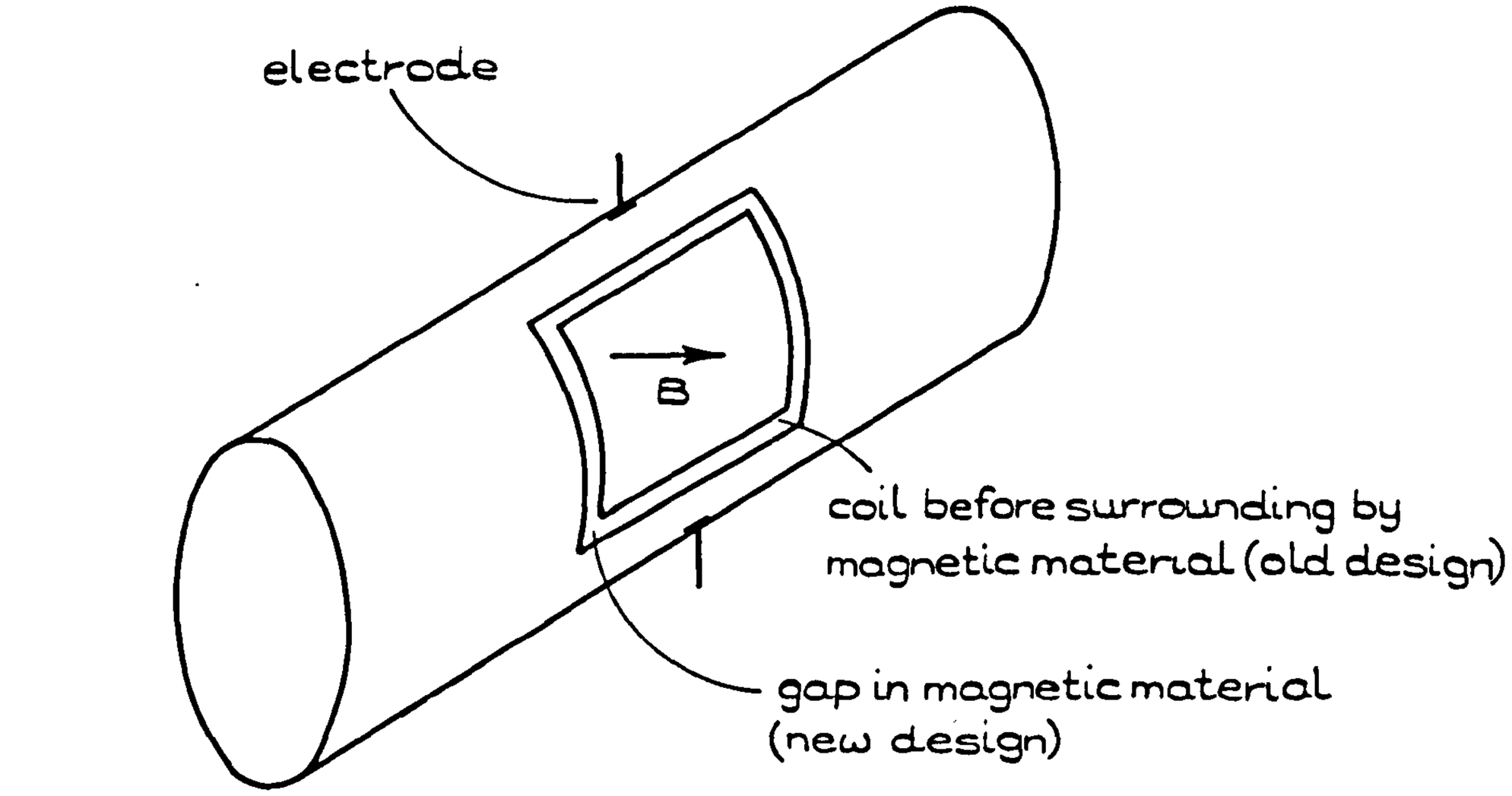

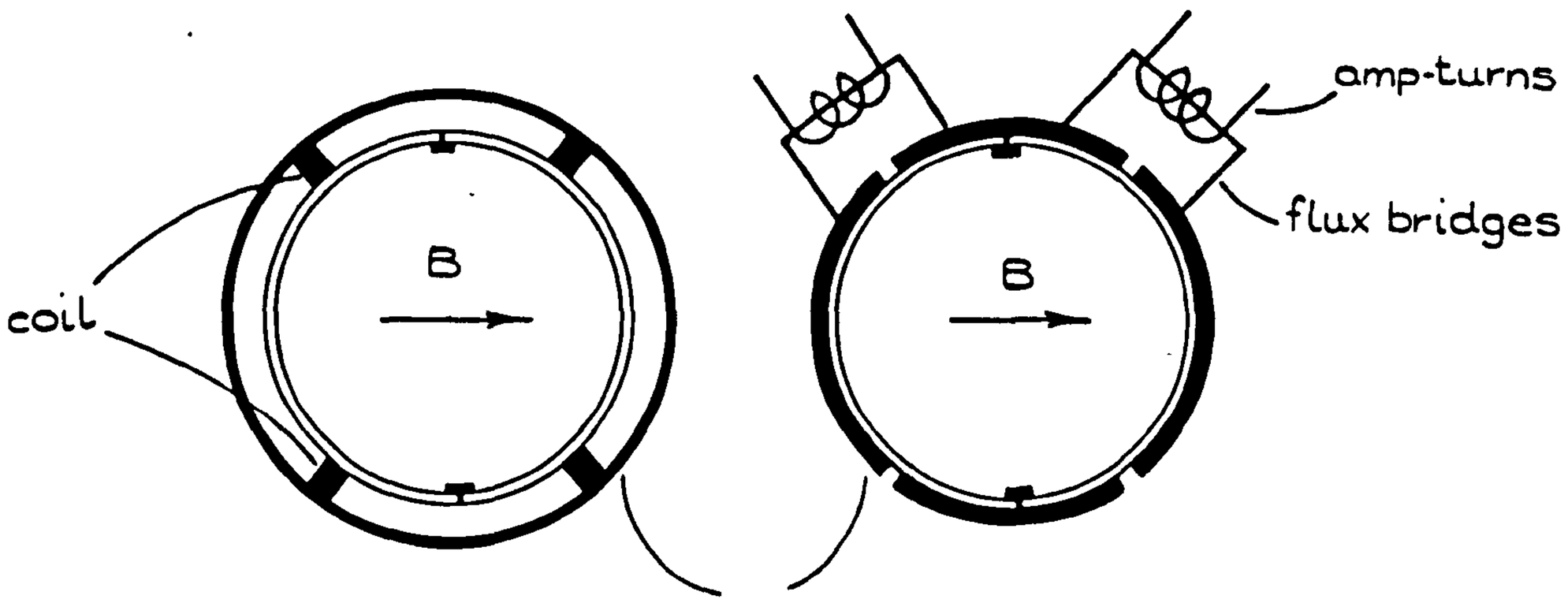

Old design New design

ALTERNATIVE MAGNETIC FIELD DESIGN

FIGURE 17.

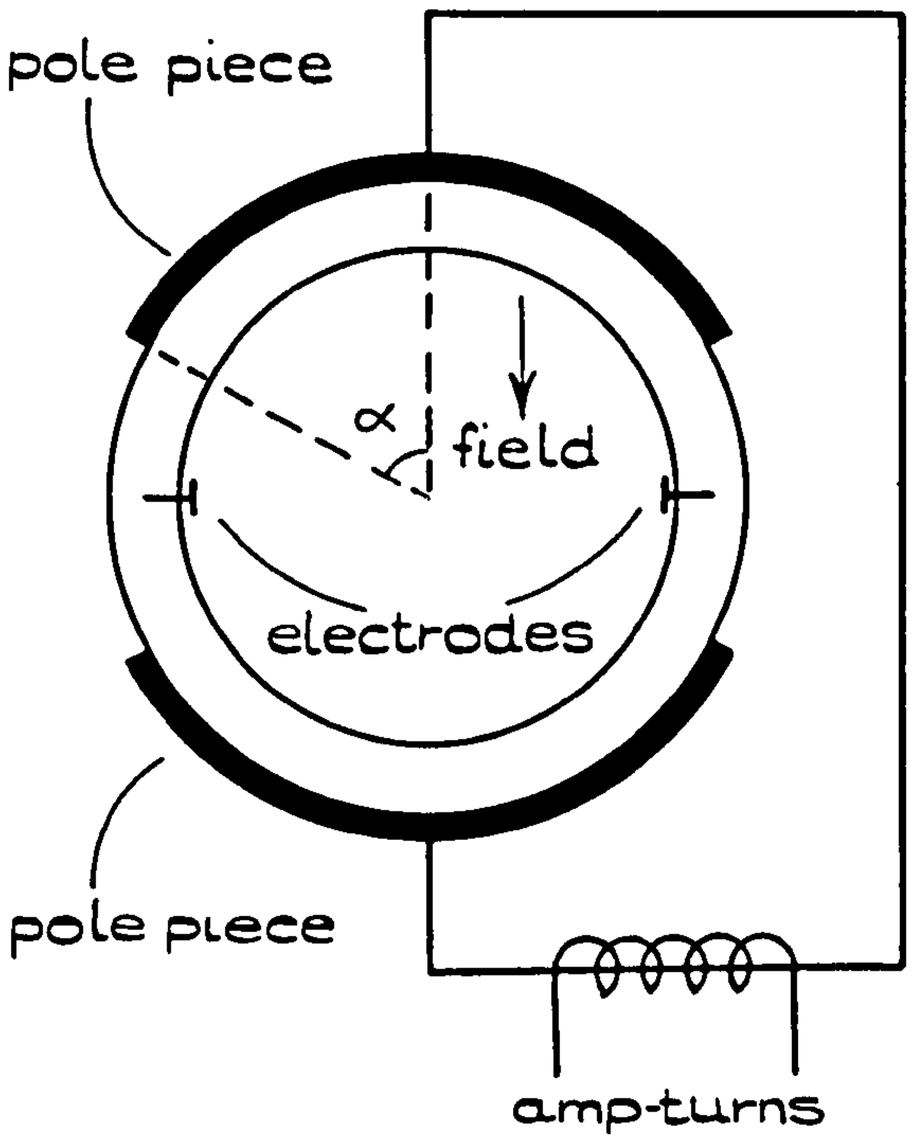

LONG VERSION: CROSS-SECTION

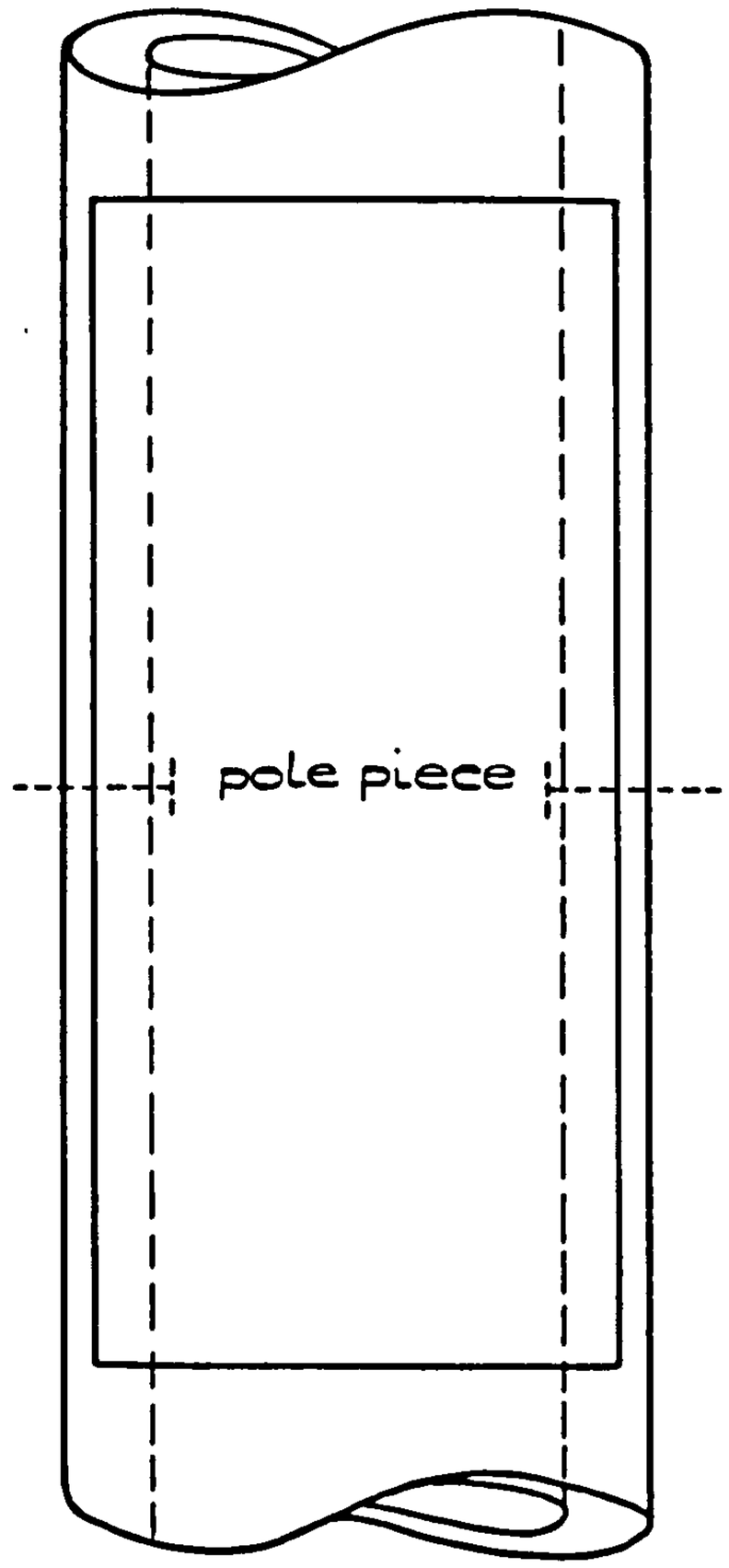

LONG VERSION : PLAN VIEW

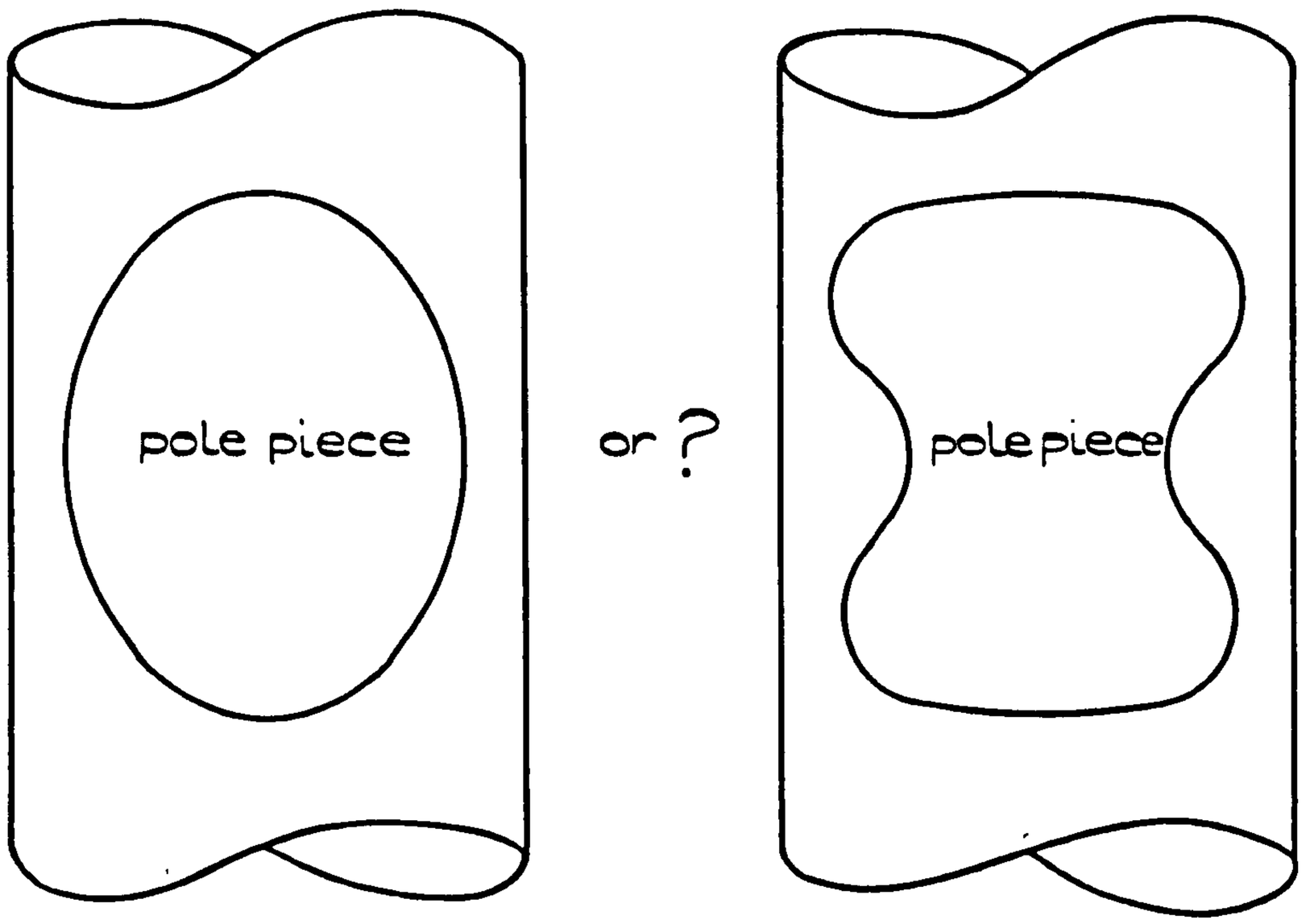

SHORT VERSIONS : POSSIBLE PLAN VIEWS

FIGURE 18

UNIVERSITY OF WARWICK

School of Engineering Science

Contributions to the theory of Induced Voltage Electromagnetic Flowmeters

Abstract

The performance of an electromagnetic flowmeter head is assessed in terms of a weight vector $\underline{W}$ and associated weight functions. The condition curl $\underline{W} = 0$ (provided $\underline{W} \to 0$ at ∞) is shown to be necessary and sufficient for the meter signal to be independent of velocity pattern. A class of such meters (called ideal) is described, but it is shown that meters with point electrodes are not ideal and a less exacting condition for them is given. Finally a class of nonideal meters is described.

Contributions to the theory of induced voltage Electromagnetic Flowmeters by MKBevir

Introduction

The principles of the induced voltage flowmeter are well known. The pipe or channel carrying the fluid is placed in a magnetic field and the voltage between suitably placed electrodes indicates the flow rate. It has become customary to define the sensitivity of a flowmeter with specified electrodes and magnetic field as

$$\frac{\text{the induced voltage between the electrodes}}{\text{the flowrate x the magnetic field at a fixed position}}$$

This definition ensures that a pro rata increase in the magnetic field at every point due to an increase of current in the field windings does not alter the sensitivity.

The sensitivity will, in general, depend on the spatial distribution of the magnetic field $\underline{B}$, the velocity $\underline{V}$ and the electrode arrangement, and the aim of the flowmeter designer is to arrange the magnetic field and electrodes so that this dependance on $\underline{V}$ disappears. In such cases the output signal will be proportional to the flowrate no matter what the form of $\underline{V}$ is. If the flow is incompressible such flowmeters, called ideal, exist, but are not in many cases practical designs. In compressible flow the idea of the sensitivity is meaningless since the flowrate Q is not uniquely defined.

These remarks refer to flowmeters of low magnetic Reynolds number, i.e. meters in which the currents induced by the motion do not distort the magnetic field appreciably. If they do, an extra nonlinearity is introduced into the problem since $\underline{B}$ now depends on $\underline{V}$. In practice this only occurs in industrial applications involving liquid metals.

This sets an upper limit to the fluid conductivity. The lowest possible conductivity is set by the largest permissible output impedance between the electrodes, and this in turn is dictated by the electronic equipment that is used for interpreting the signal. Present day practice is such that distilled water represents the bottom of the range.

Usually, then, some assumption must be made about the velocity $\underline{V}$, based on practical experience and/or the theoretical behaviour of the fluid. In the case of pipe flowmeters of circular cross-section, it has been normal to assume that the flow is rectilinear, and also axisymmetric. In these cases, where $\underline{V}$ has only a component along the pipe, we may talk of asymmetric and axisymmetric velocity profiles, and the dependance of the sensitivity on the velocity profile.

In practice, provided a certain length of straight pipe is

incorporated upstream of the flowmeter, an axisymmetric and well behaved profile (i.e. all flow in the same direction, and the profile smoothly varying with the highest velocity in the centre) may be expected.

However it is well known that for flowmeters with diametrically opposed electrodes in a nonconducting pipe and a constant transverse magnetic field the sensitivity is constant so long only as the velocity profile is axisymmetric, and these are the conditions which most designs have been based on.The sensitivity of such meters does depend on the asymmetry of the profile, though in practice the asymmetry is not as severe as might be expected. The sensitivity also depends on the exact form of an axisymmetric profile once magnetic field becomes non-uniform due to the attempts of the designer to shorten the field coils. A strictly uniform field requires very long coils, but flowmeters with short coils are cheaper to make and shorter, hence easier to install.

Until recently flowmeter design has requ: red a compromise between these two factors. However, Rummel and Ketelsen (5) have shown that deliberately non-uniform fields of the sort that would be produced by short coils can actually improve the performance of a flowmeter by rendering it more or less insensitive to asymmetric velocity profiles. Just how insensitive is being debated, but there is no doubt that performance of such flowmeters is much better than hitherto and they are also industrially desirable for the reasons given above.

Mezburd (3) has found from experiments that there seems to be more than one set of coils and magnetic field that will achieve the same result.

Clark and Wyatt (2) have tested a circular meter with point electrodes and a range of short rectangular aircored coils approximately one diameter long, and measured its sensitivity as the Reynolds number was increased and and the flow changed from laminar to turbulent. Their results show that there is a coil in the range they considered whose use would result in a flowmeter where the sensitivity did not alter with increasing Reynolds number. Such a flowmeter may not be insensitive to axisymmetric profiles in general, but would be to most practical profiles.

Such experiments show that the era of the constant field meter has passed but the extent to which specially chosen magnetic fields and electrode configurations can improve flowmeter performance needs clarification. In this paper, we provide a partial answer to this question by:

1) putting the idea of a weight function on a more rigorous basis, by introducing a weight vector $\underline{W}$ and weight functions defined from it that are suitable for different types of velocity pattern,
2) giving the condition on $\underline{W}$ for an ideal meter, and describing a class of ideal meters,
3) proving that a flowmeter with point electrodes cannot be ideal,

4) specifying a suitable weight function for point electrode meters, and

5) describing a class of mathematically simple non-ideal meters that can approximate to ideal ones.

The Weight Vector $\underline{W}$

We consider the motion of an electrically conducting fluid, with velocity $\underline{V}(\underline{r})$, inside a typical flowmeter head which supplies a magnetic field $\underline{B}(\underline{r})$. $\underline{V}$ and $\underline{B}$ both depend on the position vector $\underline{r}$. The induced electric potential U satisfies (Shercliff (6),p.12)

$$\nabla^2 U = \text{div}\,(\underline{V} \wedge \underline{B}) \quad \ldots\ldots\ldots\ldots\ldots\ldots\ldots\ldots\ldots\ldots(1)$$

Far upstream and downstream of the flowmeter head the motion of the fluid contributes very little to the potential U. We designate the volume of fluid that does contribute by τ and the surface surrounding it by S. S consists of the inside surface of the flowmeter walls and two surfaces spanning the pipe cross-section: one, far upstream, denoted by Su and the other, far downstream, by Sd.

It remains only to specify some boundary conditions on U at the surface S. The simplest, non-conducting walls on which $\underline{V} = 0$, requires $\frac{\partial U}{\partial n} = 0$ on S. This would be the case in many flowmeters, but we shall later consider flowmeters with large electrodes, and walls of variable finite conductivity, so we need a suitable boundary condition, where $\underline{V} \neq 0$ on the wall.

If the wall conductivity is σ_f, the wall thickness t and the fluid conductivity σ we write $\lambda = \frac{\sigma}{t\sigma_f}$: by walls of variable conductivity we mean variable λ. If ∇_s^2 denotes the Laplace operator in locally plane coordinates in the wall, the relevant boundary condition is

$$\nabla_s^2 U + \lambda\left[\frac{\partial U}{\partial n} - (\underline{V} \wedge \underline{B}).\,\underline{n}\right] = 0 \quad \ldots\ldots\ldots\ldots\ldots\ldots(2)$$

This condition is not as general as it could be. For the following argument it need only be linear in U and its derivatives, and would then represent any electrical arrangement on and outside the wall. The important point is that the boundary condition on ϕ, in equation 3 below, is obtained by dropping the term $(\underline{V} \wedge \underline{B}).\ \underline{n}$ in equation 2.

On the surfaces Su and Sd all derivatives $\to 0$, so the precise form of the boundary condition is not important, though in fact it will be a linear condition representing the rest of the fluid outside Su and Sd.

We now establish a formula for the potential difference between the points in the moving fluid.

Suppose the potential at the point $\underline{r}$ due to a unit pole at the point $\underline{r}'$ is $\phi(\underline{r}, \underline{r}')$, where ϕ satisfies the boundary conditions (see equation 2)

$$\nabla_s^2 \phi + \lambda \frac{\partial \phi}{\partial n} = 0 \quad \ldots\ldots\ldots\ldots\ldots\ldots\ldots\ldots\ldots\ldots\ldots\ldots (3)$$

Then denoting $\underline{V} \wedge \underline{B}$ by $\underline{P}$ the potential at the point $\underline{r}$ due to the motion is:

$$\int_\tau \phi(\underline{r}, \underline{r}')\, d\omega' \underline{P}\, d\tau' - \int_S \phi(\underline{r}, \underline{r}')\, \underline{P}.\, \underline{dS}'$$

or, using Gauss's theorem

$$- \int_\tau \nabla' \phi .\, \underline{P}\, d\tau'$$

The difference in potential ΔU between two points, e.g. two electrodes, E_1 and E_2 will be

$$(-) \int_\tau \nabla' [\phi(E_1, \underline{r}') - \phi(E_2, \underline{r}')] .\, \underline{P}\, d\tau'$$

and using Green's reciprocal theorem this may be written as

$$\Delta U = \int_\tau \nabla G .\, \underline{P}\, d\tau$$

where G is the potential due to a unit pole on E_1 and a negative unit pole on E_2 and satisfying the boundary condition (3).

Using $\underline{P} = \underline{V} \wedge \underline{B}$ we finally achieve:

$$\Delta U = \int_\tau \underline{V} .\, (\underline{B} \wedge \nabla G)\, d\tau$$

$$= \int_\tau \underline{V} .\, \underline{W}\, d\tau \quad \ldots\ldots\ldots\ldots\ldots\ldots\ldots\ldots\ldots\ldots\ldots\ldots (4)$$

Where we have denoted $\underline{B} \wedge \nabla G$ by $\underline{W}$, which by analogy with Shercliff's weight function we call the weight vector. $\underline{W}$ has dimensions volts $L^{-1}T$. (G has dimensions L^{-1}) and measures the relative contribution of $\underline{V}$ at difference places to the output signal. The integral (4) will give the correct absolute value of the signal, as long as the poles on the electrodes are unit poles.

If the magnetic Reynolds number is very small, as it will be in all except some liquid metal applications, then

$$\underline{B} = \nabla F$$

$$\text{and} \quad \underline{W} = \nabla F \wedge \nabla G \quad \ldots\ldots\ldots\ldots\ldots\ldots\ldots\ldots\ldots\ldots (5)$$

where F and G are both solutions of Laplace's equation, and div $\underline{W} = 0$ identically.

Important points to note are:

1). G is the potential due to unit flux flowing from one electrode to the other under identical electrical conditions to those in the flowmeter in normal operation, and may be obtained, as may ∇G, (apart from a scaling factor,) by imposing a fixed voltage between the electrodes and measuring the size and direction of the resulting current field. We shall call ∇G the virtual current.

2). F depends only on the magnetic field, and G only on the electrode shape and electrical geometry. In equation (5) they occupy dual positions, so that the performance of the flowmeter would be unaffected by interchanging them (apart from an

alteration in the absolute value of the signal). Whether this would be practicable is another question.

2.1 The Condition on W in ideal flowmeters

Equation (4) shows the way in which the output signal of a flowmeter depends on the flow pattern and the weight vector $\underline{W}$ as defined in equation (5). The question now arises whether there are any flowmeters in which the sensitivity is independant of the flow pattern, i.e. meters in which the signal is always proportional to flow rate irrespective of the velocity distribution. Such meters will be called ideal. In this section we state and prove a necessary and sufficient condition on $\underline{W}$ that ensures that the flowmeter is ideal, and later we examine whether there are any flowmeters where $\underline{W}$ does obey this condition.

If the fluid is incompressible (div $\underline{V} = 0$) and if the electrodes and/or magnetic field are confined ($\underline{W} \to 0$ at ∞) then the necessary and sufficient condition for the signal to depend only on the flowrate is curl $\underline{W} = 0$.

Sufficiency. If curl $\underline{W} = 0$, then $\underline{W} = \nabla t$. Also, if $W \to 0$ at ∞, $t \to$ constant at ∞, but may take different values upstream and downstream of the flowmeter head. Then from equation (4) the signal is

$$\int_\tau \underline{v} \cdot \nabla t \, d\tau \qquad \text{.....(6)}$$

$$= \int_S \underline{v} t \cdot \underline{dS} \qquad \text{since div } \underline{V} = 0$$

Now on the pipe walls, $\underline{V} \cdot \underline{dS} = 0$, and upstream and downstream t is constant, so that the signal is:

$$t \text{ (upstream)} \int_{S_u} \underline{v} \cdot \underline{dS} + t \text{ (downstream)} \int_{S_d} \underline{v} \cdot \underline{dS}$$

or (t up - t down) x the flowrate Q.E.D.....(7)

Necessity If curl $\underline{W} \neq 0$, then there is a loop C around which

$$\oint_C \underline{W} \cdot \underline{dr} \neq 0$$

Consider the flow pattern in which the fluid is stationary everywhere except along the tube of (small) constant cross-section A in the direction $\underline{dr}$. Then the velocity along this tube must be constant, since div $\underline{V} = 0$. Let it be Vo.

Then this velocity pattern, which produces no flowrate, gives rise to a signal:

$$A V_o \oint_C \underline{W} \cdot \underline{dr}$$

Where $\underline{V} \, d\tau = V_o A \, \underline{dr}$ has been substituted in equation (4). Thus $\oint_C \underline{W} \cdot \underline{dr}$ must be zero around every possible loop C, i.e. by Stokes theorem curl $\underline{W} = 0$.

2.2 Long flowmeters

In flowmeters where F, G, and $\underline{v}$ are not permitted to vary in the flow direction the only component of $\underline{W}$ is in this direction, the z -

direction in figure 3, and the condition curl $\underline{W}$ = 0 reduces to W_z = constant.

More generally we only require two of F, G and $\underline{v}$ to be independant of z, since we may perform an integration w.r.t. z on the third as part of the volume integral in equation (4).

If F and G are independant of z, then the flowmeter is ~~ideal~~ long anyway, but if $\underline{V}$ and either F or G, say F, are independant of z, then the problem becomes that of making W_z constant, where $\underline{W}$ is defined in terms of F and $G^1 = \int_{z=-\infty}^{z=+\infty} G \, dz$.

In the particular case of an axisymmetric profile V_z (r) and a constant magnetic field (∇F = const), we may do the integration w.r.t. to θ as well in equation (4) and, using the fact that the average value of a plane solution of Laplace's equation (in this case G^1) over a circle is the value at the centre of the circle, see that G^1, and hence G, is arbitrary.

Thus, provided the magnetic field is constant, and the velocity profile axisymmetric, the sensitivity of a meter with electrodes of any shape is independant of the profile.

3. Ideal flowmeters (for which curl W = 0)

We must now investigate whether there are flowmeters for which curl $\underline{W}$ = 0. This is initially a mathematical problem. Do solutions of Laplace's equation F and G exist such that (see equation 5)

$$\text{curl } (\nabla F \wedge \nabla G) = 0 \quad \ldots\ldots\ldots\ldots\ldots\ldots\ldots\ldots (8)$$

If this is the case, we must then consider the practical difficulties of producing the necessary F and G. F (giving the magnetic field) will not be difficult, since any non-singular magnetic field may be produced by suitable coils distributed around the flowmeter. In most cases G is dictated by practical considerations, and without great inconvenience little can be done to alter it.

In the appendix we give two sets of F and G that satisfy equation (8) and also show that for certain G (approximating to the case of point electrodes) there exists no F such that (8) is satisfied. The enumeration of possible F and G is incomplete, since we have not been able to show that there are definitely no other cases than the two sets given.

The first of the two sets is useless for practical purposes, since F and G both $\to \infty$ at ∞. The second, however, is not only very simple, but also provides us with a class of ideal flowmeters that have some very remarkable properties.

In these meters either ∇F or ∇G must be constant, and the other lie in planes perpendicular to it. We shall consider the case of constant ∇F (constant magnetic field B_o). There is a dual set of flowmeters with

constant ∇G, but the dual of the case when there is more than one set of electrodes and a constant magnetic field is of little practical use.

The requirement that ∇G is perpendicular to the magnetic field, Bo, means that all sections through the flow channel perpendicular to the magnetic field must be the same, i.e. the flow channel must be a cylinder with generators parallel to the field and with insulating walls perpendicular to the field at either end. A simple form of meter is shown in figure 1.

With G, a plane solution of Laplace's equation, we may associate a stream function ψ_g. Then

$$\underline{W} = Bo \nabla \psi_g \quad \ldots\ldots\ldots\ldots\ldots\ldots\ldots\ldots\ldots\ldots\ldots\ldots\ldots\ldots(9)$$

$Bo\,\psi_g$ is in fact the function t of equation (6).

The condition that unit flux (per unit width) emerge from an electrode gives, in the notation of equation (7)

$$\psi\,(\text{upstream}) - \psi\,(\text{downstream}) = 1$$

and substituting this in (7) we find that the output signal is:

Bo x the flow rate per unit width.

The sensitivity of the meter is thus independant of its shape, (provided it is of constant width) and depends only on the magnetic field. The shape may be changed without altering the sensitivity; indeed it may be changed while the flowmeter is operating, and if suitable (cylindrical) moving flaps, arms etc. are provided be used as a valve at the same time. There is no restriction on the number of entrances and exits and each may be provided with its own valve and set of electrodes. Such a device could be used as a multiple metering valve: figure 2 shows an example incorporating most of the possible features.

The distance over which the magnetic field must be kept constant is important. This depends on the flowmeter: more precisely on the distribution of the streamlines of constant ψ_g. Consider the simple flowmeter in figure (1). As a rough guide as long as the field is constant between the lines $\psi_g = 0.005$ and $\psi_g = 0.995$ (i.e. for 99% of the flux between the electrodes) then the signal will be at least 99% of what it should be. In practice B will alter gradually and the extra regions containing 1% of the flux will contribute to the signal (with the right algebraic sign if the flow is well behaved) so some non-uniformity of the magnetic field may be tolerated at the edges of the 99% region.

In the case of the flowmeter in figure (2) the addition of extra entrances actually prevents the lines of constant ψ_g from spreading out as far as in the case in figure (1). Each set of electrodes must be considered individually, but it can be seen that the extent of the uniform

magnetic field need not be quite as great as in the case in figure 1. The accuracy of these flowmeters will depend, among other things, on

1). the uniformity of the magnetic field,

2). the accuracy of manufacture,

3). the validity of the assumptions about the fluid e.g. that its conductivity is constant.

In fact, if the velocity $\underline{V}$ was invariant in the magnetic field direction, then there would be no currents, since curl $(\underline{V} \wedge \underline{B}) = 0$, and the conductivity would be immaterial. In practice $\underline{V}$ drops to zero on the side walls. The currents flowing are due entirely to the effect of boundary layers on the side wall.

This class of meters, where $\underline{B}$ is uniform and the boundary conditions invariant in the $\underline{B}$ direction, may also be proved ideal by integrating (1) and the condition div $\underline{V} = 0$ in the direction of $\underline{B}$ and noticing that curl $(\underline{V}^1 \wedge \underline{B}) = 0$, where $\underline{V}^1$ is the resulting integral of $\underline{V}$.

The lines of constant ψ_s for the flowmeter in figure 1 are shown in Bewley (1) figure 37, page 55. The distance between the lines enclosing 99% of the flux is 3.1 W at the centre line: for 90% and 99.9% the figures are 1.6W and 4.7W. For flowmeters with large electrodes similar details may be found in Rossow (4). In both cases the flux lines have been required for purposes other than flowmetering.

For more complicated shapes, flux plotting is probably the easiest way of finding the lines of constant ψ_s especially in combined meters and valves where the geometry is variable.

4.1 Flowmeters with point electrodes

Flowmeters with point electrodes set in a nonconducting wall are not ideal in the sense we have defined. If R is the distance from a point electrode and d a typical dimension of the flowmeter cross-section, e.g. a radius of curvative of the wall at the electrode, then for $R \ll d$ (and $\gg$ the electrode dimensions)

$$G = -\frac{1}{4\pi R} + O\left[\frac{\log R}{d}\right]$$

In the appendix we make this assumption, that near the electrodes G behaves like $\frac{1}{R}$, and show that for this G there is no nontrivial magnetic field $\underline{B}$ that satisfies curl $\underline{W} = 0$. This indicates that flowmeters with point electrodes cannot be made ideal.

This being the case, we must make some assumptions about the velocity $\underline{V}$. If we assume that the flow is rectilinear, i.e. only V_z in figure (3) is non-zero, then since div $\underline{V} = 0$ implies $\frac{\partial V_z}{\partial z} = 0$ we must have (writing $d\tau = r\,d\theta\,dr\,dz$ in equation (4))

$$\bar{W}(r,\theta) = \int_{-\infty}^{\infty} W_z\, dz$$

constant if the sensitivity of the meter is to be independant of the

form of $V_z(r,\theta)$.

If we may further assume that V_z is axisymmetric as it may be in flowmeters with circular cross-section, i.e. $\frac{\partial V_z}{\partial \theta} = 0$, then we only require

$$\overline{W}'(r) = \frac{1}{2\pi}\int_0^{2\pi} \overline{W}\, d\theta$$

constant.

These two conditions are necessary for the flows with asymmetric and axisymmetric profiles mentioned in the introduction.

The effect of swirl in circular flowmeters.

Flowmeters that only satisfy the conditions $\overline{W}(r,\theta)$ or $\overline{W}'(r)$ constant will be affected by the presence of swirl velocity components V_r and V_θ, which contribute nothing to the flow rate, but may contribute to the signal. Due to the symmetry we may expect in $\underline{W}$, however, some forms of swirl will contribute no signal.

In a circular flowmeter with diametrically opposed point electrodes and symmetrical coils (i.e. where any movement that either leaves the electrodes where they were or at most interchanges them leaves the appearance of the meter unchanged) changing θ to $\pi + \theta$ does not alter W_r or W_z, and W_r is even in θ, W_θ odd.

The largest swirl component will very likely be $V_r = 0$, $V_\theta = f_n(r,z)$. Owing to the symmetry in W_z this contributes nothing. Nor would swirl where $V_r = 0$, V_θ even in θ, though if V_θ were odd in θ it would. These cases would arise in flowmeters with a bend upstream, when in the former the electrode axis lay in the plane of the bend, and in the latter was perpendicular to it.

4.2 Flowmeters based on certain choices of F and G suitable for axisymmetric profiles.

These meters are not particularly practicable, but are based on some mathematically simple choices of F and G, and the use of a mean value theorem, used before, which states that the average value (taken over a circle) of plane solutions of Laplace's equation is the same as the value at the centre of the circle. If we can show, therefore, that $\overline{W}(r,\theta)$ is a solution of Laplace's equation, then $\overline{W}'(r)$ is constant.

In figure (4a), consider circular flowmeters, and choose

$$F = F(x, z)$$
$$G = G(x, y)$$

This choice of G implies infinitely long electrodes of arbitrary shape and disposition, which in practice, for suitable F, need only be about three flowmeter diameters long. A suitable F would be the function G of figure (1), modified to put the singularities outside the flowmeter. The coils (surround by high permeability iron) required to produce any magnetic

field are simple to define. The field is schematically shown in figure 4a.

The important point about these F's is that there is net flux across the flowmeter and that, being plane, with no component in the electrode directions there is an associated stream function ψ_F such that

$$\frac{\partial \psi_F}{\partial x} = \frac{\partial F}{\partial z} \quad , \quad \frac{\partial \psi_F}{\partial y} = - \frac{\partial F}{\partial x}$$

and $$\left[\psi_F \right]_{z=-\infty}^{\infty} = \text{constant}$$

this constant being the flux/unit length from the poles of F.

Using equation (5) for Wz and these equations we find

$$\overline{W}(r,\theta) = \left[\psi_F \right]_{z=-\infty}^{+\infty} \frac{\partial G}{\partial y}$$

Since $\frac{\partial G}{\partial y}$ is Laplacian, $\overline{W}'(r)$ is constant.

$\overline{W}(r,\theta)$ is same as W_z would be for a long flowmeter with the same electrodes and a constant magnetic field, and the results for long flowmeters can therefore be applied. For line electrodes, the distribution of $\overline{W}(r,\theta)$ is that shown on page 29 of (6). It is possible, using walls of variable conductivity (not easily realised in practice) to make $\frac{\partial G}{\partial y}$ constant, thus making $\overline{W}(r,\theta)$ constant (and incidentally curl $\underline{W} = 0$, so that these meters are ideal). The most practicable approximation to constant $\frac{\partial G}{\partial y}$ in circular flowmeters is to use large diametrically opposed (long, in the sense used above) electrodes which each cover 1/4 of the meter circumference.

The same approximation as above may be achieved by using a constant magnetic field and 1/4 circumference line electrodes. Both approximations may be regarded as duals of each other. In the first case an ideal square flowmeter, with large electrodes top and bottom and a plane magnetic field is physically distorted until it is circular; in the second case the meter shown in figure (1) is similarly distorted.

Conclusions

Firstly, it is possible to make a flowmeter ideal, in the sense defined, without having a rectangular channel, uniform field and large long electrodes. Some of these features are still needed, and the main industrial disadvantages are big electrodes, which may become partially covered with insulating deposits, quasi-rectangular channels and the need for a uniform field, though this last problem can be considerably eased by careful shaping of the flow channel. Since the resulting flowmeters can be used as valves as well they may have some specialised applications.

Secondly insistance on the use of point electrodes means that the resulting meter cannot be ideal. Considerable discussion in the appendix

is given to showing that it is just possible to cope with rectilinear flow of arbitrary profile, the broad conclusion being that to do this extreme complication of the field coils is necessary.

Thirdly the only ways that seem to be at present available for approximating an ideal flowmeter in a circular pipe (if this was necessary, immediately after a valve for instance) are to use one of the two meters with quarter circumference electrodes mentioned at the end of 4.2 and shown in figure 4b. The meter with line electrodes might also admit the use of a butterfly valve in the middle without too serious an effect on its performance. Just how serious would be a matter for experimental testing.

Future developments

In this paper I have only been concerned with showing, sometimes not conclusively, what is possible and not possible, but have not given any means of predicting the performance of a flowmeter with point electrodes and a given magnetic field. In another paper (7) I have given formulae for $\overline{W}$ and $\overline{W}'$ when the magnetic fields are produced by rectangular coils (and other simple coil shapes) wrapped around the flowmeter and surrounded by high permeability iron. A set of tables for $\overline{W}'$ have been produced on a digital computer that reduce the problem of coil design for axisymmetric profiles to looking up a few judiciously chosen figures in the tables and doing a few sums. I have not been at pains to demonstrate that it is possible to make $\overline{W}'$ constant since there are an infinite number of ways of doing so, and the tables confirm this.

Tables for $\overline{W}$ could be produced, but they would be too bulky to handle, and, as the discussion in the appendix shows, the design problem here is much more difficult and requires optimising numerically on the computer. In this case there is not much point in printing out the entire information only to feed it back in again.

At some stage I hope to publish some fairly comprehensive investigations of long flowmeters. Chronologically they precede this work, and the possibilities can be much more clearly defined, but by their very nature (long) they are not of great practical interest.

We are doing some experimental work, mainly on a three inch diameter plastic flowmeter with point electrodes, to check theoretical predictions, but we are also building an elementary valve-flowmeter to establish the principle, with electrodes that rotate with the valve.

Acknowledgment

I wish to acknowledge the advice and criticism of Prof.J.A.Shercliff, the interest shown by George Kent Ltd., and the financial support of the

English Electric Co. Ltd.

Appendix

Cases where curl W = 0

Equation (8) is satisfied (excluding interchanging F and G) if:

1) $F = x^2 - y^2$

$G = y^2 - z^2$

(x, y and z may be interchanged)

2) ∇F = constant, and ∇G lies in the plane perpendicular to ∇F.

The behaviour of W near a point electrode

We first show that using point electrodes no magnetic field can be chosen so that curl $\underline{W} = 0$. Secondly we examine the behaviour of $\overline{W}$ near the electrode. In both cases we make the assumption that

$$G = -\frac{1}{R}$$

following the notation in figure 5 where (R,θ,ϕ), (r,ϕ,z), (x,y,z) are spherical, cylindrical and cartesian coordinates with their origin at the electrode.

Firstly, assuming $G = -\frac{1}{R}$, and an unknown F satisfying Laplace's equation, calculation shows that

$$\underline{W} = \frac{1}{R^2}\left[0, -\frac{1}{\sin\theta}\frac{\partial F}{\partial \phi}, \frac{\partial F}{\partial \theta}\right] \qquad \ldots\ldots\ldots A1$$

and the three components of curl $\underline{W} = 0$ lead to

$$\sin\theta \frac{\partial}{\partial \theta}\left(\sin\theta \frac{\partial F}{\partial \theta}\right) + \frac{\partial^2 F}{\partial \phi^2} = 0 \qquad \ldots\ldots\ldots A2$$

$$\frac{\partial}{\partial R}\left(\frac{1}{R^2}\frac{\partial F}{\partial \theta}\right) = 0 \qquad \ldots\ldots\ldots A3$$

$$\frac{\partial}{\partial R}\left(\frac{1}{R^2}\frac{\partial F}{\partial \phi}\right) = 0 \qquad \ldots\ldots\ldots A4$$

Since $\nabla^2 F = 0$ as well, A2 may be written

$$\frac{\partial^2}{\partial R^2}(RF) = 0 \qquad \ldots\ldots\ldots A5$$

A3 and A4 show that $\frac{\partial}{\partial R}\left(\frac{F}{R^2}\right) = f_n(R)$

i.e. $F = f_n(R) + R^2 f_n(\theta,\phi)$

A5 then shows that the $f_n(\theta,\phi)$ must be zero and F be of the form

$$A + \frac{B}{R}$$

This magnetic field, apart from having a pole at the electrode, makes $\underline{W} = 0$.

Secondly, $W_z = -W_\theta \sin\theta$

$$= \frac{1}{R^2}\frac{\partial F}{\partial \phi}$$

so that $\overline{W}(r,\phi) = \int_{-\infty}^{\infty} W_z\, dz = \frac{1}{r^2}\int_0^{\pi} \frac{\partial F}{\partial \phi}\sin\theta\, d\theta \qquad \ldots\ldots\ldots A6$

It is clear ∇F must be zero at R = 0, and since it must also be well behaved there, F may be expanded in a series of associated legendre functions. F must be odd in ϕ, and even in $\pi/2 - \theta$ (figure 5).

This restricts the choice to

$$F = R^2 \left[\phi \, P_2^0(\cos\theta) + P_2^2(\cos\theta) \sin 2\phi \right]$$ + terms in higher powers of R. A7

The first term is not strictly admissable, since F is not single valued w.r.t. ϕ, but may be approximated to if the current windings are very close to the electrodes. The two terms are more easily recognised as the elementary solutions of Laplace's equation $\frac{1}{2}(2z^2 - r^2)$ and 6 xy.

The first term in A7 diverges when integrated in A6, contributions from large z giving a logarithmic type integral. The solution is not accurate for large z, however, since the terms in higher powers of R in A7 have an effect.

The important point is that in both cases the $\frac{1}{r^2}$ factor in A6 disappears and the first solution yields $\overline{W}$ = divergent integral (constant)

the second yields $\overline{W}$ = constant x $\cos 2\phi$.

So for $r \ll$ the thickness of the flowmeter walls $\overline{W}$ varies as $\cos 2\phi$ and for $r \gg$ the wall thickness might be made uniform, provided that in both cases $r \ll$ the characteristic size of the flowmeter.

If the magnetic field produced by any reasonable coil configuration is adjusted so that it is zero at the electrodes, then the second term in A7 will arise naturally. In theory it would be possible to suppress this term by making the field vanish to a higher order in R, so that $\overline{W} \to 0$ at the electrodes, and then, by making the walls very thin near the electrodes and placing the necessary windings just outside them to conjure up the first term in A7.

The coils required to produce this term are sketched in figure 6a. We have to assume the walls are infinitely thin, so that the coils lie, in figure (5), in the plane x = 0 and are the lines of constant $\frac{1}{2}(2z^2 - r^2)$. This becomes $\frac{\pi}{4}(2z^2 - y^2)$ for $y>0$, $-\frac{\pi}{4}(2z^2 - y^2)$ for $y<0$ giving an odd sort of singularity on the line y = 0.

In the absence of attempts to use such coils, $\overline{W} \propto \cos 2\phi$ as long as the magnetic field is zero at the electrodes. This unsatisfactory situation, which is no improvement over the situation in long flowmeters, can only be resolved by making some assumption about the velocity profile near the electrodes. It is reasonable to suppose that near the wall the velocity depends only on the distance from the wall: in figure (5) that V_z depends only on x. We may then integrate $\overline{W}$ w.r.t. y and find that its value is the same as on the flowmeter walls viz -1.

The aim of the flowmeter designer should therefore be, in the absence of more sweeping approximations, to make $\overline{W}$ uniform, 1 say, over most of the electrode plane but on the electrode diameter drop sharply to -1 as the electrode is approached, since this will make $\overline{W} = 1$ on the

flowmeter wall near the electrode.

I am not yet sure to what extent it is possible to make $\overline{W}$ uniform over the rest of the cross-section:the following arguments are speculative. If G had no singularity at the electrodes then it would be possible to adjust the shape of the magnetic field coils to make $\overline{W}$ uniform everywhere. One may convince oneself of this as follows:

Suppose the magnetic field is produced by specifying the value of F, the magnetic potential, on a surface surrounding the flow meter. This surface distribution of F gives rise to a distribution of W over the flowmeter cross-section, which may be made uniform by suitably adjusting the values of F on the specified surface.

This adjustment would probably be done numerically. That the specification of F may differ in detail does not alter the argument. For ease of manufacture, approximations in the form F might be necessary. Now the worse behaved G is at the electrodes the more difficult this numerical adjustment would become, probably resulting in high numerical values of F oscillating in sign and producing a low net field that varies sharply near the electrodes.

When G becomes singular at the electrodes the numerical process would not work, since uniform $\overline{W}$ now requires a discontinuous magnetic field. The singular behaviour of W must tolerated if the magnetic field is produced by coils outside the pipe.

The argument above does no more than suggest the existence of well behaved magnetic fields that would give uniform $\overline{W}$ for well-behaved G, and it would be more convincing if we could produce an explicit formula for F when given a simple form of G. The most useful case is $G = \frac{1}{R}$, the difference between this case and the original assumption that $G = \frac{1}{R}$ being that we are now considering regions not particularly close to the electrodes. The necessary F is again given by the first term of A7.

Since the G for the practical case diametrically opposed point electrodes is still dominated by the term $\frac{1}{R}$ even some distance from the electrodes, the suggestion is that a suitable geometry for the coils of a flowmeter (surrounded by high permeability iron) is found by utilising the coil distribution in figure 6a at each electrode and joining them together, as in figure 6b. The exact shape of such coils must be predicted using the exact solution for G, but this analysis does suggest what form of coils to try.

With such coils we may expect $\overline{W}$ to be singular in regions near the electrodes of the same order of size as the wall thickness, and more or less uniform elsewhere. The small coils are necessary to make the magnetic field at the electrodes zero.

References

1.	L.V.Bewley	1963	"Two Dimensional Fields in Electrical Engineering" Dover Pub. Inc.
2.	Delia M.Clark & D.C.Wyatt	1967	"The Effect of Magnetic Field Inhomogeneity on Flowmeter Sensitivity". Electromagnetic Flowmeasurements Symposium. Oslo.
3.	V.Mezburd	1968	Private Communication.
4.	V.J.Rossow	1960	Rev.Mod.Phys. 32.4. p.987
5.	Th.Rummel & B.Ketelsen	1966	"Practical Electromagnetic Flowmeasurement using Non-uniform Fields" (trans.) Regelungstecknik •6, p.262.
6.	J.A.Shercliff	1962	"The Theory of Electromagnetic Flowmeasurement" C.U.P.
7.	M.K.Bevir	1968	"Some Design Data for Induced Voltage Electromagnetic Flowmeters with Non-uniform Fields. M.H.D.Symposium. (Riga)

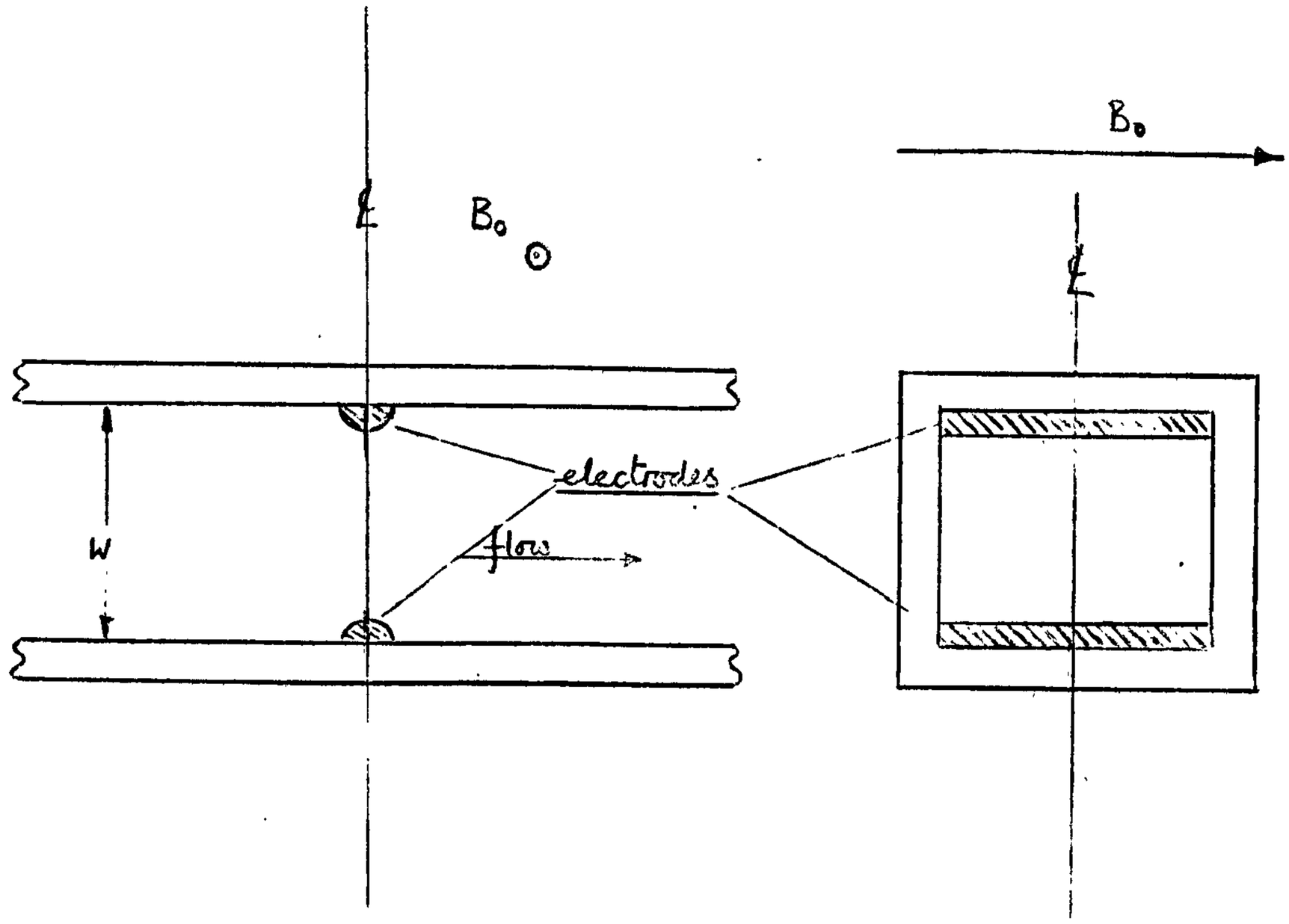

Figure 1 A Simple Ideal Flowmeter

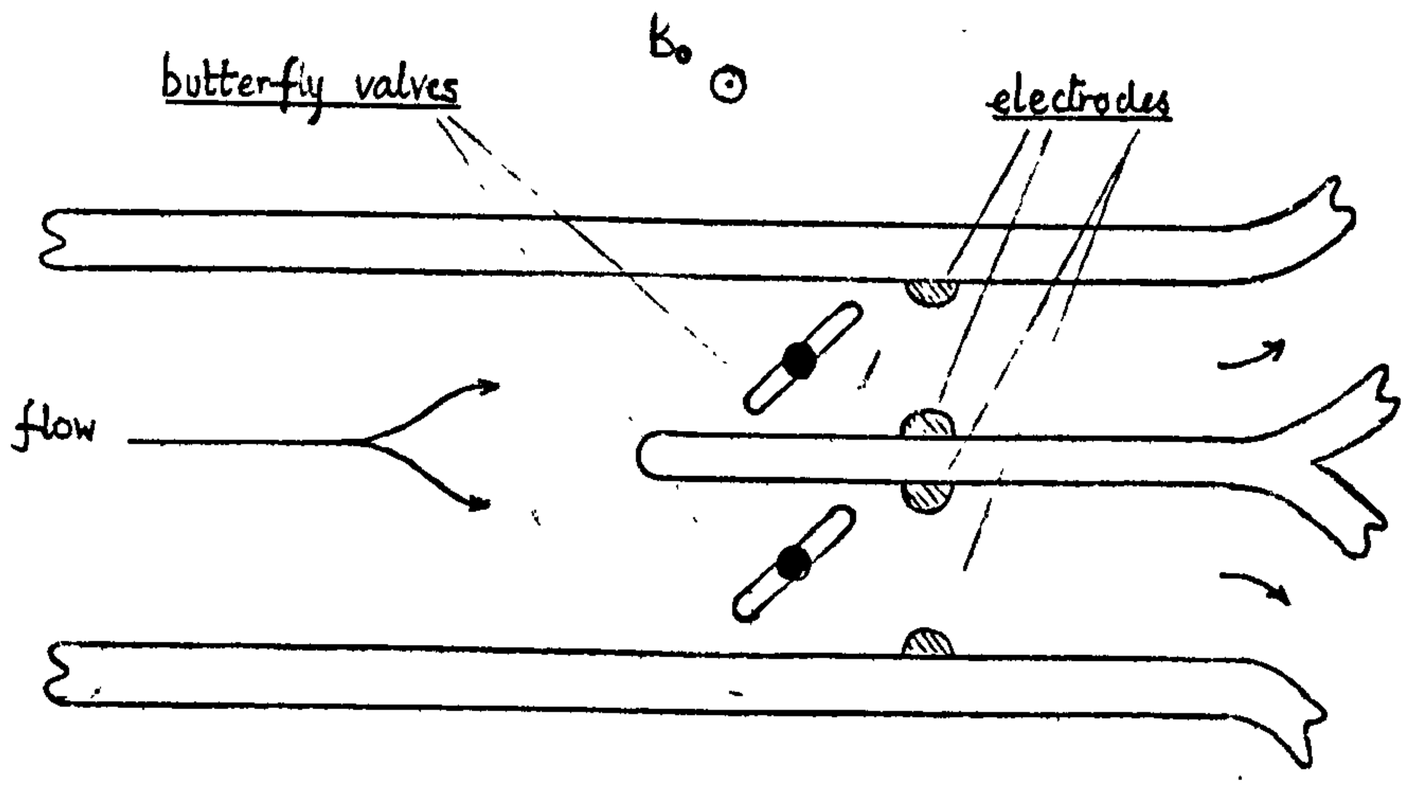

Figure 2 A Multiple Valve-Flowmeter

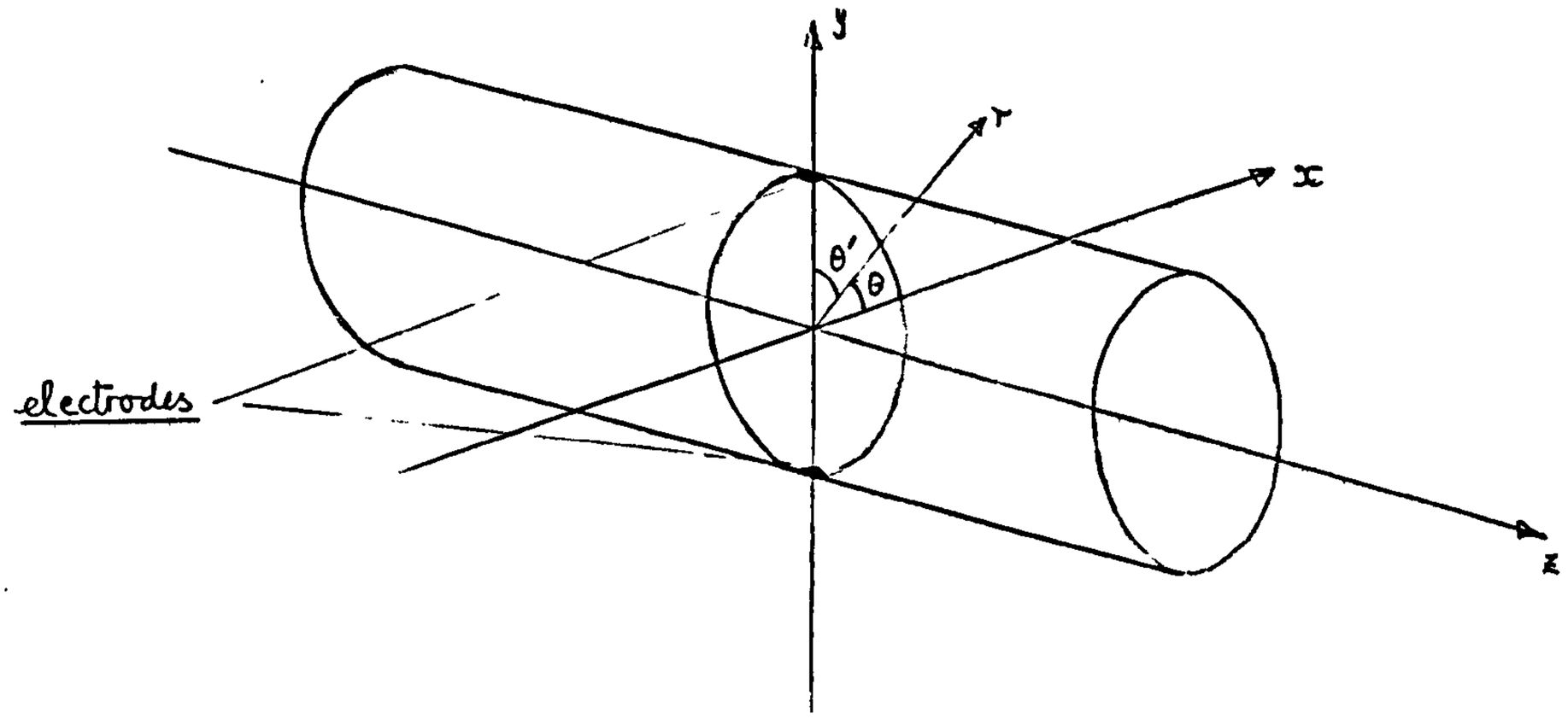

Figure 3 Notation

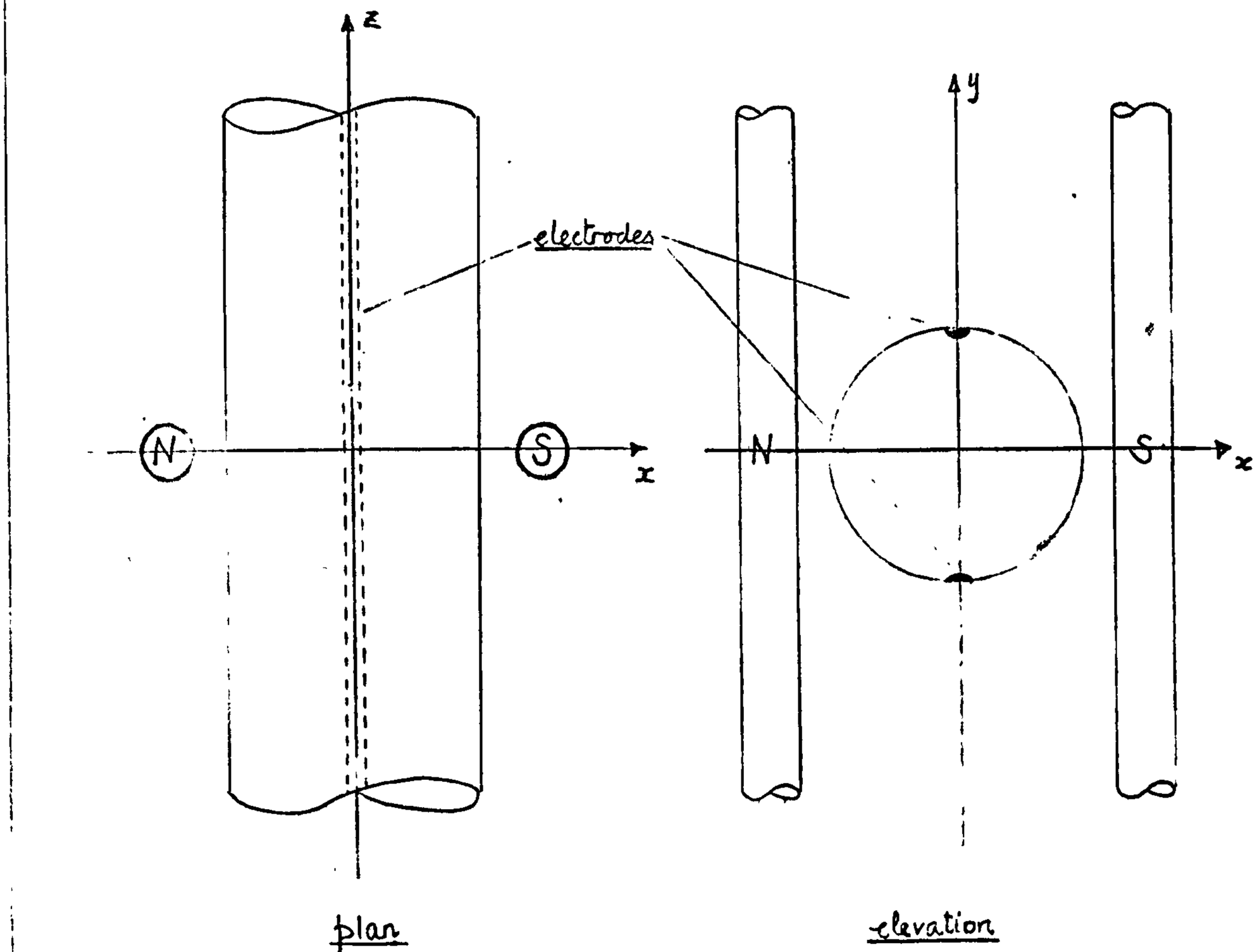

Figure 4a A Flowmeter for Axisymmetric Profiles

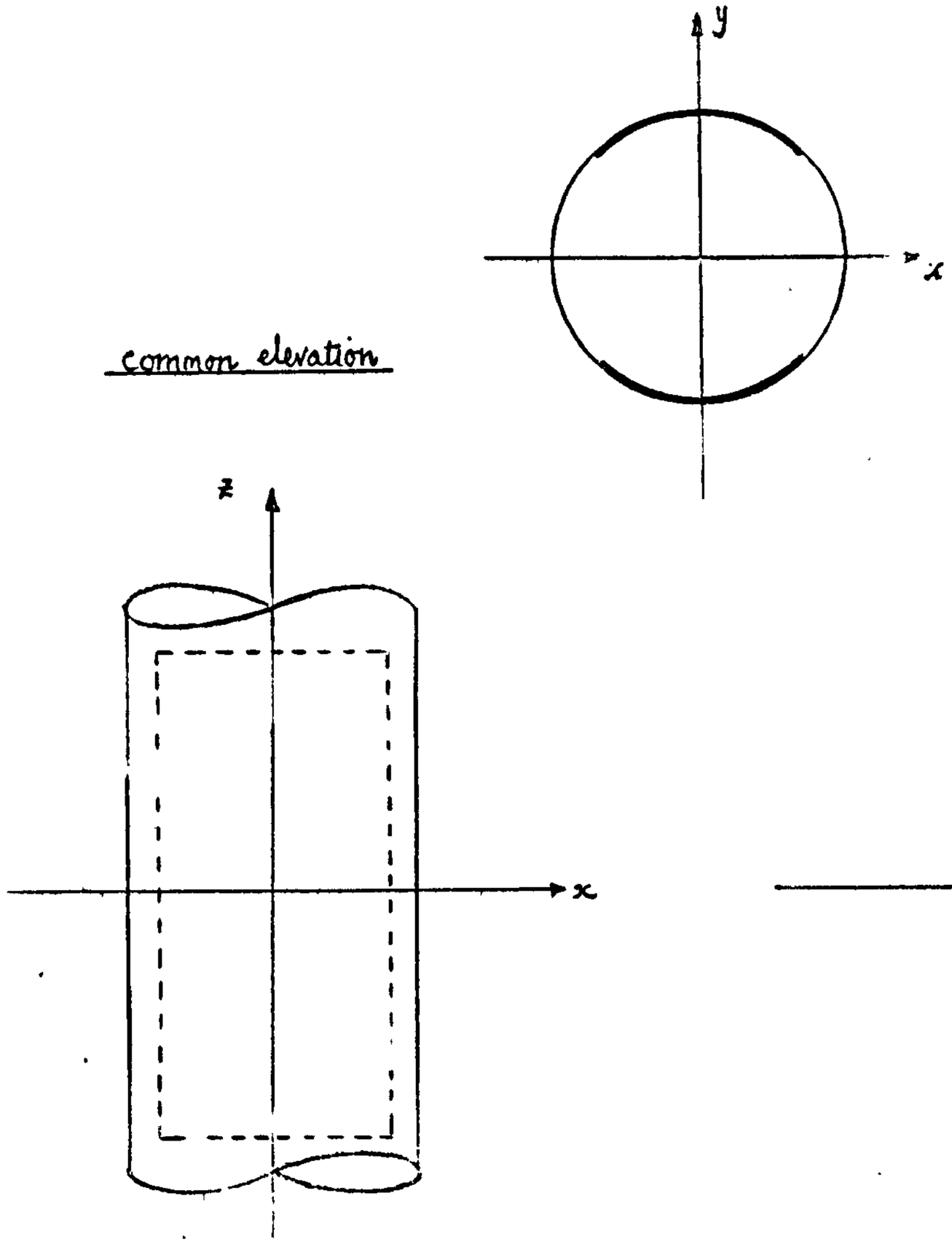

Figure 4b Quarter Circumference Electrodes

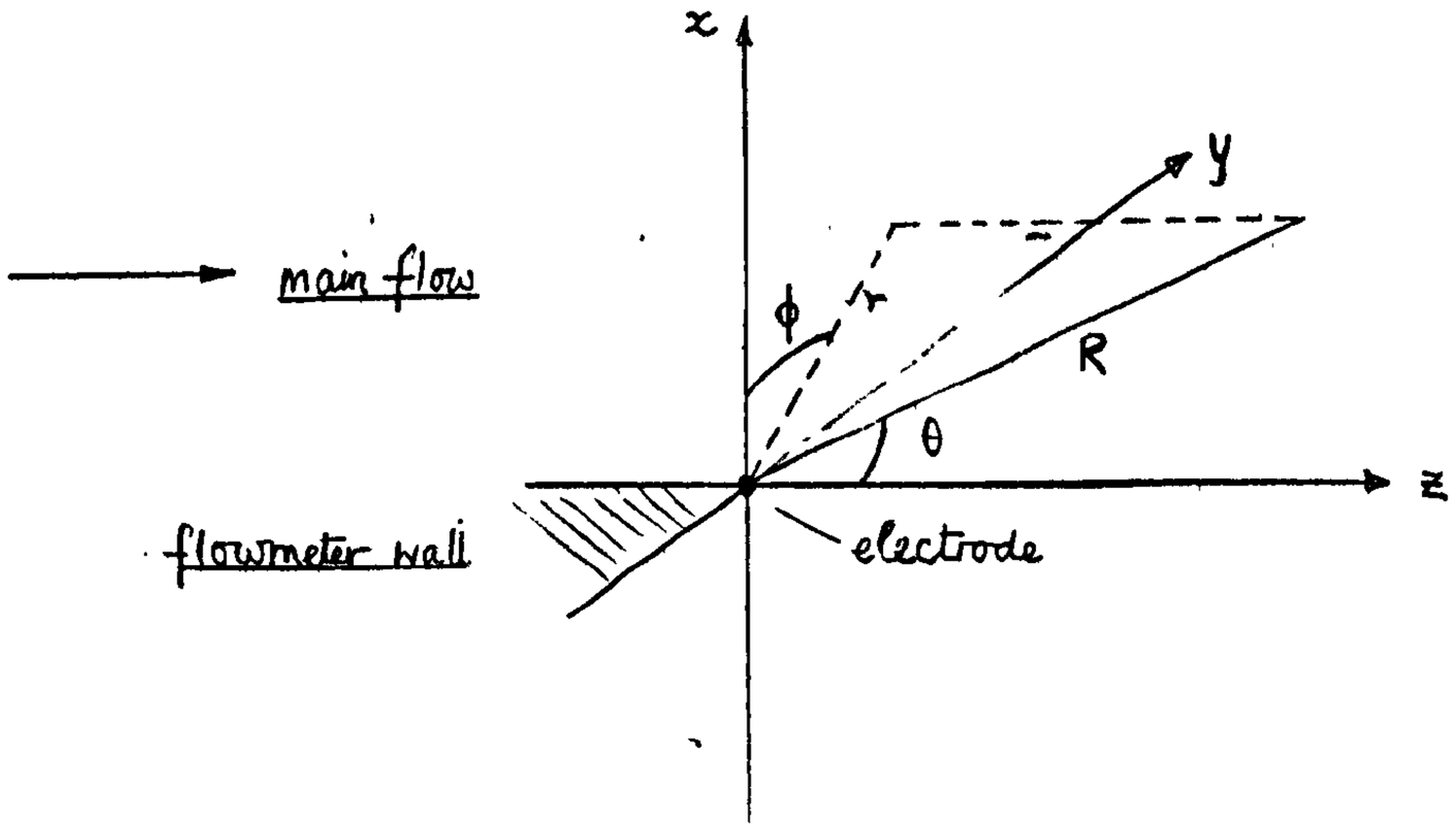

Figure 5 Appendix Notation

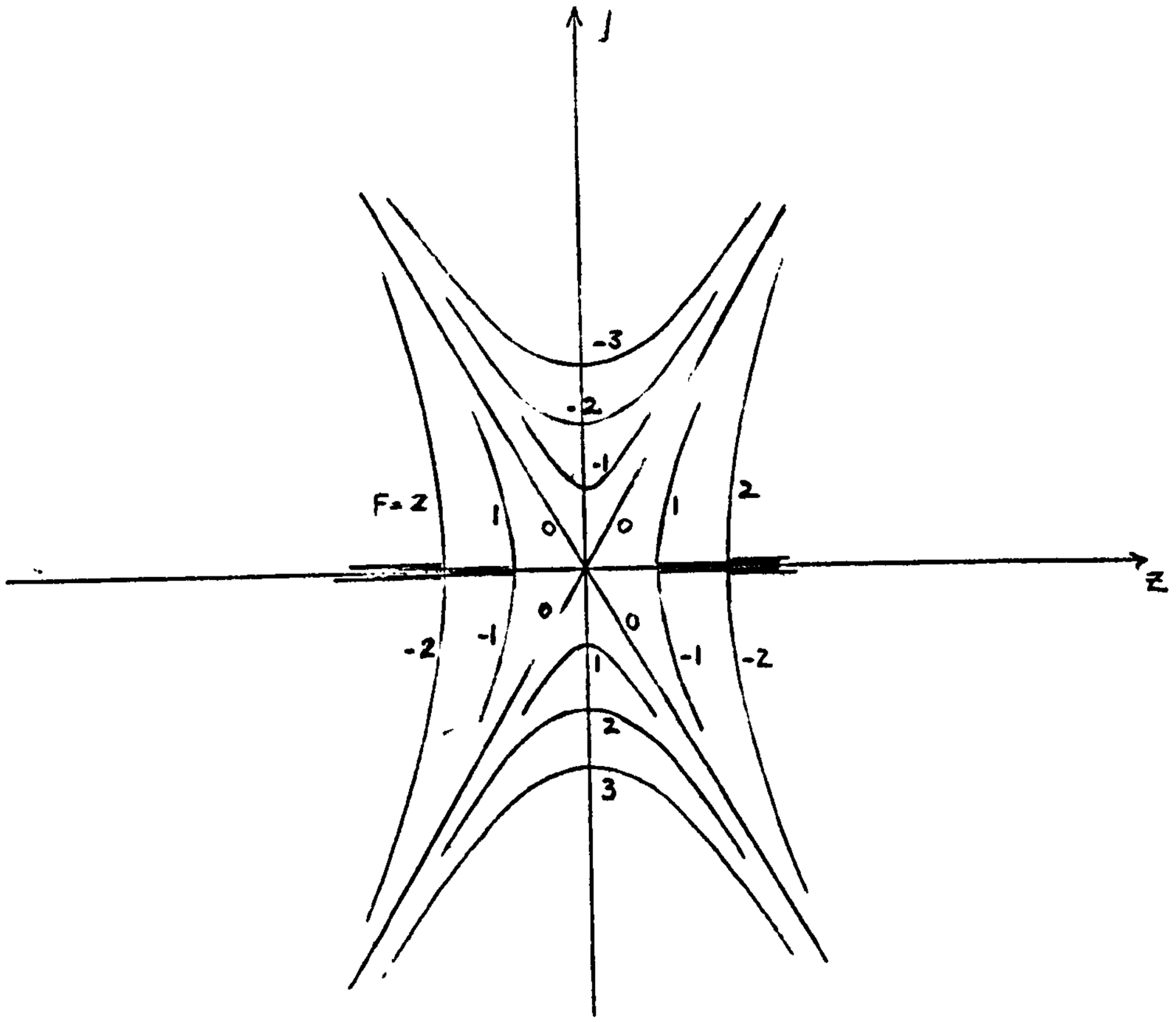

Figure 6a Lines of Constant F near an Electrode

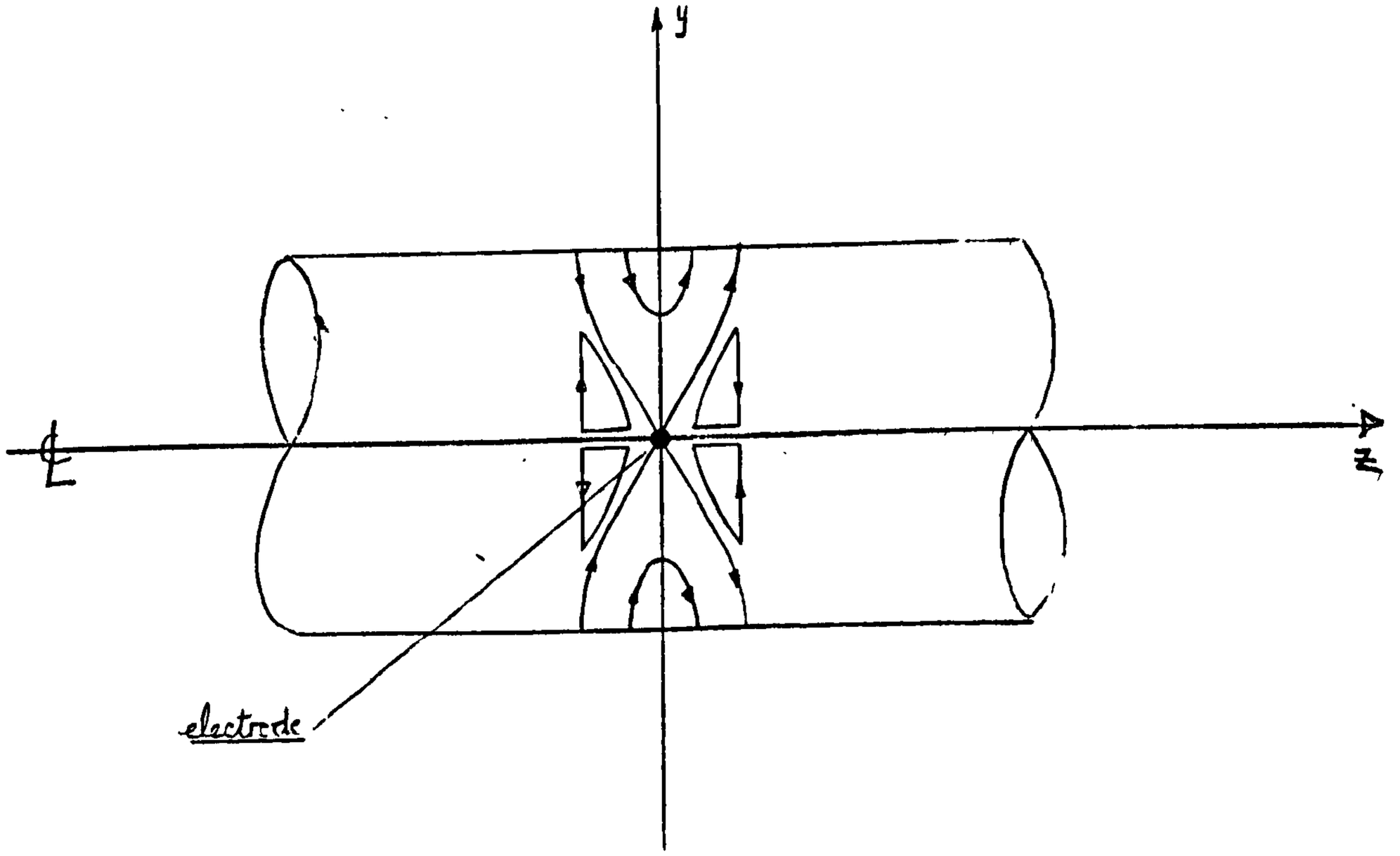

Figure 6b Possible Constant $\bar{W}$ Coils : plan view

The Theory of Long Induced Voltage Electromagnetic Flowmeter Heads

by M.K.Bevir†

Abstract

A detailed account of the dependance of a flowmeter signal on velocity profile is given, under the assumption that the magnetic field, electrode system and streamwise component of velocity (the only one relevant) are invariant in the streamwise direction. The theory still applies if one of these three quantities is not invariant, and can be applied to flowmeters of any shape with any plane magnetic field, including those with external flow. The results serve as an introduction to the theory of short flowmeters.

† The English Electric Co. Ltd., Whetstone, Nr.Leicester, seconded to the School of Engineering Science, University of Warwick.

Introduction

By the word long in the title we mean that all relevant quantities, such as the velocity, magnetic field or electrical boundary conditions, are independant of the distance in the flow direction. Until very recently this assumption was, as far as we know, always used in any analysis that took account of variation of the velocity profile in the cross-section of the flowmeter; it was certainly used by Shercliff (7a), Baker (1b), Mills (5), Yakubenko (8) and, as far as we can judge without translation, by Kanai (4).

Recently interest in the problem of designing short flowmeters has arisen, see for example Ketelsen (6). Here the variation of quantities in the streamwise direction is of great importance.

There is little doubt that future flowmeters will be short. In this paper, however, only the theory of long flowmeters is examined which, while not of direct practical relevance, may be regarded as part of the more general theory and one for which a complete theory can be put forward. Many readers will no doubt be acquainted with Shercliff's weight function demonstrating how the flow at different places in a circular flowmeter with point electrodes in a uniform field contributes to the signal. The work presented here generalises that idea taking into account different electrode configurations and non-uniform magnetic fields, but still retaining the assumption of invariance in the streamwise direction.

Basic Theory

In any motion of fluid moving with velocity $\underline{V}$ in a magnetic field $\underline{B}$ the induced voltage between two electrodes is (Bevir 2)

$$\int \underline{W} \cdot \underline{v} \, d\tau \qquad \ldots\ldots\ldots\ldots\ldots\ldots\ldots(1)$$

where τ is the volume in which the fluid is moving and $\underline{W}$ is a weighting vector given by

$$\underline{W} = \underline{B} \wedge \nabla G \qquad \ldots\ldots\ldots\ldots\ldots\ldots\ldots(2)$$

where G is the potential set up by imposing a voltage between the electrodes (normalised so that unit flux of ∇G emerges from the electrodes). Since ∇G is the current in the liquid when unit current enters at the electrodes it is called the virtual current.

If we also restrict ourselves to fluids in which the induced currents distort the magnetic field negligibly then we can write $\underline{B} = \nabla F$ where F, as well as G, is a solution of Laplace's equation so that

$$\underline{W} = \nabla F \wedge \nabla G \qquad \ldots\ldots\ldots\ldots\ldots\ldots\ldots(3)$$

In long flowmeter theory the virtual current and the magnetic field both lie in planes perpendicular to the meter axis and the only remaining component of $\underline{W}$ may be written as a scalar W. Only the component of velocity v in the streamwise direction contributes to the signal. In this situation we may write the volume element $d\tau$ in (1) as LdS where L is the length of the flowmeter. This L disappears in the integration since ∇G has a factor $\frac{1}{L}$ in it and we find, using the notation of figure (4a), the induced voltage is:

$$\int V(x, y) \; W(x, y) \, dS \qquad \ldots\ldots\ldots\ldots\ldots\ldots\ldots(4)$$

where all quantities are referred to the (invariant) cross-sectional plane of the flowmeter and dS is a surface element there.

Note that long flowmeter theory may be extended in practice to cases in which one only of the quantities $\underline{V}$, $\underline{B}$ and ∇G depend on distance in the streamwise direction, since in this case this part of the integration may be performed separately in (1), still giving (4). This applies particularly to flowmeters which have point electrodes but otherwise are long. In such cases

the preliminary integration replaces the virtual current produced by point electrodes by that produced by line electrodes (whose plan view in a cross-section, of course, shows points). While we actually analyse the case with line electrodes the results apply to the case of point electrodes, both referred to as the case of line/point electrodes. Though the same would be true of any flowmeter that was assumed long apart from its electrodes, the equivalent set of long electrodes is not always so obvious.

The weight function relevant when the velocity profile is axisymmetric is:

$$W'(r) = \frac{1}{2\pi}\int_0^{2\pi} W d\theta \quad \ldots\ldots\ldots\ldots\ldots\ldots\ldots\ldots(5)$$

This, of course, is only likely to occur in circular flowmeters. For long flowmeters to have a sensitivity independant of the velocity profile we require W' constant if the profile is axisymmetric: if it is not W must be constant over the whole cross-section.

<u>The form taken by W</u>

Now

$$W = \frac{\partial F}{\partial x}\frac{\partial G}{\partial y} - \frac{\partial F}{\partial y}\frac{\partial G}{\partial x} \quad \ldots\ldots\ldots\ldots\ldots\ldots\ldots(6)$$

Since F and G are plane solutions of Laplace's equation we may write

$$\left.\begin{aligned} F &= \mathrm{Re}\ f(z) \\ G &= \mathrm{Re}\ g(z) \end{aligned}\right\} \quad \ldots\ldots\ldots\ldots\ldots\ldots\ldots\ldots(7)$$

and then $$W = \mathcal{J}\left[f'(z)\ \overline{g'(z)}\right] \quad \ldots\ldots\ldots\ldots\ldots\ldots\ldots(8)$$

where dashes denote differentiation w.r.t. the complex variable $z(= x + iy)$.

In the normal way $$Bx - iBy = f'(z)$$

$$\frac{\partial G}{\partial x} - i\frac{\partial G}{\partial y} = g'(z) \quad \ldots\ldots\ldots\ldots\ldots\ldots\ldots\ldots(9)$$

From (8) the following observations can be made.

(1) <u>Asymmetric profile</u>

By taking z and $\bar{z}$ as independant variables and setting $\frac{\partial W}{\partial z}$ and $\frac{\partial W}{\partial \bar{z}}$ equal to zero it may be shown that W is only constant when f' and g' are constant. This means a uniform magnetic field and suitable electrical boundary conditions

to give a uniform virtual current. Much of the rest of the paper consists of finding approximately and exactly, the boundary conditions necessary to make the virtual current uniform.

(2) Axisymmetric profile.

Here the problem is easier because $W'(r)$, not W, needs to be constant. From (5) and (8) we have

$$W'(r) = \frac{1}{2\pi}\int_0^{2\pi} \jmath \left[f'(z)\,\overline{g'(z)}\right] \quad d\theta \quad \ldots.(10)$$

which can be evaluated in particular cases with the aid of the substitutions $d\theta = \imath\frac{dz}{z}$ and $\bar{z} = \frac{r^2}{z}$, r being constant.

Apart from certain freak cases $W'(r)$ is constant if and only if one of the two functions f' and g' is constant; that is to say W' is independant of r if the magnetic field is uniform, whatever the electrode arrangement or if the electrodes are arranged in a particular way whatever the magnetic field. In either case W is a solution of Laplace's equation and the constancy of W' may be shown either by contour integration or directly from a theorem which states that the average value of a plane solution of Laplace's equation, taken over a circle, equals its value at the centre of that circle.

In brief a long flowmeter of constant sensitivity and axisymmetric velocity profile requires either a uniform magnetic field or a uniform virtual current: if the profile is not specified it needs both.

It is very likely, however, that for practical reasons only a limited choice can be made in the electrode arrangement and in circular flowmeters the resulting virtual current is almost certain to be non-uniform, with singularities at the electrodes (or their edges if they are large). In these cases there are two alternatives.

Either we use a uniform field, in which case W' will be uniform, but W will be non-uniform and infinite at the electrodes, or we use a non-uniform field, in which case both W' and W are non-uniform, but W can be made finite at the electrodes. The choice would be between a flowmeter which would measure axisymmetric flows perfectly and asymmetric flows badly or all flows tolerably well.

Given a particular electrode arrangement, i.e. given the virtual current $g'(z)$, a mathematically simple choice of magnetic field that ensured that W was finite everywhere would be

$$f'(z) = \frac{1}{g'(z)}$$

where upon $$W = \mathrm{Re}\left(\frac{\overline{g'(z)}}{g'(z)}\right) \qquad \Big\} \ldots\ldots\ldots\ldots\ldots\ldots\ldots\ldots (11)$$

W, though finite, would still have singular behaviour at the zeros and singularities of $g'(z)$, the exact nature of which depends on the behaviour of $g'(z)$ there.

The physical explanation of the weight function in (11) is as follows: If the angle between the direction of the virtual current streamlines and the line joining the electrodes (or the line of symmetry if the electrodes are large) is γ W in (11) is $\cos 2\gamma$. γ is itself a measure of the non-uniformity of the virtual current. Where the walls are insulating γ, hence W, is automatically fixed by their orientation. The minimum values of W will occur on the walls since, whatever their conductivity, the extreme values of γ (a solution of Laplace's equation) must occur there.

The magnetic field required to achieve the W of (11) will be called the field 'matching' the virtual current and is better regarded as a guide to what is possible rather than a practical proposition, since it can be inconvenient to set up. Later the distributions of W, given a flowmeter with specified electrodes (i.e. $g'(z)$ given), are calculated, for both a uniform field and the matching one. It might appear the lines of constant W in the two cases are perpendicular; in fact the angle between them is $\pi/2 - \gamma$ and they only appear perpendicular in so far as we have succeeded in making γ small.

Matching the field to the virtual current for a line/point electrode set in a flat wall results in $W \sim \cos 2\theta'$ at the electrode, where θ' is the local azimuthal angle whose origin depends on the relative orientation of the field to the wall. At the edge of a large electrode in a flat wall $W \sim \cos\theta'$, which is an improvement since we can prevent W from being negative by making it zero on the wall.

Figures 2a and 2b show typical examples of such behaviour. In many cases (including the second case just mentioned) the magnetic field $f'(z)$ has a singularity, not a plain zero, at the point in question, which can only be approximately reproduced in practice since magnetic windings or pole pieces cannot be brought directly into contact with the electrode edge.

Other magnetic fields could be used. We might try $f'(z) = \frac{h(z)}{g'(z)}$ where h was some arbitrary regular function and then use a suitable criterion for finding the best h(z). We have tried this in the case of a circular flowmeter and diametrically opposed electrodes using a polynomial $A + Bz^2 + Cz^4$ for h(z) and minimising $\int(W - 1)^2 dS$ but is not a very fruitful task since we know that we require both $f'(z)$ and $g'(z)$ uniform to achieve constant W and for line electrodes $g'(z)$ is far from uniform.

We now calculate the distribution of W and W' for some particular shapes of flowmeter. First, we consider rectangular flowmeters with line/point electrodes and circular flowmeters with both line/point and large curved rectangular electrodes. For each type of flowmeter W is calculated for a uniform magnetic field and for the matching field described above. Where relevant, W' using the matching field is calculated and shown in figure 3. One example of the virtual current resulting from the preliminary integration of the virtual current for a particular set of short electrodes is also included.

Then we consider some methods of achieving a uniform virtual current in a circular flowmeter, using thin walls of finite conductivity and variable thickness. Finally we consider external flowmeters, which have electrodes on the outside and magnetic field windings inside with the fluid flowing externally.

The definition of sensitivity adopted is:

$$\frac{\text{the flowmeter-signal with a given magnetic field and velocity profile}}{\text{the signal with the same field and a uniform profile with the same flowrate.}}$$

It is a measure of how a flowmeter signal depends on the velocity profile, and is unity by definition for a uniform profile.

Rectangular and Square Flowmeters

The results here are of rather limited practical interest. Of course, it is well known that infinitely conducting electrodes completely spanning two

opposite walls are desirable: in this context it is because the resulting virtual current is uniform.

Using point/line electrodes the formulae for the virtual current involve elliptic functions. Fortunately a set of tables of complex elliptic functions is available (Henderson 3).

Using a uniform field B_o and placing the electrodes in the mid-point of opposite sides of an otherwise nonconducting square flowmeter we achieve the distribution of W shown in figure 1a.

$$W = \frac{B_o}{\pi} \quad \mathrm{Re} \left[\mathrm{dn} \left(z, \tfrac{1}{2} \right) \right]$$

which has the typical singular behaviour of point electrodes set in flat non-conducting wall. No point in attempting the matching field in this case because of the known bad behaviour of point/line electrodes on a flat wall with their matching field.

If we turn the flowmeter through 45°, still using a uniform field, and put the electrodes in the corner we find:

$$W = \frac{\sqrt{2}}{\pi} \; B_o \; \mathrm{Re} \left[\mathrm{cn} \left(z, \tfrac{1}{\sqrt{2}} \right) \right]$$

which is shown in figure 1b. The point of doing this is that using the matching field the singular behaviour of W at the electrodes is cut off by the presence of the side walls, so that W is never negative, but still finite. For this case, shown in figure 1c,

$$W = \mathrm{Re} \left[\frac{\mathrm{cn} \left(z, \frac{1}{\sqrt{2}} \right)}{\mathrm{cn} \left(\bar{z}, \frac{1}{\sqrt{2}} \right)} \right]$$

None of these W distributions are satisfactory. In practice, given the use of a rectangular channel, a short flowmeter may be designed whose sensitivity is completely independent of the actual velocity distribution, provided the fluid is incompressible (Bevir 2).

Circular Flowmeters with Line/Point Electrodes

We consider line/point electrodes set in a nonconducting circular flowmeter diametrically opposite each other, as in figure 2a. Analysis shows that:

$$g'(z) = \frac{2i}{\pi (z^2 + 1)} \qquad \ldots\ldots\ldots\ldots\ldots\ldots (12)$$

so that for an unknown magnetic field function $f'(z)$

$$W = \frac{2}{\pi} \mathrm{Re} \quad \frac{f'(z)}{z^2 + 1} \qquad \text{.....(13)}$$

and the axisymmetric weight function W' may be calculated using the calculus of residues:

$$W'(r) = \frac{2}{\pi} \mathrm{Re} \quad f'(ir^2) \qquad r<1 \quad \text{...(14)}$$

$$= \frac{1}{\pi} \mathrm{Re} \quad f'(ir^2) \qquad r=1$$

This must be compared with Baker's formula (1b), which gives the signal between two diametrically opposite electrodes on a circle of radius a as

$$U = 2\int_{s=o}^{a} V(\sqrt{as})\, B_\theta\, (s, \theta)\, ds$$

According to this formula the velocity at radius $s'(=\sqrt{as})$ must be weighted with the transverse component of the magnetic field at radius $\frac{s'^2}{a}$ (the remaining s' in the integral gives the area of the annulus). This is the same result as (14).

For a uniform transverse magnetic field B_o, $f'(z) = B_o$ and

$$\left.\begin{aligned} W &= \frac{2B_o}{\pi} \mathrm{Re} \left\langle \frac{1}{z^2 + 1} \right\rangle \\ W' &= \frac{2B_o}{\pi} \end{aligned}\right\} \text{.....(15)}$$

The lines of constant W in this case were first given by Shercliff and are reproduced in figure 2a for comparison. They are the constant potential lines of dipoles situated at the electrodes. W' is constant as expected, and the sensitivity for all axisymmetric profiles is unity.

The matching magnetic field is given by $f'(z) = B_o (z^2 + 1)$, giving

$$\left.\begin{aligned} W &= \frac{2B_o}{\pi} \mathrm{Re} \quad \frac{z^2 + 1}{z^2 + 1} \\ \text{and} \qquad W' &= \frac{2B_o}{\pi} \quad (1 - r^4) \end{aligned}\right\} \text{.....(16)}$$

The sensitivity for $V \propto 1 - r^2$ is 1.25 and for $V \propto 1 - r$ is 1.28. These agree with the formula given by Shercliff in (7b) where he calculates his† sensitivity for $f'(z) = 1 - \varepsilon z^2$ and $v(r) \propto 1 - r^n$ as $1 - \frac{\varepsilon}{3} \frac{n+2}{n+6}$. The formula for W' in this case is $\frac{2B_o}{\pi} (1 + \varepsilon r^4)$. The contours of constant W as given by (16) are shown in figure 2a and W' in figure 3. It will be seen that there are areas of negative W near the electrodes.

† The definitions of sensitivity are different. For a flat profile Shercliff has $1 - \frac{\varepsilon}{3}$ whereas we have 1, by definition.

Equation 16 is a good example of the non-uniformity in W' resulting from making W finite everywhere. Because the virtual current $g'(z)$ is so non-uniform the behaviour of both W' and W is unsatisfactory: the remedy, with the long flowmeter assumption, is not in optimising the magnetic field but in making $g'(z)$ more uniform. This can only be achieved by altering the electrodes. To this end we now analyse the case of large electrodes opposite each other (figure 2b).

Circular Flowmeters with Large Electrodes

We know that the virtual current in a rectangular flowmeter with large electrodes on opposite walls, whose conductivity is high compared to that of the liquid, is uniform. In the particular this is true for a square and since the deformation required to make a square into a circle is not great, except at the corners, we may expect a circular flowmeter with large electrodes to have a much more uniform virtual current than one with point electrodes.

If the electrodes are opposite each other and such subtend an angle 2α at the centre of the flowmeter, then analysis shows that the virtual current is

$$g'(z) = \frac{i}{K(\sin\alpha)\sqrt{(z^2+1)^2 - 4z^2\sin^2\alpha}} \quad \ldots\ldots(17)$$

where K is an elliptic integral of the first kind of modulus $k = \sin\alpha$. We see the virtue of making $\alpha = \pi/4$ since in this case the terms in z^2 under the square root sign disappear, thus for quadrant electrodes

$$g'(z) = \frac{1}{1.854}\,\frac{i}{\sqrt{z^4+1}} \quad \ldots\ldots\ldots\ldots\ldots\ldots(18)$$

so that for a magnetic field $f'(z)$

$$W = \frac{1}{1.854}\,\frac{f'(z)}{\sqrt{z^4+1}} \quad \ldots\ldots\ldots\ldots\ldots\ldots(19)$$

The distribution of W for a uniform field is shown in figure 2b and should be compared with the corresponding case of line/point electrodes and uniform field originally given by Shercliff (figure 2a). W still tends to infinity at the electrode edges, but more weakly. W', of course, is uniform since this is a case with uniform magnetic field, but the effect of large electrodes is to reduce the signal by $\frac{1}{1.854}$ compared to $\frac{2}{\pi}$ i.e. by a factor of 0.85.

The reader is also invited to compare the formula (17) for $g'(z)$ for an electrode half angle α with the work of Yakubenko (8) in which he gives the

output voltage and impedance of a flowmeter with large electrodes, an axisymmetric velocity profile and a uniform field. The reduction in open circuit voltage according to both calculations is $\frac{\pi}{2K(\sin\alpha)}$.

If we now utilise the matching field given by $f'(z) = \sqrt{z^4 + 1}$ then

$$\left.\begin{aligned} W &= \frac{1}{1.854} \quad \mathrm{Re} \sqrt{\frac{z^4 + 1}{\bar{z}^4 + 1}} \\ \text{and} \qquad W' &= \frac{1}{1.854} \quad \frac{2}{\pi} \; E(r^4) \end{aligned}\right\} \qquad \ldots\ldots\ldots\ldots\ldots\ldots (20)$$

where $E(r^4)$ is the complete elliptic integral of the second kind of modulus $k = r^4$. The distribution of W is given in figure 2b. There are now no areas of negative W and only small areas around the electrode edges where it is appreciably non-uniform. The W plot also has a higher degree of symmetry than the corresponding case using point electrodes in figure 2a.

W' is plotted in figure 3, without the factor $\frac{1}{1.854}$. It is a pity that W' is most non-uniform at r = 1. which is where two profiles are likely to differ, but at least it does not fall to zero there as it did in the case of point electrodes.

The sensitivities for various axisymmetric profiles can be calculated and are listed below. The ratio between the first and last figure is $\frac{\pi}{2}$ and the figures are only accurate to $\pm\frac{1}{2}\%$ since an infinite series was used for evaluating $E(r^4)$.

	quadrant electrodes	point/line electrodes
All flow through centre (delta function)	1.06	1.50
Parabolic velocity profile	1.04	1.25
Uniform velocity profile	1.00	1.00
All flow through edge (r = 1)	0.68	0

Between laminar and turbulent flow, assumed to be parabolic and flat respectively, there is a difference at 4%; too much for accurate flow measurement, but perhaps not too high a price to pay for such a well behaved W if the inlet conditions are bad and accuracy is not at a premium. Taking account of the fact that even in turbulent flow the velocity falls with increasing radius would decrease the difference.

The magnetic field required to give this W has singularities right at the edge of the electrodes. These would cause difficulties in practice for reasons explained before: unless pole pieces or current carrying wires could be brought right up to the electrode edges the field would depart from its design distribution at the edges. The effect of this on the sensitivity and weight function distributions would be approximately proportional to the flowmeter wall thickness.

The performance of a flowmeter with quadrant electrodes is, apart from a drop of 0.85 in output signal, much superior to one with point/line electrodes. The non-uniformity of W still remaining is due to the behaviour of the virtual current $g'(z)$ at the electrode edges, and a later section deals with problem of removing the non-uniformity and making the virtual current uniform everywhere in the flowmeter. Before we do this we examine a short flowmeter in which only the virtual current varies in the streamwise direction.

Line electrodes - Quasi 2-D Virtual Current

The case of the line electrodes (treated as singular lines of zero thickness) lying on the surface of a nonconducting circular flowmeter, perpendicular to the main flow direction (as in figure 4b of (2)) do not fall within the scope of long flowmeter theory. For reasons given in (2), however, they have a promising performance and here we calculate how they behave if the magnetic field and flow are assumed invariant in the flow direction. Then, as mentioned earlier on page 3/4, we need the fictitious virtual current found by integrating the actual virtual current in the streamwise direction. This may be derived directly as if we were dealing with long flowmeters, though there is no simple set of long electrodes that will produce the resulting virtual current.

The cross-sectional view of the flowmeter in the electrode plane will look the same as it does for long electrodes in figure 2b, but whereas the boundary conditions on the electric-potential ϕ for these electrodes was $\frac{\partial \phi}{\partial n} = 0$ on the insulating walls and ϕ = constant on the electrodes, here $\frac{\partial \phi}{\partial n}$ = constant is required on the electrodes.

If the electrodes subtend an angle 2α at the flowmeter centre, then

$$g'(z) = \frac{i}{2\alpha\pi z} \log \frac{z^2 + 1 + 2z\sin\alpha}{z^2 + 1 - 2z\sin\alpha} \quad \ldots\ldots(21)$$

Note that both this formula and (17) give the formula (12) for point electrodes as $\alpha \to 0$, and also that the singularity at the electrode "edges" is of the type $g'(z) \sim \log z'$ (z' referred to the "edges") which is much weaker than the corresponding $\frac{1}{\sqrt{z}}$ or $\frac{1}{z'}$ in the previous two cases.

The following table compares the drop in signal due to these three different electrode schemes when the magnetic field is uniform and the velocity profile axisymmetric. To do this we simply compare the values of $g'(z)$ at $z = 0$, normalised so that the point electrode case takes the value unity.

Signal Drop

	Point/Line	Long	Transverse line
	1	$\frac{\pi}{2K(\sin\alpha)}$	$\frac{\sin\alpha}{\alpha}$
e.g. $\alpha = 0$	1	1	1 , as expected
$\alpha = \pi/4$	1	0.85	0.90
$\alpha = \pi/2$	1	0	$\frac{2}{\pi} = 0.64$

It is interesting that even when the transverse line electrodes extend right round the pipe, the signal is only reduced by 0.64, though for long electrodes it vanishes.

Figures 2c, d, e give the distribution of W for the transverse line electrodes using a uniform magnetic field and the matching field, for the three cases of $\alpha = 45^\circ$, 66.5°, 90°. I have not been able to find an analytic formula for W' for arbitrary α, but it can be evaluated numerically and is shown for these three cases in figure 3. The cases $\alpha = 45^\circ$ and 90° are better than the case of $\alpha = 45^\circ$ using long electrodes. As α varies from 0° to 90°, the value of the axisymmetric weight function W' on the flowmeter edge using the matching field has a maximum, at $\alpha = 66.4^\circ$, of 0.937. The maximum is not sharp, and W' is above 0.90 for $80^\circ > \alpha > 55^\circ$ approximately. The case of $\alpha = 45^\circ$ was chosen because it was suggested in (2) as the best approximation to an ideal flowmeter using line electrodes and circular pipes. It now appears

that the case $\alpha = 66.4^\circ$ may be better, though a proper assessment requires taking the three dimensional variation of the virtual current into account.

The case of $\alpha = 66.5^\circ$ was chosen because at that value of α the value of W' (figure 2d) on the flowmeter wall is the same at $\theta = 0^\circ$ and $\theta = 90^\circ$, namely 0.856. Its closeness to the previous value of α suggests that maybe they are exactly the same, and that there might be a general theorem that for $g'(z, \alpha)$ (with the relevant symmetry) the maximum value of Re $\overline{g'}$ as α varies is given by the solution of the equation in α $g'(1, \alpha) = g'(i, \alpha)$ though I have not been able to prove this (it holds for the $g'(z)$ for large electrodes (17) but this is obvious by symmetry anyway).

$\alpha = 90^\circ$ is interesting only in so far as it is the case of "touching" line electrodes. To achieve the result in practice the gap between the ends of the wires would have to be considerably greater than the line thickness. Its performance is not as good as that of the previous case since the singularities at the electrode ends coincide and reinforce each other.

Flowmeters with Finitely Conducting Walls

Up till now we have only considered flowmeters with walls made of insulating and infinitely conducting sections. The main cause of the non-uniformity of the virtual current $g'(\xi)$ has been the join between these sections and the question arises whether smoothing out these discontinuities in wall conductivity can make it uniform. More precisely we may ask ourselves what boundary conditions are required at the wall to make $g'(\xi)$ uniform.

If we think in terms of thin walls, we may use the thin wall boundary conditions on page 27 of (7a).

Consider the case of a circular flowmeter of radius a surrounded by a thin wall of thickness w and conductivity k, where $wk(\theta)$ is a yet undecided function of θ, the azimuthal angle round the wall (figure 4a). Since it is easy to do so we take into account uniform contact resistance τ. σ is the conductivity of liquid.

Imagine two electrode leads placed diametrically opposite each other, as in figure 4a, and a voltage set up between them. If we demand that the resulting current flow, which is the virtual current, is uniform then substitution of this fact into the thin wall boundary conditions gives the following formula relating w, k, τ and σ .

$$\frac{wk}{\sigma a} = \frac{\lambda \sec\theta - 1}{1 + \frac{\tau\sigma}{a}} \qquad -\pi/2 < \theta < \pi/2 \quad \ldots\ldots\ldots\ldots(22)$$

where λ is arbitrary, but must be >1 since wk must be positive everywhere. For $|\theta| > \pi/2$ read $\theta - \pi$ for θ.

If we now compare the output signal of such a flowmeter with the signal from a meter with point electrodes, uniform field and axisymmetric velocity profile we find a reduction in signal of $\frac{\pi}{4\lambda}$. This factor is independent of contact resistance, provided that is constant.

As expected (22) shows that $\frac{wk}{\sigma a} \to \infty$ at $\theta = \pi/2, \ -\pi/2$ but $\to 0$ at $\theta = 0, \pi$ only for $\lambda = 1$. For $\lambda > 1$ $\frac{wk}{\sigma a}$ is always >0 and the extra shorting through the side wall is reflected in the fact that the shorting factor $\frac{\pi}{4\lambda}$ is smaller for larger λ.

Variable contact resistance

Similar calculations show that provided $\frac{wk}{\sigma a}$ is taken as very large, that is the walls are taken as infinitely conducting, thin non-uniform contact resistance τ given by

$$\frac{\sigma\tau}{a} = \lambda' \operatorname{cosec}\theta - 1 \qquad \lambda' > 1, \ 0 < \theta < \pi \quad \ldots\ldots\ldots(23)$$

will make the virtual current uniform. Obviously the infinitely conducting walls outside the layer of non-uniform contact resistance must be insulated at $\theta = 0,$ and the shorting factor is $\pi/4$, independent of λ'. $\tau \to \infty$ at $\theta = 0, \pi$ which prevents shorting between the walls via the fluid there.

Obviously there is a continuous range of $\frac{\sigma\tau}{a}$ and $\frac{wk}{\sigma a}$, both depending on θ, which will make the virtual current uniform and there are other boundary conditions which can be proposed that will do so as well. The point is whether they can be achieved in practice.

Possible Methods of achieving walls of variable conductivity

Liquids of known conductivity in circular pipes

A possible method is to choose a material of conductivity considerably larger than the liquid and making a thin wall of variable thickness. Except at the lead connections the wall will be thin enough to satisfy the thin wall approximation.

With mercury, for example, and copper walls where $\frac{\sigma_{Cu}}{\sigma_{Hg}} \simeq 62$ and $\tau = 0$, taking $\lambda = 1$ we require from (22):

$$\frac{W}{a} = \frac{1}{62} (\sec\theta - 1)$$

At $\theta = 90^\circ \pm 1^\circ$ $w = a$ and at $\theta = 90^\circ \pm 10^\circ$ $w = 0.1a$ so that only very close to $\theta = 90^\circ$ is the thin wall approximation bad. Such a wall could be machined out of solid, or made by laying strips of constant thickness and varying width on top of one another, or made by a mixture of the two methods. Figure 4b shows the wall shape. Constant contact resistance reduces $\frac{w}{a}$ but makes no difference to the principle; nor for that matter does θ - dependent contact resistance provided we know what it is.

The lower the conductivity of the wall, the thicker it becomes. For any conductivity there is always a wall shape that will make the virtual current uniform, though it is more difficult to calculate and the arrangement of the lead connections becomes important.

Walls made of infinitely conducting and insulating strips

This method is very promising at first sight, but is not feasible in practice. However it raises some interesting points.

The disadvantage of making a continuous wall out of a certain conducting material is that the resulting flowmeter is only good for a liquid of the same conductivity as that for which it was designed. If σ alters, then the required $\frac{wk}{\sigma a}$ changes by a constant factor. The expressions on the right hand side of (22) are not constant multiples of each other for different values of λ and hence each is only suitable for one value of $\frac{wk}{\sigma a}$.

It is possible in principle (though as we shall see, not in practice) to make an approximation to a conducting wall out of successive insulating and

infinitely conducting segments. Figure 4c shows the cross-section of such a wall where the pitch ϕ is small compared to the linear dimensions of the flowmeter and δ (which is the fraction of surface covered by infinitely conducting material) is assumed for the purposes of calculation not to vary along the wall. In practice we may therefore only consider slow variations, in which δ changes appreciably in distances much larger than ϕ.

If an emf was imposed along the wall, some shorting across the electrodes would be expected. At distances much greater than ϕ from the wall it may be shown that such an arrangement behaves like a thin conducting wall of thickness X conductivity wk given by

$$\frac{wk}{\sigma\phi} = \frac{1}{\pi} \log \sec \frac{\delta\pi}{2} \quad \ldots\ldots\ldots\ldots\ldots\ldots(24)$$

For a circular flowmeter with uniform virtual current and no contact resistance $\delta(\theta)$ (varying slowly with θ) is, from (22) and (24), given by

$$\frac{1}{\pi} \log \sec \frac{\delta\pi}{2} = \frac{a}{\phi} (\lambda \sec \theta - 1) \quad \ldots\ldots\ldots(25)$$

The fluid conductivity σ does not appear at all. Walls made like this are self-regulating, but there are severe practical difficulties. For instance, if the formula (25) is to apply at all reasonably we must at least have, say, ten segments between $\theta = 0$ and $\pi/2$, i.e. $\phi/a = 0.1 \times \pi/2$. Then, putting $\lambda = 1$ and evaluating $\delta(\theta)$ at the midpoint of each pitch we find

1st segment	:	$\theta = 4\frac{1}{2}^{\circ}$	:	$\delta = 0.8$
6th segment	:	$\theta = 49\frac{1}{2}^{\circ}$	:	$1 - \delta \simeq 10^{-5}$
10th segment	:	$\theta = 85\frac{1}{2}^{\circ}$	:	$1 - \delta \simeq 10^{-100}$

The insulating gaps are hopelessly small after the first few segments. This is because ϕ/a is small. In fact for a fixed δ, i.e. for a fixed ratio of conducting to insulating surface, the equivalent wall conductivity is proportional to ϕ so that by making the pitch ϕ small enough the wall behaves as an insulator to emfs imposed along it, no matter how high a fraction of conducting material there is in it.

In practice it might be possible to surround the electrodes with large infinitely conducting electrodes, say from $\theta = 45^\circ$ to 135°, and then make the rest of the wall out of segments. A trial and error approach would be needed, based on some unjustified use of (25) when b/a is not particularly small and backed up by some experimental work on an analogue like teledeltos paper. It is not very promising since the use of a small pitch requires minute gaps as we have seen above, and the effect of a larger pitch is to make the virtual current non-uniform some way into the pipe.

It is also possible to simulate a wall of varying contact resistance, either by putting partly porous material over two infinitely conducting electrodes spanning the whole circumference of the flowmeter, or by placing strips of insulator of varying width and spacing on the electrode surface. The same sort of difficulties arise with the second method as with simulating the conducting wall described above. It may be possible to combine the two methods.

External flowmeters

The name is used to cover all those flowmeters in which the magnetic field windings are placedinside the meter, the electrodes outside and the whole device is put in the flow to be measured. The meter is, of course, assumed long enough for the problems of endshorting to be ignored.

The main use of such meters is in the measurement of blood flows in veins and arteries but they could also be used as a ship's log. Although the present trend in the first application is towards shorter and smaller meters, the assumption of no end shorting is reasonable not too far from the meter (compared with its length). Length to diameter ratios are in the region of 8 to 1 or somewhat less.

In order to analyse such situations we require the virtual current $g'(z)$. For circular meters (of unit radius) with line/point electrodes or large electrodes and surrounded by an infinite sea of fluid $g'(z)$ has same form as for the internal meter of the same geometry, though now the formulae apply in

$|z| > 1$. In the case of blood vessels though, the meter is surrounded by a wall of tissue of debatable conductivity, and it may not even be in the centre. The virtual current in such a case has not been found. If necessary, we can bound the behaviour of such a flowmeter by using the virtual current for the cases of immersion in an infinite sea of fluid and immersion in fluid surrounded by an insulating concentric wall of larger radius. Using point electrodes and a surrounding wall of radius R, the formula is

$$g'(z) = \frac{K'(k)}{\pi^2 z} \left[k\, cn\left(\frac{2K'}{\pi} \log z,\ k\right) + dn\left(\frac{2K'}{\pi} \log z,\ k\right)\right]$$

where the modulus k of the elliptic functions cn and dn and the integral K' is defined by

$$\log R = \pi \frac{K(k)}{K'(k)}$$

There is a more complicated formula for the same case with large electrodes. Neither has been used, though it would be possible to do so using tables of complex elliptic functions.

Fortunately it seems that the assumption of no wall is better than that of an insulating one and anyway the difference between the two assumptions is small when regions close to the flowmeter compared with the wall radius are considered.

For all two-electrode systems in an infinite sea of fluid far from the meter the electrodes behave like a dipole i.e.

$$g'(z) \sim \frac{i}{z^2} \quad \text{for large } z$$

and since we are considering the magnetic field to be produced by windings inside the meter it also behaves like a dipole:

$$f'(z) \sim \frac{1}{z^2} \quad \text{for large } z$$

Thus far from the meter $W \sim \frac{1}{r^4}$, a highly unsatisfactory state of affairs (since far from the meter the contribution of the flow to the signal will be negligible) which is, moreover, independent of the exact electrode and magnetic field arrangements.

The physical explanation for this is that while it is still true that

we require the virtual current $g'(z)$ uniform in order to make W constant it is, far from being uniform, in opposite directions in various places no matter what electrode system is used. There is no virtue in using large electrodes, which in the case of internal flowmeters achieve a fairly uniform current distribution (except at electrode edges), unless there are other reasons such as the reduction of the meter impedance.

For point electrodes

$$\left.\begin{aligned} W &= \mathrm{Re}\,\frac{f'(z)}{\bar{z}^2+1} \\ \text{and}\quad W' &= \mathrm{Re}\left[f'(ir^2) - f'(\infty)\right] \end{aligned}\right\} \qquad \ldots\ldots\ldots\ldots\ldots\ldots (26)$$

W has the same form as before but in calculating W' the extra term $f(\infty)$ appears. Compare Baker's formula in (1b), in a constant magnetic field, when f' is constant. $W' = 0$. External flowmeters still retain the property that W' is constant in a uniform field, but, as can be seen by integrating around the circle at infinity, this constant is zero.

In spite of this, an external flowmeter that was inserted in an infinite flow field of uniform velocity and uniform magnetic field would give a signal. That this is true is obvious in the case of point electrodes since the induced electric field is constant and there is no current flow. The reason is that although W' is zero, the range of integration is infinite. Physically there is no shorting by the fluid at infinity. This point is clarified later.

However where the meter is inserted in an infinite sea of fluid only a finite portion of which is moving (axisymmetrically) there is no signal with a uniform field. It is only because the magnetic field is non-uniform (and to a much smaller extent because blood vessel walls do not have the same conductivity as blood) that there is any signal at all.

From now on we confine ourselves to the case of point electrodes. For any practical magnetic field $f'(\infty) = 0$ and $W' = \mathrm{Re}\, f'(ir^2)$. As we have seen before for all internally generated magnetic fields $W \sim \frac{1}{r^4}$ so there is no chance of making W constant. It is just possible, however, that by arranging the windings in the right way inside the flowmeter, probably with currents

varying very sharply from positive to negative over short distances, that we could make W' fairly constant over a few diameters. This is not a practicable possibility with bloodflow catheter tip meters even if theoretically possible as it is difficult enough putting the present relatively simple current windings in the available space.

Figure 5 is the cross-section of a catheter tip instrument recently built by Mills (5). The outside diameter of the meter is 3mm and the current windings are considered as circles (or line currents) centred on the y-axis at $y = \pm 0.85$mm. The electrodes are taken to be point electrodes though the ones used by Mills were in fact circular discs of platinum 1 mm diameter attached to the surface. If the wall is taken to be the unit circle then the line currents are at $y = \pm \lambda$ where $\lambda = \frac{0.85}{1.5}$ or 0.565.

The resulting magnetic field is given by

$$f'(z) = \frac{1}{z^2 + \lambda^2}$$

so that

$$W = \mathrm{Re}\ \frac{1}{(\bar{z}^2 + 1)(z^2 + \lambda^2)}$$

The lines of constant W are shown in figure 5 where it will be seen that they very quickly become circles as r increases.

Also

$$W' = \frac{1}{r^4 - \lambda^2}$$

The moral is clear: external flowmeters producing their own magnetic field by windings carried internally are useless as flow measuring devices, as Mill's experience has shown. They may however be used as velocity probes, when inserted into a sea of fluid moving at a uniform velocity, in which case the problem is to see that the region near the flowmeter, where the fluid flow is upset in a variable way by the presence of the probe, contributes nothing to the signal. Since the flow may be assumed axisymmetric this requires a much more feasible adjustment in the magnet field. Schemes have been put forward by Baker (1b) using two windings on a shaped iron core. The problem is to ensure $W' = 0$ on the wall ($r = 1$).

Conclusions

Firstly it must be stressed that a constant magnetic field is only necessarily best for circular pipes with an axisymmetric profile under the assumption that the flowmeter is long. This assumption applies also to the requirement of uniform field and uniform virtual current for an ideal meter.

Secondly the special electrode arrangements required to give uniform $g'(z)$ are not easily realisable in practice. Most of the electrode arrangements described do not have a sufficiently superior performance to justify the extra practical difficulties. The case of transverse circular arc line electrodes are the exception, long flowmeter theory suggesting that their performance, taking the three dimensional nature of their virtual current into account, may be the best practical approximation to an ideal circular flowmeter yet found.

Thirdly catheter tip probes are poor flowmeters though if the boundary layer on the probe is prevented from contributing to the signal as described in the text they can serve as velocity probes (Baker and Mills).

The general conclusion must be that none of the long flowmeters described in this paper are more practical propositions than the design of long circular flowmeter now in use. It would be better to regard the analysis given here for one class of flowmeter (namely long ones) as an initial step to analysing short flowmeters, some of which have very useful properties.

Acknowledgements

The author wishes to acknowledge the advice of Professor J.A.Shercliff, useful discussions with George Kent Ltd., and Dr's D.G.Wyatt, R.C.Baker and C.J.Mills and finally the English Electric Co. Ltd. for supporting him financially at the University of Warwick.

References

1. BAKER, R.C. a) 1968 Journal of Fluid Mechanics 33.1.p.73.
   b) 1968 Brit. Journal Appl.Phys. (J.Phys.D) series 2, 1, p.895.

2. BEVIR, M.K. 1968 Contributions to the theory of Induced Voltage Electromagnetic Flowmeters. Warwick University, School of Engineering.

3. HENDERSON, F.M. 1960 Elliptic Functions with Complex Arguments. University of Michigan Press.

4. KANAI, H. a) 1965 J.Jap.Soc.Inst.Cont.Eng. 4.5.p.328.
   b) 1966 Trans. Jap.Soc.Inst.Cont.Eng. 2.2., p.152.
   c) 1966 Trans. Jap.Soc.Inst.Cont.Eng. 2.4., p.295.

5. MILLS, C.J. 1966 Phys.Med.Biol. 11.2. 323.

6. RUMMEL, T.H. & KETELSEN, B. 1966 Regelungstechnik 6.262.

7. SHERCLIFF, J.A. a) 1962. The Theory of Electromagnetic Flow Measurement C.U.P.
   b) 1965. Symposium on Electromagnetic Flow Measurement, Warwick.
   c) 1967. Symposium Electromagnetic Blood Flow Metry. Oslo.

8. YAKUBENKO, A.E. 1964 Z.P.M.T.F. No.5. p.151 also reviewed in VATAZHIN, A.B. & REGIRER, S.A. 1965, Supplement to Russian edition of (7a) (In Russian, English Translation available from N.L.L.).

UNIFORM MAGNETIC FIELD

FIGURE 1a

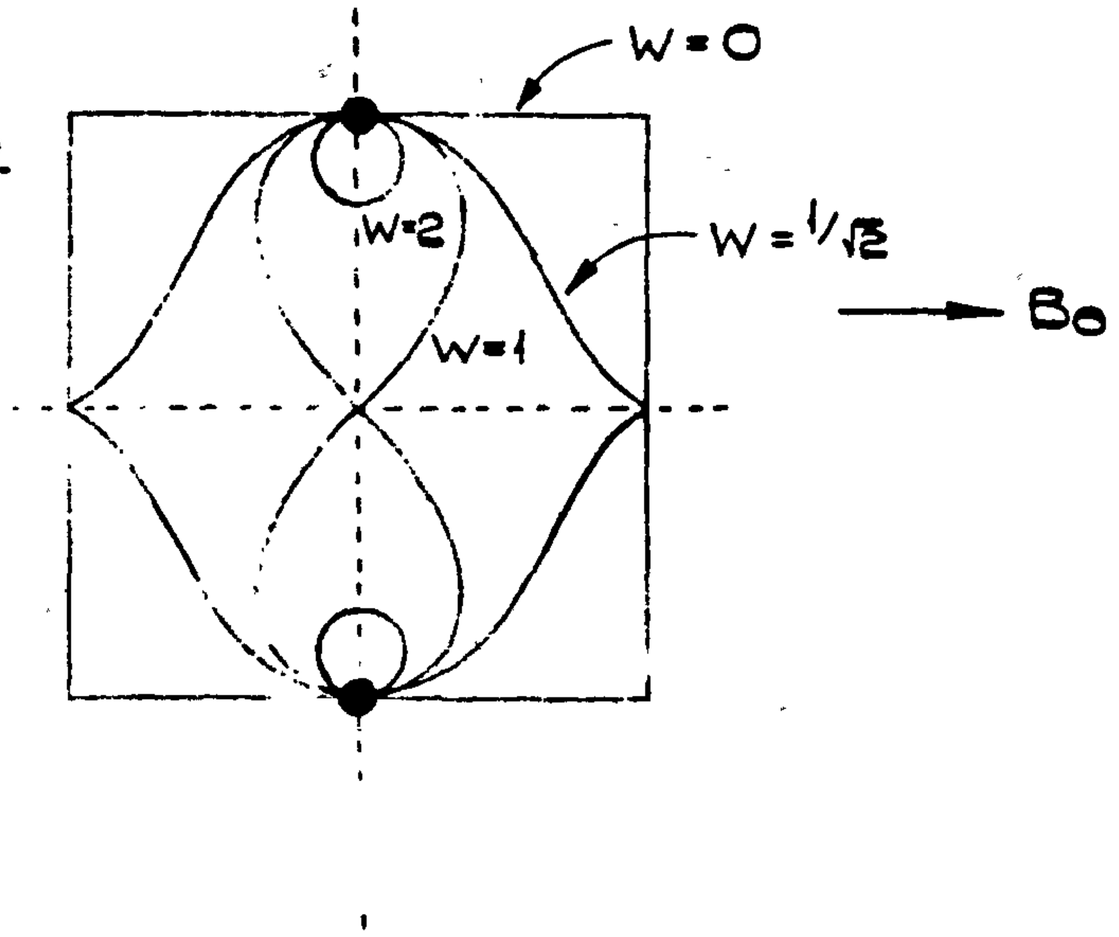

UNIFORM MAGNETIC FIELD

FIGURE 1b

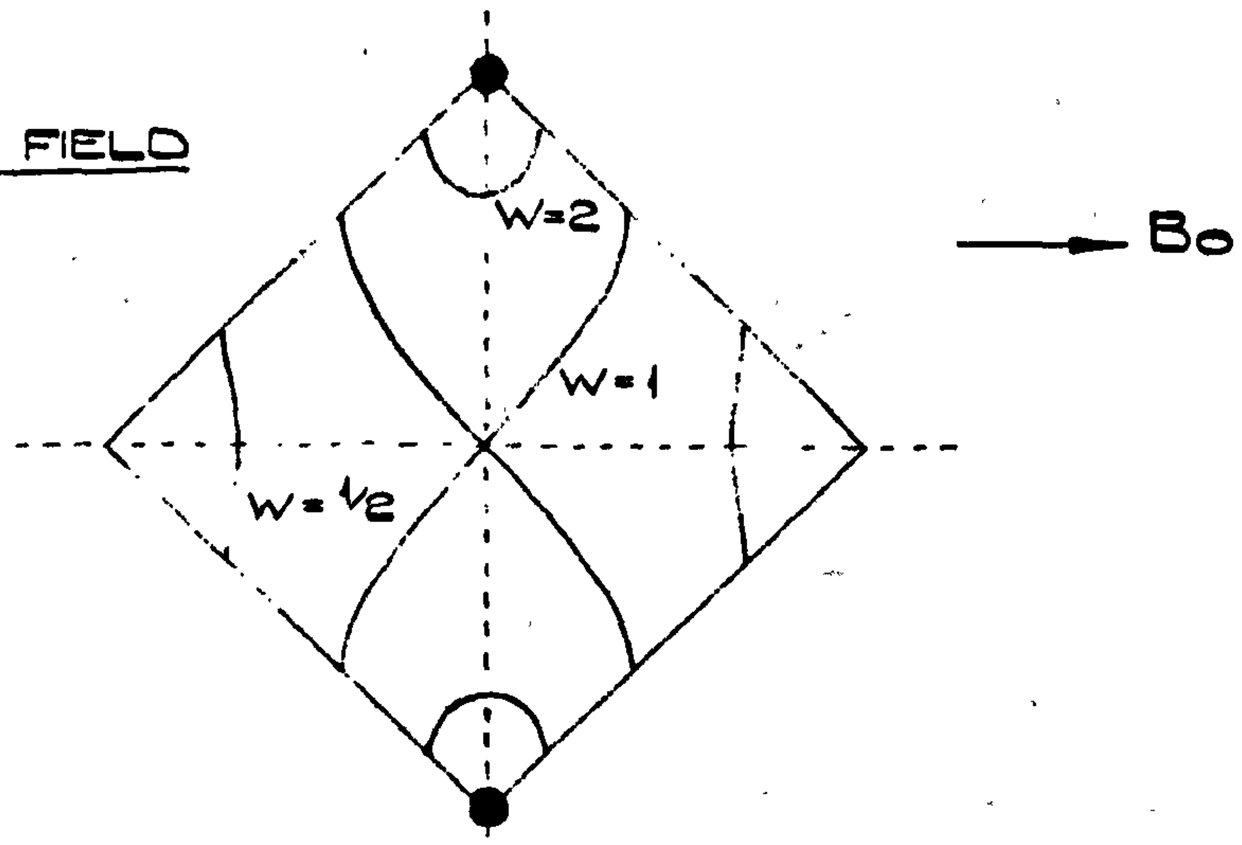

MATCHING MAGNETIC FIELD

FIGURE 1c

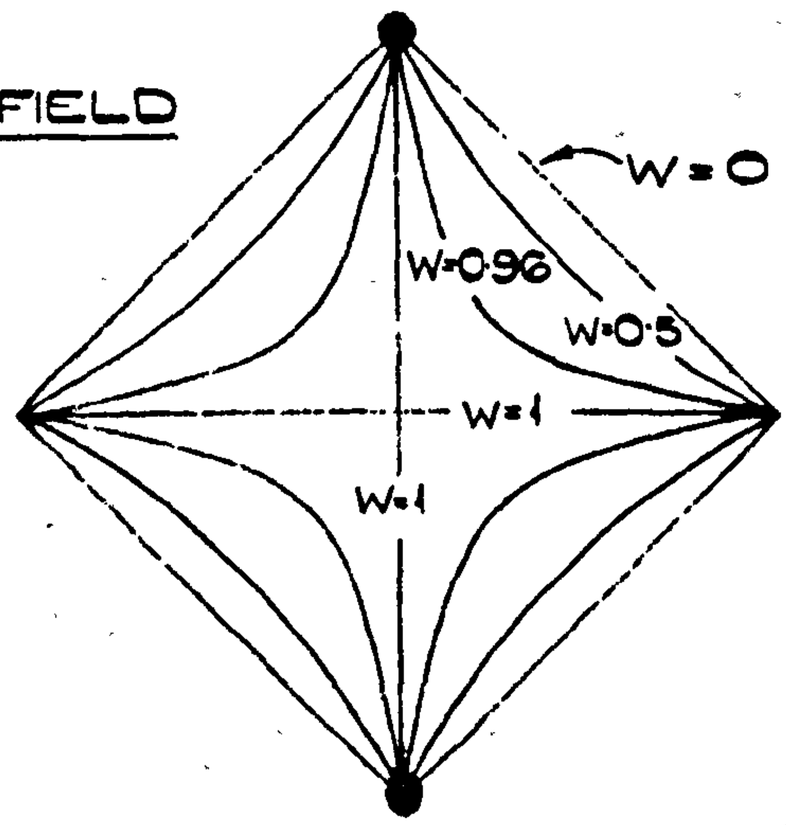

SQUARE FLOWMETERS WITH POINT/LINE ELECTRODES

FIGURE 1

UNIFORM MAGNETIC FIELD

(After Shercliff)

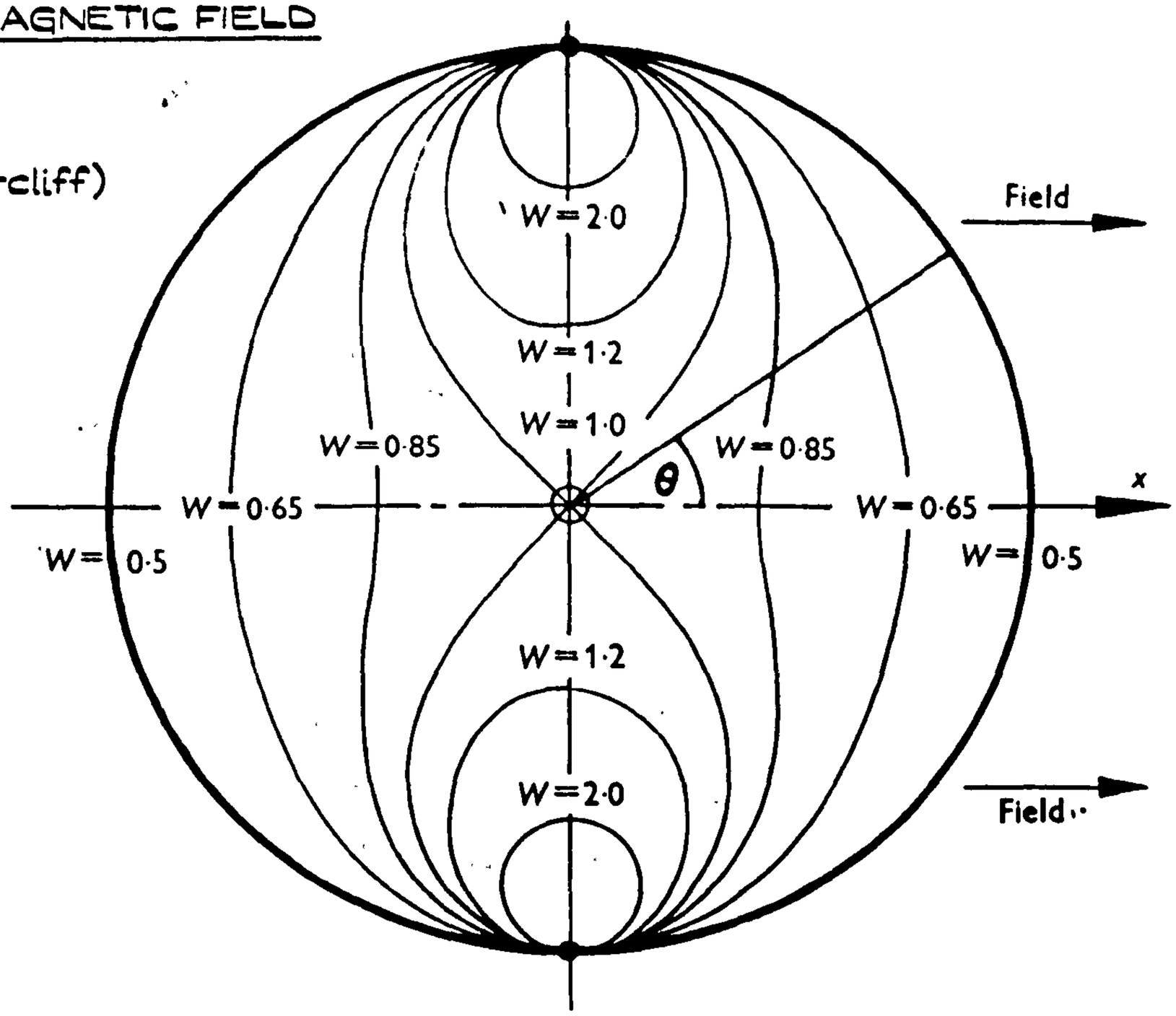

MATCHING MAGNETIC FIELD

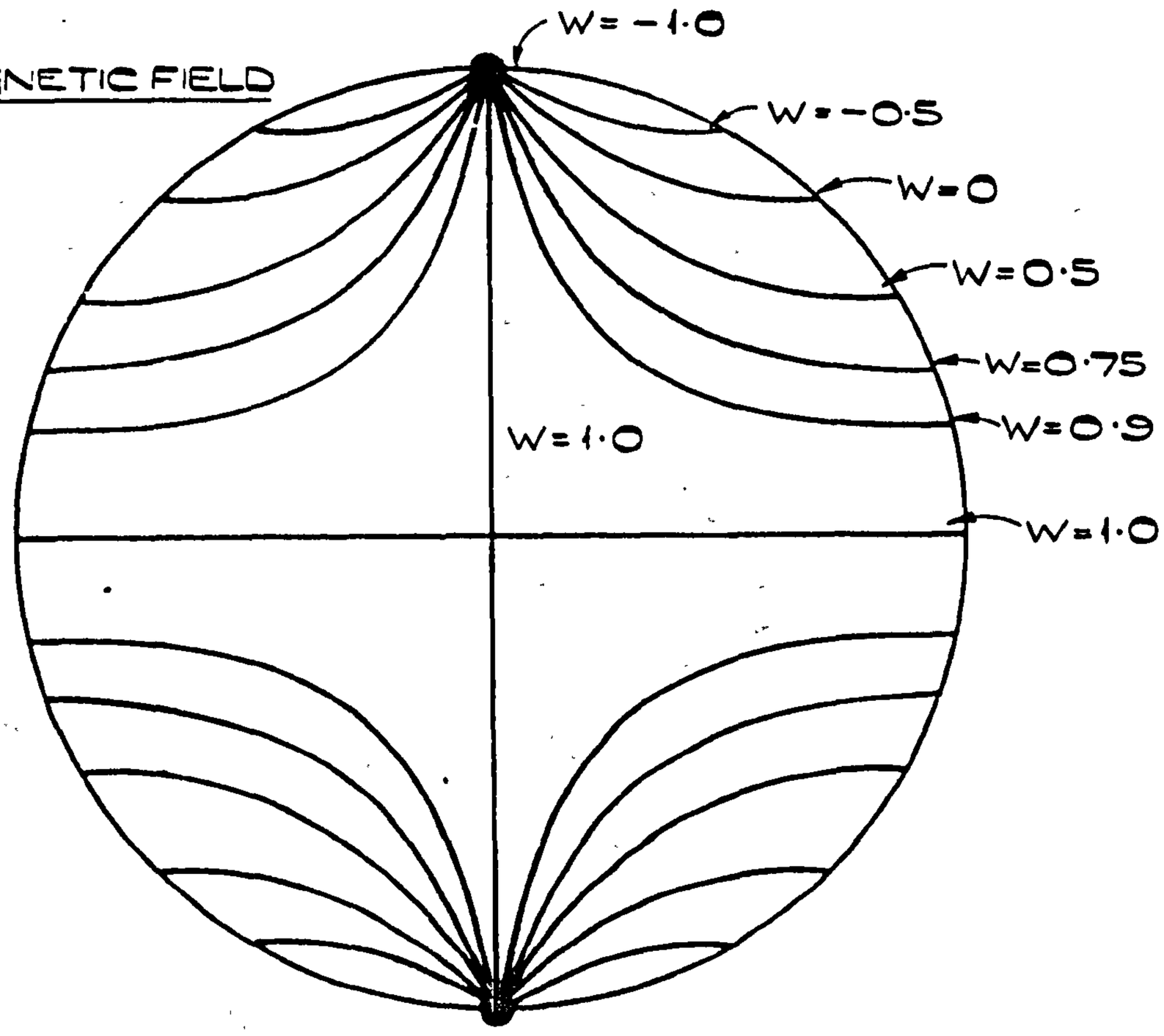

LINE/POINT ELECTRODES

FIGURE 2a

UNIFORM MAGNETIC FIELD

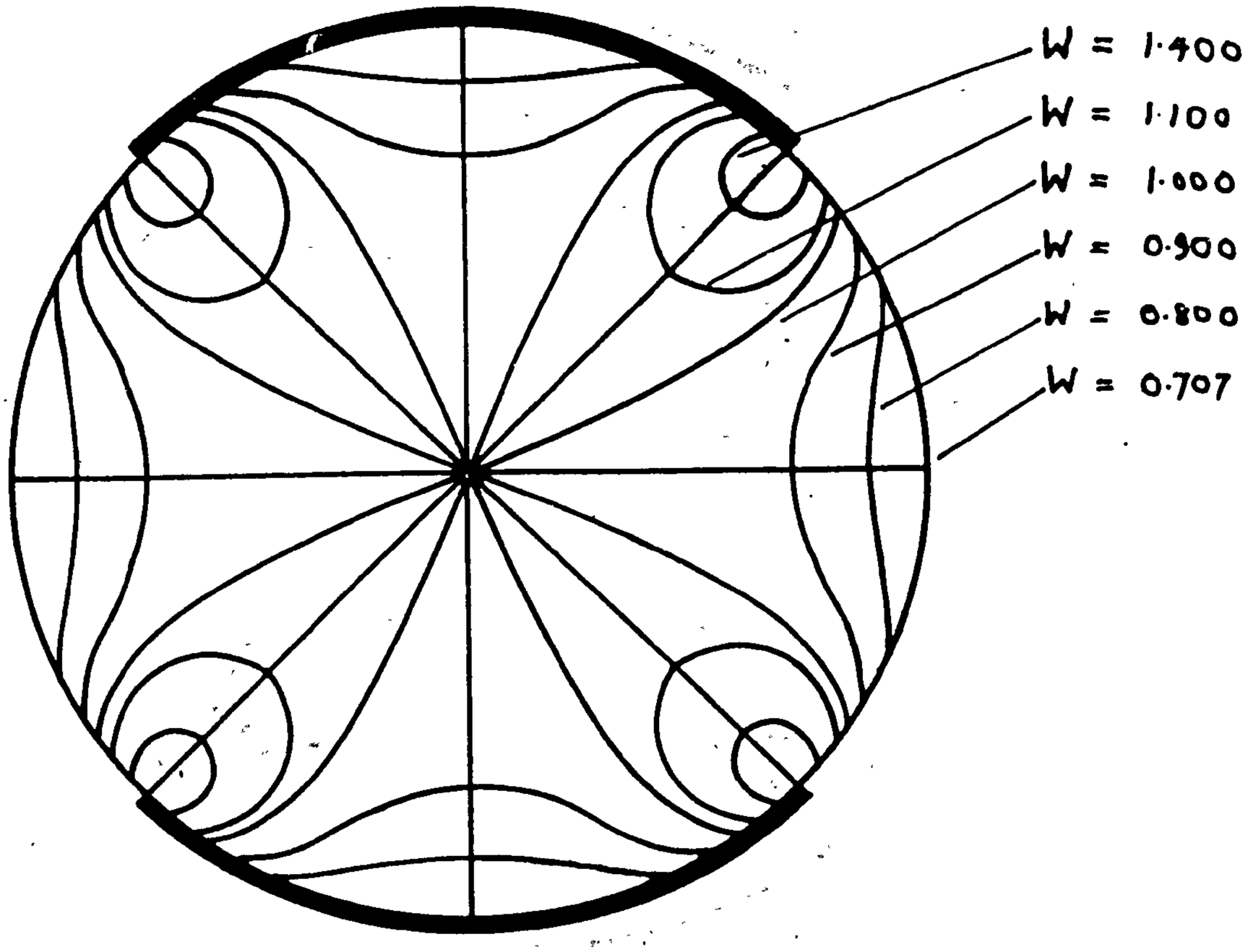

MATCHING MAGNETIC FIELD

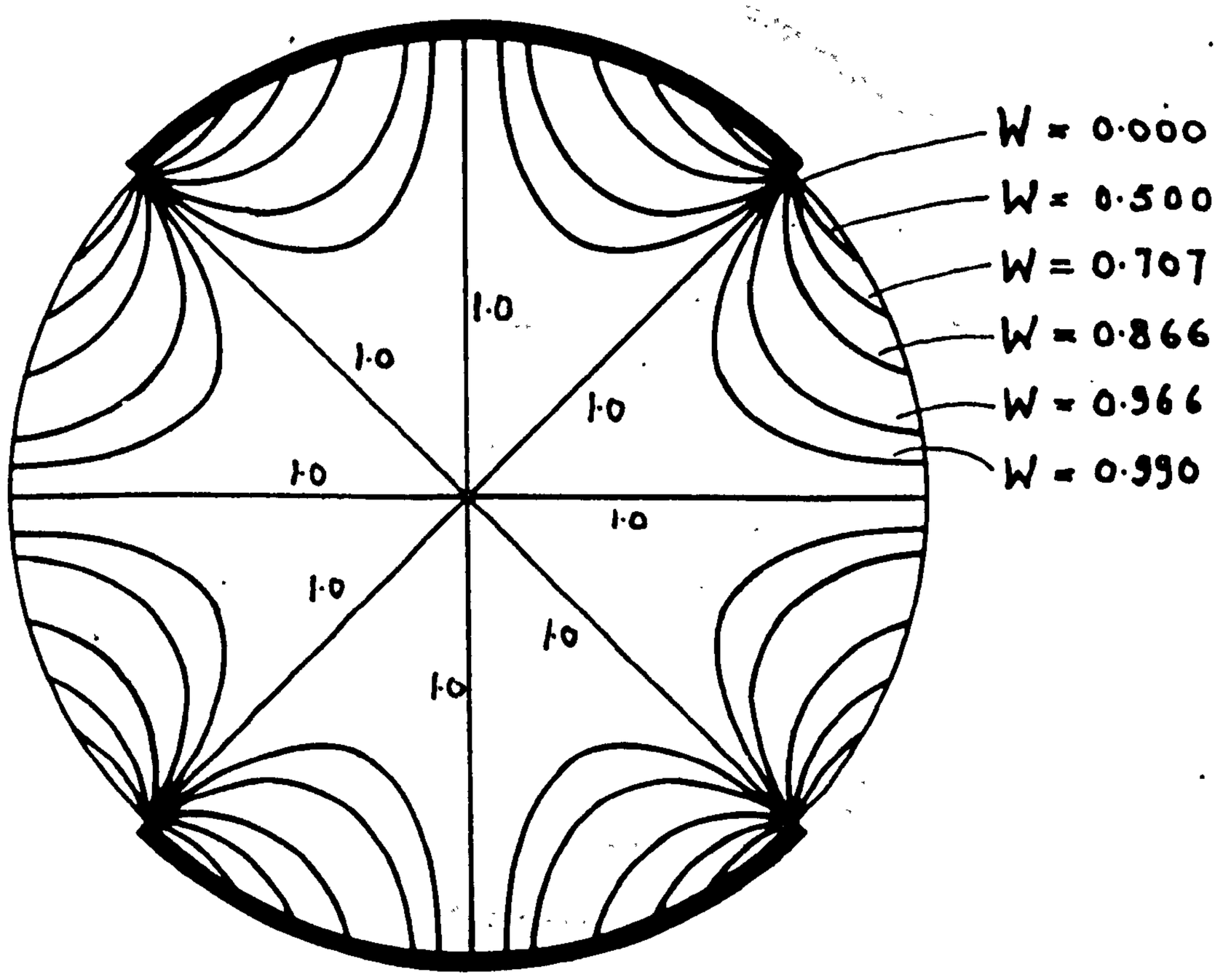

LONG QUADRANT ELECTRODES

FIGURE 2b

UNIFORM MAGNETIC FIELD

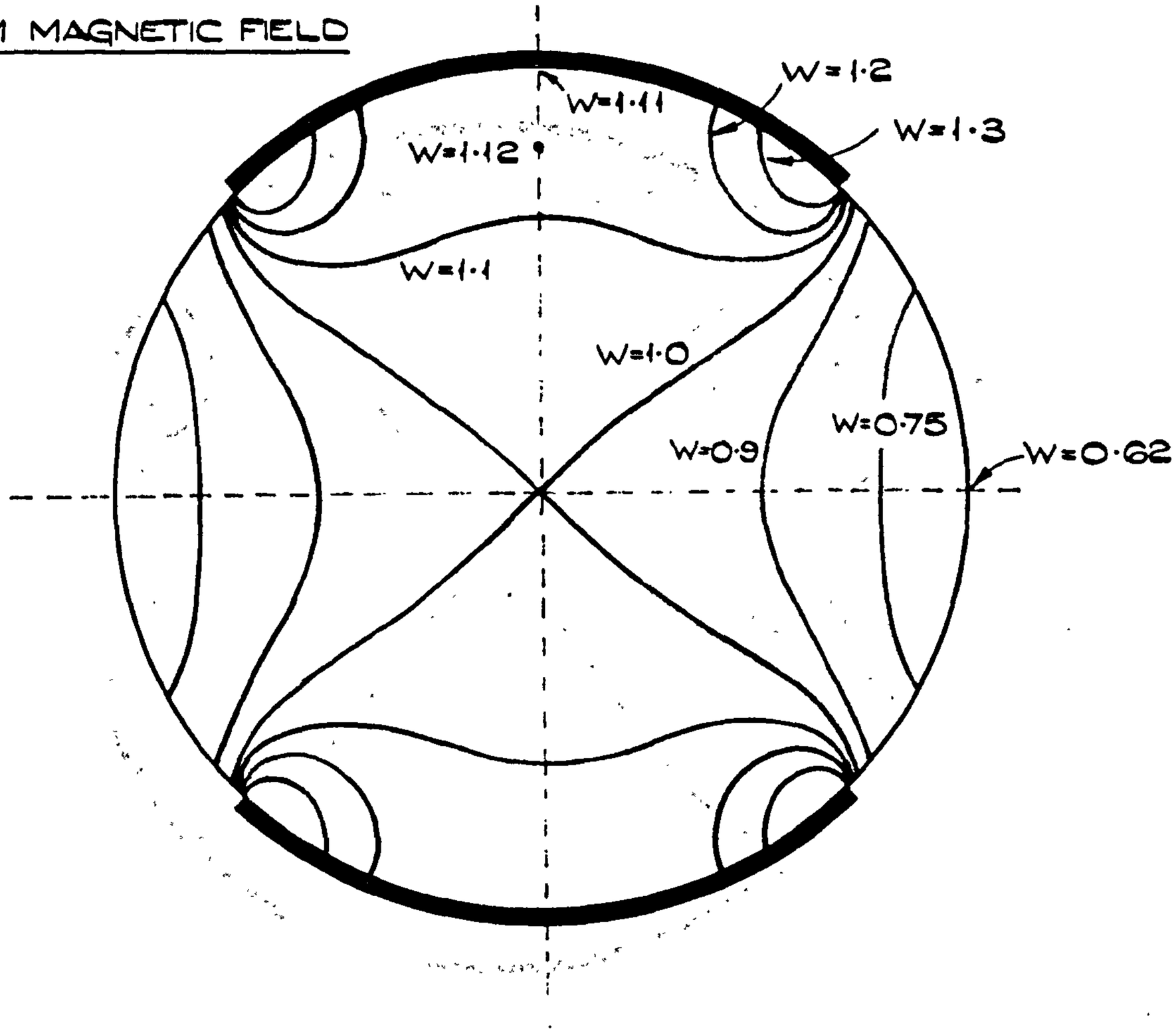

MATCHING MAGNETIC FIELD

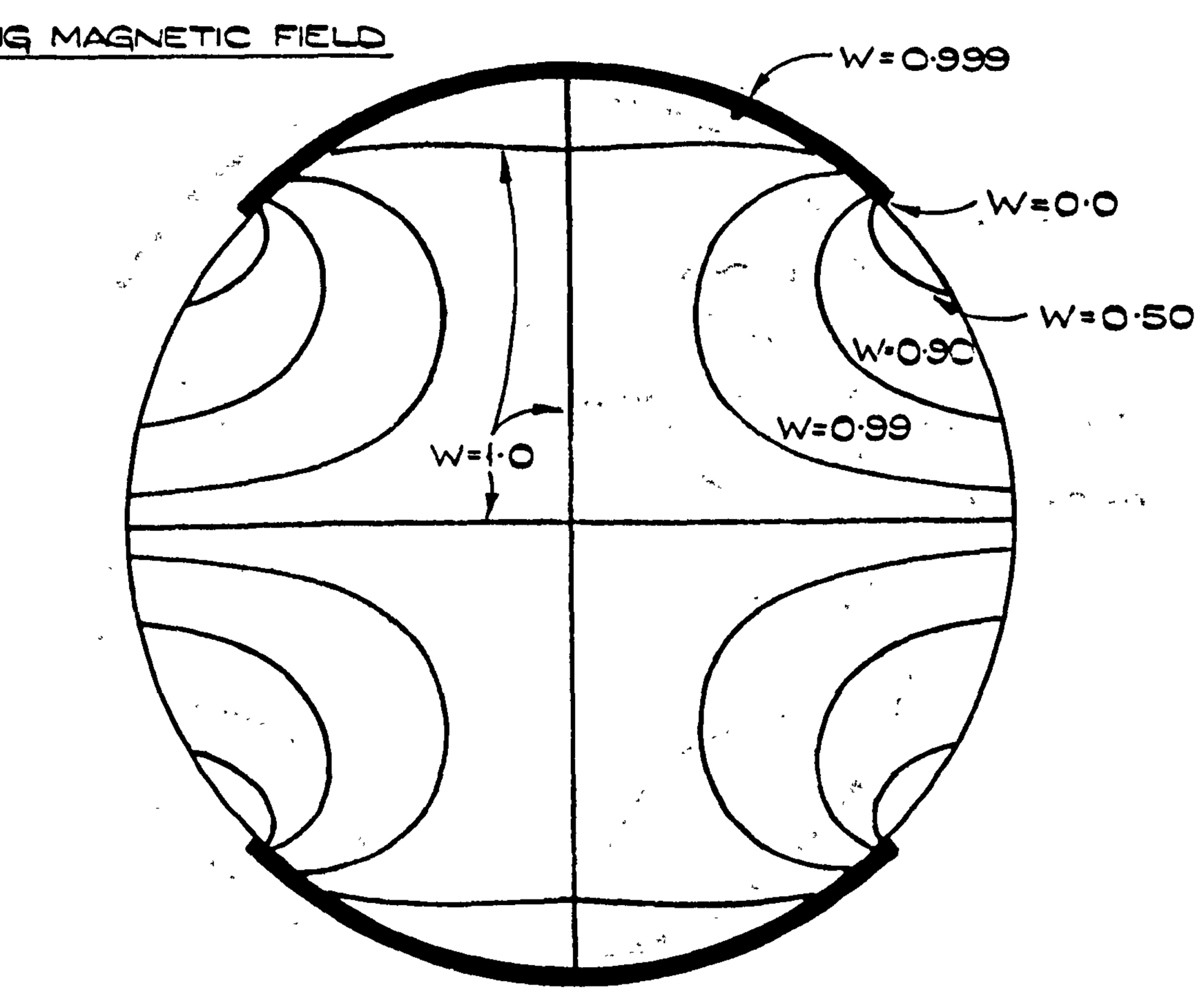

TRANSVERSE LINE ELECTRODES: HALF ANGLE $\alpha = 45°$

FIGURE 2c.

UNIFORM MAGNETIC FIELD.

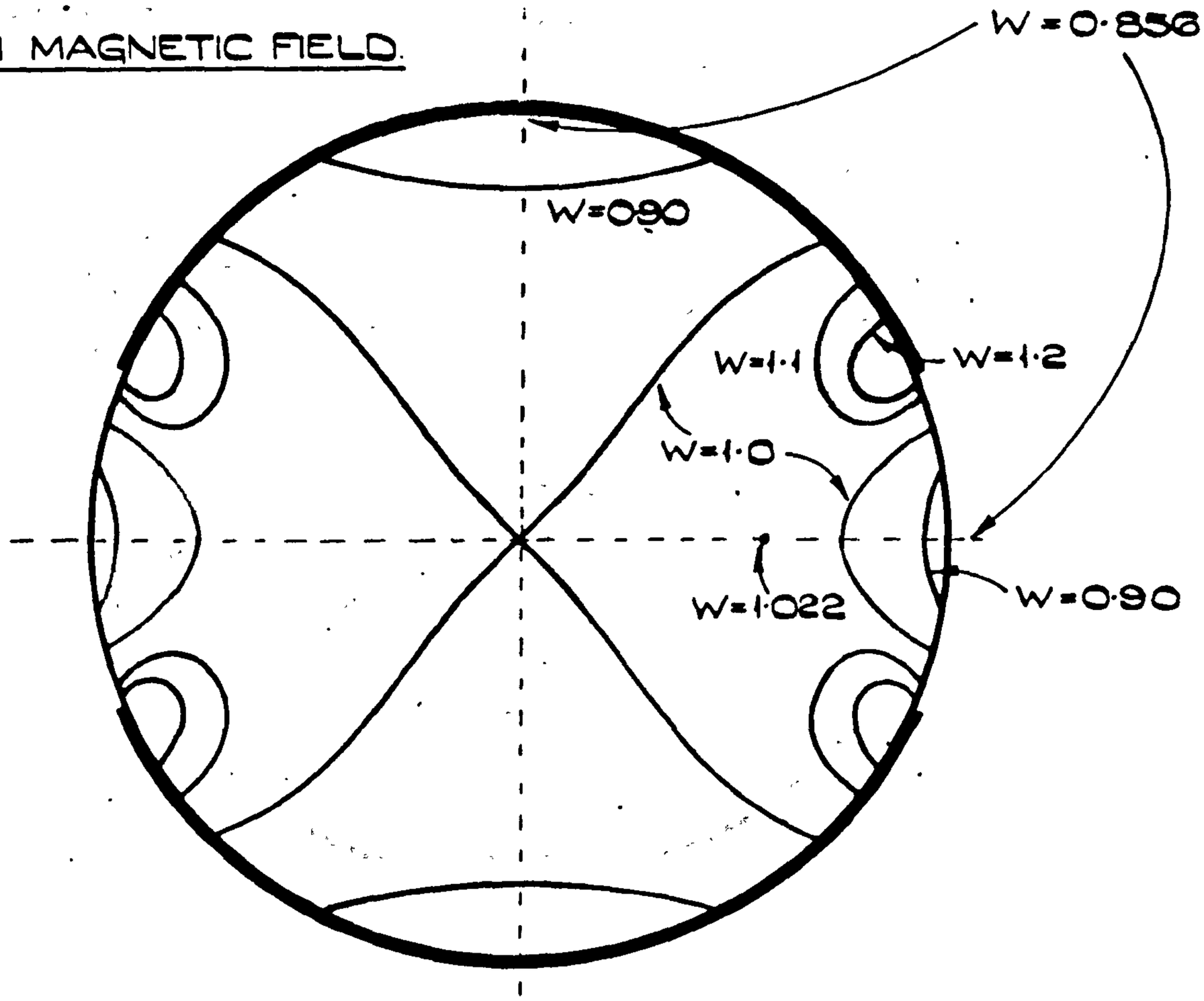

MATCHING MAGNETIC FIELD

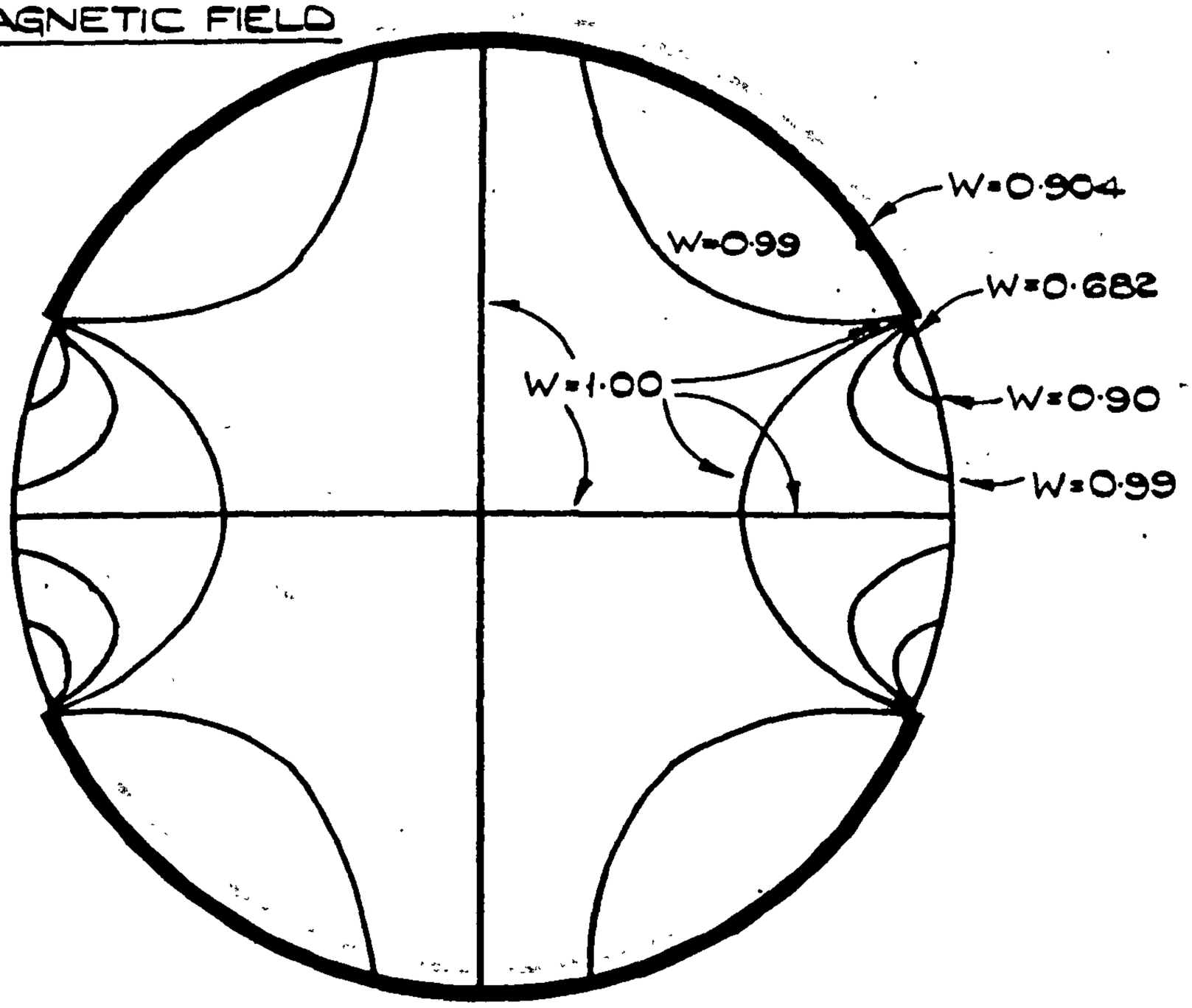

TRANSVERSE LINE ELECTRODES: HALF ANGLE $\alpha = 66{\cdot}5°$

FIGURE 2d

UNIFORM MAGNETIC FIELD

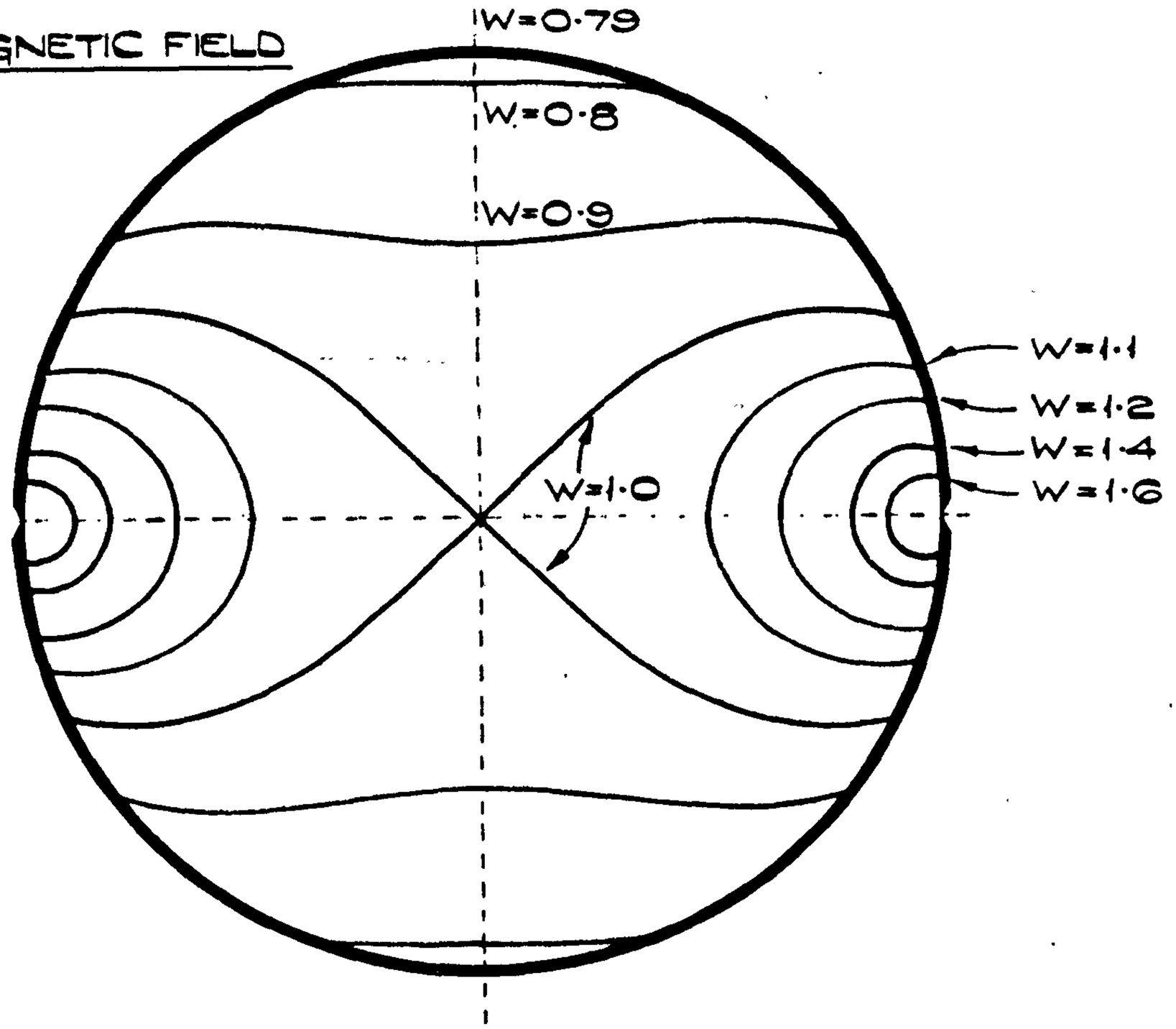

MATCHING MAGNETIC FIELD

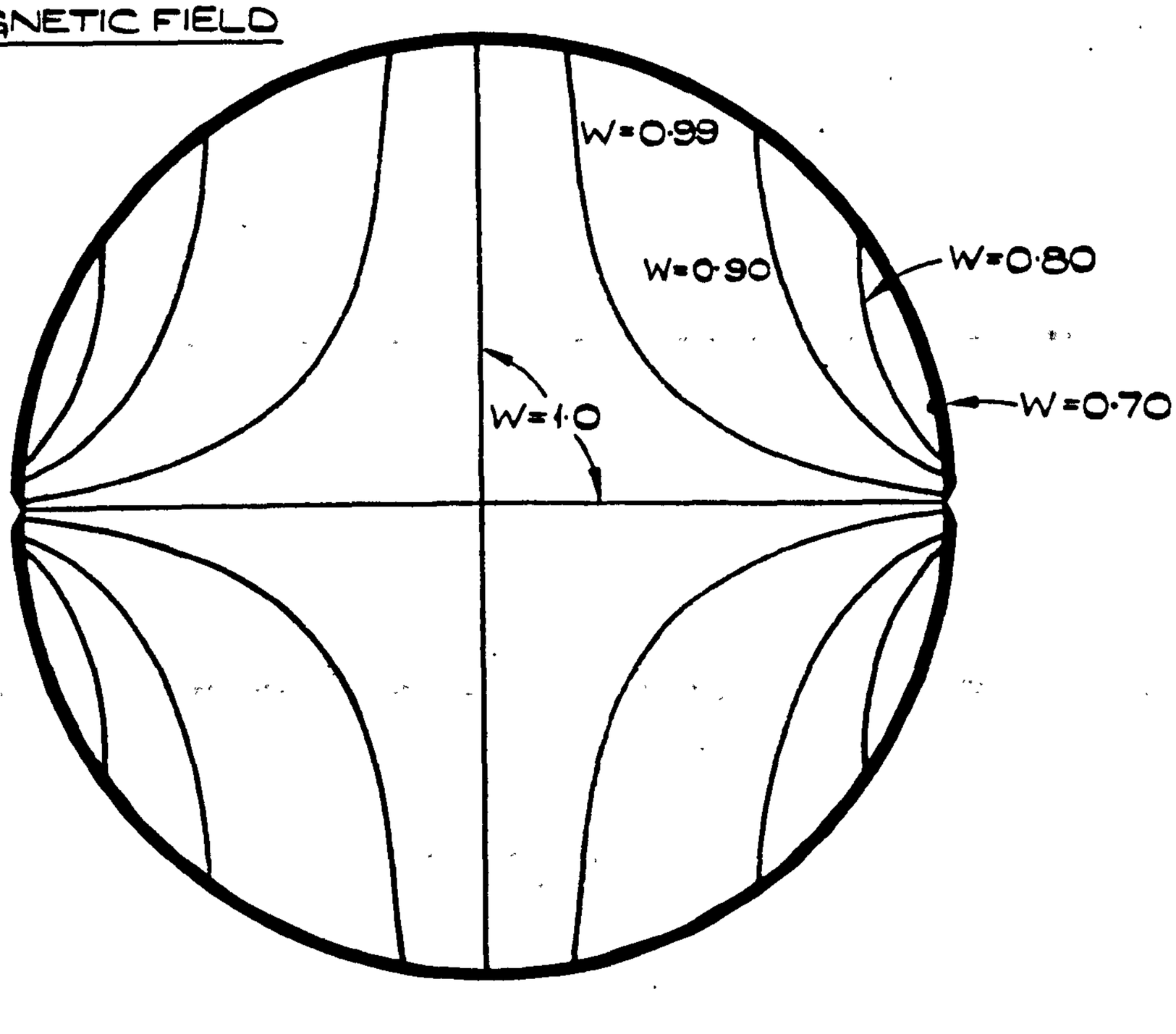

TRANSVERSE LINE ELECTRODES : HALF ANGLE $\alpha = 90°$

FIGURE 2e.

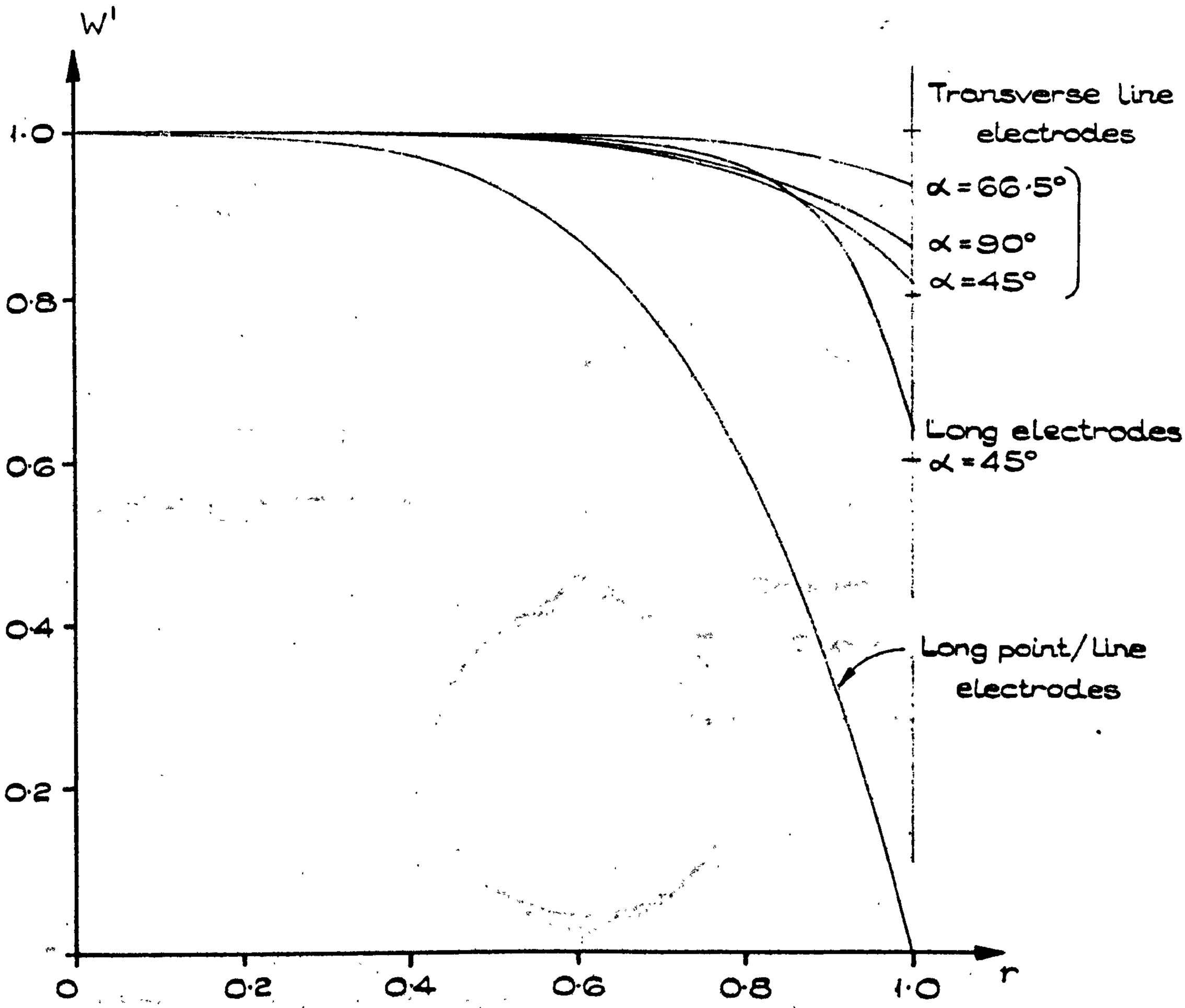

AXISYMMETRIC PROFLE WEIGHT FUNCTION $W'(r)$ FOR MATCHING MAGNETIC FIELDS.

FIGURE 3.

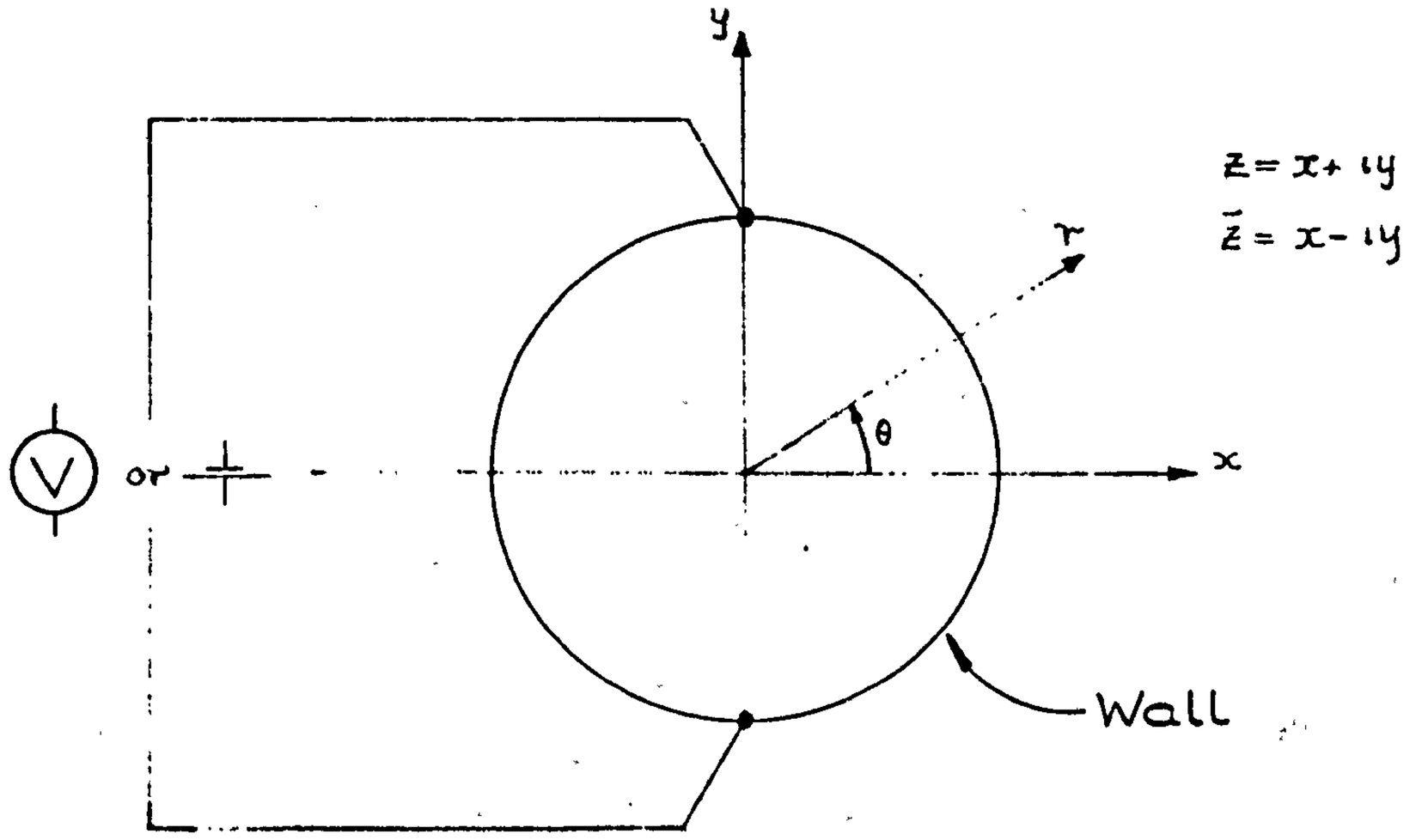

FIGURE 4a. NOTATION.

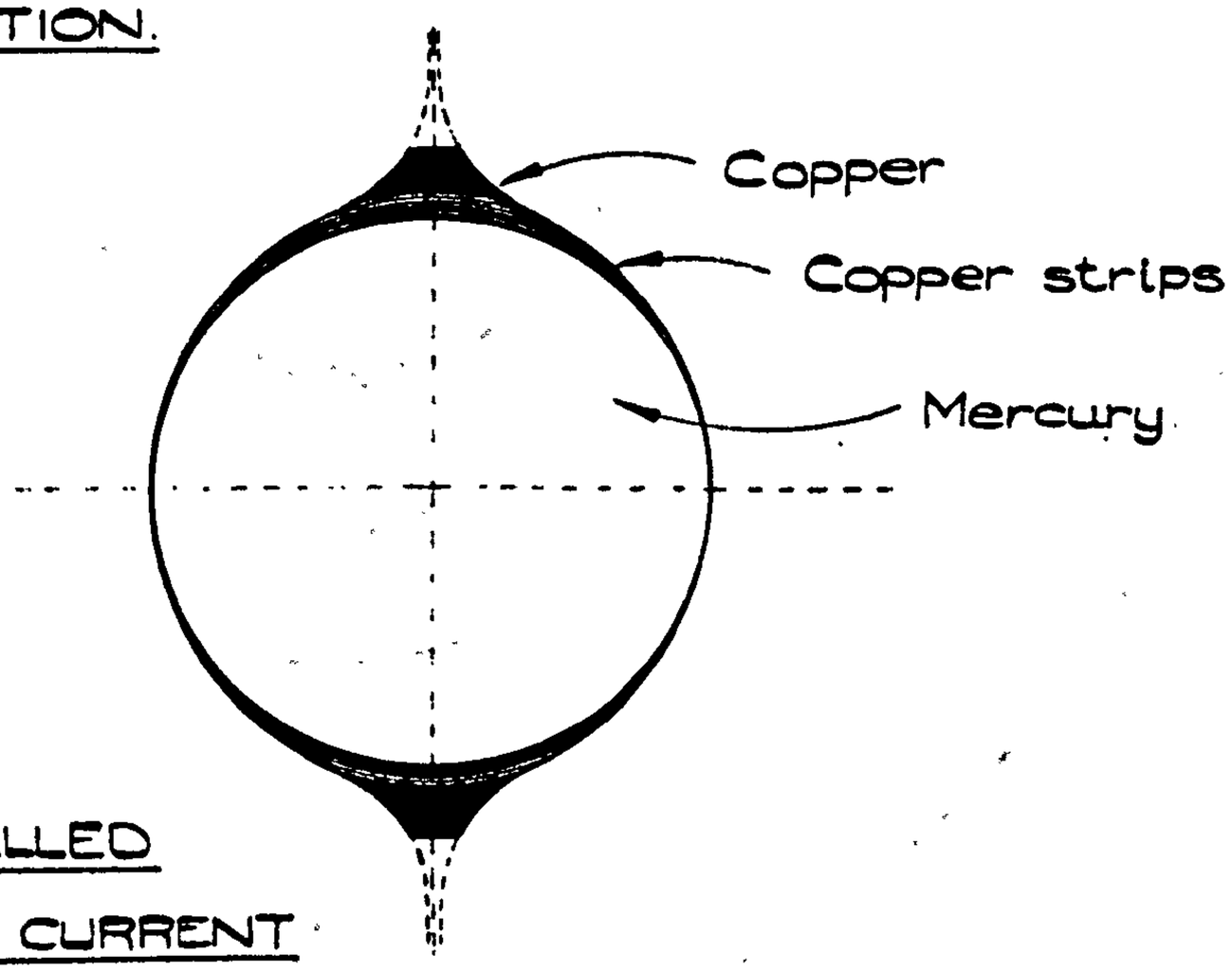

FIGURE 4b. THIN-WALLED UNIFORM VIRTUAL CURRENT FLOWMETER.

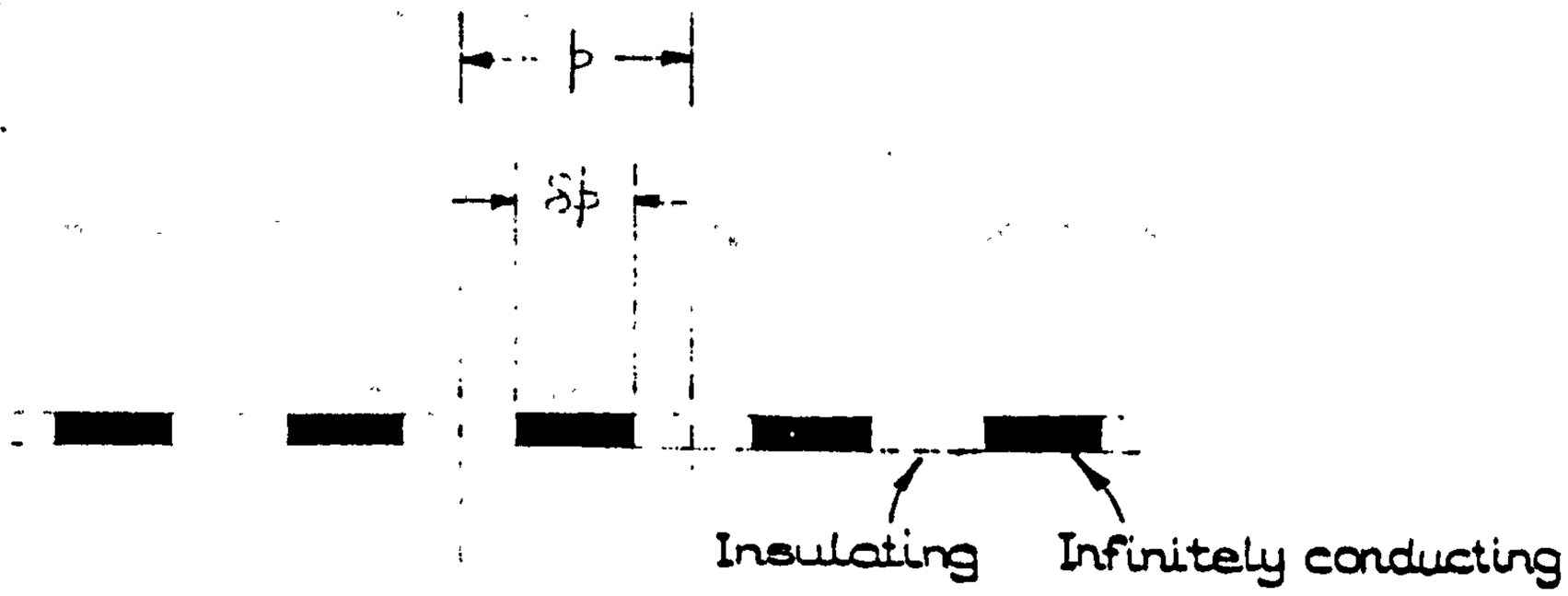

FIGURE 4c. APPROXIMATION TO A THIN WALL OF FINITE CONDUCTIVITY.

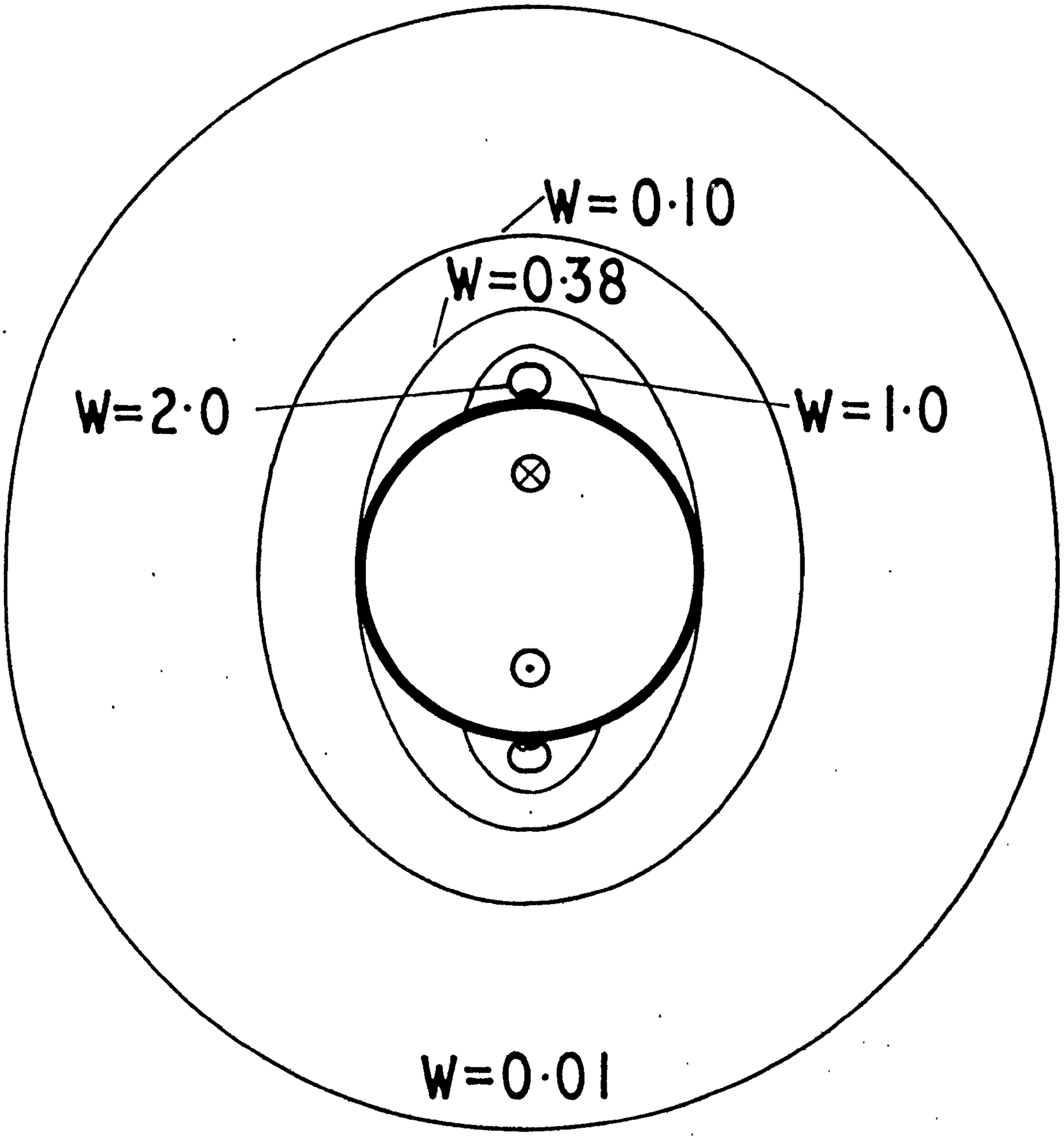

EXTERNAL FLOWMETER (MILL'S DESIGN)

FIGURE 5.

Abstract

A summary of the extent to which the performance of a flowmeter can be made independent of the velocity pattern is given. The case of practical interest, a flowmeter with diametrically opposed point electrodes and short magnetic field, is analyzed making certain (practical) assumptions about the way in which the magnetic field is produced. In the case of axisymmetric rectilinear flow the results are set out in a series of design tables. Finally the effects of unknown magnetic and electric boundary conditions at the ends of a short flowmeter are briefly discussed.

SOME DESIGN DATA FOR INDUCED VOLTAGE ELECTROMAGNETIC FLOWMETERS WITH NON-UNIFORM FIELDS

by
M.K. Bevir*

Introduction

Ketelsen[5] has recently claimed that deliberately non-uniform magnetic fields can improve the performance of induced-voltage electromagnetic flowmeters, and he has used this idea to design a range of short flowmeters, in which the magnetic field and associated coils do not extend very far either side of the electrodes. His design procedure seems to have been based largely on numerical and analogue methods. There is no doubt that the performance of flowmeters may be improved in this way. The question is how much.

In another paper[2] we have explored the general problem of designing the magnetic field, electrodes and pipe geometry so that the flowmeter calibration is wholly or partially independent of velocity distribution. These conclusions are briefly summarised in this paper, before the particular case of designing a magnetic field for a circular flowmeter with point electrodes is discussed. For reasons given in (2) we assume the flow is rectilinear and distinguish between flowmeters with an axisymmetric velocity profile and those in which the profile is unknown (referred to as having an asymmetric profile).

It turns out that it is feasible to produce a set of tables that greatly ease the design of a short flowmeter whose signal is independent of the flow rate, provided the velocity profile is axisymmetric, but that if the profile is asymmetric this desirable property may only be approximately achieved and the design is better optimised on a computer. This has not yet been finished, so in this paper we concentrate on the problem of axisymmetric flow.

* The English Electric Co. Ltd., Whetstone (seconded to the University of Warwick) England

Background

The general situation with regard to induced voltage flowmeters is as follows:

1. The signal between two electrodes is given by

$$\int_\tau \underline{v}.\underline{W}\, d\tau \qquad (1)$$

where $\underline{v}$ is the fluid velocity, τ the volume occupied by the fluid, and $\underline{W}$ a weight vector given by:

$$\underline{W} = \underline{B}\times\nabla G \qquad (2)$$

where $\underline{B}$ is the magnetic field and G a Green's function. ∇G is proportional to the current that would flow between the electrodes if a voltage was placed across them, subject to the same electrical boundary conditions as the flowmeter itself, and may be called the "virtual" current.

2. The necessary and sufficient general condition for the signal to be entirely independent of velocity distribution is, provided div $\underline{v}$ = 0 and $\underline{W}\to 0$ at ∞,

$$\text{curl } \underline{W} = 0 \qquad (3)$$

3. It is possible to achieve this condition using certain electrodes, geometrical arrangements and magnetic fields, and even to vary the geometry while keeping the flowmeter calibration constant, but it is <u>not</u> possible using point electrodes.

4. This being the case, some conditions must be put on the velocity $\underline{v}$ so that conditions on $\underline{W}$ are less stringent. Briefly, taking the axis of the flowmeter in the z-direction (figure 1) we require the flow to be in this direction only, and hence by continuity independent of z, and seek to make

$$\bar{W}(r,\theta) = \int_{-\infty}^{+\infty} W_z\, dz \qquad (4)$$

$$\text{or} \quad \bar{W}'(r) = \int_0^{2\pi} \bar{W}(r,\theta)\, d\theta \qquad (5)$$

constant. The first condition is suitable for asymmetric rectilinear profiles, and includes the second which is suitable only for axisymmetric profiles. In the paper mentioned previously

we have discussed at some length whether it is possible to make $\bar{W}$ constant, to which the provisional answer is yes, except in regions close to the electrodes compared with the flowmeter wall thickness. There are many ways of making $\bar{W}'$ constant.

In this paper we give formulae for $\bar{W}$ and $\bar{W}'$ using a canonical set of magnetic fields which can be simply produced and added together to produce the required distributions of $\bar{W}$ and $\bar{W}'$. The question is how to choose this canonical set and this is discussed in the next section.

Magnetic field production

In order to produce some useful design procedures, we must take account of the aims and needs of designers and in particular how they produce their magnetic fields. Let us restrict ourselves to industrial applications. Here we may distinguish three main sizes of flowmeters: small, up to 2.5 cm. in diameter; medium, up to 30 cm.; large, up to 300 cm. or more.

Most designers require a fixed output signal per unit mean velocity from all sizes of flowmeters, typically 1.5mV/m/sec. and for uniform-field designs the magnetic field is therefore inversely proportional to the flowmeter diameter. For a 2.5 cm. diameter meter the above figure requires a field of 600 gauss and a total current of 1200 AT to maintain this field over a gap equal to the flowmeter diameter. This total current is independent of diameter since the required field drops as the diameter is increased.

For a given rate of heat dissipation in the copper, the volume of copper required is proportional to the diameter, whereas for geometrically similar designs the volume available is proportional to the $(\text{diameter})^3$. The result is that for small flowmeters there is no room to put the necessary copper around the outside; yokes are required and the whole device occupies so much space in relation to the flowmeter that the length of pipe needed to ensure that the flow is rectilinear with axisymmetric profile is automatically incorporated. There is little scope or need for design improvements here.

For large flowmeters the situation is quite the reverse; in fact the windings are so sparse that itis remarkable they

produce any magnetic field at all. Medium flowmeters represent the transition region in which it is still possible to place the windings on the surface, although they now cover nearly all of it, to a depth of a few layers in the smaller sizes.

In the past, the designers of large and medium flowmeters have used some non-magnetic material, often stainless steel, for the flowmeter pipe, put the windings on the outside and then surrounded it with iron to keep the field in. The recent trend is towards a rationalization of this design in which a piece of ordinary steel piping keeps the field in and the windings are encapsulated in some suitable nonmagnetic glue, which also holds the electrodes. The whole capsule forms a short piece of cylindrical piping which fits neatly inside the steel piping, and acts as the insulating liner at the same time. Figure 2 schematically compares the two designs.

The model we shall adopt as amenable to analysis is based on the rationalized scheme. We shall suppose the magnetic field to be produced by twin symmetrical rectangular coils, of thickness small compared to the pipe diameter. Their shape is defined by their length L and the angle they subtend at the centre line of the flowmeter $\pi-2\theta_o$. They are surrounded by a cylindrical iron sheath of infinite magnetic permeability, assumed infinitely long in the analysis. The arrangement is shown in figure 3a. We shall take account of the thickness of the flowmeter wall, but not of the coil thickness, so that strictly speaking the results will only hold at distances from the coil windings large compared with the coil thickness. All coil dimensions are defined on the centre of the coil cross-section. For the purposes of calculation, the diameter of the iron sheath is its actual diameter and <u>not</u> the diameter based on a circle through the centre of the coil cross-section.

We shall also assume that the insulated portion of the inside wall of the flowmeter is infinite in extent. In practice both the insulating liner and the magnetic sheath are a few diameters long. If this effect was taken into account, the analysis of the resulting magnetic field and virtual current would require the solution of mixed boundary value problems, which we shall not attempt here. The solution for infinitely long liner and sheath may be written down, and from these we can estimate the distances upstream and downstream at

which the magnetic field and virtual current fall to some specified small fraction of their maximum values. For liner and sheath lengths shorter than this the more sophisticated analysis would be necessary, but fortunately there is another factor that makes it unlikely that such analysis would be required. This is that the designer is normally not sure what sort of pipes will be attached to the flowmeter; that is he does not know the electrical and magnetic boundary conditions at the ends of the flowmeter, and he must thereforemake it long enough for their unknown effects to be sufficiently small, in which case the analysis based on infinitely long liner and sheath is valid.

The analysis is given in terms of formulae for G and F (the magnetic field potential such that $\underline{B} = \nabla F$). F on the outer surface of the flowmeter is the stream function for the coil current (for F read ΔF in the case of coils without any iron sheath), and so the lines of constant F (constant stream function) on the outer wall surface are the coils. On the outer surface F is therefore zero outside the rectangular coils and constant inside them. By taking $\frac{-\partial}{\partial\theta_0}$ or $\frac{\partial}{\partial L}$ or both of the formulae for $\bar{W}$ and $\bar{W}'$ for rectangular coils (with F = 1 inside) we obtain formulae for strip coils (of unit strength/unit length) in the z-direction or θ-direction or point source coils (δ-function coils) of unit strength. These coils form further canonical sets. The strip coils in the z-direction are particularly suitable for predicting the performance of non-rectangular coils. The point source coils may be used for calculating the performance of more complex coil shapes, but in practice they are not so useful, since the formulae for them do not converge too well close to the electrode plane. A typical strip coil and point source coil is shown in figure 3b, the multiple coils being due to the symmetry assumed in the original rectangular coils.

Notation for Bessel Functions

J_m	Bessel function of the first kind
I_m, K_m	Modified Bessel functions of the first and second kind
$j_{m,s}$	The s^{th} zero of $J_m(t)$
$j'_{m,s}$	The s^{th} zero of $J'_m(t)$ ($' \equiv \frac{d}{dt}$)

Analytic expressions for $\bar{W}$ and $\bar{W}'$

With the symmetry we have chosen, F and G will be symmetrical in z (see figure 1), F will be odd in θ and even in θ', G will be even in θ and odd in θ'.

We therefore write:

$$F(r,\theta,z) = \int_{\alpha=0}^{\infty} d\alpha \sum_{m\ odd} A(m,\alpha)\, I_m(\alpha r) \cos\alpha z \sin m\theta \qquad (6)$$

$$G(r,\theta,z) = \int_{\beta=0}^{\infty} d\beta \sum_{n\ odd} B(n,\beta)\, I_n(\beta r) \cos\beta z \cos n\theta \qquad (7)$$

To evaluate $A(m,\alpha)$, when the magnetic field is produced by the rectangular coils in figure 3, surrounded by the infinite iron sheath, we use the conditions

$$\begin{aligned} F(r=b,\ \theta,\ z) &= 1 \quad |z|<\ell,\ \theta_o<\theta<\pi-\theta_o \text{ and } \pi+\theta_o<\theta<2\pi-\theta_o \\ &= 0 \text{ otherwise} \end{aligned} \qquad (8)$$

$$\text{This requires } A(m,\alpha) = \frac{8 \sin\alpha\ell \cos m\theta_o}{\pi^2 \alpha m\, I_m(\alpha b)} \quad (m \text{ odd}) \qquad (9)$$

Suppose, however, that we require the magnetic field due to the same coils, without the iron sheath. We write F for r<b as in (6) and for r>b as

$$\int_{\alpha=0}^{\infty} d\alpha \sum_{m\ odd} A^T(m,\alpha)\, K_m(\kappa r) \cos\alpha z \sin m\theta$$

$\frac{\partial F}{\partial r}$ must be continuous at r=b, and $F(b-,\theta,z) = F(b+,\theta,z)$ replaces F in condition (8). After a little manipulation we find

$$\begin{aligned} A(m,\alpha) &= -\frac{8b}{\pi^2 m} \sin\alpha\ell \cos m\theta_o\, K'_m(\alpha b) \\ A^T(m,\alpha) &= -\frac{8b}{\pi^2 m} \sin\alpha\ell \cos m\theta_o\, I'_m(\alpha b) \end{aligned} \qquad (10)$$

Similarly, to evaluate G for point electrodes set diametrically opposite each other in a non-conducting circular pipe as in figure 1, we use:

$$\left(\frac{\partial G}{\partial r}\right)_{r=a} = \delta(\theta = 0,\ z = 0) - \delta(\theta = \pi,\ z = 0)$$

where δ is a δ-function such that $\int \delta ds$ over the pipe surface is unity.

This gives $B(n,\beta) = \frac{2}{a\pi^2 \beta I'_m(\beta a)}$ (11)

Now $W_z = \frac{1}{r}\left(\frac{\partial F}{\partial r}\frac{\partial G}{\partial \theta} - \frac{\partial F}{\partial \theta}\frac{\partial G}{\partial r}\right)$

so that using (6) and (7) we find

$$W_z = \int_{\alpha=0}^{\infty} d\alpha \int_{\beta=0}^{\infty} d\beta \sum_{m\,\mathrm{odd}} \sum_{n\,\mathrm{odd}} A(m,\alpha)\, B(n,\beta) \cos\alpha z \cos\beta z$$
$$\frac{1}{r}\left[\alpha n \sin m\theta \sin n\theta\, I'_m(\alpha r)\, I_n(\beta r) + \beta m \cos m\theta \cos n\theta\, I_m(\alpha r)\, I'_n(\beta r)\right] \quad (12)$$

This expression is rather intractable, but in this approach to the problem we are not concerned with W_z itself.

Using the relations:

$$\int_{-\infty}^{\infty} \cos\alpha z \cos\beta z\, dz = \pi\, \delta(\alpha-\beta) \quad (13)$$

and $$\int_0^{2\pi} \sin m\theta \sin n\theta\, d\theta = \int_0^{2\pi} \cos m\theta \cos n\theta\, d\theta = \pi\, \delta(m-n) \quad (14)$$

We find:

$$\bar{W} = \int_{-\infty}^{\infty} W_z\, dz = \frac{\pi}{r} \int_{\alpha=0}^{\infty} d\alpha \sum_{m\,\mathrm{odd}} \sum_{n\,\mathrm{odd}} \alpha\, A(m,\alpha)\, B(n,\alpha)$$
$$\left[n \sin m\theta \sin n\theta\, I'_m(\alpha r)\, I_n(\alpha r) + m \cos m\theta \cos n\theta\, I_m(\alpha r)\, I'_n(\alpha r)\right] \quad (15)$$

and $$\bar{W}' = \int_0^{2\pi} \bar{W}\, d\theta = \frac{2\pi^2}{r} \int_{\alpha=0}^{\infty} d\alpha \sum_{m\,\mathrm{odd}} \alpha m\, A(m,\alpha)\, B(m,\alpha)\, I'_m(\alpha r)\, I_m(\alpha r) \quad (16)$$

The formula for $\bar{W}'$ in (16) was originally obtained by separating the variables when the problem was formulated in terms of the electric potential ϕ induced by the motion, and using the condition $\frac{\partial \phi}{\partial n} + (\underline{v} \times \underline{B})_n = 0$ on the boundary. This boundary condition only applies, of course, with point electrodes, whereas the method used here is more general since, although we shall only deal with the case of point

electrodes, the relevant $B(m,\alpha)$ (if known) for any electrodes may be substituted in (16).

The separation of variables method was originally used by Baker[1] for the case of an infinitely long flowmeter with nonconducting walls, and the way in which the magnetic field potential $I_m(\alpha r)\sin m\theta$ in (6) gives rise to the component $I'_m(\alpha r)I_m(\alpha r)$ in $\bar{W}'$ in (16) is an extension of the way in which the two dimensional magnetic field potential $r^m \sin m\theta$ gives rise to the component r^{2m-1} in $\bar{W}'$ according to Baker's calculations. If we let $\alpha \to 0$ in (6) and (16), we find that $I_m(\alpha r)$ and $I'_m(\alpha r)I_m(\alpha r) \to r^m$ and r^{2m-1} (the α's dividing out due to α's in the $A(m,\alpha)$ and $B(m,\alpha)$).

Three points may be made about the case of axisymmetric flow profiles, for which $\bar{W}'$ was defined.

Firstly that from the way in which the term $A(m,\alpha)B(m,\alpha)$ occurs in (16), we see that given any $B(m,\alpha)$ (set of electrodes) we can choose $A(m,\alpha)$ (the magnetic field) to achieve any required product $A(m,\alpha)B(m,\alpha)$. That is, whatever form we require for $\bar{W}'$, there is no restraint on the magnetic field or electrode arrangement independently, but only on them together.

Secondly, we may remove one of the rectangular coils, thereby introducing terms $\sin m\theta$, where m is even, in equation (6) and eventually in (15), and, because of relation (14) and the fact that there are only terms with n odd in equation (15), find that $\bar{W}'$ in (16) is unaltered (except by a factor of $\frac{1}{2}$). Indeed we may also for both $\bar{W}$ and $\bar{W}'$ remove half of both the coils in $z>o$, so that terms in $\sin \alpha z$ appear in (6), since these terms contribute nothing to (15) and (16). Of course, we again get half the signal.

Thirdly, that although $\bar{W}'$ is a function of one variable only, the radius r, we are at liberty to choose $A(m,\alpha)$ (the magnetic field) which is a function of two variables, so that we expect there to be many ways of doing this. Even though we shall later restrict ourselves to the case of rectangular coils, the tables, a specimen of which is shown in figure 4, show that there are still infinitely many ways of achieving a given distribution of $\bar{W}'$.

Axisymmetric weight function $\bar{W}'$

In this section we deal with the axisymmetric weight function $\bar{W}'$, using point electrodes and rectangular coils surrounded by the iron sheath. Substituting for $A(m,\alpha)$ and $B(m,\alpha)$ from (9) and (11) in (16) we find

$$\bar{W}'(r) = \frac{32}{\pi^2 ar} \sum_{m\,odd} \cos m\theta_0 \int_{\alpha=0}^{\infty} \frac{\sin \alpha l}{\alpha} \frac{I'_m(\alpha r)\, I_m(\alpha r)}{I'_m(\alpha a)\, I_m(\alpha b)}\, d\alpha \qquad (17)$$

The $\int_{\alpha=0}^{\infty}$ is evaluated by writing the integrand as

$$\mathcal{J}\left[\frac{e^{j\alpha l}}{\alpha} \frac{I'_m(\alpha r)\, I_m(\alpha r)}{I'_m(\alpha a)\, I_m(\alpha b)}\right]$$

and using contour integration in the complex α-plane. The residues of the expression in the square brackets [ ] lie on the imaginary axis and at the origin. The integration is taken around a large semicircle centred on the origin and along the real axis. The integral over the circle contributes nothing provided $l>0$ and after evaluating the residues, and using a few relations about Bessel functions, we find

$$\bar{W}'(r) = \frac{16}{\pi a^2} \frac{a}{r} \sum_{m\,odd} \cos m\theta_0 \left[\frac{r^{2m-1}}{a^{m-1} b^m} - 2 \sum_s \frac{e^{-j'_{m,s} l/a}\, J'_m(j'_{m,s} r/a)\, J_m(j'_{m,s} r/a)}{j'_{m,s}\left(1 - \frac{m^2}{j'^2_{m,s}}\right) J_m(j'_{m,s})\, J_m(j'_{m,s} b/a)}\right.$$

$$\left. + 2 \sum_s \frac{e^{-j_{m,s} l/b}\, J'_m(j_{m,s} r/b)\, J_m(j_{m,s} r/b)}{j_{m,s}\, J'_m(a/b\, j_{m,s})\, J'_m(j_{m,s})}\right] \qquad (18)$$

The formula is characterised by the ratio b/a (=T in the tables), l/a ($=L/D$ in the tables), the coil half-angle $\frac{\pi}{2}-\theta_0$ and the non-dimensional radius r/a. The first term in (18) gives the value of $\bar{W}'$ when the coils are long ($\bar{W}'_\infty$, i.e. for $l=\infty$), and may be derived directly from long flowmeter theory. The summation over m gives:

$$\bar{W}'_\infty(r) = \frac{16}{\pi ab} \frac{\cos\theta_0 \left(1 - r^4/a^2b^2\right)}{\left(1 + r^8/a^4b^4 - 2\, r^4/a^2b^2 \cos 2\theta_0\right)} \qquad (18)'$$

Note the singular behaviour of $\bar{W}'_\infty$ on the wall of the flowmeter r=a as b→a and $\theta_o \to 0$ (when the four coils in figure 3a, now infinitely long, merge into two, immediately above and below the electrodes). For b=a when $\theta_o \neq 0$ $\bar{W}'_\infty(a) = 0$, but for b≠a and $\theta_o = 0$ $\bar{W}'_\infty(a) \propto \frac{1}{1-a^2/b^2}$. For a thin-walled long flowmeter $\bar{W}'_\infty(a)$ is small, provided θ_o is not close to zero, but for $\theta_o = 0$ $\bar{W}'_\infty(a)$ becomes large. The behaviour of $\bar{W}'_\infty(a)$ depends on the relative closeness of b to a and θ_o to zero.

In (18) the formula for $\bar{W}'(r)$ is dominated by the first-term until $\ell/a<1$ so that the same behaviour can be seen in the tables and persists, in fact, for $\ell/a \ll 1$.

Asymmetric weight function $\bar{W}$

The integral $\int_{\alpha=0}^{\infty} d\alpha$ in (15) may be evaluated in the same way, giving an answer similar to (18), but with an extra summation over n with terms in $J'_n J_m$ etc., instead of $J'_m J_m$. $\bar{W}$ is a function of two variables, and if it was calculated for, say, ten different values of r and θ the set of tables corresponding to the ones for $\bar{W}'(r)$ would be ten times as large. Though this could be avoided by removing the less useful information, the process of producing a specified distribution of $\bar{W}$ is not as easy as it is for $\bar{W}'$, since $\bar{W}$ must be made independent of both r and θ. The problem is better handled inside the computer, whether judicious guesses of suitable coil distributions are fed in, or the computer used to produce the best solution, or a mixture of both methods. In (2) a suitable coil shape is suggested, but there are no definite results to support the suggestion yet.

Explanation of the tables

The formula for $\bar{W}'(r)$ was worked out on a digital computer, the summations over s and m being taken up to s,m<20, except that the first term was summed analytically for m→∞.

1. b/a (T in the tables) is fixed.

2. Then for each ℓ/a ranging from 3.0 to 0.25 in steps of 0.1 and also the values 0.75 and 0.25 the computer printed

out a double page of results.

3. On each double page there is:

(a) a heading giving the value of $^{b}/a(=T)$, $^{\ell}/a(=^{L}/D)$.

(b) the terms in (18), before doing the summation in m but including the factor $\frac{a}{r}$, for $^{r}/a = 0.1$ to 1.0 in steps of 0.1. This shows how the different harmonics $\sin m\theta$ of the magnetic field in (6) contribute to $\bar{W}'$. In particular we see how the first harmonic $\sin\theta$ contributes since this is the $\bar{W}'$ produced by current windings that would produce a constant magnetic field if infinitely long, but are cut off at the relevant value of $^{\ell}/a$. In terms of the magnetic field potential $F(r=b, \theta, z)=\sin\theta$ for $|z|<\ell$ and = 0 other wise. Such a magnetic field is referred to as quasi-constant.

(c) the values of the sensitivity using a quasi-constant field for parabolic and flat velocity profiles and their ratio. The sensitivity is given by

$$S = \frac{\int_0^a \bar{W}'(r)\, v(r)\, rdr}{\int_0^a v(r)\, rdr} \qquad (19)$$

where $v(r) = a^2-r^2$ or constant respectively. Flat and parabolic profiles were chosen as they are the extreme profiles likely to be encountered in industrial practice. The profile variation is not likely to be as much as this; in many cases there is so little variation that the shape of the magnetic field is immaterial, although the customer has always demanded design against axisymmetric profile variation.

(d) three sets of weight functions, each given for $^{r}/a = 0.1$ to 1.0 in steps 0.1, and θ_o ranging from 0° to 90° in steps of 6°. θ_o is the azimuthal angle, $^{\pi}/2-\theta_o$ is the coil half angle. The second of these weight functions is $\bar{W}'(r)$ from (18) without the factor $\frac{16}{\pi a^2}$, and after this table the sensitivities referred to in (c) above are given for each value of θ_o. The other two weight functions are for the strip coils and point source or

δ-function coils shown in figure 3b, and are found by taking $\frac{\partial}{\partial\theta_o}$ and $\frac{-\partial^2}{\partial\theta_o\partial(\ell/a)}$ of (18).

<u>The accuracy of the computed values of $\bar{W}'$</u>

Two points should be made:

1. The accuracy of $\bar{W}'$ for small ℓ/a is limited by the number of terms in the various summations. Assuming b/a is not far from 1.0, an approximate estimate of the accuracy is found by considering the size of the factors $\frac{e^{-j_{m,s}\,\ell/a}}{j_{m,s}}$ or $\frac{e^{-j'_{m,s}\,\ell/a}}{j'_{m,s}}$ in (18), which is much the same for both for large m or s.

For m=1, s=21 $\quad \frac{e^{-j'_{m,s}\,\ell/a}}{j'_{m,s}} = \frac{e^{-65\,\ell/a}}{65}$

For m=21, s=1 $\quad$ " $\quad = \frac{e^{-23\,\ell/a}}{23}$

These are to be compared with its value for s=1, m=1 which is $\frac{1}{1.8}e^{-1.8\,\ell/a}$, which for small ℓ/a is about $\frac{1}{2}$. For $\ell/a=0.25$, the smallest value in the tables, the larger of the two factors $\frac{1}{23}e^{-23\,\ell/a}$ is 10^{-4}. Since the figures in the tables are given to four places of decimals, we may expect some error in the fourth place.

The situation is different with the other two weight functions. The operator $\frac{-\partial}{\partial\theta_o}$ brings in a factor m, so that the same factor is now about 2.10^{-3}, and $-\frac{\partial^2}{\partial\theta_o\partial(\ell/a)}$ brings in the factor $mj'_{m,s}$, so that the error is now 4.10^{-2}.

In order to reduce the error to 10^{-4}, we must have $\ell/a>0.4$ for the strip weight function, and $\ell/a>0.55$ for the δ-function weight function. For ℓ/a less than this they become progressively more inaccurate. (The reason that the summation in s has been extended to s=20 when s=10 would have been enough, given that that summation on m would not be taken past m=20, is historical. It means that the weight functions of the separate harmonics will be rather more accurate.)

2. It may be that when evaluating the bottom line of the second and third set of terms in (18), given a value of $^{b}/a$, that for some m and s $^{b}/a\ j'_{m,s}$ might unfortunately be $aj_{m,s}$, which would give rise to a zero on the bottom line. In this case, $\frac{a}{b}j_{m,s}$ would be $aj'_{m,s}$ so that both terms would have a zero. In practice these terms would be large and have opposite signs thereby cancelling each other, provided that the summations extended far enough to include both terms. The bottom lines of both these expressions are computed as a set of coefficients and printed out at the head of the tables so that this point can be checked.

Use of the tables

Even in the case of axisymmetric profiles, it is clear that the tables, containing some thirty double pages like the one in figure (4), contain a lot of information, some of which can be more easily digested in graphical form. Some examples follow.

1. Quasi-uniform-field flowmeters

Figure 5 is a graph of the sensitivity ratio for flat and parabolic velocity profiles plotted against $^{L}/D$, the non-dimensional length of the field windings, for different values of the wall thickness parameter $T(=^{b}/a)$. Also included are the values of the sensitivity for both profiles for one (arbitrary) value of T, showing how they change in the same manner with $^{L}/D$, so that their ratio does not change so fast. At $^{L}/D=1.5$, an industrially typical length of coil, the difference between the sensitivities is somewhat more than the one per cent commonly required, but, as mentioned before, industrial profiles are not likely to be flat or parabolic.

2. "C onstant sensitivity" rectangular coils

For each value of $^{L}/D$, there is a rectangular coil of a certain coil angle for which the flat and parabolic profile sensitivities are equal. Figure (6) shows the line giving the relationship between $^{L}/D$ and coil half angle for equal

sensitivities. If we assume that any velocity profile occurring in practice may be represented by the sum of a flat and parabolic profile, then a flowmeter with such a rectangular coil would have constant sensitivity, even though the distribution of $\bar{W}'(r)$ with respect to r is far from uniform (see figure 7). Clark and Wyatt[3] have done experiments using a range of coils of fixed length and variable angle to determine the change of sensitivity as the flow changes from laminar to turbulent. The experiments indicate a coil angle at which there is no change of sensitivity, but the coils were air-cored, i.e. without the iron sheath, and we have done no computations for this case.

3. Best signal to copper ratio

A designer may be interested in the minimum amount of copper required to give a certain output signal. To some extent this will depend on the shape of the coil windings, but for the sake of illustration suppose the designer required a rectangular coil and equal parabolic and flat profile sensitivities. For each L/D there is one coil angle for which they are equal (figure 6). Since this angle does not vary much with L/D we shall take a mean value of 66^{o} for the half angle and T=1·1. The ratio of the absolute output signal (taken from the flat profile entry in the tables) to the total length around the coil may be called the signal to copper ratio, since profile sensitivities are the output signal for unit current in the coil and unit current specifies the cross-sectional area of the coil for a given current density in the copper so that the total coil length measures the amount of copper.

This ratio is plotted in figure 8 against L/D, which shows that the best coil length is about $L/D = 0.9$.

4. Constant $\bar{W}'$ coils

The aim of the designer who requires a flowmeter insensitive to changes in axisymmetric profile is to make $\bar{W}'$ constant. A possible method would be to take a linear sum of the ten harmonics given in the first table in figure 4 for

a chosen value of $^{l}/a(^{L}/D)$ and $^{b}/a(T)$, somewhere near the length for the optimum signal/copper ratio, and arrange the coefficients C_m in this sum so that $\bar{W}'(r)$ took the same value at the ten values of $^{r}/a$. This would result in a distribution of F over the flowmeter surface which could then be approximated by a series of rectangular coils.

F would be given by $\sum_{m=0}^{19} C_m \sin m\theta$

There are difficulties with this approach:

(a) Since the higher harmonics (in m) contribute very little except when $^{r}/a$ is close to 1, solu tion of the resulting simultaneous equations results in large values of C_m for the larger m, which have to be produced by high current densities on the surface which alternate quickly in sign, which is wasteful, if not impossible, to achieve.

(b) By permitting $\bar{W}'$ to depart very slightly from being constant, the C_m can be kept down to a reasonable size, but the resulting current distribution still needs a large number of carefully spaced wires.

It is much simpler to pick out from the tables a linear sum of rectangular coils that makes $\bar{W}'$ constant to within some specified tolerance. Since $\bar{W}'$ falls to $r \to a$, except for large coil angles, we expect to have at least one large coil. By judicious choice, bearing in mind that the coils have to fit inside one another, it is possible to arrange that $\bar{W}'$ is constant to within about 10% using two coils, and about 3% using three, though it appears that in some cases coils carrying current in opposite directions may be necessary. 10% may sound a large variation, but the variation in $\bar{W}'$ for a quasi-uniform field of length $^{L}/D = 1.5$ is about 15%, depending slightly on the value of T, and such coils are known to give good results in practice, which must be due mainly to the fact that the profile variation is not nearly as large as assumed.

The behaviour of the virtual current ∇G

So far we have avoided the explicit determination of G, partly because it is not easy to find a formula that holds everywhere, and partly because the outstanding question is always what to do with it when it has been found. It is necessary to do so, in order to discuss how fast the virtual current ∇G falls to zero away from the electrodes, and hence to estimate the minimum length of insulating liner for the infinitely long liner assumption to be valid. We shall calculate $\frac{\partial G}{\partial x}$ at various points in the plane x=0 in figure 1.

Substituting (11) in (7) we find

$$G = \frac{2}{\pi a^2} \sum_{n=0}^{\infty} \cos n\theta \int_{\beta=0}^{\infty} \frac{I_n(\beta r)}{I_n'(\beta a)} \cos \beta z \, \frac{d\beta}{\beta} \qquad (20)$$

Provided z>0 it is possible to integrate (20) using the same contour as before in (18), as Mezburd[4] and others have done. The result is:

$$G = \frac{2}{\pi a} \sum_{n=0}^{\infty} \cos n\theta \sum_{s=1}^{\infty} \frac{J_n(j'_{n,s} r/a)\, e^{-j'_{n,s} z/a}}{j'_{n,s}\left(1 - \frac{n^2}{j'^2_{n,s}}\right) J_n(j'_{n,s})} \qquad (21)$$

for z>0. G is even in z.

Note that $\int_{-\infty}^{\infty} G\,dz$, using a standard series of Bessel functions, has the value:

$$\frac{2}{\pi} \sum_{n=0}^{\infty} \frac{1}{n} \left(\frac{r}{a}\right)^n \cos n\theta$$

or

$$Re \; \frac{1}{\pi} \log \frac{a + re^{i\theta}}{a - re^{i\theta}}$$

as expected.

From the formula for G, ∇G may be calculated at places for which z=0. The expression (21) does not converge for z=0, since the method of contour integration used is not valid. (The integral over the semicircle at ∞ does not converge.)

Along the axis r=0

$$\frac{\partial G}{\partial x} = \left(\frac{\partial G}{\partial r}\right)_{\substack{r=0 \\ \theta=0}} = \frac{1}{\pi^2 a^2} \sum_{s=1}^{\infty} \frac{e^{-j'_{1,1} z/a}}{\left(1 - \frac{1}{j'^2_{1,s}}\right) J_1(j'_{1,s})}$$

For $z/a>1$, the first term dominates and

$$\frac{\partial G}{\partial x} = \frac{0.78}{a^2} \; e^{-1.84 z/a} \qquad (22)$$

On the side wall, at $r=a$ and $\theta=\pi/2$,

$$\frac{\partial G}{\partial x} = -\frac{1}{a}\left(\frac{\partial G}{\partial \theta}\right)_{\substack{r=a \\ \theta=\pi/2}} = \frac{2}{\pi^2 a^2} \sum_{n \text{ odd}} (-1)^{\frac{n-1}{2}} n \sum_{s=1}^{\infty} \frac{e^{-j'_{n,s} z/a}}{j'_{n,s}\left(1-\frac{n^2}{j'_{n,s}}\right)}$$

Again for $z/a>1$, the first term $n=s=1$ dominates, though not quite so strongly and

$$\frac{\partial G}{\partial x} = \frac{0.50}{a^2} \; e^{-1.84 z/a} \qquad (23)$$

We must now calculate the value of ∇G, if possible, in the electrode plane. We cannot use (21) for this since it does not converge for $z=0$, but by using two different methods we can obtain an estimate of $\frac{\partial G}{\partial x}$ on the line $x=0$, $z=0$. We shall not attempt more than this.

Firstly, at the centre of the flowmeter, (20) gives

$$\frac{\partial G}{\partial x} = \left(\frac{\partial G}{\partial r}\right)_{\substack{\theta=0 \\ r=0}} = \frac{2}{\pi^2 a} \int_{\beta=0}^{\infty} \frac{I_1'(0)}{I_1'(\beta a)} \, d\beta$$

all the other terms disappearing,

or $$\left(\frac{\partial G}{\partial x}\right)_{x,y,z=0} = \frac{1}{\pi^2 a^2} \int_{t=0}^{\infty} \frac{dt}{I_1'(t)} \qquad (24)$$

The integral in (24) is perfectly well behaved, since $I'(0)=\frac{1}{2}$ at $t=0$ and behaves like $t^{-\frac{1}{2}} e^{t}$ at ∞. It may be evaluated numerically, or by a similar method which in this case saves effort. The integral has the value 3.53 so that

$$\left(\frac{\partial G}{\partial x}\right)_{x,y,z=0} = \frac{0.36}{a^2} \qquad (25)$$

However, if we try to use (20) for ∇G at $r=a$, $\theta=\pi/2$, $z=0$, i.e. on the wall, we find both the integral and the sum diverge.

It may be possible to overcome this difficulty, but the following approach gives a good estimate of $\frac{\partial G}{\partial x}$ along the whole of the line x=0, z=0 in figure 1.

On the corresponding line in the case of insulated circular pipe with long line electrodes, and an insulated spherical ball with point electrodes the distribution of $\frac{\partial G}{\partial x}$ is easily found. It is:

$$\text{line electrodes:} \quad \frac{G}{\partial x} \propto \frac{1}{a^2+y^2}$$

$$\text{sphere:} \quad \frac{\partial G}{\partial x} \propto \frac{3a^2+y^2}{a(a^2+y^2)^{3/2}} \qquad (26)$$

The shape of these functions is very similar, and if the function for the case of point electrodes in a circular pipe lies between them a good estimate of $\frac{\partial G}{\partial x}$ can be obtained. At the wall $(\frac{\partial G}{\partial x})_{y=a}$ must lie between 0.5 and $\frac{\sqrt{2}}{3}$ of its value at y=0, which we have already calculated in equation (25), i.e. between 0.5 and 0.47 of $(\frac{\partial G}{\partial x})_{y=0}$.

To give some justification of the above remark, we write the condition that the z-component of curl $(\nabla G)=0$ in intrinsic coordinates s(along a streamline) and n, the unit normal in the direction of the centre of curvature. R is the radius of curvature of the streamline. If the stream lines do not lie in a plane z=constant, we take their projections onto this plane. The condition gives

$$\frac{\partial}{\partial n}(\frac{\partial G}{\partial s}) - \frac{1}{R}(\frac{\partial G}{\partial s}) = 0$$

On a line x=0, z=constant $\frac{\partial}{\partial n} \equiv -\frac{\partial}{\partial y}$ and $\frac{\partial G}{\partial s} \equiv \frac{\partial G}{\partial x}$ and we find

$$\frac{\partial}{\partial y}(\frac{\partial G}{\partial x}) = -\frac{1}{R(y)}\frac{\partial G}{\partial x} \qquad (27)$$

where R(y) is the radius of curvature of any of the streamlines of ∇G. Figure 9 shows the streamline shape that may be expected in the electrode plane of any of the three cases we have considered.

By successively deforming a nonconducting cylinder with line electrodes to one with point electrodes, and then to a spherical ball with point electrodes, we may plausibly argue that the R(y) for these cases is a set of monotonic functions.

A general lower bound for the ratio of $(\frac{\partial G}{\partial x})_{y=a}$ to $(\frac{\partial G}{\partial x})_{y=0}$ may be found by substituting R(y)>a in (27). The ratio for R(y)=a is $^1/e$. Note that away from the electrode plane the streamlines are flatter, in agreement with the higher value of the ratio, which for large $^z/a$ is from (22) and (23) 0.64.

The behaviour of the magnetic field B

The magnetic field behaves in a similar way to the virtual current, except that, since the magnetic boundary conditions require zero potential on the wall whereas the virtual current boundary conditions require zero potential gradient, the magnetic field decreases faster away from the electrodes.

The behaviour of the transverse component B_y on the centre line x,y=0 produced by a rectangular coil of length $2\ell(=L)$ and coil angle $\pi-2\theta_o$ may be found by substituting (9) in (6) and using the same method of contour integration as before to produce formulae for F somewhat similar to formula (21) for G. The formula gives the value of B_y at all z except for $z=\pm\ell$, where it does not converge.

For $^\ell/b>1$ and $\frac{||z|-\ell|}{b}>1$ the formulae are dominated by the first term. We find

$$(B_y)_{x,y,z=0} = \frac{4}{\pi b}\lambda\left\{1+\frac{e^{-j_{1,1}\,\ell/b}}{J_1'(j_{1,1})}\right\}^{\cos\theta_o}$$

$$= \frac{4}{\pi b}\lambda\left\{1 + 2.5\ e^{-3.83\,\ell/b}\right\}^{\cos\theta_o} \qquad (28)$$

and for $z > \ell+b$

$$(B_y)_{x,y=0} = \frac{5.0}{\pi b}\lambda\, e^{-3.83\left(\frac{z-\ell}{b}\right)}{}^{\cos\theta_o} \qquad (29)$$

The behaviour of the weight vector $\underline{W}$ for large z

We are now in a position to estimate the rate at which W_z falls off away from the flowmeter head. Typical industrial practice would be to make the coil length $L/D = \frac{3}{4}$ and the insulating liner length $1\frac{1}{2}D$.

Using these figures and assuming $a \sim b$ the ratio of $\frac{\partial G}{\partial x}$ on the centre line at z=0 to its value at $\frac{z}{a}=1\frac{1}{2}$ is, from (25) and (22), 0.137. The same ratio for B_y, using (28) and (29), is 0.082, so that the same ratio for W_z is 0.011. W_z falls off very fast, like $e^{-(1.84 z/a + 3.83 z/b)}$ for large z, due more to the magnetic field $(e^{-3.83 z/b})$ than the virtual current $(e^{-1.84 z/a})$

In order to be certain that the effects of unknown boundary conditions at the ends of the flowmeter are small, the flowmeter ought to be somewhat longer than $1\frac{1}{2}D$.

Shortening the flowmeter introduces uncertainty, not only about the rate at which $\frac{\partial G}{\partial x}$ and B_y fall to zero, but also about the shape of the fields ∇G and $\underline{B}$. Though it might be possible to estimate the first of these effects, the second would need proper analysis. It would affect the way in which the flowmeter sensitivity depended on the velocity profile though in practice this is likely to be less important than the absolute change in output signal.

Conclusion

1. The work in this paper has been based on certain assumptions about the iron-work producing the magnetic field, and the design data is given in terms of the necessary field windings.

The result is a comprehensive design procedure, at this stage only for flowmeters with axisymmetric velocity profiles, but applicable only if the magnetic field is produced in the specified way.

2. In many cases the flowmeter performance is required from a knowledge of the magnetic field itself, and to do this the virtual current distribution (W.G) must be known especially in the electrode plane. No-one, as far as I know, has yet produced formula that behaves well there and since the resulting calculations using the given magnetic field distribution will probably be carried out on a computer there is a strong case for finding the virtual current numerically. At the time of writing the values of $(\frac{\partial G}{\partial x})_{x=0}$ so found agree well along the line $z=0$, but not so well along $y=0$.

It should also be noted that the analytical solutions for $\bar{W}'$, $\bar{W}$ and W_z, which must themselves be evaluated numerically on a computer, involve two, three and four summations respectively, the amount of computation correspondingly increasing, whereas in the methods relying on direct numerical integration, the computation is correspondingly less.

3. The tables produced from the analysis are in the process of being checked, by determining the performance of flowmeters designed from them and comparing it with experiment and direct numerical integration. Though they are printed at the moment it is possible to produce them on paper tape as well.

Acknowledgements

I would like to acknowledge the advice and criticism of Professor J.A. Shercliff and Dr. G. Rowlands, the interest shown by George Kent Ltd., and the financial support of the English Electric Co. Ltd.

References

1. R.C. Baker. 1967. "Solutions of the Electromagnetic Flowmeter Equation for Cylindrical Geometrics". Brit. J. App. Phys. (Physics D).

2. M.K. Bevir. 1968. "Contributions to the Theory of Induced Voltage Electromagnetic Flowmeters".

3. Delia M. Clark and D.G. Wyatt. 1967. "The Effect of Magnetic Field Inhomogeneity on Flowmeter Sansitivity". Electromagnetic Flowmeter Symposium, Oslo.

4. V. Mezburd. 1968. Private communication.

5. Th. Rummel and B. Ketelsen. 1966. "Practical Electromagnetic Flowmeasurement using Non-uniform Fields" (trans.). Regelungstecknik 6, p. 262.

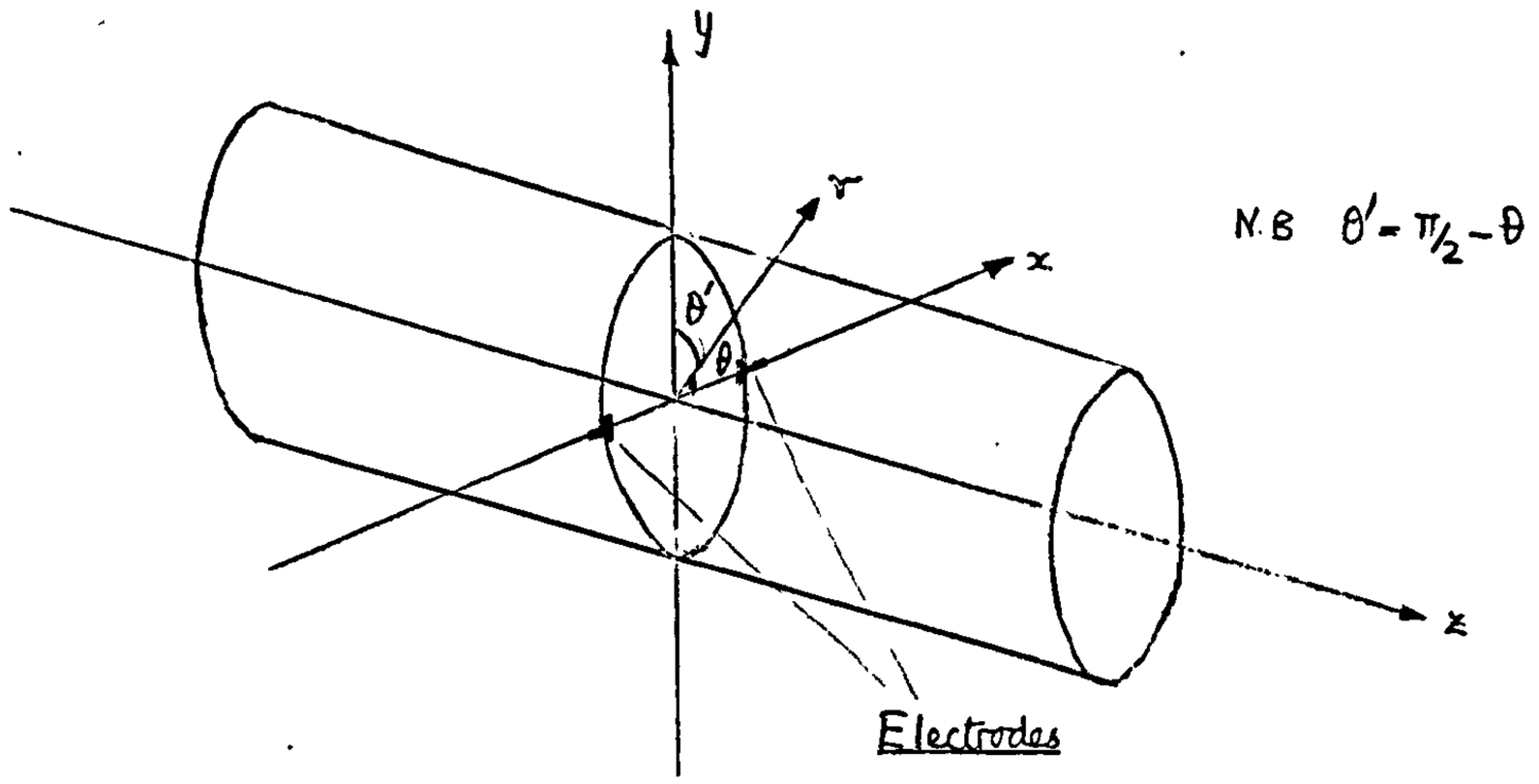

N.B $\theta' = \pi/2 - \theta$

Figure 1 Coordinate Notation

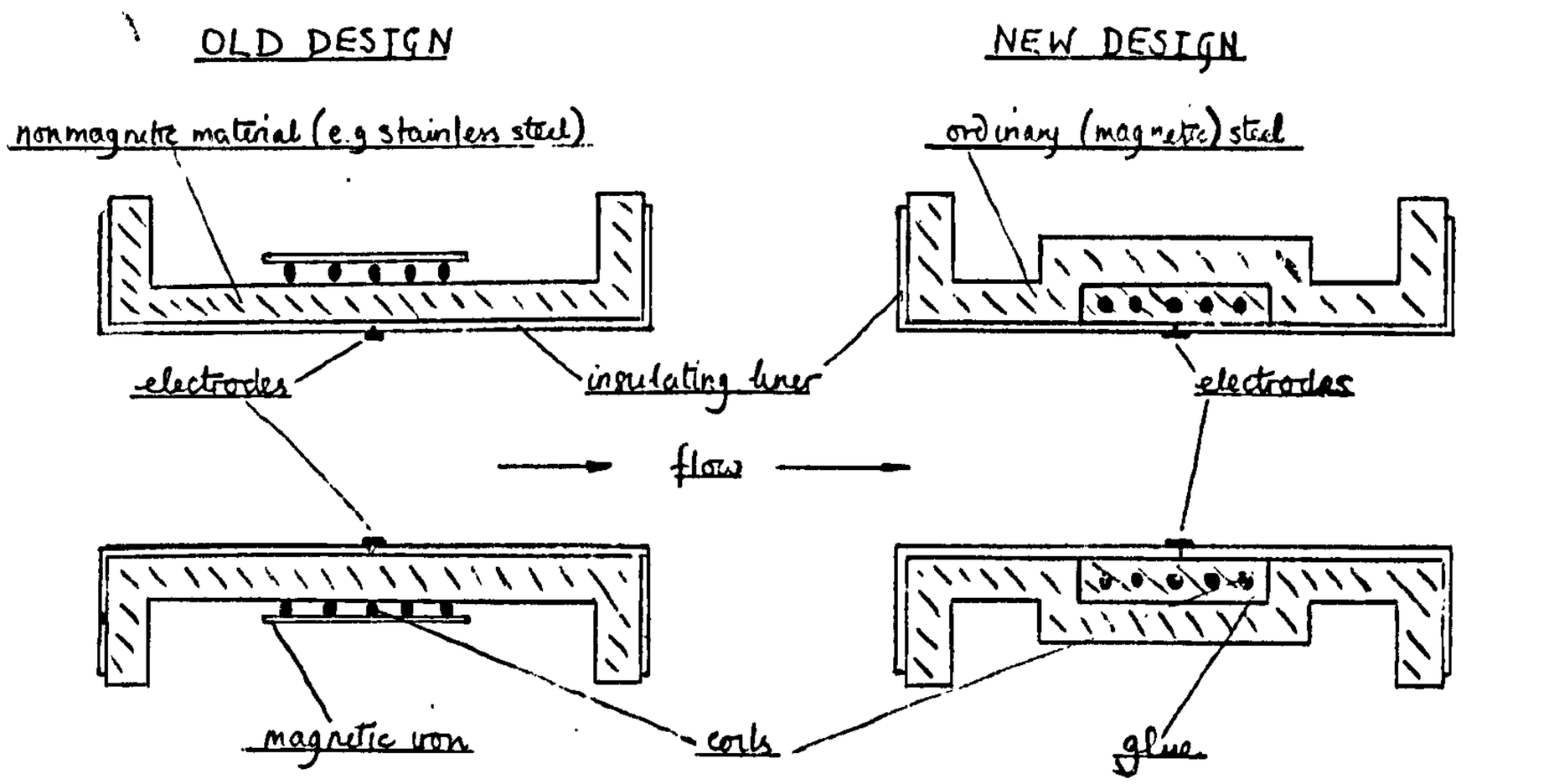

NB. The old designs were commonly longer than the new.

Figure 2 Schematic Design Comparison

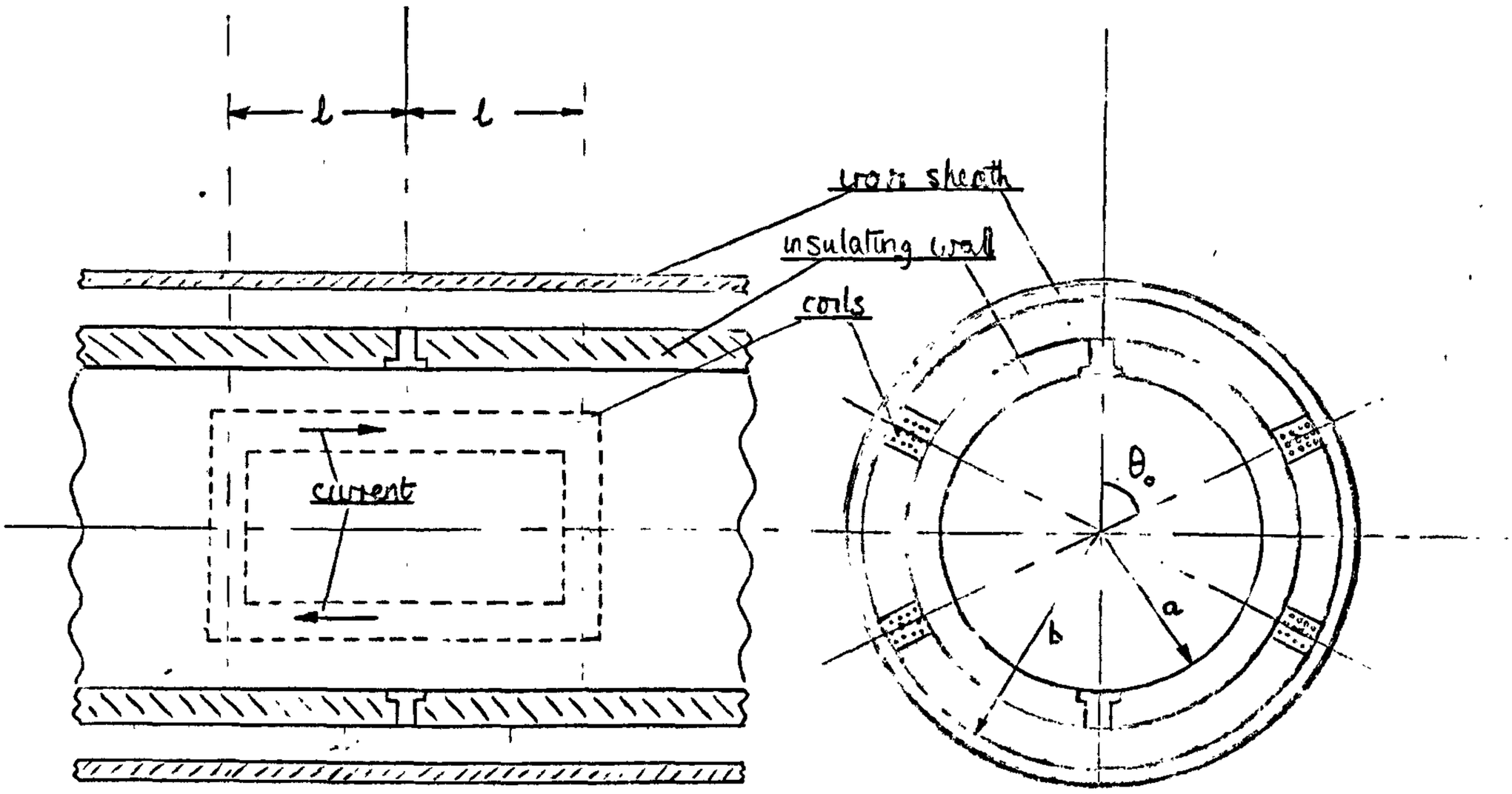

N.B. $L = 2\ell$
$D = 2a$
$T = b/a$

Figure 3a Arrangement of Rectangular Coils

Strip Coil

Point Source Coil

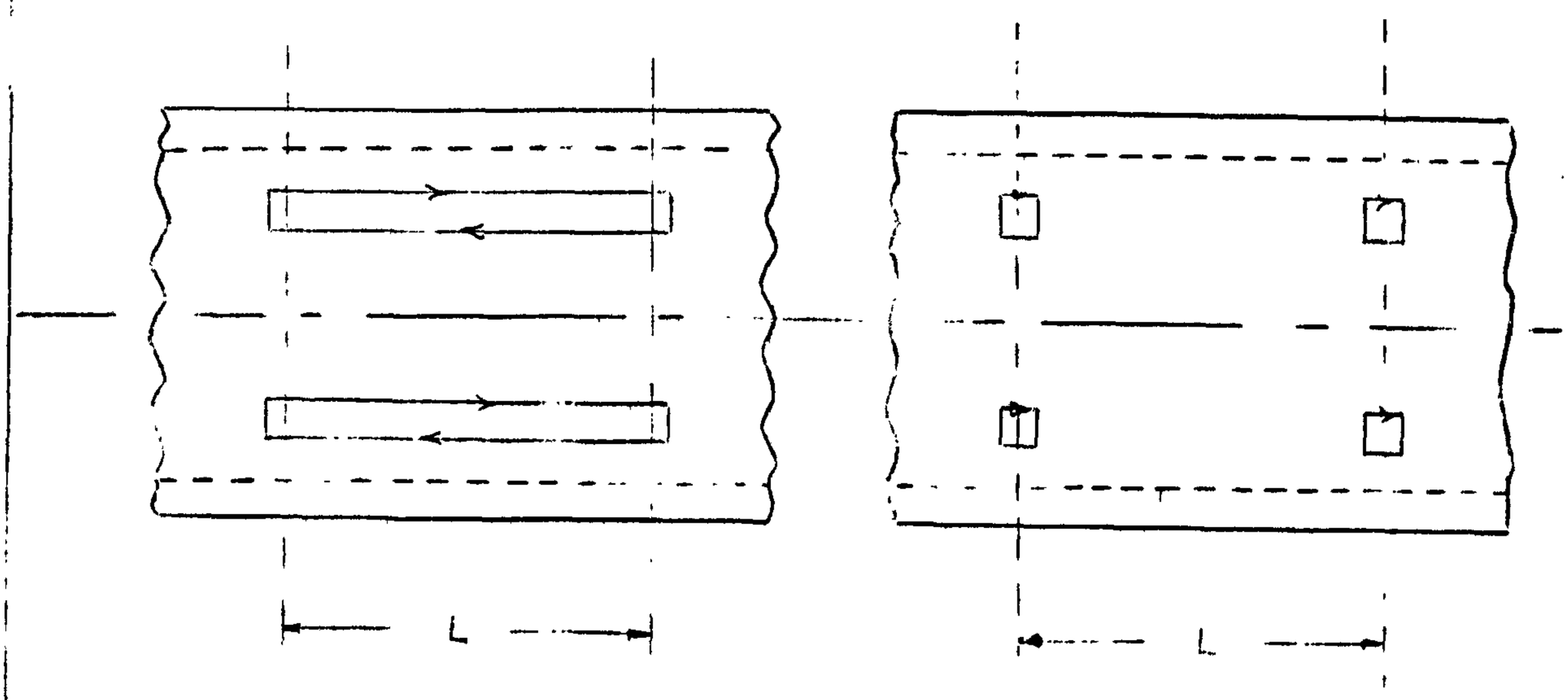

Figure 4 Arrangement of Coils

AXISYMMETRIC WEIGHT FUNCTION FOR CURRENT STREAM FUNCTION=COSNTHETA FOR T= 1.30 L/D= 0.79

RADIUS	N= 1	N= 3	N= 5	N= 7	N= 9	N= 11	N= 13	N= 15	N= 17	N= 19
0.10	0.42236732	0.00063486	0.00000008	0.00000008	0.00000008	-0.00000008	-0.00000008	-0.00000008	-0.00000006	-0.00000010
0.20	0.42827127	0.00056241	0.00000060	0.00000008	0.00000008	0.00000008	-0.00000008	-0.00000008	-0.00000008	-0.00000010
0.30	0.43847540	0.00288434	0.00001550	0.00000008	0.00000008	0.00000008	0.00000008	-0.00000008	-0.00000008	-0.00000010
0.40	0.45356230	0.00920473	0.00019674	0.00000250	0.00000004	0.00000008	0.00000008	0.00000008	0.00000008	-0.00000004
0.50	0.47441798	0.02321533	0.00094864	0.00003678	0.00000130	0.00000005	0.00000008	0.00000008	0.00000008	0.00000008
0.60	0.50228426	0.04957568	0.00415391	0.00033175	0.00002597	0.00000201	0.00000016	0.00000001	0.00000008	0.00000008
0.70	0.53876373	0.09587793	0.01455088	0.00213598	0.00030825	0.00004414	0.00000630	0.00000090	0.00000013	0.00000002
0.80	0.58561395	0.16059082	0.04325569	0.01073337	0.00262908	0.00064033	0.00015596	0.00003775	0.00000915	0.00000222
0.90	0.64393272	0.28187793	0.11320635	0.04456685	0.01739984	0.00677122	0.00263148	0.00102207	0.00039687	0.00015409
1.00	0.71211988	0.44432686	0.26708391	0.15888096	0.09419190	0.05577426	0.03301135	0.01953535	0.01155904	0.00684079

QUASICONSTANT FIELD SENSITIVITIES: FLAT PROFILE 0.9584 PARABOLIC PROFILE 0.9013 RATIO 1.0000

STRIP AXISYMMETRIC WEIGHT FUNCTION

RADIUS: AZIMUTH WRT ELECTRODES

	0	6	12	18	24	30	36	42	48	54	60	66	72	78	84	90
0.1	0.0000	0.0442	0.0879	0.1306	0.1719	0.2113	0.2484	0.2827	0.3139	0.3417	0.3658	0.3858	0.4016	0.4131	0.4200	0.4223
0.2	0.0000	0.0453	0.0900	0.1337	0.1758	0.2158	0.2533	0.2879	0.3193	0.3478	0.3709	0.3907	0.4063	0.4175	0.4243	0.4266
0.3	0.0000	0.0465	0.0963	0.1426	0.1866	0.2279	0.2668	0.3004	0.3309	0.3573	0.3797	0.3979	0.4119	0.4219	0.4279	0.4299
0.4	0.0000	0.0564	0.1114	0.1635	0.2117	0.2598	0.2931	0.3256	0.3527	0.3748	0.3921	0.4054	0.4150	0.4215	0.4253	0.4269
0.5	0.0000	0.0737	0.1439	0.2079	0.2634	0.3091	0.3448	0.3712	0.3893	0.4007	0.4078	0.4098	0.4104	0.4108	0.4095	0.4093
0.6	0.0000	0.1106	0.2124	0.2982	0.3641	0.4088	0.4344	0.4440	0.4420	0.4324	0.4198	0.4046	0.3914	0.3811	0.3745	0.3728
0.7	0.0000	0.1936	0.3666	0.4827	0.5543	0.5866	0.5929	0.5829	0.5616	0.4577	0.4162	0.3801	0.3513	0.3305	0.3179	0.3137
0.8	0.0000	0.4042	0.7095	0.8788	0.8999	0.8436	0.7458	0.6377	0.5367	0.4503	0.3805	0.3265	0.2869	0.2599	0.2443	0.2392
0.9	0.0000	1.0739	1.6413	1.6767	1.4357	1.1315	0.8611	0.6494	0.4927	0.3796	0.2992	0.2427	0.2048	0.1798	0.1650	0.1609
1.0	0.0000	4.2908	4.2843	2.0836	1.7849	1.1124	0.7168	0.4803	0.3347	0.2426	0.1829	0.1438	0.1183	0.1024	0.0936	0.0908

Figure 4

AXISYMMETRIC VELOCITY PROFILE L/D= 0.79

RECTANGULAR COIL WEIGHT FUNCTION

RADIUS: COIL HALF ANGLE

	90	84	78	72	66	60	54	48	42	36	30	24	18	12	6	0
0.1	0.4224	0.4201	0.4132	0.4017	0.3859	0.3658	0.3417	0.3139	0.2826	0.2482	0.2112	0.1718	0.1309	0.0878	0.0441	0.0000
0.2	0.4268	0.4245	0.4174	0.4076	0.3914	0.3709	0.3463	0.3179	0.2861	0.2512	0.2136	0.1737	0.1319	0.0887	0.0446	0.0000
0.3	0.4414	0.4388	0.4312	0.4187	0.4015	0.3797	0.3538	0.3241	0.2911	0.2550	0.2164	0.1756	0.1332	0.0895	0.0450	0.0000
0.4	0.4630	0.4608	0.4512	0.4368	0.4171	0.3927	0.3639	0.3315	0.2959	0.2578	0.2176	0.1758	0.1328	0.0898	0.0446	0.0000
0.5	0.4906	0.4947	0.4833	0.4648	0.4401	0.4100	0.3757	0.3381	0.2982	0.2568	0.2145	0.1717	0.1287	0.0858	0.0429	0.0000
0.6	0.5564	0.5505	0.5335	0.5066	0.4718	0.4311	0.3868	0.3407	0.2942	0.2484	0.2038	0.1607	0.1198	0.0796	0.0391	0.0000
0.7	0.6569	0.6486	0.6113	0.5667	0.5128	0.4522	0.3916	0.3330	0.2783	0.2281	0.1824	0.1407	0.1025	0.0669	0.0330	0.0000
0.8	0.8117	0.7988	0.7385	0.6465	0.5529	0.4611	0.3777	0.3052	0.2438	0.1923	0.1498	0.1121	0.0841	0.0519	0.0252	0.0000
0.9	1.1113	1.0522	0.9847	0.7274	0.5631	0.4287	0.3249	0.2443	0.1869	0.1416	0.1063	0.0781	0.0548	0.0349	0.0170	0.0000
1.0	1.8132	1.5526	1.0762	0.7883	0.4681	0.3115	0.2175	0.1559	0.1138	0.0839	0.0619	0.0449	0.0313	0.0198	0.0096	0.0000

SENSITIVITY (FLAT)

0.7894	0.7521	0.6608	0.5769	0.4919	0.4174	0.3529	0.2978	0.2488	0.2042	0.1647	0.1283	0.0943	0.0628	0.0308	0.0000

SENSITIVITY (PARABOLIC)

0.5043	0.5031	0.5028	0.5109	0.4639	0.4155	0.3678	0.3216	0.2778	0.2341	0.1927	0.1526	0.1135	0.0753	0.0375	0.0000

RATIO FLAT/PARABOLIC

1.3282	1.2899	1.2898	1.1291	1.0604	1.0044	0.9595	0.9237	0.8951	0.8725	0.8547	0.8411	0.8318	0.8248	0.8199	0.8196

DELTA FUNCTION WEIGHT FUNCTION

RADIUS: AZIMUTH WRT ELECTRODES

	0	6	12	18	24	30	36	42	48	54	60	66	72	78	84	90
0.1	0.0000	0.0467	0.0938	0.1382	0.1818	0.2235	0.2627	0.2991	0.3321	0.3615	0.3870	0.4082	0.4249	0.4370	0.4443	0.4468
0.2	0.0000	0.0473	0.0939	0.1395	0.1835	0.2254	0.2647	0.3009	0.3338	0.3630	0.3882	0.4091	0.4255	0.4374	0.4445	0.4469
0.3	0.0000	0.0490	0.0974	0.1443	0.1892	0.2314	0.2706	0.3063	0.3381	0.3660	0.3896	0.4090	0.4241	0.4349	0.4414	0.4435
0.4	0.0000	0.0535	0.1058	0.1559	0.2027	0.2456	0.2848	0.3177	0.3466	0.3708	0.3904	0.4059	0.4175	0.4255	0.4302	0.4318
0.5	0.0000	0.0625	0.1228	0.1788	0.2298	0.2724	0.3085	0.3375	0.3598	0.3764	0.3881	0.3960	0.4013	0.4040	0.4056	0.4060
0.6	0.0000	0.0786	0.1526	0.2182	0.2727	0.3149	0.3451	0.3644	0.3747	0.3784	0.3775	0.3742	0.3698	0.3659	0.3642	0.3638
0.7	0.0000	0.1042	0.1989	0.2768	0.3338	0.3696	0.3867	0.3890	0.3811	0.3671	0.3507	0.3344	0.3201	0.3092	0.3034	0.3001
0.8	0.0000	0.1384	0.2579	0.3455	0.3971	0.4168	0.4144	0.3998	0.3796	0.3581	0.3383	0.3225	0.3110	0.3049	0.3279	0.3244
0.9	0.0000	0.1661	0.2994	0.3815	0.4124	0.4044	0.3731	0.3318	0.2892	0.2502	0.2172	0.1907	0.1796	0.1571	0.1449	0.1442
1.0	0.0000	0.1486	0.2413	0.2974	0.2957	0.2712	0.2350	0.1984	0.1654	0.1388	0.1165	0.1001	0.0883	0.0803	0.0757	0.0742

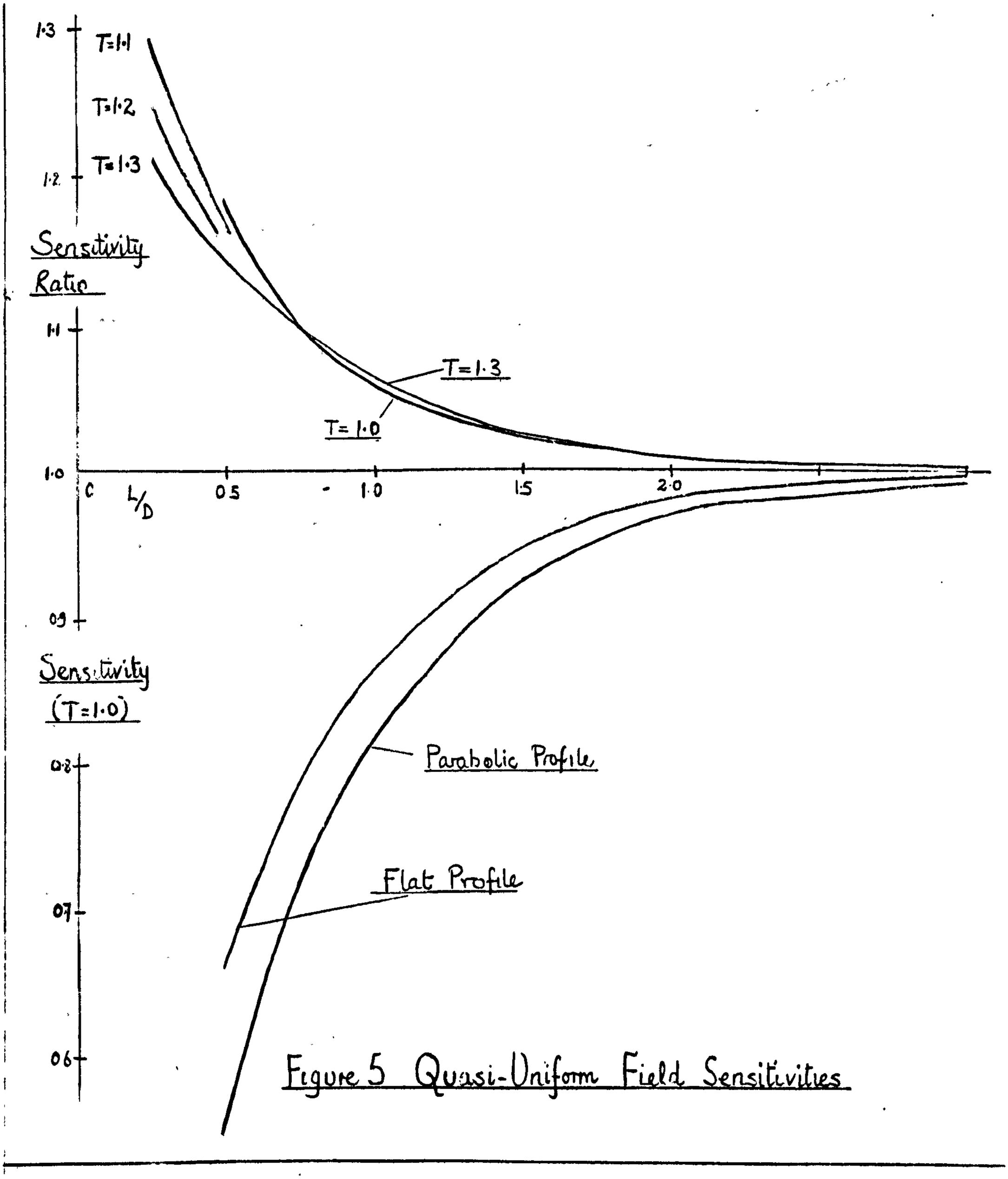

Figure 5 Quasi-Uniform Field Sensitivities

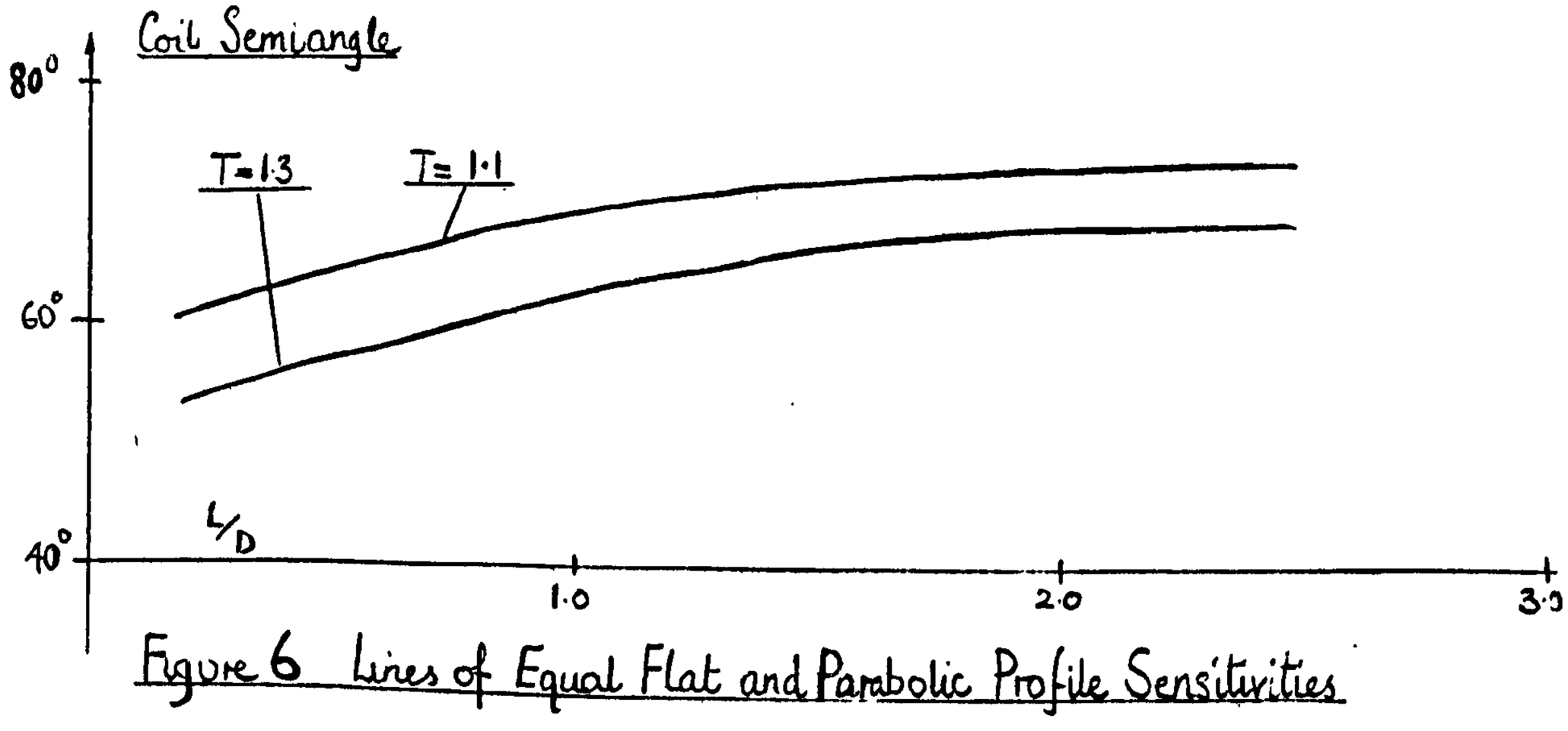

Figure 6 Lines of Equal Flat and Parabolic Profile Sensitivities

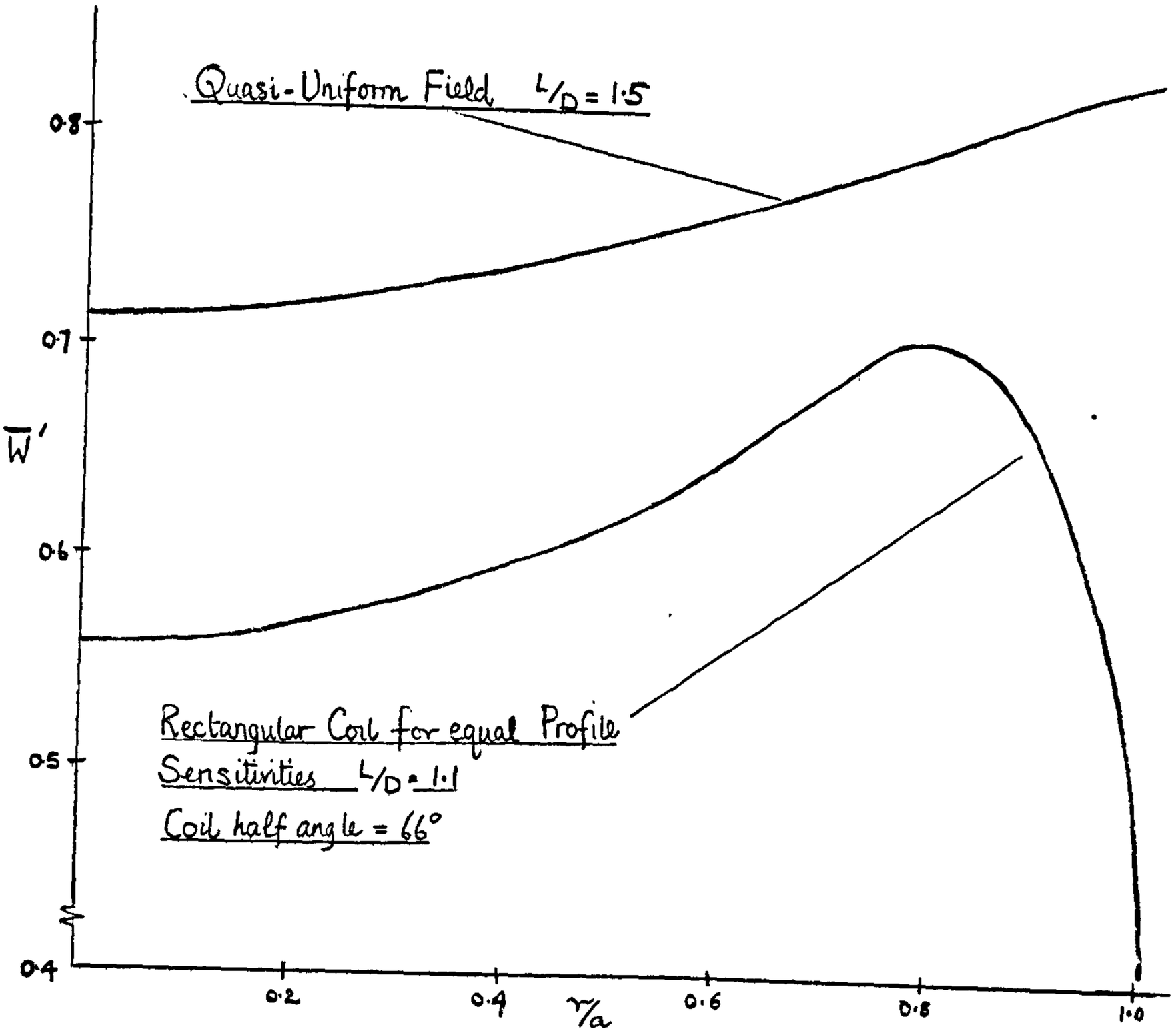

Figure 7 Axisymmetric Weight Function T = 1.2

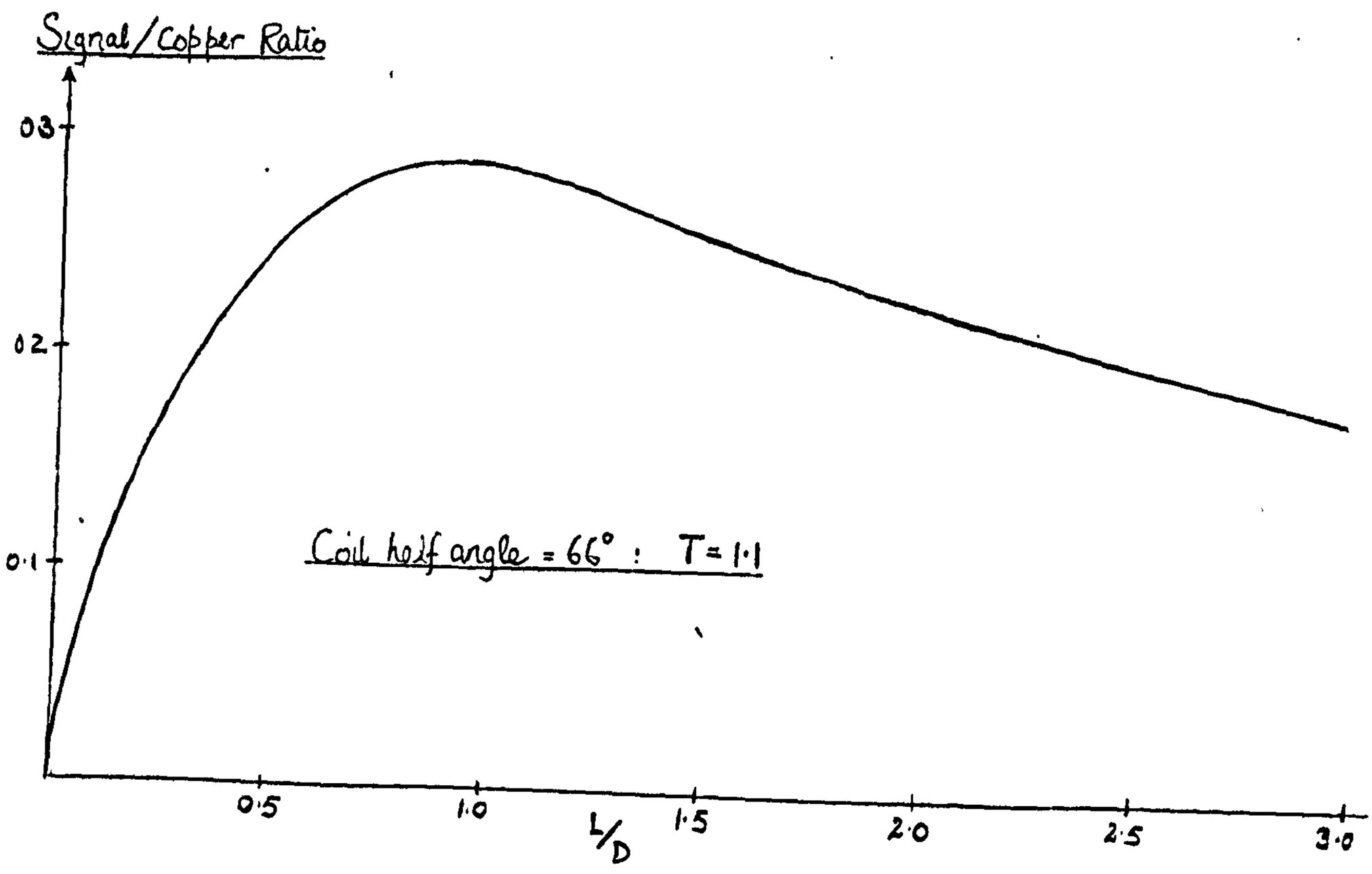

Figure 8 Signal/Copper Ratio

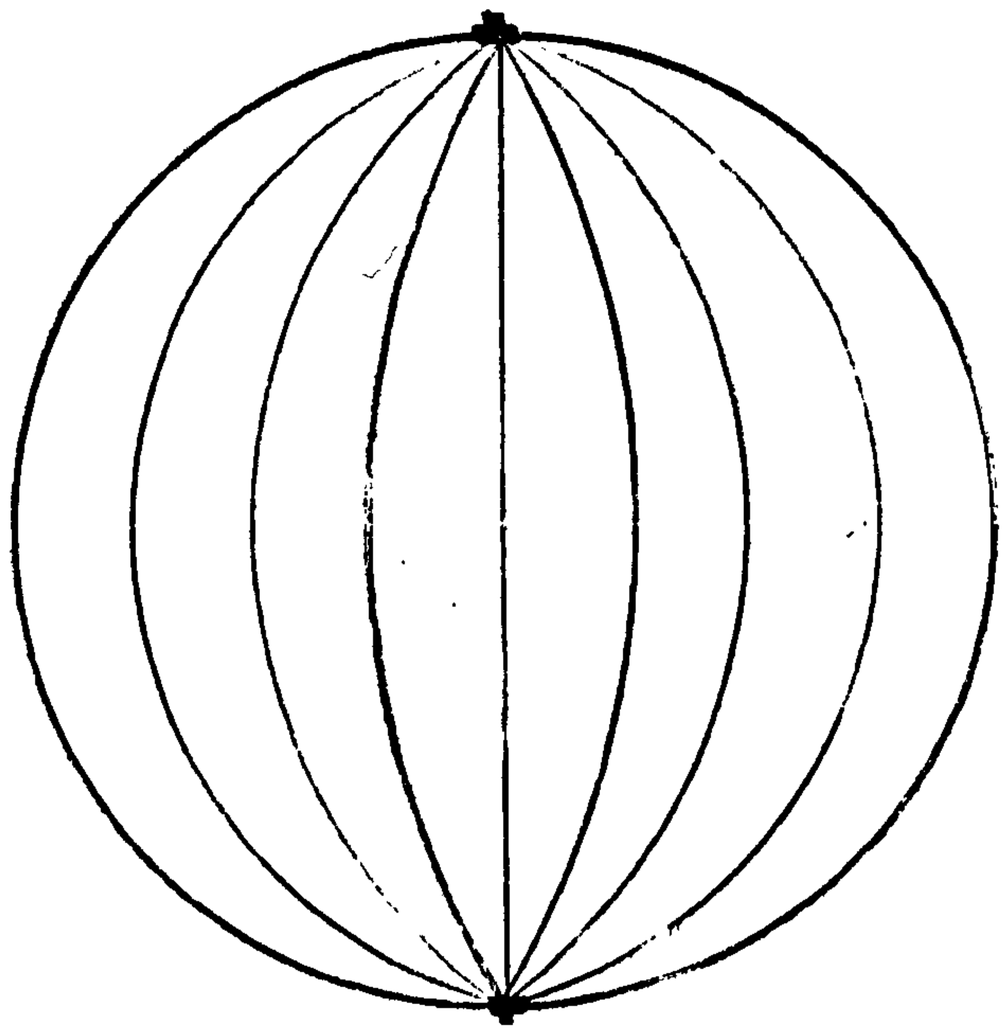

Figure 9 Typical Virtual Current Lines in the Electrode Plane